KU LEUVEN

ARENBERG DOCTORAL SCHOOL

FACULTY OF SCIENCE

Recovery of Neodymium and Dysprosium from NdFeB Magnets using Ionic Liquid Technology

Sofía Riaño Torres

Dissertation presented in partial

fulfilment of the requirements for the

degree of Doctor of Science (PhD):

Chemistry

May 2017

Supervisor:

Prof. Dr. Koen Binnemans

Recovery of Neodymium and Dysprosium from NdFeB Magnets using Ionic Liquid Technology

Sofía Riaño Torres

Supervisors:
Prof. Dr. Koen Binnemans

Members of the
Examination Committee:
Prof. Dr. Tatjana Parac-Vogt
Prof. Dr. Tom Van Gerven
Prof. Dr. Stefan De Gendt
Prof. Dr. Thierry Verbiest
Dr. Jan Luyten

Dissertation presented in partial fulfilment of the requirements for the degree of Doctor of Science (PhD): Chemistry

May 2017

To my parents

Acknowledgments

I would like to thank everyone who, directly or indirectly has contributed to the materialization of this PhD thesis.

First of all, thank you *Koen* for receiving me in your group, for everything you have taught me and for your patience and support through these years. Your trust, encouragement and guidance have made of me a better scientist and a better person. Your ideas, comments, thoughts, questions and your memory (what a memory!) have always motivated me to continue expanding the borders of what I think is chemically possible. I greatly appreciate that although you have a lot of students and lead several different projects you always find time for us. I deeply respect you.

I would like to thank *Tanja, Tom, Stefan, Thierry* and *Jan* for reading this thesis and improving it with their corrections and suggestions and also for the fruitful discussions. Special thanks go to *Tanja* for supporting and giving visibility to the role of women in science.

Peter Tom Jones, you changed my life with a call in November 2014. Thank you for all the motivation and support during the EREAN (European Rare Earth Magnet Recycling Network) project, for always securing the food of the vegetarians in the meetings, for being consistent and coherent helping the environment not only with your research but also with your daily actions.

Rita, thank you for all your support, kindness and encouragement, for everything you do to make sure things get done properly and on time. *Dirk, Paul, Bart* and *Dominik*, thank you for your help in the labs and with the orders, without you everything would be much more complicated.

My gratitude to the FP7 Marie Curie Actions of the European Commission that have funded the EREAN project. They have made of this experience more than a normal PhD. I am very thankful for all the training I got, the support and the encouragement to become a better professional. I always felt very proud to be a Marie Curie fellow and I honored it as much as I could, I took every task with responsibility and did my best. I would like to thank all the people who participated in the EREAN project, for the scientific discussions, team building, long meetings

and great times that we shared. Big thanks to *Marino* and *Misha* for their friendship and support. *Mr. Başkan* (a.k.a. *Recai*), thank you for the scientific discussions, the coffees, the conversations about life, the detailed emails, and overall for always extending your hand to help me.

Thanks to all the nice people I met in Chalmers, thanks to *Christian, Britt-Marie* and *Martina* for the useful discussions. *Kristian*: the best thing that happened to me during the time I was in Sweden was to meet you again and share the office with you. Thank you for showing me Sweden and its culture, for adopting me and taking care of me during those months, for the interesting conversations!

Thank you *Stefan* for giving me the opportunity to join Treibacher Industry AG and increase my experience on R&D. My stay at Treibacher would have not been the same without *Lars* and *Frauke*, thank you guys for sharing all your industrial experience with me and showing me the beauty of Austria and Slovenia, you made of everyday a wonderful experience!

Thanks to *Federica, David, Dzenita, Clio, Michiel, Kumar, Lukas, Pieter, Isadora, Liubov, Nerea, Martina, Simona, Thomas, Stijn R, Stijn VR, Thupten, Lieven, Piet, Raju, Babu, Sharron, Gijs, Bram* and *Nand*, I am very happy to have the opportunity to learn something about different cultures through each one of you. Thanks to *Şenol* for the political/religious/cultural discussions, for the parties and the Turkish candies. *Ernestinho!* Thank you for all the good moments in Belgium and in Brazil, for all the joy that you always bring. *Jonas*: thank you for keeping the apple time tradition alive. *Arne* thank you for being the human jukebox who always has the perfect song for every situation, the jokes and the help in the lab. *Bieke*: you were the first person I met from the group and since the very first moment I got a very nice impression of you, through these years that impression has just gotten better and better. Thank you for your kindness, the trips, the shopping days, the honest advices on clothing and the cafes that we have shared, for showing me Belgium and encouraging me to practice my Dutch. *Tom*: if one googles "Smart person, good at sports, father, kind, humble, always ready to help, professional" the first result you get is a website called TomVanderHoogerstraeteIsTheModelToFollow.com. I really admire you, and I am very grateful for everything I have learned from you. Thank you for sharing all the knowledge you have, for helping me to be better. I also have to thank you for being the only one

who trusted my intuition when Mercedes went missing! *Mercedes*: many thanks for your support, words, emails and all the help that you have offered me. *Joris*: you are the definition of what it is to be a person of integrity, thank you for all the good times and the laughs. *Jeroen*: when you said "so yeah, there is this thing called Dodentocht… you have to walk 100 km in less than 24h… would you like to do that?" I don't know what I was thinking when I said "yeah sure, I am in!" Honestly I had no idea about what 100 km were. I don´t drive a car so those numbers mean nothing to me, the only think I know is that between Leuven and Bogota there are 8.800 km… so 100 km, that´s nothing, right? Slowly I became more aware of the magnitude of my decision when people started saying "gosh, you are doing what? You sure? 100 km?" Although it was a bit painful I have to say that it was a nice experience and I am really glad we did it together. We walked the Dodentocht as we have walked through this PhD, we talked a lot, we gossiped, we were quiet, we talked about the chemistry, we got angry, we felt frustrated, we had moments of happiness, ~~we cried~~, we thought we were invincible, right immediately we thought we were going to quit, but we were always there to support each other and at the end we finished it, as now we are finishing our PhDs. Thank you for everything! *Sven*, thank you for all the moments we have shared together, the Dodentocht of 2015, the walk to the Corcovado, the end of the PhD, for all the story tiiiiimes and jokes, for caring about me and asking how things were going and of course, for eating with joy that a.w.e.s.o.m.e. vegetarian food in Rio. Best restaurant ever. *Daphne*, I am really glad to have you as a friend and there are no words to describe the amazing woman you are. Thanks for your support and motivation, for the talks, the pieces of advice, the cookies and overall for sharing a part of your world with me. You are in my heart. *Ken*: thank you for being there when I thought there was no one. For every lunch, text, talk and absolutely everything you did for me. I am convinced that the world needs more people like you. Thank you for offering me your friendship and your help in the difficult and good times.

Thanks to the old friends who are still there: Carolina, Natalia, Jennifer, Wilder, Kana, Mauricio, Juan, Laura, Paticas, Caroline, Natalie, Esthi, Edu, Nico and Nelly.

Mom, *dad*: thank you for the education you gave me, for having the perfect combination between being strict and flexible, for trusting me and giving me freedom so I could learn how to be independent. Thank you for encouraging me to follow my dreams, for supporting each one of my

decisions and for all the infinite love that only good parents know how to give. I miss you every day. *Brother*, thank you for always taking care of me and for encouraging me to open my mind and see the world in different ways. Every time I hear someone playing a piano I think of you.

And the last one to thank is my favorite human being! Thank you *Fernando* for all these years together, for your unconditional love and support, for motivating me to pursue this PhD since the moment I told you I was coming to Belgium. I always remember that you left many things behind and moved to Leuven so we could just start a new life together, I am very grateful for that!!!! Without you and your love I wouldn't be where I am right now.

And yeah, I have to put this last paragraph here:

The research leading to these results has received funding from the European Community's Seventh Framework Programme ([FP7/2007–2013]) under grant agreement no. 607411 (MC-ITN EREAN: European Rare Earth Magnet Recycling Network). This publication reflects only the author's view, exempting the Community from any liability. Project website: http://www.erean.eu.

Abstract (English)

The rare-earth crisis of 2010 taught the whole world a lesson: the supply of elements that are of high importance for the economy and the development of new technologies (*i.e.* the critical raw materials) must not rely only on a specific country or region. Investing in primary mining, research for the substitution of rare earth elements in their applications, development of rare-earth recycling schemes and training of highly skilled personnel constituted a set of strategies proposed by Europe to tackle the shortage of rare earths.

The recycling of neodymium-iron-boron (NdFeB) permanent magnets is more interesting from an economic and environmental point of view than the opening of new mines. Additionally, elements high in demand and less abundant, such as dysprosium, can be easily recovered. Other critical and valuable metals can also be recovered as byproducts from the recycling of NdFeB permanent magnets. The recovery and purification of individual rare earths opens the possibility to their reuse in the fabrication of magnets with different compositions for specific applications.

The first part of this PhD thesis shows how ionic liquids can be employed as a green alternative to replace the conventional organic phase in solvent extraction processes of rare-earth elements. In a first approach, the selective leaching of rare earths from NdFeB magnets and their solvent extraction from a nitrate media is presented. More specifically, neodymium and dysprosium were separated from cobalt by extracting them to the ionic liquid trihexyl(tetradecyl)phosphonium nitrate (Cyphos® IL 101 nitrate). Afterwards neodymium and dysprosium were separated using ethylenediaminetetraacetic acid (EDTA) as a selective stripping agent. The purified metals were recovered as oxalates and then transformed into the corresponding oxides by calcination. In a second approach, the recovery and separation of rare earths from chloride media is presented. Neodymium and dysprosium were separated by using Cyphos® IL 101 in its thiocyanate form combined with the molecular extractant Cyanex® 923. The addition of a molecular extractant provided a beneficial lower viscosity of the organic phase and a higher loading capacity in comparison with the pure ionic liquid. Stripping of the metals from the loaded organic phase was carried out with water and the rare earths were also recovered as oxalates.

In the second part of this PhD dissertation, the deep-eutectic solvent choline chloride:lactic acid (molar ratio 1:2) was employed to dissolve the magnets. The solvent extraction process was

carried out by contacting the deep-eutectic solvent (more polar phase) with ionic liquids and conventional extractants diluted in toluene (less polar phase). Iron, boron and cobalt were separated from neodymium and dysprosium using the ionic liquid tricaprylmethylammonium thiocyanate (Aliquat® 336 SCN) diluted in toluene. The separation of neodymium and dysprosium was assessed by using two different types of extractants, a mixture of trialkylphosphine oxides (Cyanex® 923) and bis(2-ethylhexyl)phosphoric acid (D2EHPA). Based on the distribution ratios, separation factors and the easiness of the subsequent stripping, Cyanex® 923 was chosen as the most adequate extractant. This new methodology offers higher selectivities and efficiencies than the corresponding aqueous system. Extended X-ray absorption fine structure (EXAFS) spectroscopy was used to elucidate the mechanisms for extraction of cobalt and iron from the deep-eutectic solvent. Furthermore, the feasibility of scaling up this separation process was tested in a mixer settler setup.

Finally, considering that the correct quantification of metal ions in aqueous solutions is essential for the evaluation of a solvent extraction system and also for the follow up of continuous systems, practical and easy guidelines for the correct preparation of aqueous samples and posterior quantification by total-reflection X-ray fluorescence (TXRF) were developed. The most important parameters that play a role in the calibration of a TXRF apparatus such as the choice of the standard element and the concentration ratio between the analyte and the standard were discussed.

Abstract (Nederlands)

De hele wereld leerde tijdens de zeldzame aarden crisis in 2010 dat de bevoorrading van elementen die economisch zeer belangrijk zijn en die essentieel zijn voor de ontwikkeling van nieuwe technologieën (de zgn. kritieke grondstoffen) niet mag afhangen van één specifiek land of regio. Het investeren in primaire mijnbouw, onderzoek naar het vervangen van zeldzame aarden in hun toepassingen door andere minder kritieke elementen, het ontwikkelen van recyclagemethoden voor en het trainen van hoog geschoold personeel zijn enkele strategieën door Europa voorgesteld om het tekort aan zeldzame aarden op te vangen.

Het recycleren van neodymium-ijzer-boor (NdFeB) permanente magneten is interessanter vanuit een economische en milieubewuste visie dan het (her)openen van mijnen. Daarnaast zijn veel gebruikte maar moeilijk te ontginnen elementen zoals dysprosium gemakkelijker te herwinnen. Ook andere kritieke en waardevolle elementen kunnen herwonnen worden als bijproducten van het recycleren van NdFeB magneten. Het herwinnen en zuiveren van de individuele zeldzame aarden geeft de mogelijkheid om ze te hergebruiken in de productie van nieuwe magneten en hun specifieke toepassingen.

Het eerste deel van dit doctoraatsproefschrift toont aan hoe ionische vloeistoffen kunnen gebruikt worden als milieuvriendelijkere alternatieven voor traditionele organische solventen in het zuiveren van zeldzame aarden door solventextractie. Het selectief uitlogen van zeldzame aarden uit NdFeB magneten en de solventextractie van uit nitraatmilieu wordt gepresenteerd als een eerste methode. Meer bepaald, neodymium en dysprosium worden gescheiden van kobalt door extractie naar de ionische vloeistof trihexyltetradecylfosfoniumnitraat (Cyphos® IL 101 nitraat). Vervolgens worden neodymium en dysprosium selectief gescheiden met behulp van ethyleendiaminetetra-azijnzuur (EDTA). De gezuiverde metalen worden daarna neergeslagen als oxalaat en gecalcineerd. In een tweede methode wordt het herwinnen en zuiveren van zeldzame aarden uit chloride milieu voorgesteld. Neodymium en dysprosium worden gescheiden door het gebruik van de ionische vloeistof Cyphos® IL 101 met een thiocyanaatanion in combinatie met het moleculaire extractans Cyanex® 923. Het toevoegen van Cyanex® 923 aan de ionische vloeistof resulteerde in een lagere viscositeit en een hogere laadcapaciteit voor het metaal in vergelijking met de zuivere ionische vloeistof. De terugextractie van de zeldzame aarden uit de

organische fase werd uitgevoerd met water en de zeldzame aarden werden eveneens neergeslagen als oxalaten.

In het tweede deel van dit doctoraatsproefschrift, werd het diep-eutectische solvent cholinechloride:melkzuur(molaire verhouding 1:2) gebruikt om de magneten in op te lossen. Het solventextractieproces werd uitgevoerd door het diep-eutectische solvent (meer polaire fase) in contact te brengen met een ionische vloeistof en conventionele extractanten opgelost in tolueen (minder polaire fase). Ijzer, boor en kobalt werden gescheiden van neodymium en dysprosium door de ionische vloeistof tricaprylmethyl ammoniumthiocyanaat (Aliquat® 336 SCN) opgelost in tolueen. Neodymium en dysprosium werden op twee verschillende manieren gescheiden: met een mengsel van trialkylfosfineoxides (Cyanex® 923) en met bis(2-ethylhexyl)fosforzuur. Cyanex® 923 gaf de beste resultaten op het vlak van verdelingsverhoudingen, selectiviteit en de eenvoud om de zeldzame aarden te verwijderen uit de organische fase. Deze nieuwe technologie geeft ook een betere selectiviteit dan de overeenkomstige waterige systemen. *Extended X-ray Absorption Fine Structure* (EXAFS) spectroscopie werd gebruikt als techniek om de extractiemechanismen van kobalt en ijzer vanuit het diep-eutectisch solvent te onderzoeken. Bovendien werd de mogelijkheid tot het opschalen van dit scheidingsproces getest in een opstelling van *mixer-settlers*.

Tenslotte werden ook praktische richtlijnen voor het correct meten van metalen in waterige oplossingen met behulp van totale-reflectie X-stralenfluorescentie (TXRF) ontwikkeld. Het correct bepalen van metaalconcentraties is essentieel in het beoordelen van solventextractiesystemen op labo- en continue schaal. De belangrijkste parameters die een rol spelen bij het kalibreren van een TXRF-toestel, zoals de keuze van de interne standaard en de concentratieverhouding tussen het analyt en de standaard, werden onderzocht.

Abbreviations and symbols

$(BH)_{max}$	Maximum energy product
$[M]_{aq}$	Metal ion concentration in the aqueous phase after the extraction
$[M]_i$	Metal ion initial concentration
%E	Percentage extraction
$\%E_L$	Percentage extraction in the leachate
%*L*	Percentage of metal leached
%*S*	Percentage recovery / scrubbing / stripping
AAS	Atomic absorption spectroscopy
aq	Aqueous
Bif-ILs	Bi-functional ionic liquids
C_8mim	1-methyl-3-octyl imidazolium
CMPO	Octyl(phenyl)-N,N-diisobutyl carbamoylmethyl phosphine oxide
$C_n$mim	1-alkyl-3-methylimidazolium
Cya	Cyanex® 923
D	Distribution ratio
D2EHPA	bis(2-ethylhexyl)phosphoric acid
DBBP	Dibutyl butyl phosphonate
DEHEHP	Di(2-ethylhexyl) 2-ethylhexil phosphonate
DES	Deep-eutetic solvent
DMSO-d_6	Deuterated dimethyl sulfoxide
DODGAA	*N*,*N*-dioctyldiglycolamic acid
EDTA	Ethylenediaminetetraacetic acid

EDXRF	Energy dispersive X-ray fluorescence
ELV	End-of-life vehicles
EOL	End-of-life
EREAN	European rare earth recycling network
ERECON	European rare earths competency network
ESRF	European synchrotron radiation facility
EU	European union
EXAFS	Extended X-ray absorption fine structure
FT	Fourier transform
FTIR	Fourier transform infrared
GBDP	Grain boundary diffusion process
HBD	Hydrogen bond donor
Hbet	Betainium
HDDR	Hydrogenation disproportionation desorption and recombination
HDDs	Hard disk drives
HP	Heavy phase
HPMS	Hydrogen processing of magnet scrap
HREEs	Heavy rare earths elements
ICP	Inductively coupled plasma
ICP-MS	Inductively coupled plasma optical mass spectrometry
ICP-OES	Inductively coupled plasma optical emission spectroscopy
IL	Ionic liquid
INAA	Instrumental neutron activation analysis
K	Stability constant

K_{eq}	Equilibrium constant
LCA	Life cycle assessment
LCD	Liquid crystal display
LEDs	Light-emitting diodes
LP	Light phase
LREEs	Light rare earths elements
M	Metal
N	Coordination number
MREEs	Middle rare earth-elements
NAA	Neutron activation analysis
org	Organic
PC88A	2-ethylexyl hydrogen 2-ethylhexyl phosphonate
PMMA	Poly(methyl methacrylate)
ppm	Parts per million
PVDF	Polyvinylidene fluoride
R	Bond distance
R_4NCy	Trioctylmethylammonium bis(2,4,4-trimethylpentyl)phosphate
R_4ND	Trioctylmethylammonium di(2-ethylhexyl)phosphate
RE	Rare earth
REEs	Rare earth elements
REOs	Rare earth oxides
RR	Recovery rate
RSD	Relative standard deviation
S/L	Solid liquid ratio

SD	Standard deviation
SX	Solvent extraction
t	Time
TBP	Tri-*n*-butyl phosphate
Tf_2N^-	Bis(trifluoromethylsulfonyl)imide
tpa	Tonnes per annum
TXRF	Total reflection X-ray fluorescence
V_{aq}	Volume of the aqueous phase
VCMs	Voice call motors
V_{org}	Volume of the organic phase
WLEDs	White-light-emitting diodes
WTO	World trade organization
$\bar{x}$	Average
XRD	X-ray diffraction
α	Separation factor
σ^2	Mean-square-displacement in the bond distance

Table of contents

Outline

This PhD dissertation entitled "Recovery of Neodymium and Dysprosium from NdFeB Magnets using Ionic Liquid Technology" is a compilation of four experimental chapters. Three of them are related to the separation and recovery of rare earth elements from used NdFeB magnets and one is related to the analysis of metal ions in aqueous solutions by total reflection X-ray fluorescence.

Chapter 1 is the introduction, in which the criticality of the rare earths is addressed and the different existing routes to secure their supply are explained. Next, the importance of the recycling of end-of-life NdFeB permanent magnets for the recovery of rare earths is highlighted and the different possible recycling routes are described. Then, hydrometallurgy is presented as a tool for the recovery of individual rare-earth elements. Special attention is paid to solvent extraction and in particular to ionic-liquid-based solvent extraction processes for the separation of rare-earth elements. A discussion concerning the scale-up of solvent extraction processes, emphasizing on mixer-settlers is also presented. Finally, the total reflection X-ray fluorescence (TXRF) technique is described.

Chapter 2 discusses the objectives of the PhD thesis.

Chapter 3 discusses the effect of different parameters that could affect the measurement of aqueous solutions by TXRF. It is shown that the choice of the standard element and the concentration ratio between the analyte and the standard are the most important parameters in the calibration of a TXRF apparatus. Practical guidelines for the correct measurement of metal ions in aqueous solutions and cleaning of the sample carriers holders are presented.

Chapter 4 describes the preparation of an iron-free leachate from used NdFeB magnets and the use of an undiluted ionic liquid (Cyphos® IL 101 nitrate) for the extraction of neodymium and dysprosium from nitrate media. The separation of neodymium and dysprosium is achieved using ethylenediaminetetraacetic acid to selectively strip the rare earths. A process flow sheet for the recovery of these rare earths in high purity is presented.

Chapter 5 focuses on the separation of neodymium and dysprosium from chloride media using Cyphos® IL 101 in its thiocyanate form combined with Cyanex® 923. The advantages of the

addition of Cyanex® 923 to the ionic liquid are described. A process flow sheet for this separation is also presented.

Chapter 6 discusses a new approach in which, a deep-eutectic solvent is used to dissolve the NdFeB magnets. Then, Aliquat® 336 SCN diluted in toluene is used to extract iron, boron and cobalt. Afterwards, Cyanex® 923 diluted in toluene is used to separate the neodymium and dysprosium that remained in the raffinate. The mechanism of extraction of iron and cobalt from the deep-eutectic solvent is elucidated by extended X-ray absorption fine structure (EXAFS) spectroscopy. The feasibility of scale-up the process is supported by the results obtained from mixer-settlers. A flow sheet of the process from the dissolution of the magnet is also presented.

Chapter 7 contains the conclusions and the outlook for future work.

At the end, notes about the safety aspects, list of publications, conferences and trainings are presented.

Chapter 1. Introduction

1.1 The rare-earth elements

The rare-earth elements (REEs) form a chemically uniform group that includes the lanthanides lanthanum (La), cerium (Ce), praseodymium (Pr), neodymium (Nd), promethium (Pm), samarium (Sm), europium (Eu), gadolinium (Gd), terbium (Tb), dysprosium (Dy), holmium (Ho), erbium (Er), thulium (Tm), ytterbium (Yb), and lutetium (Lu) plus yttrium (Y), scandium (Sc).[1] The REEs are usually classified into sub-groups, the light rare earth-elements (LREEs) that comprise the elements from La to Gd, the heavy rare-earth elements (HREEs) that include the elements from Tb to Lu, and occasionally some authors add a third sub-group, namely the middle rare earth-elements (MREEs) in which the elements from Pm to Ho are contained.[2-8] A good way to describe the division between the LREEs and the HREEs is considering the electronic configuration of the REEs. The division between the LREEs and the HREEs is usually placed between Gd and Tb, since Gd has a very stable one-half filled 4f electron shell with seven unpaired electrons. Before Gd in the lanthanides series in the periodic table, the elements are characterized for having unpaired electrons in the 4f electron shell. After Gd onwards, paired electrons are progressively added to the 4f electron shell until the 4f electron shell of Lu is fill with 14 electrons.[3,9] Ytrium is considered a REE because it is also found together with other lanthanides in the same minerals.[3] Ytrium is furthermore included in the HREE group because its chemical behavior is similar to the members of this group and its ionic radius falls in between the ionic radii of Ho and Er. In the case of scandium, it does not have enough similar properties with any of the two groups so therefore it is not usually included in any of them. Still Sc resembles Y and the REEs more than what it resembles aluminum (Al) or titanium (Ti) and in aqueous systems it behaves more like the REEs.[10]

In the lanthanide series, the ionic radii get smaller while increasing the atomic number, which is known as the lanthanide contraction. The latter is due to the fact that across the lanthanide series there is an increase in the effective nuclear charge due to the poor shielding of the valence f-orbitals that results in a decrease in the ionic radii.[8,10] The lanthanides share similar properties and they usually have the 3+ oxidation state, although some can also have a 2+ or a 4+ oxidation

state. The coordination numbers are usually greater than 6, and they bind preferably with strong electronegative elements. They are usually grey, silvery-white metals with electrical conductivity.[11] Some REEs have important magnetic properties which are useful in the fabrication of magnets, for instance rare earths such as Nd, Sm, Gd, Dy, Tb, Ho and Er have high magnetic anisotropy and coercivity and thus are usually employed with this aim.[12] Rare-earth based magnets are of high importance and almost indispensable in different industries such as, aerospace, wind turbines, automotive, electronics, magnetic resonance imaging and military. These kind of magnets are chosen over other magnets due to their high magnetic and mechanical strength with a reduced size.[13]

Up to 1960, most permanent magnets were based on the combination of iron with other transition metals. During the 1960s, magnets based on Sm and Co were discovered and investigated, while in the 1980s, magnets containing mainly Nd, Fe, B and small quantities of another rare earth or transition metals were developed.[14] Nowadays, REE-based magnets dominate the market and it is expected that their demand will increase in the upcoming years due to the wide range of applications in which they are used.[13,15] The main advantage that SmCo magnets have over NdFeB magnets is that they can be used at higher temperatures without losing their magnetic properties, besides the fact that they are less prone to corrosion than NdFeB magnets. Still the market for SmCo magnets is smaller compared to the one of NdFeB magnets and currently there is more concern about the supply of Nd rather than that of Sm.[16]

In NdFeB magnets, Nd is the predominant REE used, while the main transition metal present is iron. The microstructure of NdFeB sintered magnets is composed mainly of $Nd_2Fe_{14}B$ grains which are surrounded by an Nd-rich gain boundary phase whose chemical composition is highly non-uniform and can contain small quantities of praseodymium, gadolinium, terbium, and dysprosium, as well as other elements.[17-20] The Nd-rich gain boundary phase may be composed of several phases depending on its oxygen content, the most common are α-Nd, NdO, Nd_2O_3, Nd_2O_3-cubic, NdO_2, $NdBO_3$ and NdFe; in the presence of other rare earths, phases such as $(Nd, Pr, Dy)_2O_3$ can be formed as well.[20-22] The properties of the magnets not only depend on the main magnetic phase ($Nd_2Fe_{14}B$) but also on the characteristics and distribution of the intergranular phases.[23] Small amounts of cobalt can be added to the grain boundary phase to increase the Curie temperature, as well as the presence of aluminum, cobalt, chromium, copper, molybdenum,

niobium, gallium, titanium, zirconium and tungsten can improve the corrosion resistance of NdFeB magnets.[24-27] Dysprosium can be added to the magnet (up to 11%) to improve its coercivity or resistance to demagnetization at higher temperatures due to the enhancement of the anisotropy field of the phase by the formation of $(Nd, Dy)_2Fe_{14}B$.[28] However, the addition of dysprosium in the main magnetic phase reduces the maximum energy product, $(BH)_{max}$ due to a reduction in the magnetization because of the antiferromagnetic coupling of the dysprosium atoms with the iron atoms.[23] To solve this problem, a grain boundary diffusion process (GBDP) can be used to enrich dysprosium in the grain boundaries without entering the magnetic phase, in this way the coercivity can be enhanced without reducing the remanence.[23,29]

1.1.1 The rare-earth crisis: the wakeup call

Despite the fact of being called rare, the rare earths are not so rare on the earth's crust, where they have a relatively high abundance. As it can be seen in Fig. 1.1. They are even more abundant than elements like gold or platinum, with Ce being the most abundant rare earth and Lu the least. The principal ore minerals for the REEs are monazite, bastnaesite and xenotime. Monazite which is mainly composed of Ce and LREEs (La, Ce, Pr and Nd), usually contains Th and/or U in low amounts. Bastnaesite also contains Ce and LREEs but additionally it comes together with very low quantities of HREEs and yttrium. In contrast to monazite and bastnaesite, xenotime contains HREEs, it can contain up to 67% rare earth oxides (REOs) and most of it corresponds to HREEs with Dy, Y, Er and Gd being more frequent than Tb, Ho, Tm and Lu. Xenotime of some locations can also contain significant concentrations of Th and/or U.[30,31]

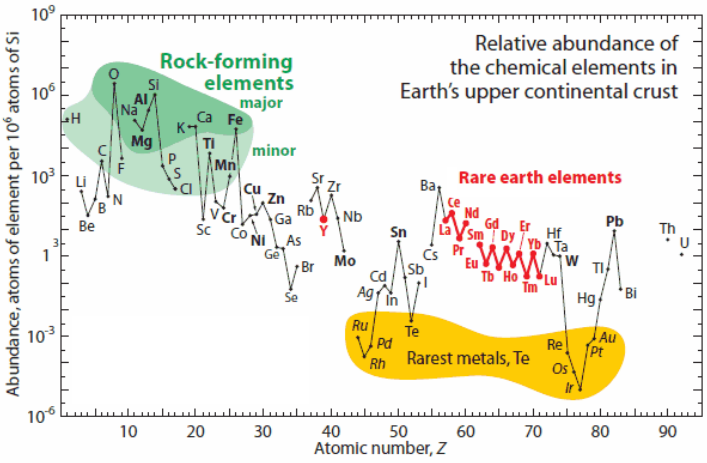

Fig. 1.1. Abundance (atom fraction) of the chemical elements in Earth's crust as a function of the atomic number Z.[32]

There are many different deposits of rare earths in the world and China rules some of the most important ones (Fig. 1.2). However, this does not imply that the majority of the deposits can be found in China, in fact, today China owns only around the 31% of the known reserves.[32,33] Through history, rare earth mines have operated in different countries all around the world, from Brazil to China passing by South Africa and India. From the 1960s and the 1980s, the largest producer in the world was the mine located in Mountain Pass, California (U.S.).[34] However after 1998, Mountain Pass rare earth sales decreased due to the low prices offered by China and also due to environmental issues. As a consequence, the separation plant was shut down in 1998, and the mining stopped in 2002. After China reduced their exportation quota in 2010, Molycorp Inc. started a process for reopening this mine and by the end of 2012 the mine started operating again.[35] Efforts were made towards the optimization of the operation and production of the mine hoping to recover the investments and to regain a place into the rare earth mining market.[36] Sadly, Molycorp Inc. filed for bankruptcy in the middle of 2015: "Rare earth pricing, which has declined dramatically over the past four years, was a key factor in the decision to suspend rare earth production at Mountain Pass."[37] As of February 2017 Molycorp and the mine were planned to be auctioned on March, 2017 after struggling with finding a buyer during more than a year.[38]

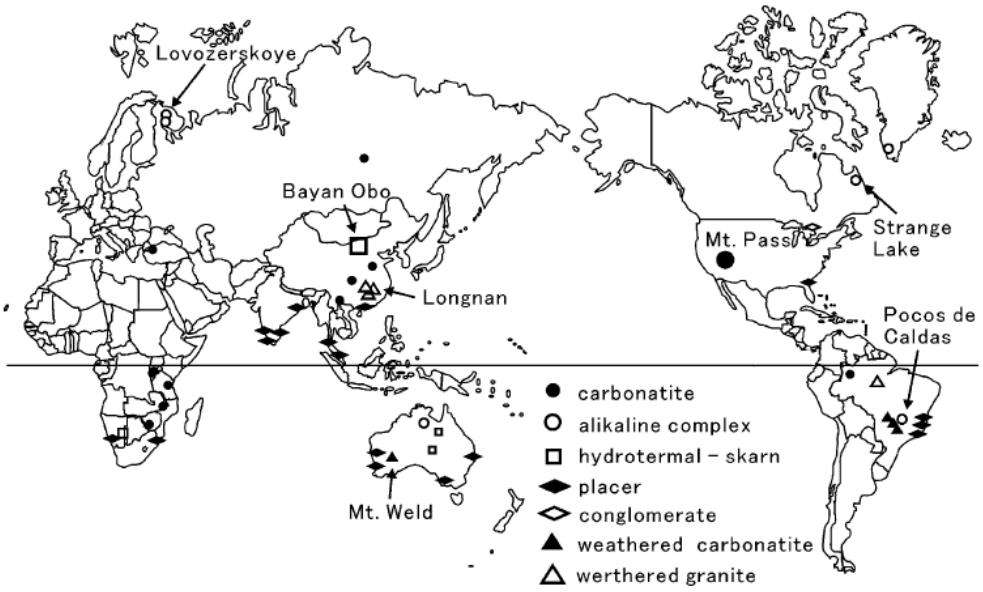

Fig. 1.2. Distribution of REE deposits in the world.[39]

China is still today the largest producer of rare earth elements in the world as it provides up to 95% of the world's supply from its mines.[39,40] Besides this, China also gained terrain in the supply of finished products containing rare earths such as magnets, phosphors, polishing compounds, generators, etc. By 2011 when China was already well positioned in the market of the rare earths and provided the world with rare earths and finished products containing rare earths, it decided to cut down the export quota of REEs (Fig. 1.3). China claimed that the reason behind this decision was that the mining of the rare earths, especially the illegal, was damaging their ecosystems and causing health problems to its population.[41,42 43-45]

In 2012, Europe, the U.S. and Japan considered that these restrictions on the export quota of rare earths imposed by China were a violation of the world trade organization (WTO) regulations. The U.S. filled in a case and brought it to the dispute settlement body of the WTO and the European Union and Japan supported the U.S. by joining the case on its side. China argued that the taken measurements were legal because the WTO regulations allow countries to impose export quotas in order to conserve the environments and to protect plant, animal and human lives. Since the REE mining was damaging the ecosystems and causing damage to the health of the people living nearby the mines, China claimed that they reduced the export quota with the aim of mitigating this environmental problem.

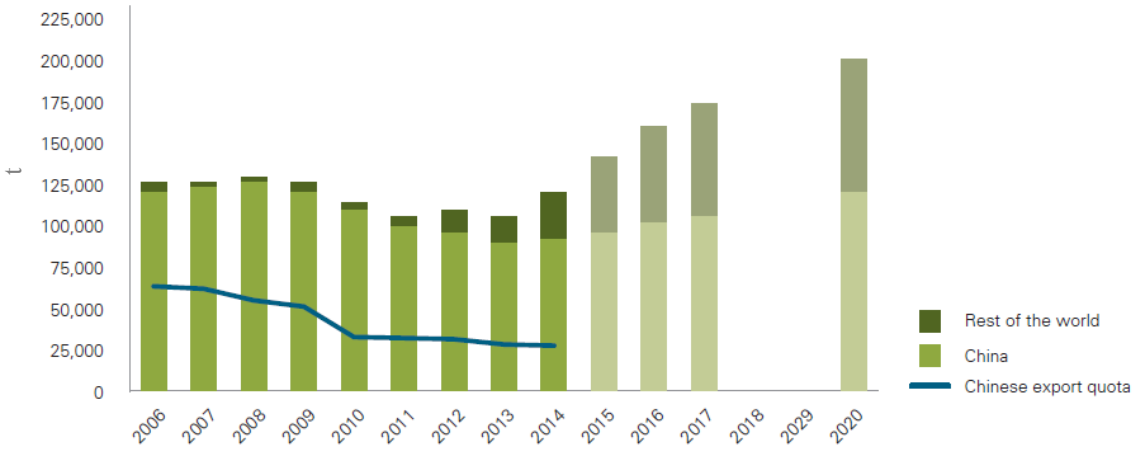

Fig. 1.3. Historical and forecasted rare earth supply, 2006 – 2020.[16]

The WTO highlighted that although the reasons China had mentioned are completely valid and that countries have the right to restrict mining for reasons of conservation and safety, the WTO members could not discriminate between domestic and foreign firms in order to benefit and give access to the mined resources. Indeed, China was giving priority to domestic firms to access the rare earths, which is against the principle of the "non-discrimination" that the WTO members must follow. In 2014 the WTO decided that China should drop the export quotas in 2015. China appealed insisting in its conservation argument but the WTO kept the decision and China dropped its export restrictions in 2015.[32,46-50] Although China was forced by the WTO to drop the export quotas and the price of rare earths has decreased since 2014, a big lesson was learned, and that is that Europe cannot rely on other countries for the supply of raw materials that are crucial for its economy. Besides this, it is not clear what the future will bring since there are other measurements that can be adopted by China in order to maintain preferential access of rare earths to its domestic industries without breaking the WTO rules.

1.1.2 How to solve the problem?

There is not a simple and unique solution to the problem of the rare-earth supply and therefore different regions in the world take different strategies and initiatives to solve it.[51] One of the proposed solutions is based on mining and especially after the 2011 spike in the prices of rare earths, Europe put more efforts towards explorative mining projects. However, economic

viability of potential mines is needed to make the REEs mining outside China a successful story. With this aim, the size of the mine deposit and the average concentration of the rare earths need to be high. Low ore grades will make the mining too expensive and small deposits will not justify the investment and the work to set up a mine.[31,52,53] In addition to the overall concentration of REEs in the deposit, it is highly important to pay attention to the rare earths that exist in the ore. Deposits with HREEs such as dysprosium that is less abundant and therefore has higher value than other REEs are much more attractive.[33,39,54,55]

Before setting up a mine, exploration studies need to be done to find a potential mine, then feasibility, environmental and financial studies have to be carried out. The high operating costs that these steps represent, the low price of the rare earths nowadays and the long time before the mines might become profitable results in many potential investors stepping back. Besides finding and setting up the mine, scalable hydro and pyro metallurgical processes need to be developed to efficiently process the ores. This represents another technical and economic challenge that also comes along with a significant environmental impact. Furthermore, REE mining has to be strictly regulated and monitored to avoid a heavy impact on the environment as it was the case in China.[41,43,56] Radioactivity is another challenge in REE mining, but this can be mitigated by strengthening the radioprotection and adjusting it according to the international and local regulations for the employees, the population living nearby and the waste management.[40] Mining also involves the processing of the ores, which can be highly energy demanding and also consumes a lot of chemicals. The flowsheets for the extraction of rare earths from different kinds of ores have been reported in detail.[53] Even taking into account all the above mentioned challenges, there is one potential exploration project for the mining of rare earths in Europe. The Kvanefjeld deposit, in Greenland which is expected to start production in 2018-2019 and to allow the production of heavy rare earth hydroxides, 4200 tpa as total rare earth oxide and light rare earth carbonate 26200 tpa total rare earth oxide. The Kvanefjeld deposit will have to deal with issues related to radioactive wasted due to the presence of U in the deposit.[16]

Since there are many different types of ores, there are also different kinds of processing technologies to extract the rare earths. In general, the most common processing technique of the crude ore after mining consists in the concentration or beneficiation by milling and flotation. Fig. 1.4 shows the main process steps in REE mining and beneficiation. In the first step, usually the

most employed surface mining technique is open pit mining, where before reaching the ore all the soil, vegetation and the waste rock (the part of the rock that has not ore or too low concentration of it) above it need to be removed. In the next step, milling, the ore is crushed and ground to a fine powder, then the valuable metals from the rest of the ore are separated by different physical methods. A common method is flotation in which hydrophobic materials are separated from hydrophilic ones by a process that is highly energy demanding and consumes a lot of water and flotation agents. Before entering the flotation, the REO concentration is in between 1 and 10%, after the flotation process, the product is enriched with REEs and the percentage of REO increases to 30-70%. The waste streams, also called tailings, are a mixture of water, chemicals and finely ground minerals. The concentrated REO product can be further processed to separate the different REE elements as necessary.[57]

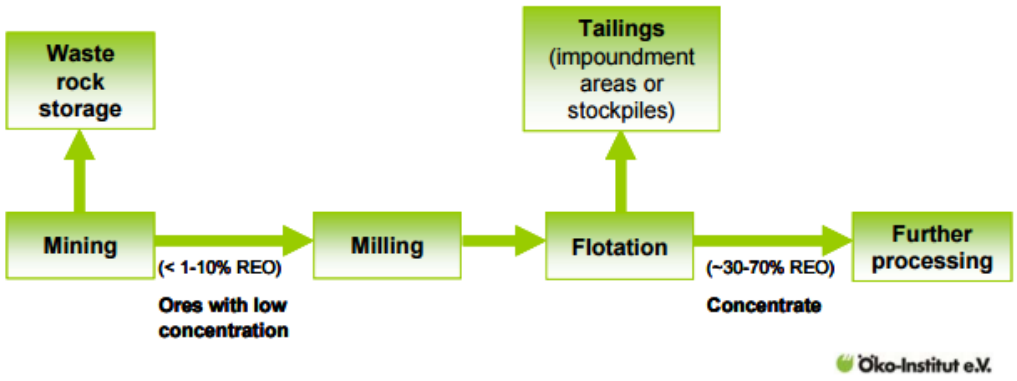

Fig. 1.4. Main process steps in REE mining and processing.[58]

The mining and processing of rare earths is a complicated process that not only requires investment in infrastructure and technology but also the hiring of highly skilled personnel that can develop and optimize an efficient REEs extraction process. The rare earth crisis also put in evidence that there was a lack of trained and experienced scientists and engineers in the rare earth field in Europe.[32] During the 80s and the 90s, when China gained the control over the rare earth market some factories decided to close their plants for the separation of rare earths and relocated the rare earth scientists of the time into other divisions. This created a gap and a lack of trained personal on the exploration and evaluation of ores, mining and beneficiation of concentrates, separation and processing of mixed and individual rare earths, recycling, production of primary materials (metals, starting chemicals, polishing compounds), manufacturing of semi-finished products (magnets, catalysts, phosphors, etc) and development of finished products (wind

turbines, cellphones, hard drives, monitors, etc).[32] Projects such as EREAN (in which this PhD thesis was developed) were created in part, in order to contribute with the solution of this problem and thus give training to young scientists in the field of basic and applied rare earths, with emphasis on extraction, separation methods, rare earth metallurgy, sustainable materials management, recycling methods and life cycle assessment (LCA).[59]

Another way to tackle the REE supply problem is to try to substitute the REEs in the finished products by other elements that are not critical. However, finding substitutes that are as effective as the rare earths elements is a complicated task. Furthermore, the development of rare earth free technology is a challenge that may take several years before it is implemented in industry.[60] Still some governments have encouraged the development of these technologies since they can help reducing the dependence on rare earth elements. In 2011 Toyota started working on the development of induction motors that could replace the magnet motors in its hybrid electric automobiles. The now discontinued Toyota RAV4 EV was an electric car that contained an induction motor that was provided by Tesla which reported the use of copper rotor cage induction machines in all of their electric devices.[61] There has been therefore a growing interest in developing electric motors for vehicles without the use of rare-earth permanent magnets.[62-64] Another approach was the one proposed by Daido Steel Co. and Honda Motor Co. last year.[65] Instead of changing completely the composition of the magnet, they changed the way they produced the magnet by employing a hot deformation method instead of the typical sintering method. This new strategy enables nanometer-scale crystal grains with high anisotropy to be well-aligned in a structure that is ten times smaller than that of a sintered magnet, which in turns makes it possible to produce magnets with higher coercivity. The magnet itself still contains Nd but it has no heavy rare earths and yet has a high resistance at high temperatures and a good magnetic performance that is suitable for its use in the motor of hybrid vehicles.[65] Concerning the development of rare-earth free magnetic materials, in 2015, Makino and co-workers successfully produced a completely rare-earth free high quality FeNi magnet.[66] Synthesis of magnetic materials in the form of nanoparticles smaller than 10 nm has emerged as an alternative method to stabilize traditional or new crystal structures. In 2013, Zr_2Co_{11} permanent-magnet nanostructures were fabricated in a single-step process using the cluster-deposition method. The obtained material presented a high coercivity and magnetic moment.[67] Indeed, in the recent 10 years there has been a lot of research concerning the development of rare-earth-free magnetic

materials, although the development is still work in progress, the real challenge is in the scaling up.[63,68] Another way to cut down the amount of demanded Nd is the implementation of hybrid drive wind turbines (power systems that combine wind turbines with other storage or generation sources, such as solar cells or hydrogen production through the electrolysis of water). Fluorescent light bulbs and LEDs depend on phosphors made from the rare earths terbium, europium and yttrium. Alternatives to these phosphors have been presented, and rare-earth-ion-free boron carbon oxynitride phosphors have been prepared from inexpensive and environmentally friendly raw materials, leading to the production of a phosphor with tunable color emission through a low-temperature method.[69] A novel rare-earth free self-luminescent $Ca_2KZn_2(VO_4)_3$ phosphor was synthesized in order to replace the rare-earth based phosphors commonly employed in white-light-emitting diodes (WLEDs) and improve its properties.[70] In the same way, it has been recently reported the straightforward synthesis of several rare-earth-free phosphors. However, their thermal stability remains an issue.[71] If these products reach the industrial scale production they can help to further reduce the dependence on other countries for the supply of rare earth elements.

An alternative strategy to solve the problem of REE supply is by the recycling of REE. REE can be recovered from magnet swarf and rejected magnets, industrial residues containing rare earths such as red mud and phosphogypsum, end-of-life (EOL) products containing phosphors (fluorescent lamps, compact fluorescent lamps, LEDs, LCD backlights and plasma screens), permanent NdFeB magnets present in vehicles (motors, switches, sensors), mobile phones (loud speakers, microphones), hard disk drives, electric bikes and wind turbine generators.[16,18] Approximately 26 000 tons of REOs are used per year in the production of NdFeB permanent magnets, conforming the largest application both in tonnage and in market value.[72] NdFeB magnets are widely used because their properties can be fine-tuned by modifying their chemical composition to meet the requirements of different applications. Dy and Tb are used to increase the anisotropy and coercivity of the magnet, which is important for magnets that will be used at high temperatures, but they decrease the remanence and the energy product. Cu and Al can be added to improve sintering of the magnet alloy, while Co is added to increase the Curie temperature of the magnet.[60,72,73] It is expected that in the near future (2017-2035) the demand of REE magnets and Dy grows considerably due to the fast growing of green technologies such as wind turbines and electric vehicles.[72] China and Japan have led the production of REE permanent

magnets but China has dominated most of the market share. It is expected that the demand of REE permanent magnets increases and reaches approximately 36 000 tons this year. It is also forecasted that China will continue dominating the market of the rare earth elements at least in the close future (Fig. 1.5).[74]

The recovery of REEs from EOL NdFeB magnets not only helps to satisfy the demand of REE in the magnet sector but also helps to mitigate the so-called balance problem of the rare earths. This is by trying to level the unbalance between the market demand for specific REEs and the natural abundance of the REEs in the ores. For instance, the demand of Dy is expected to increase in the upcoming years, but the supply of Dy from mining will likely lead to an oversupply of other rare earths that are more abundant in the ore (*e.g.* Nd, La, Ce and Y). Besides this, recycling avoids the need to deal with the radioactive elements that can be found in the mines, since as a result of the large Dy demand, large quantities of thorium would be also co-produced.[54,75,76]

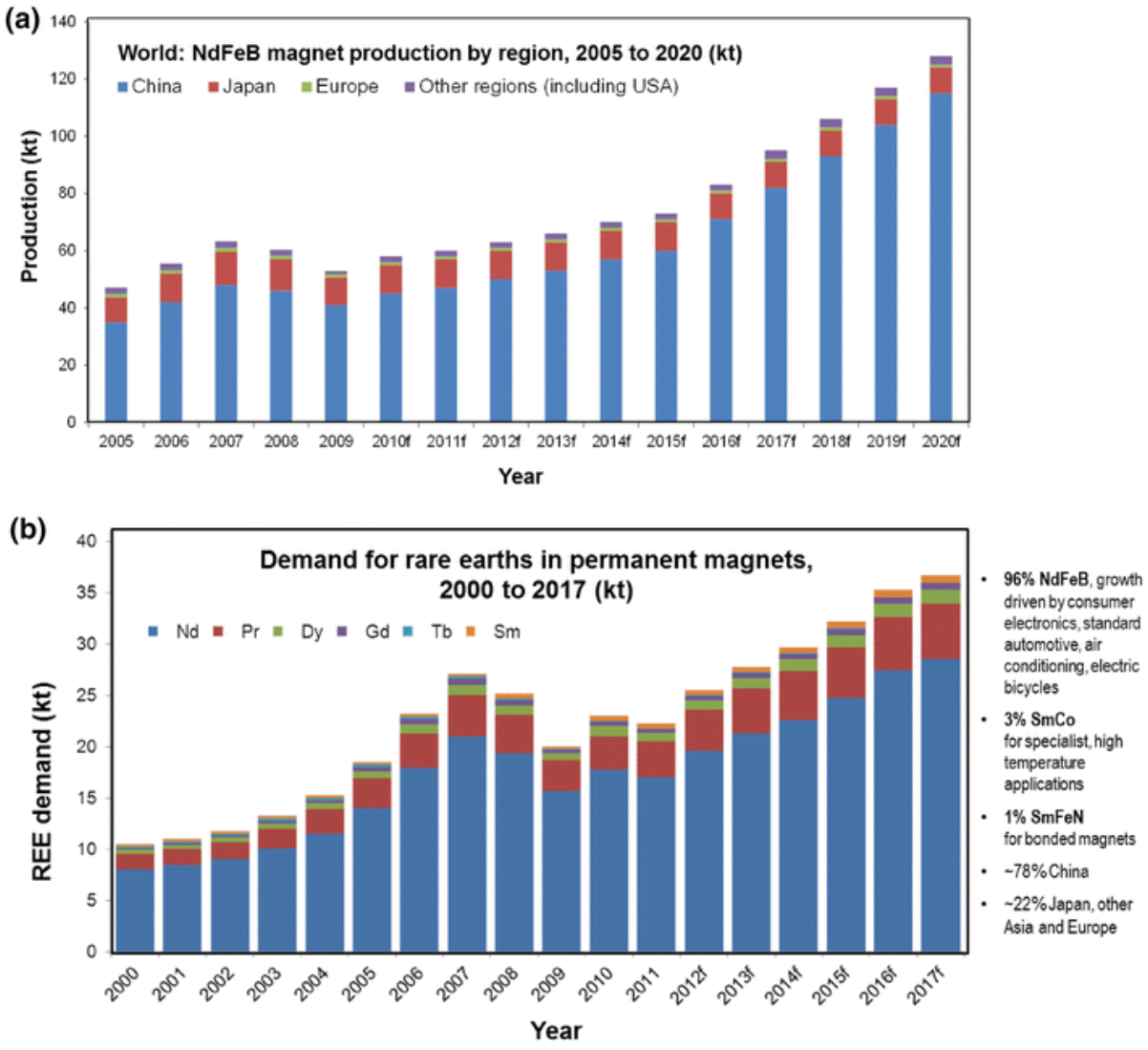

Fig. 1.5. Global production of NdFeB permanent magnets and the demand for the REEs (a) Total global NdFeB magnet production and prediction: 2005-2020, (b) Total global REE demands for permanent magnets.[74]

1.1.3 Recycling of NdFeB magnets

Life-cycle assessment (LCA) is a technique to estimate the environmental impacts associated with all the stages of the fabrication of a product or a process. Although the production of NdFeB permanent magnets is of high importance and plays a key role in the economy, to date, there are very limited LCA studies on the production of REEs and their recycling. A review on the available LCA studies related to the production of REEs has been published in 2014,[77] where it

has been discussed how rare earth elements such as Nd and Dy are in a supply risk and how they are indispensable for the production of rare earth permanent magnets. Last year LCAs on the production of NdFeB magnets from newly mined material and from recycled magnets were also published.[78] As a result of this study it was shown that REEs recycling has a less environmental impact than the virgin process and also offers magnets with a stronger magnetic performance and better microstructure. Fig. 1.6 shows the different steps involved in a common recycling of permanent magnets procedure and the virgin production route based on mining.

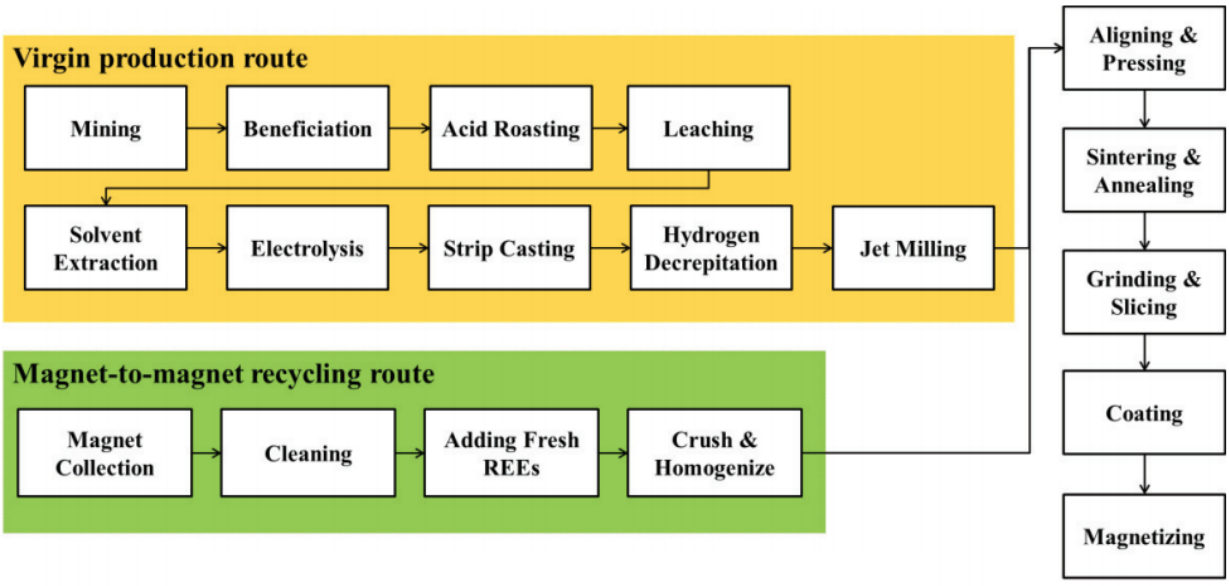

Fig. 1.6. Detailed processes: virgin production vs. magnet to magnet recycling.[78]

In a previous study, it was also concluded that recycling of permanent magnets through the manual dismantling of computer hard disk drives combined with a hydrogen based recycling process (hydrogen decrepitation) is preferable over the primary production and other processes in which the hard disk drives are shredded.[15,79] It has also been highlighted recently that in 2020-2030 about 18-22 percent of LREE (Nd and Pr) and 20-23 percent of HREE (Dy and Tb) global demand for NdFeB magnet production can be met by REEs recycling from EOL magnets and industrial scrap.[80] In 2015 the European Rare Earths Competency Network (ERECON) listed the devices containing REE permanent magnets that could be recycled, such as hard disk drives, automotive applications, motors in industrial applications, loudspeakers, air conditioning compressors, magnetic separators, mixed electronics (mobile phones, electric toothbrushes,

shavers, drills, etc), electric bicycles and wind turbines.[16,81] However, the long-term demand of NdFeB cannot be established with total certainty, since the market changes constantly, different applications can be found, new materials can be developed and the REE content on the EOL products of today might not be the same of the one in 30 years. Today, the recovery rates of these types of products are low, but they can increase with the time as collection and recycling schemes are established and the users get involved into the recycling process. Still it is important to take into account when creating recycling schemes, that China not only drives the demand for the REE but also for the NdFeB applications since they are also one of the main producers of the finished products. As a result, it could be expected that the amount of produced scrap in China is likely to arise in large quantities in the upcoming years. Moreover, China is also a large consumer of magnets, which means that many of the EOL magnets to be recycled will be located in China. Therefore it would be beneficial if recycling collaborations with China are explored in order to find a sustainable strategy for the recycling of REEs and meet the global REE demands.[80]

Since the REEs prices dropped significantly in 2011, the implementation of promisory processes for the recycling of REEs at larger scale has gotten difficult. Since the prices are low, there are not economic incentives to start implementing the recycling schemes of NdFeB magnets. The latter is especially true in countries where the labor costs also pose a challenge for the economic feasibility of REEs recycling in an industrial scale.[80] To alleviate this situation the government in Japan has issued subsidies to help the setting up of REE recycling from NdFeB magnets.[82] An additional advantage of REE recycling is associated with a lower investment cost in comparison to the establishment of a new mine. If in addition to such initiatives it is taken into account that the REE composition of the EOL magnets/industrial processing scrap is closer to the desired REE ratio required in the production of new magnets than the ratio that is found in the ores and that REE recycling is more efficient, take less time and is more environmentally friendly than the mining process, it is expected that the REE recycling process will contribute on the global supply of REE and to the economy. It has to be highlighted that although substitution of REE in products can be beneficial to mitigate the criticality of the heavy rare earths or the rare earths in general, substitution and competition could become competing strategies.[63,80] The cut down or substitution of REE in products can mitigate the shortage of rare earths today but this will have an impact on the future because less material containing REE will be available to be recycled. An excess of substitution can make the recycling of REEs less economically viable. In the same way,

an excess of recycling can make the substitution less economically viable. A balance in the substitution and the cut down of REE is a good strategy that can help to stabilize the market of the required REEs and will facilitate the planning for the recyclers.[83]

There have been several advances in the recycling of REEs contained in phosphors at industrial scale. However, the recycling rates for REEs from end-of-life products across the world are still reported to be very low (< 1 %).[16,84-86] In the case of NdFeB magnets, they are only being recycled in Japan by Tokyo Eco Recycle Co., Ltd. a company from the Hitachi group that was founded with the aim of recovering resources from personal computers and household appliances.[87] Since 2012 this company has been recycling magnets from hard disk drives (HDDs) and air conditioner compressors with a process capacity in the order of tons. Their process can be summarized as follows: (1) A HDD dismantler removes the voice call motors (VCMs) from HDDs and demagnetizes them. (2) A magnet recovery machine removes and separates the magnets from the demagnetized VCMs, (3) and a material recovery machine recovers the different materials from the scrap left over by the HDD dismantler. (4) The magnet recovery machine separates the rare-earth magnets from the yoke. The scrap contains iron, glass, electronic circuit board pieces, aluminum and stainless steel. These materials are recovered by using different techniques such as magnetic separation, vibrating filtration, gravity concentration, etc. Electronic circuit board fragments contain precious metals, so this process also serves as a starting point for the precious metal recovery. Hitachi has improved and redesigned some parts of their equipment to make it compatible with the processing of compressors that have different shapes.[87]

In general terms, the steps involved in the recycling of rare earths from EOL NdFeB magnets include:[16]

Identification of the products that contain rare earths.

Collection of these products in quantities that are large enough to make the recycling viable.

Detection of the rare-earth-containing component in the scrap.

Separation of these components by manual or mechanical dismantling or sorting.

Extraction of the rare earth-containing material as an alloy, rare earth oxide or salt.

Refining of the separated rare earth fraction to an alloy, compound or element.

Re-processing of the elements or alloys into a new form of material.

The identification, collection, detection and separation steps are key on the efficiency of the recycling process. For instance, it has been amply demonstrated how carrying out conventional shredding without separation of end of life vehicles (ELV) and household appliances reduces the concentration of Nd below 130-290 g of Nd/ton, which is even much lower than the REEs content in some mine tailings (1000-1500 g/ton). Recovering from such low concentrations is not attractive from an economic point of view.[72,88] A similar situation is presented when shredding from electronic waste without dismantling and separating the magnets from the magnet-containing component, which results in the complete loss of REEs.[89]

There are different ways to carry out the separation step, one is the hydrogen processing of magnet scrap (HPMS), in which the rare-earth containing component of the HDD is exposed to hydrogen at atmospheric pressure and room temperature to generate a soft magnetic powder that is no longer magnetically attracted to the ferrous components in the scrap. Afterwards, the magnet powder containing also Ni (from the coating of the magnet) is mechanically sieved and separated from the nickel flakes.[90]

After the extraction, there are several paths that can be taken in order to arrive to the re-processing of the magnet, these paths are summarized in Fig. 1.7.[18,72,86] When a clean, non-oxidized form of NdFeB magnet can be separated from EOL products as a solid magnet or as a hydrogenated powder magnet, it is possible to reprocess it by using a direct alloying route that is also used in the primary production of magnets. However, modifications are needed in order to reduce the oxygen content in the magnet since it is usually higher in the recycled source of sintered NdFeB than in the primary cast NdFeB material. Also, the composition of the magnet can be modified by blending with extra REE material in order to achieve certain properties. Advantages of the direct alloy recycling are that few steps are required in these processes and typically these routes have smaller environmental footprint and fewer steps compared to other recycling routes. Among this group the re-sintering of scrap NdFeB magnets,[91] hydrogenation disproportionation desorption and recombination (HDDR) of scrap-sintered NdFeB magnets,[92-94]

re-casting and melt pinning of sintered NdFeB magnet scrap can be found.[95] This kind of approach is very useful when dealing with big magnets such as the ones found in wind turbines and electric motors of electric vehicles. However, direct alloy recycling can be difficult when processing small magnets and it is not possible to use when direct shredding is employed because of the high amount of impurities present. Even in the case of manually dismantled HDDs the heterogeneity of the scrap magnet material can be so high that it could make it incompatible with the re-sintering process.[96] Metallurgical extraction, separation and refining have been proposed as an alternative to solve this issue. In the metallurgical path, there are mainly three ways that can be recognized, namely, pyrometallurgy, solvometallurgy and hydrometallurgy. Pyrometallurgy selectively converts the REEs in the magnet into another phase that separates the main non-REE components.[72] It can be divided into 5 groups, specifically roasting, liquid metal extraction, molten salt extraction, molten slag extraction and electrochemical processing. These methods are usually applicable to all types of magnet compositions and has the additional advantage of generating zero wastewaters or effluents, but at the expense of a high-energy consumption.[97] [18,72] In solvometallurgy, non-aqueous solvents such as molecular organic solvents, ionic liquids, deep-eutectic solvents (DESs) and inorganic solvents such as liquid ammonia, concentrated sulfuric acid or supercritical CO_2 are employed. The advantages that this strategy provides are the limited water, energy and acid consumption, the possibility to have higher efficiencies and different selectivities, as well as the possibility to work with water sensitive complexes or metals that can hydrolyze easily in water.[98] Finally, hydrometallurgy, that involves the use of aqueous chemistry to recover metals from different sources, can be divided into two main categories including leaching and solvent extraction. Hydrometallurgy allows the recovery of individual rare earths from magnet scrap, EOL magnets, slags and tailings. This strategy is of high importance when the recycled rare earths are employed in the fabrication of other products or magnets with different compositions and characteristics than the recycled one.[16,18]

1.2 Hydrometallurgy as a tool for the recovery of rare earth elements

In general, hydrometallurgical processes are highly flexible, since complex material can be treated (*e.g.* ores, low-grade ores, or magnets) and individual metals or groups of metals can be recovered by correct design and fine-tuning of the parameters and the leaching agents and

extractants. The latter is rather complicated or almost impossible by using other methods such as pyrometallurgy. On the other hand, the scaling up of hydrometallurgical processes is more difficult, since several steps are involved and therefore their full understanding before scale up is required.[99]

1.2.1 Leaching

Leaching (or solid-liquid extraction) is the first step to dissolve the metals that are present in a shredded material, a recovered used magnet, magnet scrap, or grinded rock from ores. One way to implement a leaching step is by dissolving completely the used NdFeB magnet or the magnet scrap with or without a roasting step in mineral acids. This usually leads to high extraction yields, but it requires of more additional steps to separate and purify the elements of interest.[72,88,100] A better strategy is to carry out a selective leaching where the scrap material is first roasted and then dissolved selectively with a mineral acid based on the different oxidation state and solubility of the obtained metal salts.[72 18,100-103] A good example of selective leaching is the one proposed by Önal and coworkers,[104] where powdered samples of EOL magnets were mixed with sulfuric acid, dried, calcined and then leached selectively with water, allowing the recovery of 95-100% of REE (Nd, Pr, Dy and Gd) while Fe (present in the magnet up to almost 70%) and other impurities remained in the residue. This REE-rich leachate can be employed in solvent extraction processes for further separation and purification of the present rare earths. Besides this, the process allows the recycling of the majority of the consumed acid.

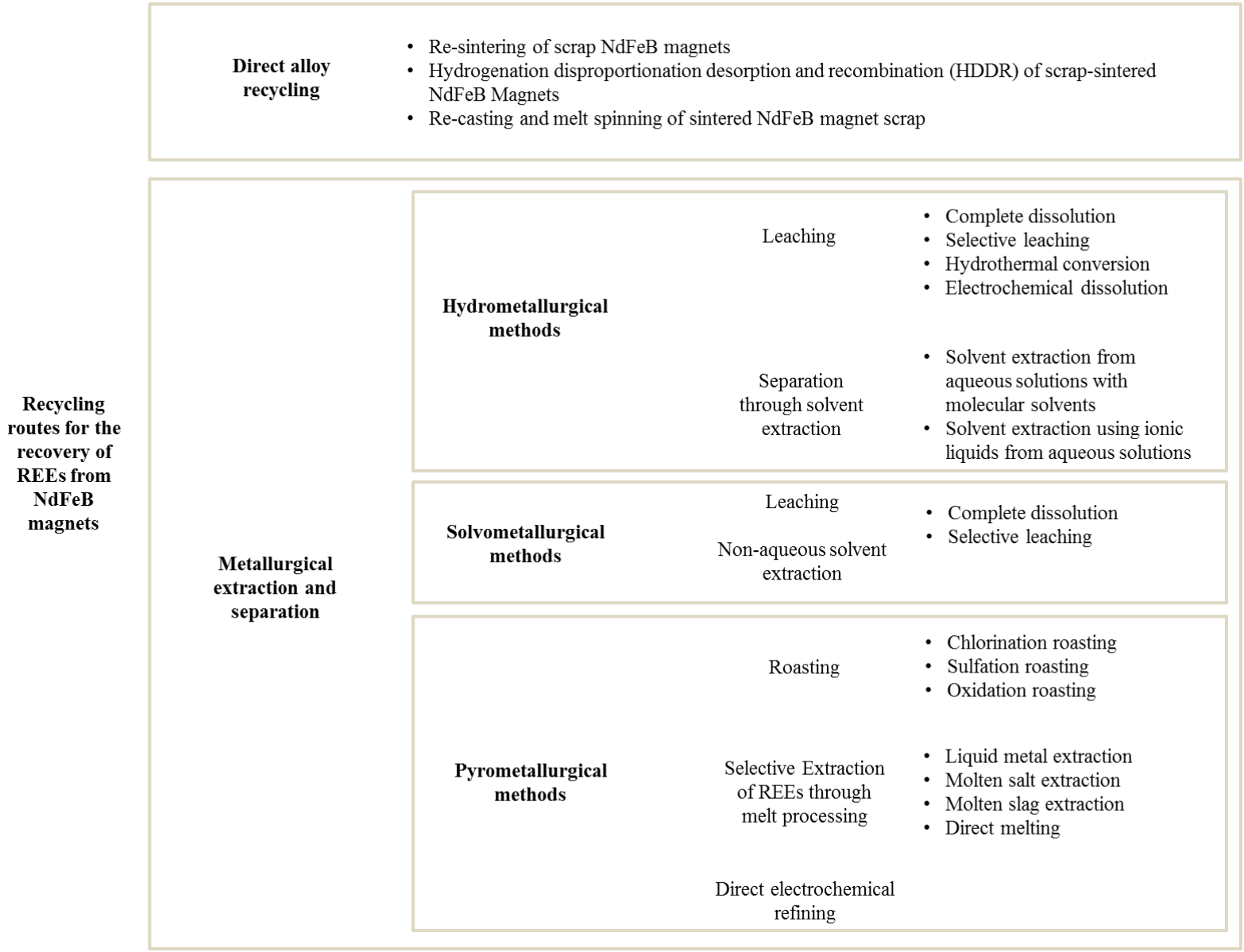

Fig. 1.7. Different recycling routes for the recovery of REEs from NdFeB magnets (EOL or scrap).

1.2.2 Solvent extraction

Solvent extraction (SX) is an important and powerful tool in the modern chemical industry. It has a wide range of applications from the recovery of metals to the recovery of organic molecules, metabolites from natural products, chemicals from waste streams, pesticides, among others.[105] Concerning the separation of rare earth elements, solvent extraction is considered as one of the most suitable technology for the separation of rare earths into groups or individual elements.[106]

In general, a solvent extraction process can be depicted as shown in Fig. 1.8. An initial aqueous solution containing a mixture of compounds or metal ions is put in contact with a hydrophobic organic phase, these two phases are then mixed until the equilibrium is reached. The success of the separation will depend on many different factors that will influence the extraction process such as temperature, stirring rate, concentration of the extractant, organic aqueous phase ratio, type of diluent, salt concentration, among others. Once the equilibrium is reached and the system has been settled, the phases are separated and can be easily recovered again.

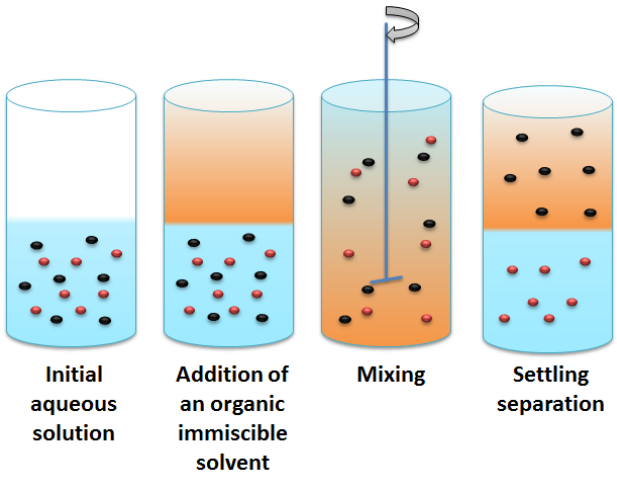

Fig. 1.8. General scheme for a solvent extraction process showing the different steps involved.

1.2.2.1 General considerations of solvent extraction processes

The efficiency of the extraction and separation of metal ions can be expressed in terms of the distribution coefficient and the separation factor. The distribution coefficient of a metal ion, M, D_M is given by:

$$D_M = \frac{\overline{[M]}}{[M]} \qquad \text{(Eq. 1.1)}$$

where $\overline{[M]}$ is the molar concentration of M in the organic phase and $[M]$ is the molar concentration in the aqueous phase after extraction. The percentage of extraction (%E) is defined as the initial amount of metal ion in the aqueous phase ([M_i]) minus the amount of metal ion in the aqueous phase after extraction ([M_f]) over the initial amount of metal ion ([M_i]). In case of equal volumes it can be expressed as:

$$\%E = \frac{([M_i]-[M_f])}{[[M_i]]} \times 100 \qquad \text{(Eq. 1.2)}$$

The separation factor of two different metal ions M_1 and M_2, α is given by:

$$\alpha = \frac{D_{M1}}{D_{M2}} \qquad \text{with} \qquad D_{M1} > D_{M2} \qquad \text{(Eq. 1.3)}$$

The metal ions are extracted into an organic phase that usually consists of an extractant, a molecular solvent, and if needed, a phase modifier (to avoid the formation of a third phase and/or to improve phase disengagement and reduce the viscosity).[106] The organic phase containing the target metal ions after extraction is called extract. If other metals are co-extracted, a scrubbing step might be necessary to improve the purity of the organic loaded phase. This is achieved by contacting the extract with an aqueous phase that allows removing the undesired metal ions, while keeping the target metal ions in the extract. Afterwards the metal ions can be removed from the organic phase by stripping, which is achieved when the extract is contacted with an aqueous solution for which the metal ions have higher affinity. Then targeted metals can be precipitated to obtain metal salts and further calcined to produce metal oxides.[107]

The chemistry of the metal solvent extraction has been well summarized and explained in the literature.[106,108-112] For the extraction of rare earths, there are basically three types of extractants (Fig. 1.9):

- Acidic extractants (cation exchange mechanism)
    - Carboxylic acids (*e.g.* Versatic acid 10, LIX 1104)
    - Organophosphorus acids (*e.g.* Cyanex® 272, MEHPA, PC 88A, D2EHPA)
    - Chelating extractants (*e.g.* β-diketonates)

- Neutral extractants (solvating mechanism)
    - Neutral extractants (*e.g.* TOPO, TBP, Cyanex® 923)
- Basic extractants (anion exchange mechanism)
    - Protonated amines (*e.g.* Primene JM-T)
    - Quaternary ammonium salts (*e.g.* Aliquat® 336)
    - Quaternary phosphonium salts (*e.g.* Cyphos® IL101)

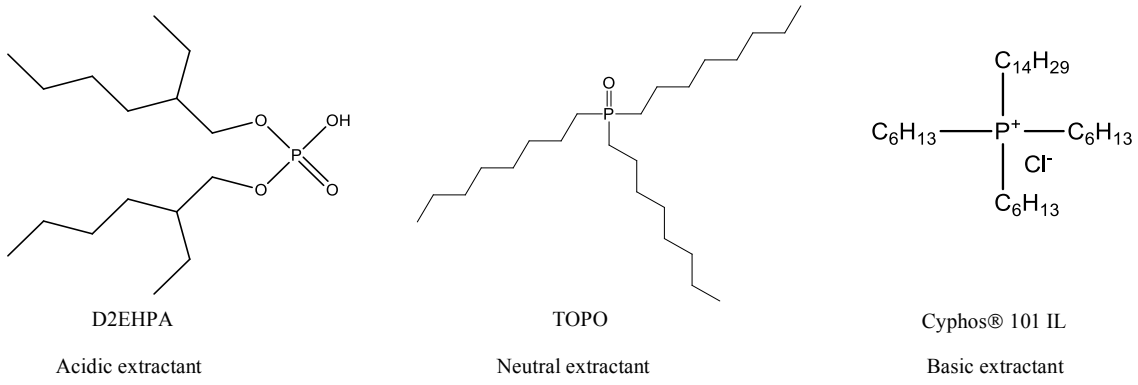

Fig. 1.9. Examples of common metal extractants.

Acidic extractants (cation exchange mechanism)

The general reaction for this kind of extractants can be written as:

$$RE^{3+} + 3\overline{(HA)} \underset{\leftarrow}{\rightarrow} \overline{(REA_3)} + 3H^+ \qquad \text{(Eq. 1.4)}$$

Usually, the process is more complicated than the described one in Eq. 1.4. The acidic extractants are usually aggregated as dimers in non-polar organic solutions that will affect the complex formed during the extraction, thus the reaction can be better depicted as,[108]

$$RE^{3+} + m\overline{(H_2A_2)} \underset{\leftarrow}{\rightarrow} \overline{(REA_3(HA)_{2m-3})} + 3H^+ \qquad \text{(Eq. 1.5)}$$

where H_2A_2 represents the dimeric form of the organic acid. From this equation it can be inferred that the extraction of rare earths with this type of extractants is promoted by increasing the pH of the aqueous phase and the stripping process is promoted by increasing the acidity of the aqueous stripping solution.[106]

The cation exchangers that are used in the separation of rare earths can be divided into carboxylic acids and alkylphosphoric acids. The extraction power depends on the acidity of the extractant as follows:

Alkylphosphoric > alkylphosphonic > alkylphosphinic > carboxylic acids

$(RO)_2PO\text{-}OH \quad > \quad (RO)RPO\text{-}OH \quad > \quad R_2PO\text{-}OH \quad > \quad R(CO)OH$

As a result, the alkylphosphoric are the strongest extractants, but they will make the stripping much more difficult and at the same time more time and economical demanding. Due to the relatively large separation factors for neighboring rare-earth ions, only one acidic extractant would be necessary to separate a mixture of rare earths. The efficiency of the extraction is strongly dependent on the acidity of the aqueous phase, which can be considered a disadvantage since the pH needs to be controlled carefully. One of the main drawbacks is that gels and emulsions can be formed when working with highly concentrated feeds.[113-117]

Neutral extractants (Solvating mechanism)

The general reaction for this kind of extraction can be written as:

$$RE^{3+} + 3NO_3^- + \overline{3B} \underset{\leftarrow}{\rightarrow} \overline{(B_3 \cdot RE(NO_3)_3)} \qquad \text{(Eq. 1.6)}$$

where B represents a neutral extractant. As it is depicted in Eq. 1.6, this extraction involves the transfer of a neutral species from the aqueous to the organic phase by solvation of the metal ion within a neutral salt species. The water molecules hydrating the complex are replaced by solvating molecules that form a more hydrophobic complex that is soluble in the organic phase. Several molecular extractants have been used for the separation of rare earths: tributyl phosphate (TBP), Cyanex® 923 and dibutyl butyl phosphonate (DBBP).[108] [53,99,106,111,118-120] These

extractants can be used to extract rare earths from very concentrated feeds having less problems with gel formation than in the case of the acidic extractants. The stripping can be achieved with water or diluted acids.

Basic extractants (anion exchange mechanism)

Anion exchangers are protonated forms of primary, secondary and tertiary amines and quaternary compounds such as quaternary ammonium salts. The general reaction for this kind of extraction is expressed in Eq. 1.7 and 1.8.

$$2\overline{RNH_2} + H_2SO_4 \underset{\leftarrow}{\rightarrow} \overline{(RNH_3)_2SO_4} \qquad \text{(Eq. 1.7)}$$

$$2Ln(SO_4)_3{}^{3-} + 3\overline{(RNH_3)_2SO_4} \underset{\leftarrow}{\rightarrow} 2\overline{(RNH_3)_3Ln(SO_4)_3} + 3SO_4{}^{2-} \qquad \text{(Eq. 1.8)}$$

The interaction of quaternary ammonium ions with rare earth metal anionic complexes is electrostatic, thus the selectivity will depend on the charge, ion size and the complex formation in the aqueous phase.[108] The concentration of the anion will be therefore of high importance, since it will directly affect the distribution coefficient. Afterwards, the back extraction is easily achieved with water as in the case of neutral extractants.[106] One major drawback when using basic extractants is that primary amines or quaternary ammonium salts can conduce to aggregation issues when the organic phase is highly concentrated and therefore increase the viscosity of the system. This problem can be addressed by the addition of a modifier, but this usually decreases the extraction efficiency.[106,108,109,111]

1.2.2.2 Solvent extraction using ionic liquids

Ionic liquids (ILs) are solvents that consist entirely of ions (Fig. 1.10). Some of the most important characteristics of ILs are their chemical and thermal stability, wide electrochemical potential window, low flammability and negligible vapor pressure. ILs are also electrically conductive, which means that there is no danger of accumulate static electricity that can result in sparks.[121] These features make them good candidates for the replacement of conventional organic phases in solvent extraction.[122] However, the relatively high viscosity of some ionic

liquids represents a challenge, since it could slow down the mass transport in the solvent extraction process. Hydrophobic ILs with fluorinated anions such as hexafluorophosphate (PF_6^-) or bis(trifluoromethylsulfonyl)imide (Tf_2N^-) are less viscous than other common ionic liquids, but ionic liquids containing these anions are expensive and the hexafluorophosphate ions can hydrolyze to hydrofluoric acid.[123] Moreover, the extraction of metals with these ionic liquids occurs through an ion-exchange mechanism in which part of the ionic liquid is lost in the aqueous phase. To alleviate this situation, hydrophobic cations that contain long alkyl chains with anions such as nitrate or chloride are preferred. The problems associated with the high viscosity of these ILs can be solved by saturating them with water before the extraction and using higher extraction temperatures. Thus the dilution of the IL in organic solvents is avoided in order to make the processes greener and take advantage of the properties of the undiluted IL.

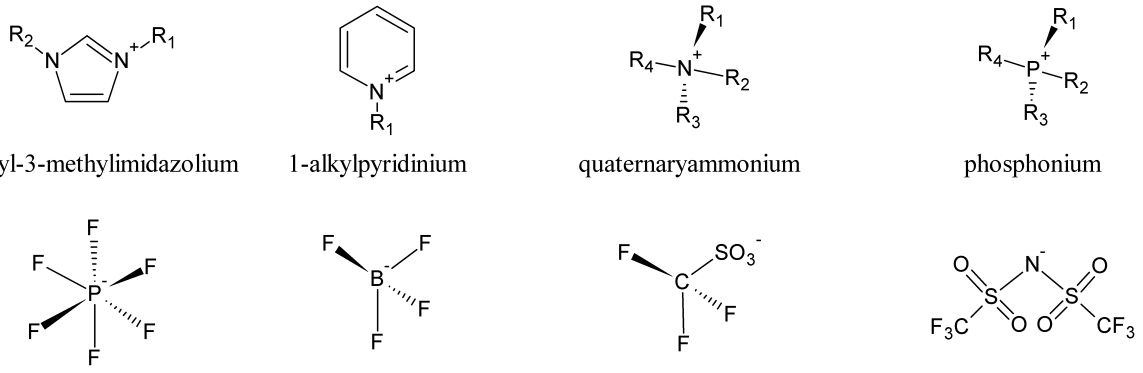

Fig. 1.10. Typical cations and anions of ionic liquids.[124]

Ionic liquids have been used alone or in combination with other extractants for the recovery of rare earths. In 2003, Nakashima and coworkers reported the use of octyl(phenyl)-*N,N*-diisobutyl carbamoylmethyl phosphine oxide (CMPO) as extractant dissolved in the ionic liquid 1-butyl-3-methyl-imidazolium hexafluorophosphate.[123] The extractability of the rare earth ions was higher than when using conventional organic solvents and the stripping step was carried out with complexing agents such as EDTA and citric acid.[125] In another study, a new extractant, *N,N*-dioctyldiglycolamic acid (DODGAA) was used in combination with 1-methyl-3-octyl imidazolium bis(trifluoromethylsulfonyl)imide [C_8mim][Tf_2N] for the separation of lanthanides. The efficiency of the extraction was higher when compared to the system in which DODGAA

was diluted in *n*-dodecane.[126] In another approach, D2EHPA was used in combination with 1-alkyl-3-methylimidazolium hexafluorophosphate [$C_n$mim][PF_6] (n = 2, 4) to separate Ce, Nd, Sm, Dy and Yb. When comparing the ionic-liquid based system to conventional organic systems using hexane as diluent, higher distribution ratios were obtained for the studied rare earths.[127] Bi-functional ionic liquids (Bif-ILs) have been also studied for the recovery of Nd and Pr from NdFeB magnet leachates. Trioctylmethylammonium bis(2,4,4-trimethylpentyl)phosphate (R_4NCy) and trioctylmethylammonium di(2-ethylhexyl)phosphate (R_4ND) were compared against conventional extractants. The extraction efficiency of different extractants for Nd and Pr was determined to have the following order: R_4NCy > R_4ND > Cyanex 272 > D2EHPA > Aliquat® 336.[128]

One of the first efforts for the recycling of rare earths from permanent magnets using undiluted ionic liquids was carried out by using trihexyl(tetradecyl)phosphonium chloride to remove cobalt from samarium and iron from neodymium. As result, the rare earths were left in the aqueous solution and the transition metals were extracted to the ionic liquid phase. The stripping of cobalt was achieved with water while the stripping of iron was carried out with EDTA.[129] The rare earths in the aqueous phase were recovered as oxalates and then calcined.[101] By changing the anion of the ionic liquid and using trihexyl(tetradecyl)phosphonium nitrate the rare earth ions can be extracted as the transition metals remain in the aqueous phase. In this case, lanthanum and samarium were separated from nickel or cobalt.[130] Dupont and Binnemans[131] developed a new recycling process for (microwave) roasted NdFeB magnets based on the ionic liquid betainium bis(trifluoromethylsulfonyl)imide ([Hbet][Tf_2N]). The thermomorphic properties of the [Hbet][Tf_2N]–H_2O system allowed the design of an efficient leaching/extraction step, where at a temperature of 80 °C the system is completely homogeneous and at temperatures below 56 °C the system is biphasic. Under these conditions, iron is distributed to the organic phase while neodymium, dysprosium and cobalt remain in the aqueous phase. Oxalic acid was then used to precipitate the rare earths along with the present cobalt, while the iron was transferred from the ionic liquid phase to the water phase as a soluble oxalate complex. Cobalt was subsequently removed from the oxalate mixture of rare earths using aqueous ammonia. The mixture of rare-earth oxalate was calcined and the rare earths were recovered as a mixture of oxides.

The split-anion extraction is an approach that can be employed for the separation of mixtures of rare earths by solvent extraction using undiluted ionic liquids.[132] The rare-earth ions are extracted from a chloride aqueous phase to an organic phase, consisting of a hydrophobic thiocyanate or nitrate ionic liquid without the need of adding an acidic extractant due to the stronger interaction between the rare-earth ions and the thiocyanate ions in the ionic liquid.[132] The process is called split-anion extraction because the aqueous and organic phases consist of different anions, for example, thiocyanate anions will have preference for the organic phase since the order of preference of the ions for the organic phase is in the ascending order: $SO_4^{2-} > Cl^- > Br^- > NO_3^- > I^- > ClO_4^- > SCN^-$. Therefore, the chloride anions that are characterized for having a high charge density are strongly hydrated and tend to remain in the aqueous phase.[133] The major advantage of split-anion extraction is that the source of the complexing anion is the ionic liquid phase. Additionally, the stripping of the rare earths from the ionic liquid phase by water is easier. The extraction mechanism is denoted by Eq. 1.9.

$$Ln^{3+} + 3SCN^- + (x-3)\overline{PR_4SCN} \rightarrow \overline{\left(\left(\left(PR_4^+\right)_{(x-3)}\right)\left((Ln(SCN)_x)^{3-x}\right)\right)} \qquad \text{(Eq. 1.9)}$$

The separation of rare earths into individual elements using ionic liquids will be presented in Chapters 3 and 4.

1.3 Upscaling

Industrial solvent extraction equipment can be classified into three categories: (1) centrifugal extractors, (2) columns and (3) stage-type extractor.[134] Centrifugal extractors are high-speed rotary machines.[135] They provide one stage of extraction per unit, which means that multiple units can be attached together. The phase separation in a centrifugal contactor is faster and more efficient than in other equipment due to the centrifugal forces. This category of extractants is ideal for systems that suffer of poor phase separation and slow phase disengagement, systems that tend to form emulsions and relatively high viscous phases. It also offers low residence times and therefore a large process capacity. The category of the column extraction equipment includes

packed towers, pulse columns, rotating disc contactors, tray columns, etc. This type of extractors maximizes the utilization of the mass transfer driving force because compared to mixer-settlers the stage retention time in a stage is only about 30% of that in the mixer-settler when the processing capacity is the same. Some disadvantages are that they are difficult to scale up to handle high flow rates and high O:A phase ratios. Concerning the stage-type contactors, one of the most common is the mixer-settler. In this type of set up, the organic phase and the aqueous phase are mixed together in one chamber by an impeller. The extraction occurs during the mixing step and it takes from seconds to minutes to reach the steady state. Then the phases are transferred to a settling chamber in which the separation of both phases occurs by gravity due to the different phase densities. Each mixer-settler represents one stage of extraction, thus units can also be linked together and the process can be operated in continuous mode. However, fast disengagement is required and mixer-settlers usually take up a lot of space. Table 1.1 summarizes the main advantages and disadvantages of the different type of solvent extraction equipment.

Table 1.1 is a good starting point for the selection of the best type of contactor for a solvent extraction process to be scaled up. It is important to notice that the selection of the contactor mostly relies on the physical properties of the extraction system. For instance, the density, viscosity and interfacial tension of the phases play a key role in the mixing process and later on in the phase separation. The kinetics of the extraction process has also a high importance on the selection of the contactor. For example, for processes requiring longer equilibration times, mixer-settlers are more suitable since they offer longer residence times than centrifugal extractors. Other parameters to take into account are the process capacity needed, the number of stages required, plant limitations in terms of area or height, fabrication material of the equipment, health and safety and maintenance of the equipment.

Table 1.1. Summary and comparison of different types of extractors.[135]

Parameters	Mixer-settlers	Columns without agitation	Columns with agitation	Centrifugal extractor
Separation Efficiency	High	Poor	Average	High
Mass transfer	Average	High	Low	High
Residence time	Long	Average	Average	Short
Stage required	Low	Average	High	Average
Capacity	Low	Low	High	High
Capital cost	High	Low	Average	High
Operation cost	High	Low	Average	High
Maintenance Cost	Average	Low	Average	High
Plant headroom	Low	High	High	Low
Floor area	Large	Low	Low	Moderate
Holdup volume	High	Average	Average	Low
Reliability	Good	Good	Good	Average
Flexibility	Good	Average	Average	Good
Complexity	Simple	Simple	Average	Complex
Quick restart	Quick/ Easy	Difficult	Difficult	Quick/easy

In general terms, mixer-settlers are suitable for systems that have good phase disengagement and require a large number of theoretical stages. Columns without agitation are mainly employed

when there is good phase disengagement and a small number of theoretical stages. Agitated columns are suitable for moderate phase disengagement and a small number of theoretical stages. Centrifugal extractors are used for difficult phase separation and small number of stages.[135]

1.3.1 Mixer-settlers

The general design of a mixer-settler is shown in Fig. 1.11. They consist of two parts, a mixer for contacting the two liquid phases and a settler for their separation after extraction either in a continuous or batch wise operation. There are different parameters that can be configured in a mixer-settler: the design and location of the impeller in the mixer, the shape of the mixing chamber, the location of inlets and outlets and the design of the baffles. Those parameters affect the flow patterns in the mixer-settler, the depth of the dispersion band and the droplet size distribution. For example, the appropriate mixing conditions have to be applied in order to create a large interfacial area and thus assure a good mass transfer and stage efficiency. However, over-mixing might cause the formation of too small droplets that will not be easily separated in the settler. A baffle located at the entrance of the mixer reduces the turbulence and therefore can contribute to fast phase disengagement. Picket fences or coalescence plates can help the droplets in the dispersion to merge and favor the phase separation. However, picket fences at larger scales might get blocked due to the presence of solids, for example. An important advantage of mixer-settlers is that the lab setup geometries can be easily scale up to industrial levels.[112,135]

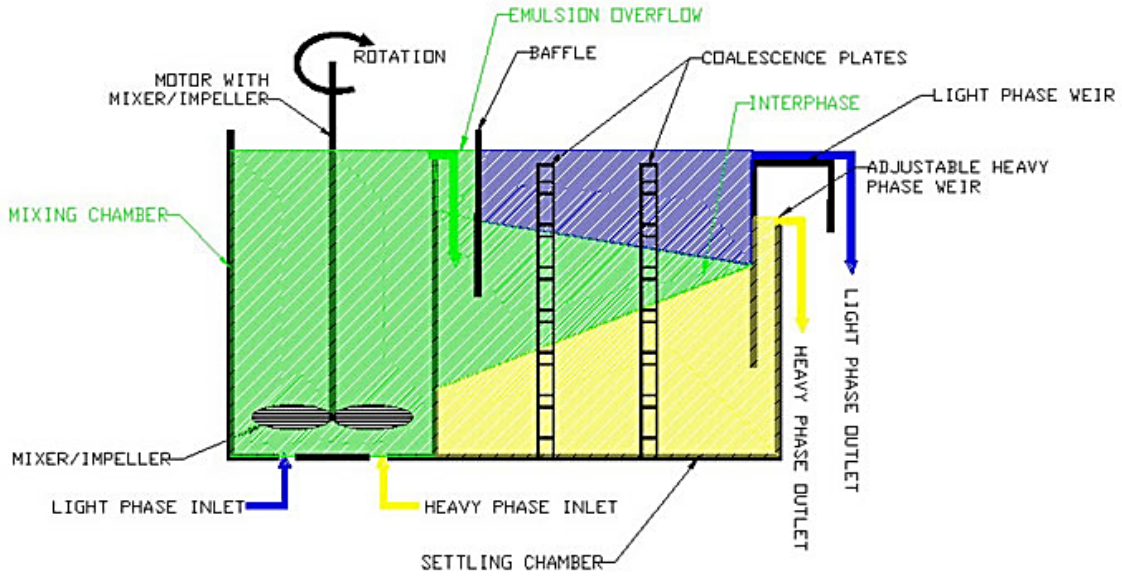

Fig. 1.11. General scheme of the process work of a mixer-settler.[136]

To design a solvent extraction process it is necessary a clear understanding of the distribution coefficients and equilibrium isotherms of the system. These data and curves are obtained in the laboratory or to some extent can be calculated by computer if enough data is available in the program. A software can operate in design mode or performance mode but in both cases it is necessary that the operator introduces the data of the extraction and stripping isotherms into the program. The software can then determine the O/A ratio and number of stages to achieve, for example, a chosen raffinate concentration. The software can also determine the concentration of metal ions of interest in the raffinate for a given set of extraction parameters. Typical software packages allow the construction of the isotherm from data generated in the lab, prediction of mass balances and percentage recovery of the target compound or metal ion, the possibility to change the number of extraction or stripping stages and determine changes in concentrations of the raffinate and calculation of O/A ratios.[137]

The number of theoretical stages required for a separation can be determined by different methods. The McCabe-Thiele diagram is one of the most employed graphical methods to determine the number of theoretical stages required in a solvent extraction process. This method is based on graphical constructions of an extraction or stripping isotherm and an operation line. Thus, a stepwise determination of the number of stages required to achieve certain grade of

separation can be defined. The slope of the operation line is equal to the volume ratio between the organic phase and the aqueous phase.[138] The operating line can be settled by any two points or by only one point and the ratio of A/O feed that decides the gradient of the line.[139] Fig. 1.12 shows an example of how a McCabe-Thiele diagram looks like. This diagram was constructed by performing extractions at different organic:aqueous phase ratios and measuring the concentration of the target metals in both phases after extraction. In this case, Lu and Yb are extracted with 0.1 M TOPS 99 from sulfuric acid media, the initial concentration of both metals is 56.7 mg L^{-1}. In the Y axis, the concentration of the metals in the organic phase is plotted, while the X axis corresponds to the concentration found in the aqueous phase. A vertical line in the X axis is placed at the value that corresponds to the initial concentration of the feed. Operating lines with different slopes (different O:A ratio) can be drawn and at some point they will intersect the vertical line at the initial concentration in the feed. This intersection point is denoted by the letter A in Fig 1.12. Then, a parallel line to the X axis can be drawn until it meets the isotherm (point B). Then a vertical line can be plotted until it touches the operating line (point C) and it continues successively until the beginning of the isotherm is reached. According to Fig. 1.12, 3 stages would be needed to carry out the separation at an A:O equal to 2:1.

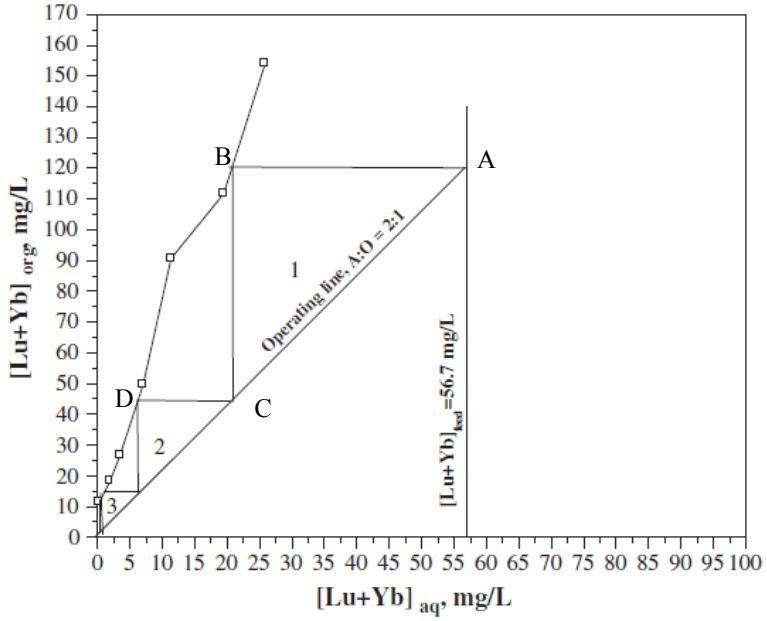

Fig. 1.12. McCabe–Thiele plot for Lu+Yb extraction. Organic: 0.1 M TOPS 99, Aqueous: [Lu+Yb]= 56.7 mg/L, $[H_3PO_4]$ = 3 M.[140]

The McCabe-Thiele method is still used in these days because it helps the researcher to develop an impression about how the system will behave in larger scales. Moreover, if there is an unusual metallurgical behavior in the system, the McCabe-Thiele diagram will show it.[141] McCabe-Thiele diagrams are useful to determine the number of stages of extraction but also the number of stages of stripping. To generate a stripping isotherm, the loaded organic phase is contacted with different volumes of the stripping solution, making sure that different O:A ratios are covered. In this case, the concentrations of the organic and aqueous phases are plotted in the X and Y axis, respectively, which is the opposite of what is plotted for an extraction isotherm.

There are many variables that can affect a McCabe-Thiele construction such as the strength and concentration of the extractant, pH of the aqueous phase, content of the metal ion in the aqueous phase, slope of the operating line, shape of the isotherm and stage efficiency. The steepness of the isotherm can be increased markedly by using a stronger extractant, which allows the use of a less number of stages of extraction than when a softer extractant is employed (using the same O/A ratio in both cases). When there is a decrease on the efficiency of extraction at the final stages of extraction, the isotherm can adopt the form of an "S", which can be translated in an increase of the number of stages required for the separation. In this case, it would be very difficult to achieve low concentrations of the metal ion in the raffinate, making the process less convenient from the economic point of view. This "S" shape is characteristic of weak extractants or poor control of the pH in the aqueous feed when the extractants are pH dependent (*e.g.* acidic extractants). This kind of extractant, for example, requires careful control of the pH to operate properly. The pH can directly influence the loading capacity of the extractant and therefore can also affect the isotherm. The O/A phase ratio chosen determines the operating line, increasing this ratio results in a decrease of the slope which reduces the number of theoretical stages required to obtain a given concentration in the raffinate.[142]

The majority of the knowledge concerning the separation of rare earths at large scale is developed and kept at industrial level. However, there is some information available concerning the design procedures for mixer-settlers, involving the importance of studying parameters such as specific gravity, viscosity, composition of the phases, interfacial tension and rate of coalescence.[134,135,143,144] Studies on the separation behavior of solvent extraction system changing the phase compositions and agitation times after completion of the mass transfer process have

been presented. Parameters affecting the dispersity of the phases and the coalescence (agitation, type of impeller, physicochemical properties of the system, etc) have been studied experimentally.[145] Also, information about the dispersion characteristics in the mixer and settler characteristics can be found in literature.[146] Most of the studies that have been published based on the separation of rare earths with conventional extractants, for instance models have been developed to predict the operating conditions, control and performance on the separation of rare earths (Nd, Pr and Ce) in a 30-stage countercurrent cascade using D2EHPA.[147] A design consisting of a mixer with double mixing chambers in series and a settler have been tested for the separation of rare earths with PC88A in kerosene.[148] In chapter 5, an example for the separation of rare earths from deep eutectic solvents using conventional extractants diluted in toluene in a mixer-settler will be presented.

1.4 Total-reflection X-ray fluorescence (TXRF)

Different analytical techniques have been used for a long time for the determination of REE in diverse samples. The most common techniques used in the determination of REE are inductively coupled plasma mass spectrometry (ICP-MS), inductively coupled plasma optical emission spectroscopy (ICP-OES), X-ray fluorescence (XRF) and neutral activation analysis (NAA). Different reviews covering the advantages and disadvantages of the different techniques employed for the determination of trace elements depending on the type of sample, as well as sample preparation and digestion have been published recently.[149-154] Fig. 1.13 shows an overview of the most common techniques that are employed for the quantification of REE depending on the nature of the sample.

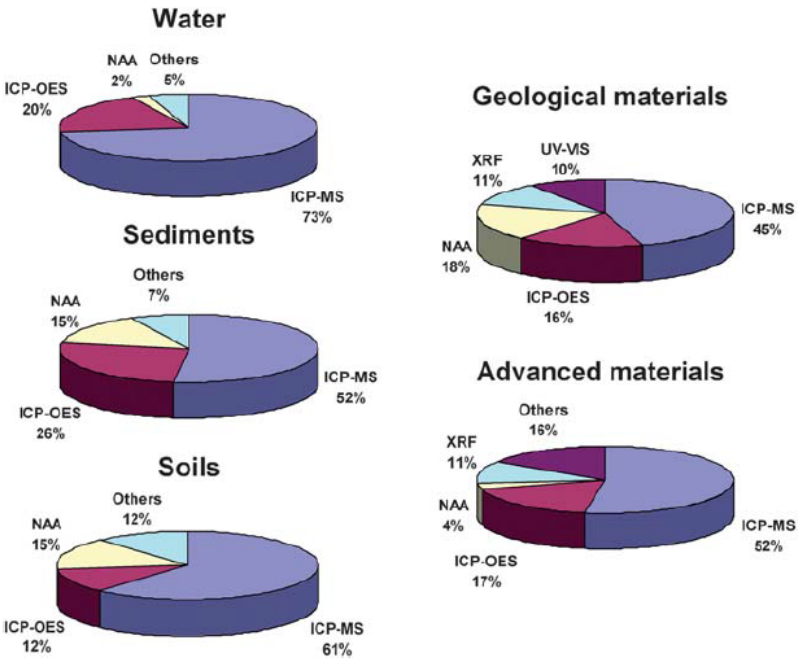

Fig. 1.13. Frequency of use of specific analytical techniques for REE determination.[154]

From Fig. 1.13, it can be seen that techniques such as ICP-OES and ICP-MS are mainly employed in the quantification of REE for most of the applications. Despite of this, TXRF seems to be a promising alternative since it offers different advantages over other spectroscopic and spectrometric techniques. For instance, low sample amount requirement, no need of constructing a calibration curve before each analysis because the quantification is done by internal standardization, fast sample preparation, low cost related to the measurement and liquids, suspensions and solids can usually be analyzed without pretreatment.

TXRF was introduced in 1971 by Yoneda and Horiuchi and it has been further developed and implemented by Aiginger and Wobrauschek, Knoth and Schwenkes and Klockenkämper and von Bohlen.[155-157] The principle of TXRF is based on the generation of an X-ray emission when an inner shell electron is ejected from an atom when it is impacted by a high energy X-ray photon. After the ejection, higher energy electrons drop to lower atomic orbitals in a series of quantum-permitted relaxations and emitting secondary X-rays of characteristic energies. The emitted X-ray photons constitute the X-ray fluorescence atomic spectrum that contains certain number of lines characteristic of the element (Fig. 1.14).[158]

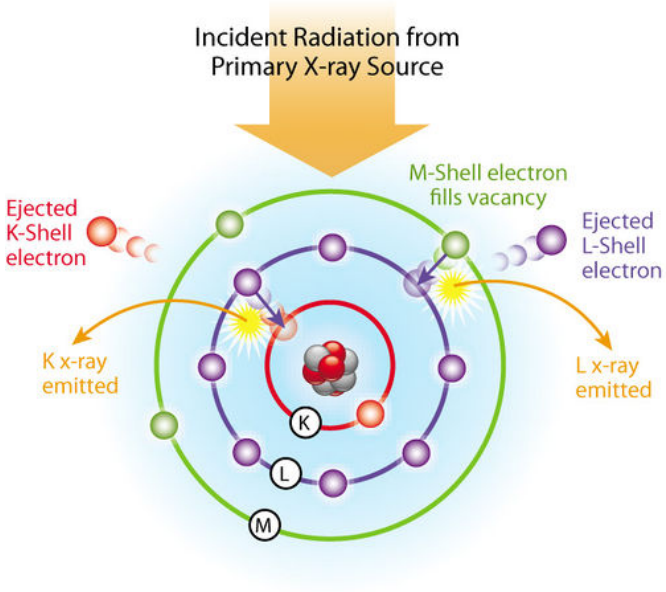

Fig 1.14. Principle of the XRF[159]

In TXRF, the sample carrier is inclined under an angle of 0.1° with respect to the direction of the incident X-ray beam. This results in the total reflection of the X-ray beam on the surface of the sample carrier, which leads to a high decrease in the background since almost no X-rays are penetrating into the sample carrier. The sample is irradiated twice by both the incident and the totally reflected X-rays, which results in an increased excitation probability of the sample elements. Furthermore, the detector is very close to the sample, which allows the collection of a large amount of the fluorescence radiation from the sample, increasing the signal-to-noise ratio and the sensitivity.[160,161] One important feature of the TXRF technique is that standing waves are formed on the surface under the total external reflection of X-rays, which promotes the effective excitation of X-ray fluorescence in the sample under study. Because of the interference of the incident and the reflected X-ray beams in a triangular zone above the reflector surface, the formation of standing waves with nodes and antinodes located parallel to this surface takes place (Fig. 1.15) The intensity at nodes is zero, and that at antinodes amounts to a fourfold intensity value of the incident beam. Unwanted effects can occur if the standard is not distributed homogeneously through the sample, the effect is even more critical if the standard is in a node and the analyte at the antinode or viceversa.[160,162]

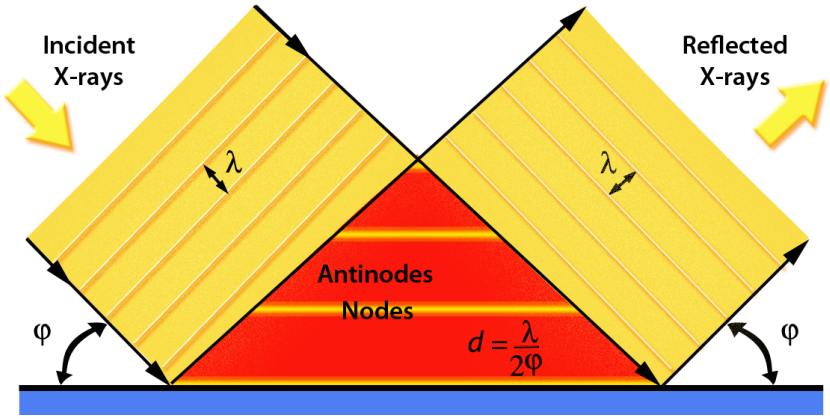

Fig 1.15. Schematic illustration of a standing-wave field above the surface caused by the interference between the incident and the totally reflected X-rays. Adapted from Klockenkämper *et. al.*[163]

The basic design of a TXRF instrument is shown in Fig. 1.16. The primary beam is generated by a fine-focus X ray tube with a fixed anode. It consists of a spiral filament acting as the cathode and a water-cooled block of copper as the anode. The filament is made of tungsten and the copper block is plated with the actual anode material: gold, tungsten, silver, molybdenum, copper, cobalt, iron or chromium.[157] In order to increase certain peaks in relation to the spectral continuum, thin metal foils can be placed in front of the X-ray tube. These foils work as filters and reduce a particular spectral peak or an entire energy band. The beam then passes through a set of aligned slits and is shaped like a strip of paper. Then the polychromatic beam is deflected by a first reflector that alters the primary spectrum. Afterwards, the primary beam hits the sample carrier and the fluorescence intensity of the sample is recorded by an energy-dispersive solid-state detector mounted perpendicularly to the carrier to obtain spectrum with a minimum scattered background. To avoid further the scattering background, the sample is prepared as a thin film on an optically flat quartz sample holder, on which the exciting beam is totally reflected. The distance to the sample can be reduced to less than 3 mm in order to collect a large amount of the fluorescence ration of the sample.[156,157,160,164]

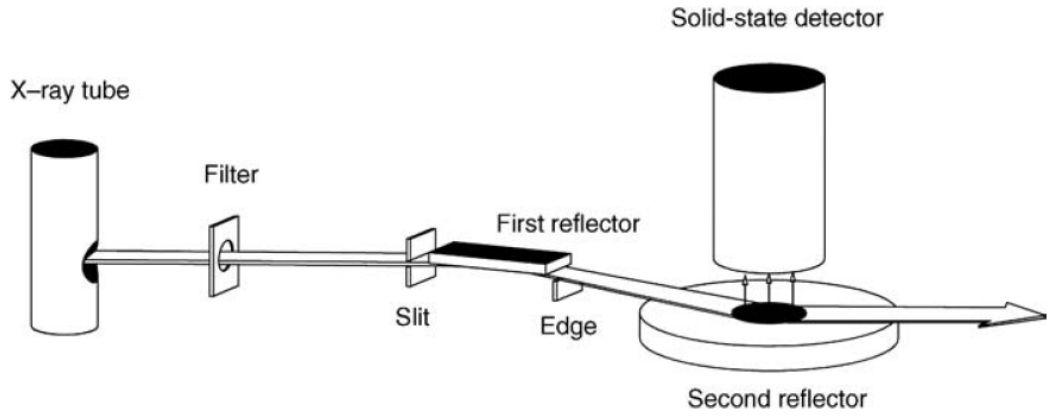

Fig 1.16. Optical pathway in a TXRF equipment.[157]

TXRF can be applied to the analysis of a wide variety of sample materials in environmental, geological, biological, medical, pharmaceutical, industrial and forensic applications. These samples include water, body fluids, oils, greases, soils, minerals, pigments, tissue samples, food and plants. TXRF is a universal an economic method for multi-element analysis, which is suitable for cases in which there is not so much sample available. One of the advantages over methods such as ICP-OES is that the sample preparation is simpler and faster. Compared to ICP-MS the detection of TXRF may be inferior but it is good enough for many applications. A major drawback is that there are restrictions for the measurement of low-Z elements and limitations for the measurement of transition elements and samples with complex matrix content. The parameters affecting the preparation and measurement of the aqueous samples will be discussed in Chapter 6.

1.5 References

1. C. NG, *Nomenclature of inorganic chemistry: IUPAC recommendations 2005. The red book.*, Cambridge, 2005.

2. H. H. Binder, *Lexikon der chemischen Elemente: das Periodensystem in Fakten, Zahlen und Daten*, Hirzel, 1999.

3. USGS, Mineral commodity summaries. Rare Earths., http://minerals.usgs.gov/minerals/pubs/commodity/rare_earths/mcs-2011-raree.pdf, Accessed 02.02.2017.
4. W. D. Jackson, Christiansen, G., International Strategic Minerals Inventory Summary Report—Rare Earth Oxides, U.S. Geological Survey Circular 930-N, U.S.Geological Survey, Map Distribution, https://pubs.usgs.gov/circ/1993/0930n/report.pdf, Accessed 02.02.2017.
5. F. P. Cesbron, in *Lanthanides, Tantalum and Niobium: Mineralogy, Geochemistry, Characteristics of Primary Ore Deposits, Prospecting, Processing and Applications Proceedings of a workshop in Berlin, November 1986*, eds. P. Möller, P. Černý and F. Saupé, Springer Berlin Heidelberg, Berlin, Heidelberg, 1989, pp. 3-26.
6. P. M. J.L. Sabot, *Lanthanides. In Kroschwitz, J.I. and Grant, M.H. (eds.), Kirk-Othmer Encyclopedia of Chemical Technology*, John Wiley, New York, 1995.
7. H. E. Kremers, *Rare earth metals. In Hampel, C.A. (ed.), Rare Metals Handbook*, Krieger Pub Co, New York, 1961.
8. V. Zepf, Rare earth elements a new approach to the nexus of supply, demand and use: exemplified along the use of neodymium in permanent magnets, Springer, Berlin, 2013.
9. P. Strange, A. Svane, W. M. Temmerman, Z. Szotek and H. Winter, *Nature*, 1999, **399**, 756-758.
10. J. H. L. Voncken, in *The Rare Earth Elements: An Introduction*, Springer International Publishing, New York, 2016, pp. 53-72.
11. D. A. Atwood, *The Rare Earth Elements: Fundamentals and Applications*, Wiley, New York, 2013.
12. R. J. Elliott, in *Magnetic Properties of Rare Earth Metals*, ed. R. J. Elliott, Springer US, Boston, 1972, pp. 1-16.
13. P. C. Dent, *J. Appl. Phys.*, 2012, **111**, 07A721.
14. J. D. Livingston, *JOM*, 1990, **42**, 30-34.
15. B. Sprecher, Y. Xiao, A. Walton, J. Speight, R. Harris, R. Kleijn, G. Visser and G. J. Kramer, *Environ. Sci. Technol.*, 2014, **48**, 3951-3958.
16. J. Kooroshy, G. Tiess, A. Tukker and A. Walton, *Strenghthening of the European Rare Earths Supply-chain,*, The european rare earths competency network (ERECON), 2015.
17. W. Mo, L. Zhang, Q. Liu, A. Shan, J. Wu and M. Komuro, *Scr. Mater.*, 2008, **59**, 179-182.

18. K. Binnemans, P. T. Jones, B. Blanpain, T. Van Gerven, Y. Yang, A. Walton and M. Buchert, *J. Clean. Prod.*, 2013, **51**, 1-22.
19. O. Gutfleisch, M. A. Willard, E. Bruck, C. H. Chen, S. G. Sankar and J. P. Liu, *Adv. Mater. (Weinheim, Ger.)*, 2011, **23**, 821-842.
20. T. G. Woodcock, Y. Zhang, G. Hrkac, G. Ciuta, N. M. Dempsey, T. Schrefl, O. Gutfleisch and D. Givord, *Scr. Mater.*, 2012, **67**, 536-541.
21. D. Brown, B.-M. Ma and Z. Chen, *J. Magn. Magn. Mater.*, 2002, **248**, 432-440.
22. C. Fredericci, M. F. de Campos, A. P. V. Braga, D. J. Nazarre, R. V. Martin, F. J. G. Landgraf and E. A. Périgo, *J. Alloys Compd.*, 2014, **615**, 410-414.
23. Q. Zhou, Z. W. Liu, X. C. Zhong and G. Q. Zhang, *Mater. Des.*, 2015, **86**, 114-120.
24. A. A. El-Moneim, A. Gebert, M. Uhlemann, O. Gutfleisch and L. Schultz, *Corros. Sci.*, 2002, **44**, 1857-1874.
25. S. Steyaert, J. M. L. Breton and J. Teillet, *J. Phys. D: Appl. Phys.*, 1998, **31**, 1534.
26. S. Szymura, Y. M. Rabinovich, H. Bala and A. D. Maysterenko, *J. Phys.: Condens. Matter*, 1994, **6**, 3573.
27. Suprapedi, P. Sardjono and Muljadi, *J. Phys. Conf. Ser.*, 2016, **776**, 012015.
28. W. F. Li, H. Sepehri-Amin, T. Ohkubo, N. Hase and K. Hono, *Acta Mater.*, 2011, **59**, 3061-3069.
29. Y. Mishin and C. Herzig, *Materials Science and Engineering: A*, 1999, **260**, 55-71.
30. J. H. L. Voncken, in *The Rare Earth Elements: An Introduction*, Springer International Publishing, New York, 2016, pp. 15-52.
31. C. G. N. Krishnamurthy, in *Extractive Metallurgy of Rare Earths, Second Edition*, CRC Press, New York, 2015, pp. 85-234.
32. J. K.A. Gschneidner, *Material Matters*, 2011, **6**, Article 2.
33. N. Haque, A. Hughes, S. Lim and C. Vernon, *Resources*, 2014, **3**, 614.
34. S. B. Castor, *Can. Mineral.*, 2008, **46**, 779-806.
35. K. R. Long, B. S. Van Gosen, N. K. Foley and D. Cordier, in *Non-Renewable Resource Issues: Geoscientific and Societal Challenges*, eds. R. Sinding-Larsen and F.-W. Wellmer, Springer Netherlands, Dordrecht, 2012, pp. 131-155.
36. D. W. Fuerstenau, *Miner. Metall. Process.*, 2013, **30**, 1-9.

37. Molycorp to Move Its Mountain Pass Rare Earth Facility to 'Care and Maintenance' Mode, http://globenewswire.com/news-release/2015/08/26/763530/0/en/Molycorp-to-Move-Its-Mountain-Pass-Rare-Earth-Facility-to-Care-and-Maintenance-Mode.html, Accessed 02.02, 2017.
38. California's Mountain Pass Mine to be Auctioned in Bankruptcy, https://www.wsj.com/articles/californias-mountain-pass-mine-to-be-auctioned-in-bankruptcy-1485955874, Accessed 02.02, 2017.
39. Y. Kanazawa and M. Kamitani, *J. Alloys Compd.*, 2006, **408–412**, 1339-1343.
40. T. Dutta, K.-H. Kim, M. Uchimiya, E. E. Kwon, B.-H. Jeon, A. Deep and S.-T. Yun, *Environ. Res.*, 2016, **150**, 182-190.
41. X. Li, Z. Chen, Z. Chen and Y. Zhang, *Chemosphere*, 2013, **93**, 1240-1246.
42. X. Wang, Y. Lei, J. Ge and S. Wu, *Resour. Policy*, 2015, **43**, 11-18.
43. S.-L. Tong, W.-Z. Zhu, Z.-H. Gao, Y.-X. Meng, R.-L. Peng and G.-C. Lu, *J. Environ. Sci. Health A.*, 2004, **39**, 2517-2532.
44. D. J. Packey and D. Kingsnorth, *Resour. Policy*, 2016, **48**, 112-116.
45. L. Wang, B. Zhong, T. Liang, B. Xing and Y. Zhu, *Sci. Total Environ.*, 2016, **572**, 1-8.
46. K. Bradsher, Amid tension, China blocks vital exports to Japan, http://www.nytimes.com/2010/09/23/business/global/23rare.html, Accessed 03.02, 2017.
47. G. P. Hatch, *Elements*, 2012, **8**, 341-346.
48. G. Bin, *J. Int'l Econ. L.*, 2011, **14**, 765-805.
49. H.-W. Liu and J. Maughan, *J. Int'l Econ. L.*, 2012, jgs037.
50. WTO, China — Measures Related to the Exportation of Rare Earths, Tungsten and Molybdenum, https://www.wto.org/english/tratop_e/dispu_e/cases_e/ds431_e.htm.
51. E. Barteková and R. Kemp, *Resour. Policy*, 2016, **49**, 153-164.
52. C. Zhanheng, *J. Rare Earth.*, 2011, **29**, 1-6.
53. C. K. Gupta and N. Krishnamurthy, *Int. Mater. Rev.*, 1992, **37**, 197-248.
54. K. Binnemans and P. T. Jones, *J. Sustain. Metall.*, 2015, **1**, 29-38.
55. A. M. Clark, in *Developments in Geochemistry*, ed. P. Henderson, Springer Berlin Heidelberg, Berlin, 1984, vol. 2, pp. 33-61.
56. B. Wei, Y. Li, H. Li, J. Yu, B. Ye and T. Liang, *Ecotoxicol. Environ. Saf.*, 2013, **96**, 118-123.
57. A. Kumari, R. Panda, M. K. Jha, J. R. Kumar and J. Y. Lee, *Miner. Eng.*, 2015, **79**, 102-115.

58. D. Schüler, M. Buchert, R. Liu, S. Dittrich and C. Merz, Study on Rare Earths and Their Recycling, http://resourcefever.eu/publications/reports/Rare%20earths%20study_Oeko-Institut_Jan%202011.pdf, Accessed 05.02, 2017.
59. EREAN, European Rare Earth (Magnet) Recycling Network, http://erean.eu/project.php, Accessed 02.01, 2017.
60. K. Smith Stegen, *Energy Pol.*, 2015, **79**, 1-8.
61. J. D. Widmer, R. Martin and M. Kimiabeigi, *SM&T*, 2015, **3**, 7-13.
62. J.-R. Riba, C. López-Torres, L. Romeral and A. Garcia, *Ren. Sust. Energy Rev.*, 2016, **57**, 367-379.
63. C. C. Pavel, C. Thiel, S. Degreif, D. Blagoeva, M. Buchert, D. Schüler and E. Tzimas, *SM&T*, http://dx.doi.org/10.1016/j.susmat.2017.1001.1003.
64. M. Emslander, Rare Earth Industry Supply: Alternatives, http://www.csus.edu/envs/documents/theses/spring%202014/815.rare%20earth%20industry%20supply%20alternatives.pdf, Accessed 03.02, 2017.
65. Honda, Daido Steel and Honda Adopt World's First Hybrid Vehicle Motor Magnet Free of Heavy Rare Earth Elements, http://world.honda.com/news/2016/4160712eng.html, Accessed 03.02.2017.
66. A. Makino, P. Sharma, K. Sato, A. Takeuchi, Y. Zhang and K. Takenaka, *Sci. Rep.*, 2015, **5**, 16627.
67. B. Balasubramanian, B. Das, R. Skomski, W. Y. Zhang and D. J. Sellmyer, *Adv. Mater. (Weinheim, Ger.)*, 2013, **25**, 6090-6093.
68. D. Li, D. Pan, S. Li and Z. Zhang, *Sci China. Phys Mech Astron*, 2015, **59**, 617501.
69. W.-N. Wang, T. Ogi, Y. Kaihatsu, F. Iskandar and K. Okuyama, *J. Mater. Chem.*, 2011, **21**, 5183-5189.
70. L. K. Bharat, S.-K. Jeon, K. G. Krishna and J. S. Yu, *Sci. Rep.*, 2017, **7**, 42348.
71. R. Boonsin, G. Chadeyron, J.-P. Roblin, D. Boyer and R. Mahiou, *J. Mater. Chem. C.*, 2015, **3**, 9580-9587.
72. Y. Yang, A. Walton, R. Sheridan, K. Güth, R. Gauß, O. Gutfleisch, M. Buchert, B.-M. Steenari, T. Van Gerven, P. T. Jones and K. Binnemans, *J. Sustain. Metall.*, 2017, **3**, 122-149.
73. S. Hoenderdaal, L. Tercero Espinoza, F. Marscheider-Weidemann and W. Graus, *Energy*, 2013, **49**, 344-355.

74. C. S. Shaw S, Permanent magnets: the demand for rare earths. Presentation in: 8th International Rare Earths Conference. 13–15 November 2012, Hong Kong., https://roskill.com/wp/wp-content/uploads/2014/11/download-roskills-paper-on-permanent-magnets-the-demand-for-rare-earths.attachment1.pdf, Accessed 01.02, 2017.
75. A. Elshkaki and T. E. Graedel, *Appl. Energy*, 2014, **136**, 548-559.
76. K. Binnemans, P. T. Jones, K. Van Acker, B. Blanpain, B. Mishra and D. Apelian, *JOM*, 2013, **65**, 846-848.
77. J. Navarro and F. Zhao, *Front. Energy Res.*, 2014, **2**.
78. H. Jin, P. Afiuny, T. McIntyre, Y. Yih and J. W. Sutherland, *Procedia CIRP*, 2016, **48**, 45-50.
79. M. Zakotnik, E. Devlin, I. R. Harris and A. J. Williams, *J. Iron Steel Res. Int.*, 2006, **13**, 289-295.
80. R. Schulze and M. Buchert, *Resour. Conserv. Recy.*, 2016, **113**, 12-27.
81. G. Xu, J. Yano and S.-i. Sakai, *J. Mater. Cycles. Waste*, 2016, **18**, 469-482.
82. P. Chancerel, V. S. Rotter, M. Ueberschaar, M. Marwede, N. F. Nissen and K.-D. Lang, *Waste Manag. Res.*, 2013, **31**, 3-16.
83. Y. Seo and S. Morimoto, *Resour. Policy*, 2014, **39**, 15-20.
84. D. Dupont and K. Binnemans, *Green Chem.*, 2015, **17**, 856-868.
85. Y. Wu, X. Yin, Q. Zhang, W. Wang and X. Mu, *Resour. Conserv. Recy.*, 2014, **88**, 21-31.
86. M. Tanaka, T. Oki, K. Koyama, H. Narita and T. Oishi, *Recycling of rare earths from scrap*, Elsevier, Amsterdam 2012.
87. K. Baba, Y. Hiroshige and T. Nemoto, Rare-earth Magnet Recycling, http://www.hitachi.com/rev/pdf/2013/r2013_08_105.pdf, Accessed 10.02, 2017.
88. H. M. Bandara, J. W. Darcy, D. Apelian and M. H. Emmert, *Environ. Sci. Technol.*, 2014, **48**, 6553-6560.
89. K. Habib, K. Parajuly and H. Wenzel, *Environ. Sci. Technol.*, 2015, **49**, 12441-12449.
90. A. Walton, H. Yi, N. A. Rowson, J. D. Speight, V. S. J. Mann, R. S. Sheridan, A. Bradshaw, I. R. Harris and A. J. Williams, *J. Clean. Prod.*, 2015, **104**, 236-241.
91. M. Zakotnik, I. R. Harris and A. J. Williams, *J. Alloys Compd.*, 2009, **469**, 314-321.
92. R. S. Sheridan, A. J. Williams, I. R. Harris and A. Walton, *J. Magn. Magn. Mater.*, 2014, **350**, 114-118.
93. M. Zakotnik, I. R. Harris and A. J. Williams, *J. Alloys Compd.*, 2008, **450**, 525-531.

94. X. Li, M. Yue, M. Zakotnik, W. Liu, D. Zhang and T. Zuo, *J. Rare Earth.*, 2015, **33**, 736-739.
95. M. Itoh, M. Masuda, S. Suzuki and K.-i. Machida, *J. Alloys Compd.*, 2004, **374**, 393-396.
96. M. Ueberschaar and V. S. Rotter, *J. Mater. Cycles. Waste*, 2015, **17**, 266-281.
97. E. G. Polyakov and A. S. Sibilev, *Metallurgist*, 2015, **59**, 368-373.
98. N. K. Batchu, T. Vander Hoogerstraete, D. Banerjee and K. Binnemans, *Sep. Purif. Technol.*, 2017, **174**, 544-553.
99. C. K. Gupta and T. K. Mukherjee, *Hydrometallurgy in Extraction Processes*, CRC Press, New York, 1990.
100. K. A. Gschneidner, J. C. G. Bünzli and V. K. Pecharsky, *Handbook on the Physics and Chemistry of Rare Earths*, Elsevier, Amsterdam, 2006.
101. T. Vander Hoogerstraete, B. Blanpain, T. Van Gerven and K. Binnemans, *RSC Adv.*, 2014, **4**, 64099-64111.
102. M. A. R. Önal, E. Aktan, C. R. Borra, B. Blanpain, T. Van Gerven and M. Guo, *Hydrometallurgy*, 2017, **167**, 115-123.
103. Y. Ho-Sung, K. Chul-Joo and K. Joon-Soo, *J. Korean Inst. Met. Mater.*, 2004, **13**, 43-48.
104. M. A. R. Önal, C. R. Borra, M. Guo, B. Blanpain and T. Gerven, *J. Sustain. Metall.*, 2015, **1**, 199-215.
105. V. S. Kislik, in *Solvent Extraction*, Elsevier, Amsterdam, 2012, ch. 1, pp. 3-67.
106. F. Xie, T. A. Zhang, D. Dreisinger and F. Doyle, *Miner. Eng.*, 2014, **56**, 10-28.
107. N. Rice, H. Irving and M. Leonard, *Pure Appl. Chem.*, 1993, **65**, 2373-2396.
108. V. S. Kislik, in *Solvent Extraction*, Elsevier, Amsterdam, 2012, ch. 3, pp. 113-156.
109. A. M. Wilson, P. J. Bailey, P. A. Tasker, J. R. Turkington, R. A. Grant and J. B. Love, *Chem. Soc. Rev.*, 2014, **43**, 123-134.
110. M. Laing, in *Coordination Chemistry*, American Chemical Society, Washington, 1994, vol. 565, ch. 31, pp. 382-394.
111. M. K. Jha, A. Kumari, R. Panda, J. Rajesh Kumar, K. Yoo and J. Y. Lee, *Hydrometallurgy*, 2016, **165, Part 1**, 2-26.
112. J. Rydberg, *Solvent Extraction Principles and Practice, Revised and Expanded*, CRC Press, New York, 2004.
113. E. V. Yurtov and N. M. Murashova, *Theor. Found Chem. En.*, 2007, **41**, 737-742.

114. M. Nascimento, B. M. Valverde, F. A. Ferreira, R. d. C. Gomes and P. S. M. Soares, *Rem: Int. Eng. J.*, 2015, **68**, 427-434.
115. T. Sato, *Hydrometallurgy*, 1989, **22**, 121-140.
116. W. Su, J. Chen and Y. Jing, *Ind. Eng. Chem. Res.*, 2016, **55**, 8424-8431.
117. R. Kopunec and J. C. Benitez, *J. Radioanal. Nucl. Chem.*, 1991, **150**, 269-280.
118. B. Gupta, P. Malik and A. Deep, *Solvent Extr. Ion Exc.*, 2003, **21**, 239-258.
119. Y. A. El-Nadi, N. E. El-Hefny and J. A. Daoud, *Solvent Extr. Ion Exc.*, 2007, **25**, 225-240.
120. N. Panda, N. Devi and S. Mishra, *J. Rare Earth.*, 2012, **30**, 794-797.
121. J. N. Chubb, P. Lagos and J. Lienlaf, *J Electrostat.*, 2005, **63**, 119-127.
122. M. L. Dietz, *Sep. Sci. Technol.*, 2006, **41**, 2047-2063.
123. A. P. De Los Rios and F. J. H. Fernandez, *Ionic Liquids in Separation Technology*, Elsevier Amsterdam, 2014.
124. Y. Liu, J. Chen and D. Li, *Sep. Sci. Technol.*, 2012, **47**, 223-232.
125. K. Nakashima, F. Kubota, T. Maruyama and M. Goto, *Anal. Sci.*, 2003, **19**, 1097-1098.
126. Y. Baba, F. Kubota, N. Kamiya and M. Goto, *J. Chem. Eng. Jpn.*, 2011, **44**, 679-685.
127. K. Shimojo, H. Naganawa, J. Noro, F. Kubota and M. Goto, *Anal. Sci.*, 2007, **23**, 1427-1430.
128. K. Sarangi, E. Padhan, P. V. R. B. Sarma, K. H. Park and R. P. Das, *Hydrometallurgy*, 2006, **84**, 125-129.
129. T. Vander Hoogerstraete, S. Wellens, K. Verachtert and K. Binnemans, *Green Chem.*, 2013, **15**, 919-927.
130. T. Vander Hoogerstraete and K. Binnemans, *Green Chem.*, 2014, **16**, 1594-1606.
131. D. Dupont and K. Binnemans, *Green Chem.*, 2015, **17**, 2150-2163.
132. K. Larsson and K. Binnemans, *Hydrometallurgy*, 2015, **156**, 206-214.
133. D. Dupont, D. Depuydt and K. Binnemans, *J. Phys. Chem. B*, 2015, **119**, 6747-6757.
134. C. Hanson, in *Hydrometallurgical Process Fundamentals*, ed. R. G. Bautista, Springer, Boston, 1984, pp. 499-514.
135. J. Zhang, B. Zhao and B. Schreiner, in *Separation Hydrometallurgy of Rare Earth Elements*, Springer International Publishing, Cham, 2016, pp. 243-259.
136. R. Robatel, Mixer settlers, http://www.rousselet-robatel.com/chemical-fine-chemical-pharmaceutical/laboratory-mixer-settlers/, Accessed 15.02, 2017.

137. D. Malhotra, P. Taylor, M. LeVier and E. Spiller, *Recent Advances in Mineral Processing Plant Design*, Society for Mining, Metallurgy, & Exploration, 2009.
138. J. T. Sommerfeld, *AIChE J.*, 1977, **23**, 406-406.
139. C. K. Gupta, *Chemical Metallurgy: Principles and Practice*, Wiley, New York, 2006.
140. S. Radhika, B. Nagaphani Kumar, M. Lakshmi Kantam and B. Ramachandra Reddy, *Hydrometallurgy*, 2011, **110**, 50-55.
141. C. Group, *MCT Redbook: Solvent Extraction Reagents and Applications*, 2007.
142. 911Metallurgist, Solvent Extraction Plants: Thiele Diagram & Theoretical Design Aspects, https://www.911metallurgist.com/solvent-extraction-plant-design/, Accessed 25.04, 2017.
143. E. Barnea, *Hydrometallurgy*, 1980, **5**, 127-147.
144. E. Barnea, *Hydrometallurgy*, 1979, **5**, 15-28.
145. G. Kyuchoukov and R. Kounev, *Chem. Eng. J.*, 1998, **69**, 63-67.
146. F. S. Gharehbagh and S. M. A. Mousavian, *J. Taiwan Inst. Chem. Eng.*, 2009, **40**, 302-312.
147. J. Wichterlová and V. Rod, *Chem. Eng. Sci.*, 1999, **54**, 4041-4051.
148. L. Lu, B. Zhao, P. Lin and J. Zhang, *Separ. Technol.*, 1992, **2**, 136-140.
149. M. Kumar, *Analyst*, 1994, **119**, 2013-2024.
150. D. S. Braverman, *J. Anal. At. Spectrom.*, 1992, **7**, 43-46.
151. T. Honda, T. Oi, T. Ossaka, T. Nozaki and H. Kakihana, *J. Radioanal. Nucl. Chem.*, 1989, **133**, 301-315.
152. V. Balaram, *Trends Anal. Chem.*, 1996, **15**, 475-486.
153. T. P. Rao and V. M. Biju, *Crit. Rev. Anal. Chem.*, 2000, **30**, 179-220.
154. B. Zawisza, K. Pytlakowska, B. Feist, M. Polowniak, A. Kita and R. Sitko, *J. Anal. At. Spectrom.*, 2011, **26**, 2373-2390.
155. T. Horiuchi and Y. Yoneda, *Rev. Sci. Instrum*, 1971, **42**, 1069-1070.
156. H. Aiginger, *Spectrochim. Acta B*, 1991, **46**, 1313-1321.
157. R. Klockenkämper and A. Von Bohlen, *Total-Reflection X-Ray Fluorescence Analysis and Related Methods*, John Wiley & Sons, New Jersey, 2015.
158. T. R. Dulski, *Trace Elemental Analysis of Metals: Methods and Techniques*, CRC Press, Amsterdam, 1999.
159. Exploration Technique: Hand-held X-Ray Fluorescence (XRF), http://en.openei.org/wiki/Hand-held_X-Ray_Fluorescence_(XRF), Accessed 25.02, 2017.

160. N. V. Alov, *Inorganic Materials*, 2011, **47**, 1487-1499.

161. P. Wobrauschek, *X-Ray Spectrom.*, 2007, **36**, 289-300.

162. D. K. G. de Boer, *Spectrochim. Acta B*, 1991, **46**, 1433-1436.

163. R. Klockenkamper, J. Knoth, A. Prange and H. Schwenke, *Anal. Chem.*, 1992, **64**, 1115A-1123A.

164. A. Knöchel, *Fresenius. J. Anal. Chem.*, 1990, **337**, 614-621.

Chapter 2. Objectives

In the previous chapter, TXRF was highlighted as a potential tool for the rapid and reliable quantification of rare earths in both aqueous phases. The objective is to develop guidelines for the correct measurement of metal ions in aqueous solutions and contribute to the understanding of the parameters that can affect the accuracy and precision of the measurement.

In chapter 1 it was emphasized the necessity of recycling of end-of-life NdFeB permanent magnets. The separation of rare earths into individual elements is of importance because it gives more flexibility to the fabricants in case they want to produce recycled NdFeB permanent magnets with different properties for diverse applications.

The main objective of this work is to develop environmentally friendly and innovative solvent extraction processes for the recovery of individual rare earths and other valuable metals such as cobalt using ionic liquid technology. The separation of rare earths has been always considered a challenge. The first goal is to separate the main components of a typical NdFeB magnet (Fe, Co, Nd and Dy) through a process combining selective leaching and solvent extraction based on an easily available ionic liquid. The objective is to study and optimize the different variables that can affect the separation of rare earths from transition metals and the rare earths into individual elements and find ways to recycle the ionic liquid. Solvent extraction processes involving ionic liquids at room temperature and highly concentrated feeds are usually facing issues with the high viscosity of ionic liquids. Therefore, another objective of this work is to find a way to lower the viscosity of the ionic liquid phase without sacrificing its efficiency as an extractant.

The development of new systems that can be scaled up for the separation of rare earths is also a challenge. A process based on the extraction of rare earths from deep-eutectic solvents using an ionic liquid and typical extractants diluted in toluene is designed. One of the aims is to test the feasibility of carrying out this process at larger scale using a set-up of small mixer settlers.

Chapter 3. Practical guidelines for best practice on total reflection X-ray fluorescence spectroscopy: analysis of aqueous solutions

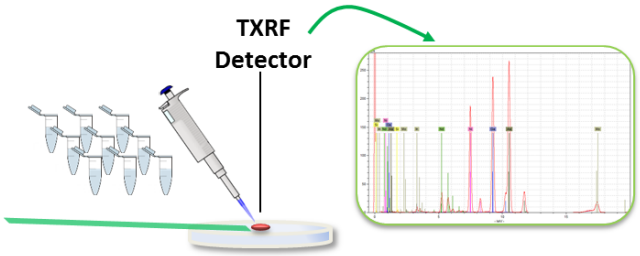

Simple guidelines for the correct preparation of liquid samples for TXRF

ABSTRACT-Despite the fact that Total Reflection X-ray fluorescence (TXRF) is becoming more and more popular as a quantification technique in analytical chemistry due to its simplicity and robustness, there are still some key aspects related to the sample preparation that need to be improved. In this work, the effect of different parameters is investigated: measurement time, carrier position, sample volume and sample drying time. The measurement time and the sample volume on the carriers mainly affect the recovery rate (RR) and relative standard deviation (RSD) of the quantified metal from aqueous solutions. The most important parameters that play a fundamental role in the calibration of a TXRF machine such as choice of the standard element and concentration ratio between the analyte and the standard are discussed. Practical and easy guidelines for the correct preparation of aqueous samples are presented. These can be used by both less and more experienced TXRF users, interested in measuring metal ion concentrations in aqueous samples.

Based on the published paper
Sofía Riaño, Mercedes Regadío, Koen Binnemans and Tom Vander Hoogerstraete
"Practical guidelines for best practice on total reflection X-ray fluorescence spectroscopy: analysis of aqueous solutions".
Spectrochimica Acta Part B: Atomic Spectroscopy, 2016, 124, 109-115.

Author contributions
S.R. performed the experimental work treated the data and wrote the article.

3.1 Introduction

Total Reflection X-ray Fluorescence (TXRF) is an often used analytical technique for metal quantification in liquids, solids, wafers and biological samples.[1-14] Despite being amply referenced for the analysis of wafers, only recently benchtop TXRF spectrometers became commercially available and more competitive with techniques such as inductively coupled plasma optical emission spectroscopy (ICP-OES), inductively coupled plasma optical mass spectrometry (ICP-MS) or atomic absorption spectroscopy (AAS).[15-20] This technique is very similar to Energy Dispersive X-ray Fluorescence (EDXRF).[7,21] However, the relative position of the incident beam to the sample carrier is significantly different. In TXRF, the sample carrier is inclined under an angle of 0.1° with respect to the direction of the incident X-ray beam. This results in the total reflection of the X-ray beam on the surface of the sample carrier.[21,22] This total reflection of the X-ray beam has three main advantages: (1) the background signal is significantly reduced as almost no X-rays are penetrating into and exciting the sample carrier. The set-up geometry reduces the background and the detection limit by a factor of at least 10^3 depending on the element in comparison with EDXRF setups; (2) The sample on the carrier is excited by both the incident and the reflected beam, which results in an increased excitation probability of the sample elements, and (3) the carrier is placed very close to the detector (≈ 0.5 mm) which makes it able to collect a large amount of the fluorescence radiation of the sample.[7] In this way, the signal-to-noise ratio is low and concentrations into the ppb range can be measured.

The TXRF technique has several advantages over atomic absorption spectroscopy (AAS), instrumental neutron activation analysis (INAA) and techniques based on inductive coupled plasma (ICP-MS, ICP-OES). In TXRF, only a small amount of sample and chemicals are required for sample analysis, the sample preparation procedure is faster and the cost related to the measurements is much lower. Furthermore, different metals can be quantified in one single measurement and calibration curves are not compulsory for each measurement because element quantification can be performed by using an internal standard.[7,23-25]

Despite its advantages, TXRF is not commonly used yet as a replacement for ICP methods or AAS.[26] This is probably due to its more recent development,[27,28] the lack of standardization procedures (*i.e.* standardization by ISO, ASTM, or DIN has just started being developed),[23,29-31] and the influence of the sample preparation procedure on the accuracy and precision of the

data.[4,32,33] In other techniques, the way and position in which the sample is entering the measurement unit is fixed and automated. In the case of TXRF measurements, the operator influences more directly the size, morphology and thickness of the sample and its position relative to the detector and the X-ray beam, aspects which can significantly influence the results.

Although several reviews, books and articles about TXRF have been published,[6,21-23,26-28,33-37] there is a lack of fundamental, simple guidelines and standard procedures for new TXRF users who would like to apply the TXRF technique for measuring on liquid samples.[7,21,27] To date, our lab is using on a routine basis three TXRF machines (Picofox S2, Bruker) to quantify elemental concentration in up to 500 liquid samples every week. In this paper, a series of experiments are reported indicating that the sample preparation procedure is a key aspect on TXRF analysis. This chapter does not focus on the technique itself, but on the practical side of performing TXRF measurements. The following questions are considered: (1) What is the influence of measuring time, sample position and the hard and software on the measurements? (2) How can highly reproducible data be obtained and what can be considered as the best sample preparation procedure? (3) How should the calibration of the machine be performed and when is it needed to be careful while processing results based on internal calibration? (4) How to clean sample carriers and what kind of impurities can be expected even after a proper cleaning procedure?

3.2 Experimental

3.2.1 Materials and methods

The 1000 ± 10 mg L^{-1} praseodymium, neodymium and gallium (Pr, Nd and Ga) standards solutions were all obtained from Merck (Overijse, Belgium). A silicone solution in isopropanol was obtained from SERVA Electrophoresis GmbH (Heidelberg, Germany). All TXRF measurements were performed with a benchtop total reflection X-ray fluorescence (TXRF) spectrometer (Picofox S2, Bruker) operating with a molybdenum X-ray source at 50 kV. Reusable quartz sample carriers (4 × 30 mm) were employed for all measurements. The optimized sample preparation was the following: Firstly, the sample carriers were pretreated with 30 µL of silicone in isopropanol at room temperature and dried for 20 min in a hot air oven at 60 °C. This procedure was followed to make the surface hydrophobic and avoid spreading of the

aqueous sample on the carrier. Secondly, 5 µL of the sample was added onto the carrier at room temperature and dried at 60 °C in a hot air oven for 30 min. The gain correction was performed before each series of measurements. Samples were measured for 200 s unless reported otherwise. All volumes were controlled gravimetrically by weighing. Spectra were analyzed with the Bruker Spectra Picofox V 7.5.3.0 software. Corrections were made for the escape peak, for pile ups and the background was corrected by a maximum of 1000 stripping cycles with a step width of 50. Samples were diluted with MilliQ water. Two identical TXRF machines (referred to in this study as TXRF1 and TXRF2) were tested to exclude effects specific to one of the machines and to validate, when necessary, the general conclusions for this type of machines.

The influence of the measuring time was studied by pipetting 5 µL of a solution containing 100 mg L^{-1} Ga and 100 mg L^{-1} of Nd on a sample carrier. The carrier was measured for different times, without any other manipulation, and the relative standard deviation (RSD) was calculated based on three measurements at the specific time interval. This experiment was performed once on TXRF1 and twice on TXRF2.

The position of the sample carrier with respect to the X-ray beam was studied by pipetting 5 µL of a solution containing 100 mg L^{-1} Ga and 100 mg L^{-1} Nd onto six different carriers. Each sample was measured six times for 200 s without removing it from the measurement position and another six times with removal from the machine in between measurements. In another experiment, three sample carriers prepared with 5 µL of the former solution were measured under different positions relative to the X-ray beam. After each measurement of 200 s, the three different samples were rotated 60° and re-measured.

The influence of the drying time of the silicone in isopropanol, added on the sample carrier before addition of the sample, was studied by adding 30 µL of this solution on the sample carriers and drying it for different times at room temperature. After the specific drying time, 3 µL of a solution containing 100 mg L^{-1} Ga and 100 mg L^{-1} Nd was added onto the carrier and dried for 30 min in an oven at 60 °C. For the optimization of the sample amount, the sample carriers were pretreated with 30 µL of silicone solution and dried for 20 min in the oven at 60 °C. Afterwards, they were cooled to room temperature, and 1, 3 or 5 µL of a solution containing 100 mg L^{-1} Ga and 100 mg L^{-1} Nd was added, the carriers were dried for 20 min at 60 °C in a hot air oven. Nine series of ten measurements were performed. The influence of the sample drying time was studied

on three different carriers containing a sample of 100 mg L^{-1} Ga and 100 mg L^{-1} Nd, the carriers were pretreated using the optimized procedure. The three samples were first measured when it was observed that all the water was evaporated from the sample. Afterwards, the sample was dried again for 5, 10, 15, 30, 45 and 60 min and measured immediately after each drying period. The RSD values at t_n are calculated based on the concentration values found in t_{n-1}, t_n and t_{n+1}.

The optimized sample procedure was tested by three different operators on six different days. The average count ratio of all measurements between Ga and Nd was used as the calibration factor. The non-linearity of the calibration factor was studied by preparing 12 different solutions containing all 100 mg L^{-1} Ga and different concentrations of Pr ranging between 1 and 900 mg L^{-1}. The sample carriers were pretreated as described above, and measured for 300 s. The 12 solutions were diluted a 10 fold and measured again for 3000 s to study the influence of possible matrix effects.

3.2.2 Formulas

The relative standard deviation (*RSD*) was calculated based on the following equation:

$$RSD\ (\%) = \frac{\sqrt{\frac{\sum_{i=1}^{N}(x_i-\bar{x})^2}{N-1}}}{\bar{x}} \times 100 \qquad (3.1)$$

Where $\bar{x}$ is the average concentration, x_i the calculated concentration for measurement i and N the number of measurements.

The recovery rate (*RR*) is defined as:

$$RR\ (\%) = \frac{Measured\ concentration}{Expected\ concentration} \times 100 \qquad (3.2)$$

3.3 Results and discussion

3.3.1 Parameter studies and optimization

All experiments were performed with Ga and the lanthanides Pr and Nd. Ga is often used as an internal standard in TXRF measurements because it is rarely found in aqueous samples. Lanthanides were chosen over more conventional and typically analyzed first row transition metals because the latter ones can be found in natural waters (Fe, Cu, Zn) or are sometimes difficult to remove from the sample carriers during the cleaning procedure (Fe, Zn). Both situations can influence the measurements, especially when working at low concentrations.

The measurement time has a relevant influence on the RSDs of the TXRF measurements (Fig. 3.1). A 5 µL sample of 100 mg L^{-1} Ga and 100 mg L^{-1} Nd was measured during different times. The RSD was calculated based on three measurements at each measurement time. All measuring times longer than 15 s gave RSDs smaller than 1%. All proceeding measurements were therefore performed for 200 s or longer in order to minimize the influence of the measuring time on the relative standard deviations. Note that the RSD values are directly depending on the number of counts rather than the measuring time. However, the use of counts rather than time is rarely done for TXRF machines requiring high sample throughput because of the uncertainty in effective measuring time and sample throughput.

After each measurement, the sample is removed mechanically from the measuring position by an automated gripper that rolls the sample carrier back into the sample holder. The relative position of the sample to the detector was therefore slightly different when the gripper placed the carrier back into the measuring position. Such rotation did not occur in the previously performed measurements. Therefore, the influence of such a rotation on the measurement was evaluated as described in the experimental section. The difference in RSD between removing and not removing the sample from the measurement position is very small (Table 3.1). Moreover, the RSD values are in the range found for the time experiments.

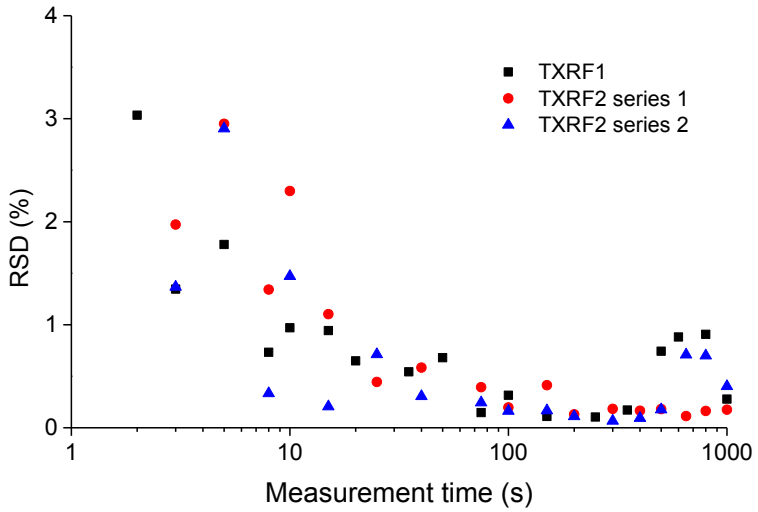

Fig. 3.1. Influence of the measurement time on the relative standard deviation (RSD) of the Nd concentration. (■): Experiments performed on TXRF1, (●) and (▲): experiments performed on TXRF2 in two different days. The RSD values are calculated based on a triplicate. 5 µL of a solution containing 100 mg L^{-1} Ga and 100 mg L^{-1} Nd standard was sampled on a TXRF carrier giving an average count rate of 8500 counts per second.

Table 3.1. Relative standard deviation (RSD) made on the measurement of six sample carriers sampled with 5 µL of 100 mg L^{-1} Ga and 100 mg L^{-1} of Nd that were measured with and without removal from the measurement position (position change).

Carrier	Without position change RSD (%)	With position change RSD (%)
1	0.20	0.65
2	0.22	0.25
3	0.16	0.39
4	0.79	0.15
5	0.13	0.08
6	0.18	0.24
AVERAGE	0.28	0.29

The next investigated parameter was the position of the sample carrier chosen by the operator. There are an infinite number of possible positions in which the sample carrier can be placed in the measuring position. The orientation of the sample relative to the ingoing and outgoing beam could also influence the results. Following the standard procedure, 5 µL of a solution containing 100 mg L^{-1} Ga and 100 mg L^{-1} Nd was disposed on a quartz sample carrier and measured for 200 s. After the measurement, the sample was rotated in the sample holder by 60°. This procedure was done in triplicate and repeated six times until the three carriers were back in their initial position. The RSDs on these measurements were 0.27, 0.30 and 0.52%. These values are slightly higher than the average RSD values reported in Table 3.1. However, it can be seen in Fig. 3.1 that such RSD values can be expected even without changing the position of the sample. Therefore, random errors introduced by the sample position are negligible in comparison with the effect of the measuring time.

Pipettes may cause random errors during the sample preparation procedure as well, but such errors are often smaller than 0.6%. Systematic errors are avoided by using the same pipette and an internal standard. It is important to mention that errors made by pipetting were avoided in this work by performing most of the experiments from one single mixed metal ion stock solution and by controlling and correcting the volumes gravimetrically. Next, the sample preparation method was optimized in which (1) the amount, drying time and temperature of silicone in isopropanol were studied as well as (2) the amount, drying time and temperature of the sample on the siliconized carrier. In contrast to poly(methyl methacrylate) (PMMA), quartz glass is not hydrophobic, but can be made hydrophobic by treating it with a silicone solution. From experience, we know that the volume of silicone in isopropanol solution, covering the whole TXRF carrier needs to be at least 30 µL at room temperature. Addition of the silicone solution to a carrier at higher temperature results often in migration of the solution to one side of the carrier and an inhomogeneous spreading of the silicone solution over the carrier. This can cause a movement of the sample droplet over the carrier resulting in significant errors in the measurement.[38]

Volumes smaller than 30 µL but at room temperature are also spread out inhomogeneously over the carrier, especially in the case of older sample carriers, which could have some scratches on their surface. The drying time of the silicone solution in isopropanol at 60 °C was varied between

30 and 240 min. Each data point represents the RSD on 10 sample carriers prepared at different moments with 3 µL of a solution containing 100 mg L^{-1} Ga and 100 mg L^{-1} Nd (Fig. 3.2). There is a slight decrease in the RSDs when the silicone solution in isopropanol was dried for a longer time, however, all RSDs remained below 2% and therefore, the drying time of the silicone in isopropanol at 60 °C does not have a significant effect on the reproducibility and accuracy of the measurements.

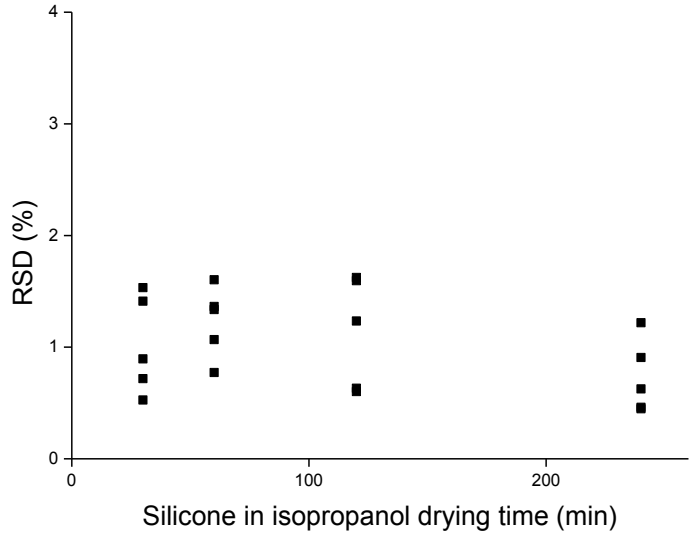

Fig. 3.2. Relative standard deviation (RSD) on the measurement of 10 sample carriers containing 3 µL of a solution with 100 mg L^{-1} Ga and 100 mg L^{-1} Nd as function of the drying time of silicone in isopropanol. Drying at 60 °C with a measurement time of 333 s.

Next, the amount of sample on the sample carrier was investigated. An aliquot of 1, 3 or 5 µL of a solution containing 100 mg L^{-1} Ga and 100 mg L^{-1} Nd was added on a carrier pretreated with silicone in isopropanol. Three series of 10 samples carriers with 1, 3 or 5 µL of sample were prepared at different moments. To keep the number of counts approximately constant, the measurement time was increased when decreasing the sample volume, thus, sample volumes of 1 µL were measured during 1000 s, sample volumes of 3 µL during 333 s and sample volumes of 5 µL during 200 s. As it can be seen in Fig. 3.3, there is a general trend of decreasing RSD values while decreasing the amount of sample. At lower volumes the droplet has less chance to move on the carrier and it remains in the center.

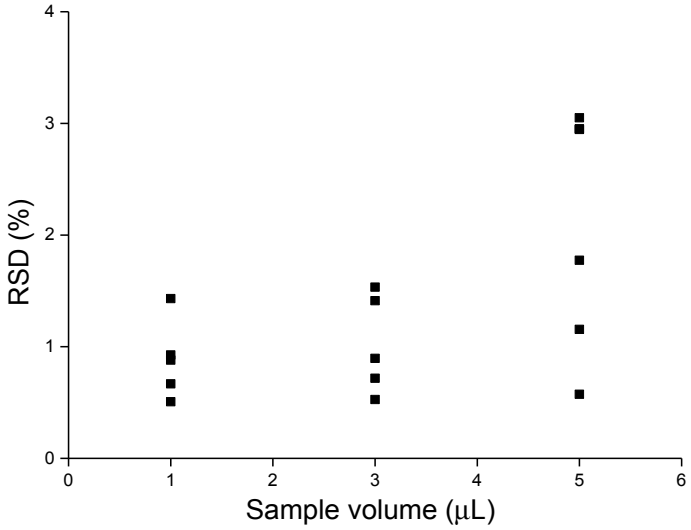

Fig. 3.3. Influence of the sample volume pipetted on the carrier on the RSD values for the recovery of Nd. 5 times 10 sample carriers sampled with different volumes of a solution containing 100 mg L^{-1} Ga and 100 mg L^{-1} Nd were measured at each volume.

The drying time of the sample was studied as well. Therefore, a triplicate of sample carriers containing 5 µL of a solution with 100 mg L^{-1} Ga and 100 mg L^{-1} Nd was prepared. The samples were measured when it was seen that all water had been removed from the sample by drying it in the oven (t = 0 min). After the measurement, the sample was placed again into the oven for a specific time interval and measured again. This sequence was followed after 5, 10, 15, 30, 45, 60 and 960 min. It was shown before that the effect of the software, counting statistic and the sample position gave RSD values around 0.3% (Table 3.1, Fig. 3.1 and the discussions). The RSD values given in Fig. 3.4 at time t_n are calculated based on the concentration values found in t_{n-1}, t_n and t_{n+1}. RSD values are in most cases significantly higher. This is probably more an effect of re-drying rather than an effect of drying time. After each drying procedure at 60 °C, the dried sample is cooled down to room temperature. As most samples contain mainly hygroscopic salts, they can take up water from the air and even become (partly) liquid. A re-drying process can cause recrystallization processes which mainly occur at places already enriched in this specific element, causing a non-uniformity across the sample affecting the accuracy of a quantitative analysis. The evaporation behavior of different kinds of droplets and studies on their morphology and homogeneity once dried have been studied and reported elsewhere.[7,39-41] In TXRF, the superposition or interference between the incoming and reflected beams at small grazing

incidence angles can cause X-ray standing waves above and below the substrates. The effect of these standing waves is usually not taken into account since two assumptions are made: first, the lateral inhomogeneity of the X-ray standing wave field is averaged in the measured signal and second, that both sample and standard are homogeneously distributed.[42-44] However, if irregular aggregates of analyte or standard are present at different points of the sample, the interference between the incoming and reflected waves cannot occur, destroying the X-ray wave field and therefore, affecting the intensity of the detected fluorescence.[42,45] Other possibilities could be the loss of material during sample preparation (although significant decreases in count rates are not observed) or decreased matrix effects by further reducing the amount of (crystal) water when drying for longer period. Even significant higher RSD values and recovery rates are observed when drying the silicone solution in isopropanol at 60 °C for only 2 min and obtaining a sample residue covering a larger surface area on the carrier.

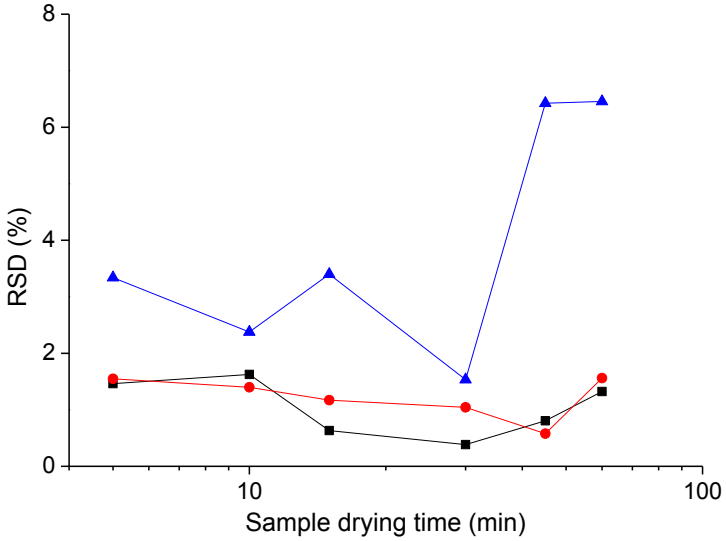

Fig. 3.4. Influence of the sample drying time on the RSD values of 3 samples containing 100 mg L^{-1} Ga and 100 mg L^{-1} Nd. The RSD values shown at time t_n are calculated based on the concentration values found in t_{n-1}, t_n and t_{n+1}. Note that the X-axis is plotted on a logarithmic scale.

The most important parameters influencing the standard deviations on TXRF measurements were investigated for samples containing 100 mg L^{-1} Ga and 100 mg L^{-1} Nd. The next step was to test if other operators could find the same results (%RR and RSD) when following the same

procedure. Table 3.2 gives an overview of six series of 10 measurements performed on different days and by different operators. The results show a very high accuracy and reproducibility of all measurements.

Table 3.2. Recovery rates and RSD values on 6 series of 10 measurements with 1 μL solution containing 100 mg L^{-1} Ga and 100 mg L^{-1} Nd measured by three different operators at six different days.

Day	Operator	RR (%)	RSD (%)
1	A	101.8	1.4
2	A	102.2	0.7
3	B	101.2	0.8
4	B	101.4	1.4
5	C	99.9	1.3
6	C	101.5	1.14

3.3.2 Calibration curves

So far, only solutions having equal Nd and Ga mass concentrations (100 mg L^{-1}) have been measured. Such conditions are rarely faced when measuring real samples with elements present in unknown concentrations. A straightforward and correct calibration method for TXRF measurements with an internal standard is of high importance. Ideally, the calibration is valid for a wide range of concentrations relative to the internal standard that is used. The calibration factor gives the ratio of the detected X-ray fluorescence intensity from an internal standard element relative to the element of interest at equal concentrations. In order to check the linearity of this calibration factor, a series of 12 calibration solutions containing 100 mg L^{-1} Ga and different amounts of Pr ranging from 1 to 900 mg L^{-1} were prepared (Fig. 3.5). All data were normalized to the recovery rate found for 100 mg L^{-1} Ga and 100 mg L^{-1} Pr.

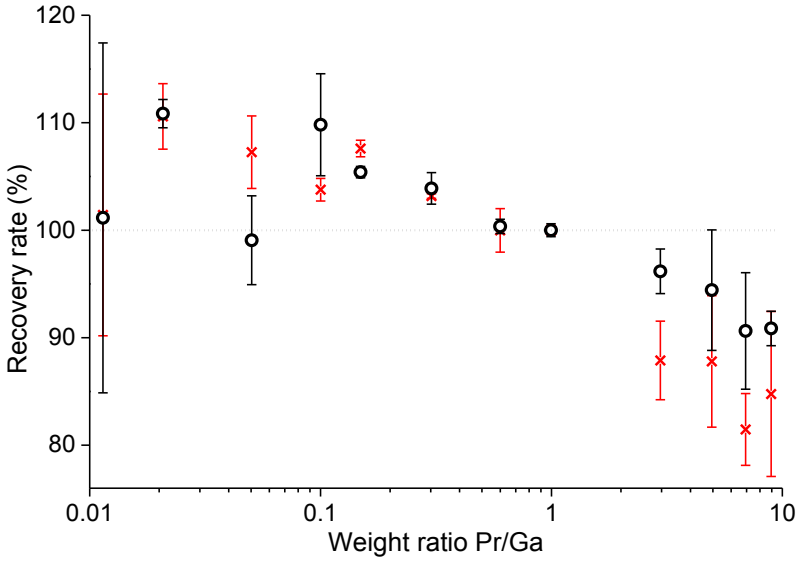

Fig. 3.5. Pr recovery rate (%) as function of the mass ratio Pr/Ga in the solution. Red = 100 mg L^{-1} Ga, Black = the red solutions 10 times diluted (10 mg L^{-1} Ga). Each data point was measured in triplicate. Note that the X-axis is plotted on a logarithmic scale. Error bars represent the standard deviation.

In Fig. 3.5, the red dots represent the results obtained with the more concentrated solutions. There is a Pr concentration overestimation at Pr concentrations that are relatively low compared to Ga and an underestimation of the Pr concentration at Pr concentrations that are relatively high compared to Ga. This non linearity in counts and recovery rate is remarkable as one of the fundamental assumptions of TXRF is that the number of counts of an element is proportional to its concentration. Moreover, these results suggest that TXRF measurements need to be performed in a very narrow, calibrated concentration range and that quite often large errors are made when using a single internal standard for quantifying multi-element solutions containing metals present in different concentrations. The graph can be split into three regions when considering the standard deviations. The standard deviation is high on the left hand side of the graph which is due to the lower detected x-ray fluorescence intensity resulting in a lower signal to noise ratio and a larger uncertainty on the peak intensity. On the right hand side, the concentrations are relatively high and matrix effects start to play a role. Therefore, the standard deviations are again higher. The standard deviation is low at medium concentrations (around a Pr/Ga mass ratio of 1 and with a gallium concentration of 100 mg L^{-1}). Afterwards, the 12 solutions were diluted a tenfold (to a

Ga concentration of 10 mg L^{-1}) to prove that this non-linearity is not caused by the fact that relative large metal concentrations are used. The measuring time was increased from 300 s to 3000 s in order to get a similar detected X-ray fluorescence intensity for the elements of interest. The black curve in Fig. 3.5 shows a similar trend although the recovery rates are closer to 100% at higher Pr concentrations.

This non-linearity when using Ga as internal standard was also observed with other rare earths and transition metals. Nd and Pr are two lanthanides having L-lines with very close energies. The effect on the recovery rates, as shown in Fig. 3.6, is very similar suggesting that, when measuring Nd, Pr should be a better internal standard, canceling out the effect that causes the non-linearity shown in Fig. 3.5. Therefore, a similar experiment was carried out in which the Pr concentration was kept at 100 mg L^{-1} and the Nd concentration was varied. Fig. 3.6 shows that indeed, the recovery rates and standard deviations are much better than in the case of Pr/Ga, however, at low Pr/Nd ratios, the peaks of Pr are overlapping more the peaks of Nd making difficult to distinguish them, resulting in lower recovery rates for Pr.

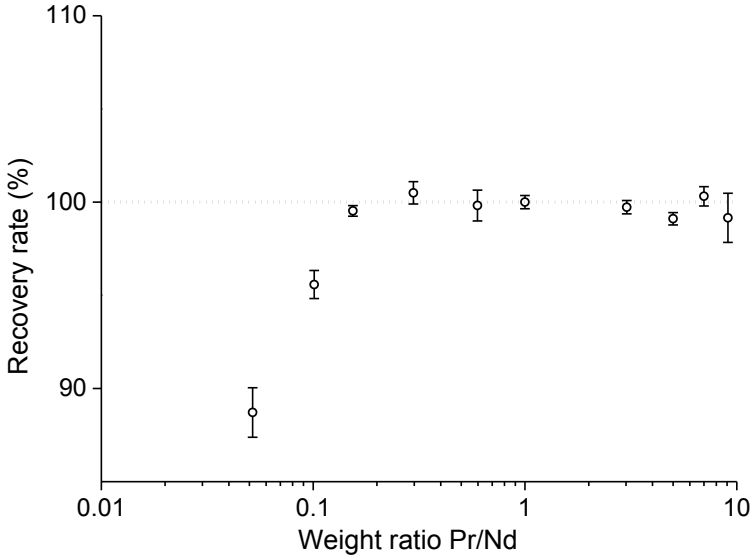

Fig. 3.6. Pr recovery rate (%) as function of the mass ratio Nd/Pr in solution. Pr concentration: 100 mg L^{-1}, each data point was measured in triplicate. Note that the X-axis is plotted on a logarithmic scale. Error bars represent the standard deviation.

Therefore, to get accurate and precise data, the calibration of the elements is performed by measuring 10 times a mixture of the element of interest and gallium as internal standard at equal concentrations (100 mg L^{-1}). Often, the calibration of the TXRF machines is carried out by making groups of four or five metals for which the X-rays are not overlapping and with concentrations of 50 mg L^{-1} to avoid matrix effects. In the case of single-element solutions is strongly suggested to re-measure a solution if the element of interest is less than half or more than double of the concentration of the internal standard used and, if possible, to measure with an internal standard that has an X- ray fluorescence energy as close as possible to the element of interest. For multi-element solutions with extremely different concentrations, it is recommended to evaluate the best conditions for the measurements in terms of the choice of the internal standard element and its concentration.

3.3.3 Carrier, blank problems and detector contamination

One of the most sensitive and expensive parts of a TXRF machine is the detector. Depending on the nature of the detector, problems due to corrosion can be faced when exposed to corrosive gases. The center of the detector shown in Fig. 3.7 is damaged and the surroundings suggest that volatile species escape from the matrix and condense on the detector assembly. First of all, improper drying of the sample can conduce to samples that still contain significant amounts of acid like HNO_3 (which comes from the internal standards used). During the measurement, it is possible that part of the remaining acid evaporates and condenses on the detector. However, it is very unlikely that still significant amounts of HNO_3 evaporate at room temperature after a drying procedure of 30 min at 60 °C. It is more likely that high chloride salt matrices are causing the corrosion. Samples with (high) chloride matrices (*e.g.* NaCl, NH_4Cl, $CaCl_2$, etc) need special attention since these hygroscopic salts can take up water from the air when standing in the sample holder, waiting to be measured. Metal salts present in the sample can hydrolyze and release highly volatile HCl gas that condenses on the detector. A way to change from a chloride to a nitrate matrix is adding a small quantity (*e.g.* 0.005 mL) of 68 wt% HNO_3 acid onto the residue that remains after drying. The removal of chloride from a 1.1 M solution of $CaCl_2$ was tested. By drying the chloride solution again in combination with HNO_3 in a hot air oven at elevated temperatures, chloride ions are oxidized by the nitrate ions and the chlorine gas that is formed

escapes from the sample before mounting the carrier into the TXRF machine, the chloride recovery rate was 0.005%.

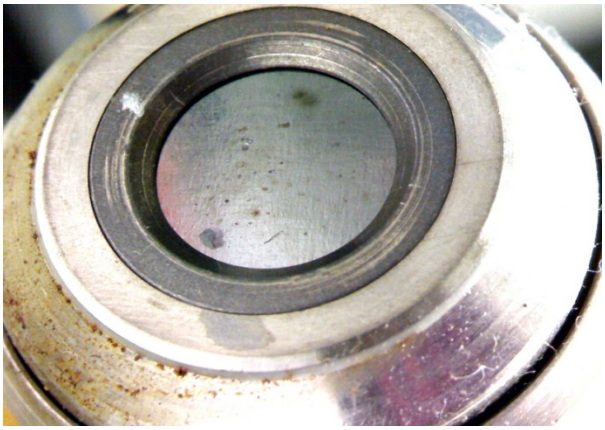

Fig. 3.7. Contamination and corrosion of the detector window.

The expensive quartz sample carriers can be cleaned after usage. However, it is sometimes difficult to get a clean spectrum and often contaminations are observed, especially when measuring into the low ppm or ppb range. Also old TXRF carriers often have metal impurities left in scratches on the carrier surface. Apart from the known elemental peaks of molybdenum (source), argon (air) and silicon (in case of a quartz carrier), other impurities that can frequently be observed in the spectrum are calcium, zinc, iron, lead and other elements depending on the type of samples analyzed. When the cleaning of the carriers is not performed properly, stable oxides of these elements can be formed which are difficult to be removed, and which interfere with the analysis. For these reasons, it is recommended to use the following cleaning procedure: (1) cleaning with water and a lint-free cleaning tissue to remove salts, (2) cleaning with acetone and a lint-free cleaning tissue to remove silicone or organic material from the carrier, (3) loading the washing cassette with the pre-cleaned sample carriers, placing the cassette inside a covered beaker and heating it with a 3 wt% HCl solution during half an hour to remove metals and especially Fe(III) and Pb(II), (4) rinsing the sample carriers with distilled water and heating the cassette with RBS 50 pF during half an hour to dissolve the silicone on the carrier, (5) rinsing the sample carriers with distilled water and heating with HNO_3 during two hours to remove the remaining metal impurities, (6) rinsing with MilliQ water, (7) rinsing with acetone, (8) drying the sample carriers in the cassette at 60 °C during half an hour, (9) placing 30 µL of silicone solution

onto the sample carrier and drying them during half an hour at 60 °C, and finally (10) measuring each sample carrier during 200 s to check their cleanness.

3.4 Conclusions

To illustrate the relevance of sample preparation in the detection and quantification of aqueous metal ion solutions by TXRF, different important parameters such as choice of standard, sample volume, drying time, measurement time and the calibration have been studied and discussed. As a result, optimal conditions needed for the correct measurement of metal ion solutions by TXRF were found and practical and simple guidelines were formulated which can improve the quality, reliability and accuracy of the measurements. For example, better results are obtained when the internal standard and the analyte have closer X-ray line energies, which is in contrast with the common practice to use gallium as the only internal standard. The concentration ratio of the standard should be close to the one of the analyte in the sample in order to assure good recovery rates. The quality of the analysis can be improved, for instance, by using smaller sample volumes in order to avoid movement of the droplet on the carrier. Further experiments are being carried out to address complex matrix effects (*e.g*. ionic liquids, high salt content) which will be addressed in a future research project.

3.5 References

1. E. K. Towett, K. D. Shepherd and G. Cadisch, *Sci. Total. Environ.*, 2013, **463-464**, 374-388.

2. T. Vander Hoogerstraete, S. Jamar, S. Wellens and K. Binnemans, *Anal. Chem.*, 2014, **86**, 1391-1394.

3. T. Vander Hoogerstraete, S. Jamar, S. Wellens and K. Binnemans, *Anal. Chem.*, 2014, **86**, 3931-3938.

4. S. Pahlke, L. Fabry, L. Kotz, C. Mantler and T. Ehmann, *Spectrochim. Acta B*, 2001, **56**, 2261-2274.

5. F. R. Espinoza-Quiñones, A. N. Módenes, S. M. Palácio, N. Szymanski, R. A. Welter, M. A. Rizzutto, C. E. Borba and A. D. Kroumov, *Appl. Radiat. Isot.*, 2010, **68**, 2202-2207.

6. M. Mages, S. Woelfl, M. Óvári and W. v. Tümpling jun, *Spectrochim. Acta B*, 2003, **58**, 2129-2138.

7. R. v. B. Klockenkämper, A., *Total-Reflection X-Ray Fluorescence Analysis and Related Methods*, John Wiley & Sons, New Jersey, 2015.

8. R. Sitko, P. Janik, B. Zawisza, E. Talik, E. Margui and I. Queralt, *Anal. Chem.*, 2015, **87**, 3535-3542.

9. M. Menzel and U. E. A. Fittschen, *Anal. Chem.*, 2014, **86**, 3053-3059.

10. R. Fernández-Ruiz, M. J. Redrejo, E. J. Friedrich, M. Ramos and T. Fernández, *Anal. Chem.*, 2014, **86**, 7383-7390.

11. S. Kunimura and J. Kawai, *Anal. Chem.*, 2007, **79**, 2593-2595.

12. V. S. Hatzistavros and N. G. Kallithrakas-Kontos, *Anal. Chem.*, 2011, **83**, 3386-3391.

13. C. Neumann and P. Eichinger, *Spectrochim. Acta B*, 1991, **46**, 1369-1377.

14. M. L. Carvalho, T. Magalhães, M. Becker and A. von Bohlen, *Spectrochim. Acta B*, 2007, **62**, 1004-1011.

15. L. Borgese, F. Bilo, K. Tsuji, R. Fernández-Ruiz, E. Margui, C. Streli, G. Pepponi, H. Stosnach, T. Yamada, P. Vandenabeele, D. M. Maina, M. Gatari, K. D. Shepherd, E. K. Towett, L. Bennun, G. Custo, C. Vasquez and L. E. Depero, *Spectrochim. Acta B*, 2014, **101**, 6-14.

16. L. Borgese, F. Bilo, R. Dalipi, E. Bontempi and L. E. Depero, *Spectrochim. Acta B*, 2015, **113**, 1-15.

17. H. Stosnach, *Spectrochim. Acta B*, 2006, **61**, 1141-1145.

18. R. Dalipi, E. Marguí, L. Borgese, F. Bilo and L. E. Depero, *Spectrochim. Acta B*, 2016, **120**, 37-43.

19. H. Stosnach, *Analyt. Sci*, 2005, **21**, 873-876.

20. E. Marguí, J. C. Tapias, A. Casas, M. Hidalgo and I. Queralt, *Chemosphere*, 2010, **80**, 263-270.

21. P. Wobrauschek, *X-Ray Spectrom.*, 2007, **36**, 289-300.

22. H. Aiginger, *Spectrochim. Acta B*, 1991, **46**, 1313-1321.

23. R. Klockenkämper and A. von Bohlen, *Spectrochim. Acta B*, 2014, **99**, 133-137.

24. I. De La Calle, N. Cabaleiro, V. Romero, I. Lavilla and C. Bendicho, *Spectrochim. Acta B*, 2013, **90**, 23-54.

25. N. H. Bings, A. Bogaerts and J. A. C. Broekaert, *Anal. Chem.*, 2010, **82**, 4653-4681.

26. R. Klockenkämper, *Spectrochim. Acta, Part B*, 2006, **61**, 1082-1090.

27. Y. Yoneda and T. Horiuchi, *Rev. Sci. Instrum.*, 1971, **42**, 169-170.

28. P. Wobrauschek and H. Aiginger, *Anal. Chem.*, 1975, **47**, 852-855.

29. ISO18507, Surface chemical analysis. Use of Total Reflection X-ray Fluorescence spectroscopy in biological and environmental analysis, 2015.

30. ISO14706, Surface chemical analysis - Determination of surface elemental contamination on silicon wafers by total-reflection X-ray fluorescence (TXRF) spectroscopy, 2014.

31. ISO17331, Surface chemical analysis. Chemical methods for the collection of elements from the surface of silicon-wafer working reference materials and their determination by total-reflection X-ray fluorescence (TXRF) spectroscopy, 2004.

32. G. H. Floor, I. Queralt, M. Hidalgo and E. Marguí, *Spectrochim. Acta B*, 2015, **111**, 30-37.

33. A. Prange, U. Reus, H. Schwenke and J. Knoth, *Spectrochim. Acta B*, 1999, **54**, 1505-1511.

34. M. Schmeling, in *Reference Module in Chemistry, Molecular Sciences and Chemical Engineering*, Elsevier, 2013.

35. N. V. Alov, *Inorg. Mater.*, 2011, **47**, 1487-1499.

36. D. Hampai, S. B. Dabagov, C. Polese, A. Liedl and G. Cappuccio, *Spectrochim. Acta B*, 2014, **101**, 114-117.

37. R. Klockenkàmper, J. Knoth, A. Prange and H. Schwenke, *Anal. Chem.*, 1992, **64**, 1115A-1123A.

38. Y. Tabuchi and K. Tsuji, *X-Ray Spectrom.*, 2016, DOI: 10.1002/xrs.2688.

39. M. Menzel, O. Scharf, S. H. Nowak, M. Radtke, U. Reinholz, P. Hischenhuber, G. Buzanich, A. Meyer, V. Lopez, K. McIntosh, C. Streli, G. J. Havrilla and U. E. Adriane Fittschen, *J. Anal. At. Spectrom.*, 2015, **30**, 2184-2193.

40. J. K. Park, J. Ryu, B. C. Koo, S. Lee and K. H. Kang, *Soft Matter*, 2012, **8**, 11889-11896.

41. A. Marin, R. Liepelt, M. Rossi and C. J. Kahler, *Soft Matter*, 2016, **12**, 1593-1600.

42. D. K. G. de Boer, *Spectrochim. Acta B*, 1991, **46**, 1433-1436.

43. M. Kramer, A. von Bohlen, C. Sternemann, M. Paulus and R. Hergenröder, *Appl. Surf. Sci.*, 2007, **253**, 3533-3542.

44. M. Kramer, A. von Bohlen, C. Sternemann, M. Paulus and R. Hergenroder, *J. Anal. At. Spectrom.*, 2006, **21**, 1136-1142.

45. D. R. Kramer M., Holz Th., Weiflbach D., Falkenberg G., Simon R., Fittschen U., Krugmann T., Kolbe M., Muller M., Beckhoff B. , *Adv. X Ray. Anal*, 2011, **54**, 209-304.

Chapter 4. Extraction and separation of neodymium and dysprosium from used NdFeB magnets: an application of ionic liquids in solvent extraction towards the recycling of magnets

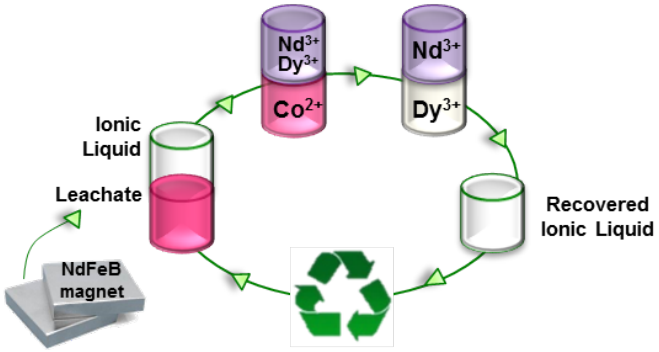

ABSTRACT-A procedure for the efficient extraction and separation of rare earths and other valuable elements from used NdFeB permanent magnets is presented. In a first step, an iron free leachate is prepared from a used magnet using nitric acid. Cobalt is separated through a liquid-liquid extraction in aqueous nitrate media using as organic phase the ionic liquid trihexyl(tetradecyl)phosphonium nitrate which is easily prepared from the commercially available ionic liquid trihexyl(tetradecyl)phosphonium chloride (Cyphos® IL 101). Afterwards neodymium and dysprosium are successfully separated using ethylenediaminetetraacetic acid (EDTA) as a selective complexing agent during liquid-liquid extraction with the same ionic liquid. Different parameters of the separation process such as shaking speed, time, temperature, pH effect and concentration of complexing agents were optimized. The designed process allowed the separation of these three elements efficiently in few steps. The separated rare earths and cobalt were precipitated with oxalic acid and then calcined in order to form the oxides. Nd_2O_3, Dy_2O_3 and CoO were obtained with purities of 99.6%, 99.8% and 99.8%, respectively. Recycling of the employed ionic liquid for reuse in rare earths separation was also demonstrated.

Based on the published paper
Sofia Riano and Koen Binnemans
"Extraction and separation of neodymium and dysprosium from used NdFeB magnets: an application of ionic liquids in solvent extraction towards the recycling of magnets".
Green Chemistry, 2015, 17, 2931-2942.

Author contributions
S.R. performed the experimental work, data analysis and wrote the article.

4.1 Introduction

Recycling of REEs is of importance from an economic, industrial and environmental point of view. For instance, the mining, transportation, processing and waste disposal of REEs have very serious environmental and occupational risks,[1] besides consequences on the surrounding ecosystems and human health.[2] Indeed, most of the rare-earth deposits contain harmful radioactive elements (e.g. thorium and uranium).[1] Moreover, in 2010, the European Commission published a list of critical raw materials at the EU level,[3] where valuable elements such as neodymium, dysprosium (both critical at short and middle term) and cobalt (not critical at short nor at middle term) can be found.

The range of REE applications has changed over time with the design and creation of new devices and processes requiring REEs.[4] Rare-earth oxides are of high importance because they cover a wide range of applications, they are employed in the glass industry (glass components and surface polishing agents), in lamp phosphors, high-power lasers, photographic industry and as catalysts.[5] Neodymium has been used since several decades as a colorant for glass, in welding goggles and more recently also in laser crystals.[4] Presently, neodymium is mostly employed in the manufacturing of permanent magnets that are used in electric motors, wind turbines and spindles for computer hard drives.[4] Dysprosium, another REE, is currently employed as an additive to NdFeB permanent magnets to improve their high temperature performance and to increase its intrinsic coercivity.[6] Furthermore, dysprosium is being applied in the nuclear industry as component for radiation shielding,[4] while dysprosium-doped phosphors are employed as radiation detectors in clinical and environmental monitoring of ionizing radiation.[7] Additionally, some NdFeB magnets contain small but considerable quantities of cobalt since it is added to the NdFeB magnets to increase the Curie temperature of the magnet.[8] Cobalt itself is a valuable and highly demanded element due to its multiple applications in the fields of super-alloys, catalysts, pigments and batteries.[9]

In contrast to the increasing REE demand, the supply of such materials is currently experiencing a shortage. Therefore different strategies such as, reopening of old REE mines or substitutions of critical elements have been proposed to solve this issue.[10-12] Alternatively, recycling of REE can be an interesting and efficient option to overcome this situation, while reducing the impact of the

balance problem and environmental issues related to mining. Indeed, through REE recycling,[13] small but representative quantities of REEs that are minor constituents in the ores but that are at the same time high in demand by the market (e.g. dysprosium), can be efficiently obtained. Therefore, the recovery of neodymium and dysprosium from end-of-life NdFeB magnets containing considerable amounts of these elements becomes a relevant issue at industrial level.[14] The most employed methods for the separation of REEs use organic solvents which due to their toxicity, volatility and flammability have led to the implementation of ionic liquids in an environmentally friendlier approach.[15]

Ionic liquids (ILs) are organic salts which consist entirely of ions and with a melting point that is generally lower than 100 °C.[16-18] Some of the most interesting properties of the ILs are their chemical and thermal stability, high ionic conductivity and wide electrochemical potential window. Due to their negligible vapor pressure and low flammability, ionic liquids have been usually labeled as "green solvents".[19,20] As the application of ionic liquids in different fields continuously grows, information related to their environmental, health and safety impact can already be found in the literature.[16,21,22]

Ionic liquids are often called "designer solvents", because their cation and anion can be chosen in order to obtain an ionic liquid with specific properties that fulfill the requirements needed for a given process.[23] For example, in the liquid-liquid extraction process proposed herein, hydrophobic and low viscous ionic liquids are needed. Additionally, it is important that the metal complex that is going to be extracted has a higher solubility into the ionic liquid than in the aqueous phase. Some of the most studied ionic liquid based extraction systems contain fluorinated anions such as hexafluorophosphate (PF_6^-) or bis(trifluoromethylsulfonyl)imide (Tf_2N^-) that allow the obtention of hydrophobic and low viscous ionic liquids.[24-27] However, ionic liquids containing these anions are usually expensive and hexafluorophosphate ions can undergo hydrolysis conducing to the formation of hydrofluoric acid.[28] Besides this, the extraction of charged metal ions in fluorinated ionic liquids often occurs through an ion-exchange mechanism that conduces to the partially loss of the ionic liquid by dissolution of the cation into the aqueous phase.[29] For this reason, ionic liquids with hydrophobic cations containing long alkyl chains are now selected which permits the use of less expensive and more available anions. Alternatives are the phosphonium based ionic liquids, which are good candidates for their use in

liquid-liquid extractions due to their high hydrophobicity, variety and availability. Moreover, phosphonium ionic liquids are able to extract anionic complexes, instead of only metal ions. As a consequence, phosphonium ionic liquids have been applied for industrial applications and a range of phosphonium ionic liquids are commercially available on a large scale.[30,31]

In this chapter, an ionic liquid was employed for the separation and recovery of rare earths from an end-of-life NdFeB magnet. We present a new, practical, efficient and environmentally friendly methodology to separate neodymium(III), dysprosium(III) and cobalt(II) by solvent extraction using an undiluted non-fluorinated ionic liquid. The separation methods were optimized considering the main involved variables (e.g. loading of the organic phase, pH, shaking rate, extraction time, temperature and complexing agent concentration). Since the master alloys needed for the production of magnets are based on the respective rare-earth oxides, the separated and recovered rare earths were precipitated as their respective oxalates and then calcined to obtain the oxides. The loading capacity of the ionic liquid was determined and thus the stoichiometry of the extracted complex close to its saturation. Moreover, the recycling of the employed ionic liquid was also demonstrated.

4.2 Experimental

4.2.1 Materials and methods

Trihexyl(tetradecyl)phosphonium chloride (>97%, Cyphos® IL 101) was purchased from IoLiTec (Heilbronn, Germany). $Nd(NO_3)_3 \cdot 6H_2O$ (99%) was obtained from Alfa Aesar (Karlsruhe Germany), $Dy(NO_3)_3 \cdot 6H_2O$ (99%), $Co(NO_3)_2 \cdot 6H_2O$ (99%) and Na_2EDTA (99%) were purchased from Acros Organics (Geel, Belgium), KNO_3 (99%) and NH_4NO_3 (99%) from Chempur (Karlsruhe, Germany), HNO_3 (65%), HCl (37%), NaOH (99%) and $H_2C_2O_4$ (99%) from J.T Baker, the silicone solution in isopropanol was obtained from SERVA Electrophoresis GmbH (Heidelberg, Germany) and the gallium standard (1000 mg L^{-1}) was purchased from Merck (Overijse, Belgium). All chemicals were used as received, without further purification. The concentrations of the rare earths in both the aqueous and the organic phase were determined by using a bench top total reflection X-ray fluorescence (TXRF) spectrometer (S2 Picofox, Bruker). The extraction experiments were performed in 4 mL vials and using a temperature controllable

Turbo Thermo Shaker (Model: TMS-200, Hangzhou Allsheng Instrument Co. Ltd., China). After the extraction, scrubbing or stripping experiments were carried out at specific conditions for each process. The aqueous and the organic phases were separated after extraction by centrifugation using a Heraeus Megafuge 1.0 centrifuge. Then, part of the aqueous phase was removed and mixed with a gallium standard solution and MilliQ water until a total volume of 1 mL was obtained. For the organic phase (ionic liquid), the gallium standard was added to a small amount of the ionic liquid phase (15-20 mg) and was further diluted with ethanol until 1 mL. The quartz glass sample carriers were treated with 20 µL of a silicone solution in isopropanol in order to make the surface hydrophobic and obtain a concentrated drop of the aqueous phase on the center of the disk. Then the sample carriers were dried for 3 min in a hot air oven at 60 °C and 5 µL of the sample were disposed on the glass carrier. The prepared samples were dried simultaneously during 30 min. The metal concentrations were measured for 200 s. All the pH measurements were performed using an S220 Seven Compact pH/Ion meter (Mettler-Toledo) and a Slimtrode (Hamilton) electrode. The viscosity of the ionic liquid and ionic liquid phases was measured using an automatic Brookfield plate cone viscometer (Model LVDV-II+P CP, Brookfield Engineering Laboratories, USA). Densities were measured with a 5 mL pycnometer. A Mettler-Toledo DL39 coulometric Karl Fischer titrator was used with Hydranal® AG reagent to determine the water content of the synthesized ionic liquid. ^{1}H NMR spectra were recorded in $CDCl_3$ on a Bruker Avance 300 spectrometer, operating at 300 MHz. Chemical shifts are expressed in parts per million (ppm), referenced to tetramethylsilane. The spectra were analyzed with SpinWorks software. FTIR spectra were recorded on a Bruker Vertex 70 spectrometer (Bruker Optics) equipped with a Bruker Platinum ATR accessory. The X-ray diffraction powder pattern was recorded at room temperature with a Siefert 3003 T/T X-ray diffractometer equipped with a scintillation detector. X-ray type: Cu Kα operating at 40 kV and 40 mA, scanning range: 10-80 degrees (2θ), step width: 0.02 degree, step scan: 2.00 s. Analysis result was progressed by "X'pert HighScore Plus" PANalytical software.

4.2.2 Synthesis of trihexyl(tetradecyl)phosphonium nitrate

Trihexyl(tetradecyl)phosphonium nitrate was synthesized by equilibrating 93.199 g (0.179 mol) of trihexyl(tetradecyl)phosphonium chloride with 100 mL of a 2 M potassium nitrate solution

during five hours. The aqueous phase was removed and the organic phase was stirred again for five additional hours with 100 mL more of the same potassium nitrate solution in order to reduce the chloride impurities. Afterwards, the two phases were allowed to separate. The aqueous phase was removed and the organic phase was washed several times with MilliQ water and dried. The ionic liquid obtained was a colorless liquid (94.9%, 94.920 g, 0.1738 mol. ^{1}H NMR (300 MHz, $CDCl_3$, δ/ppm): 2.28 (m, 8H, 4× CH_2), 1.50 (m, 18H, 9× CH_2), 1.32 (s, 12H, 6× CH_2), 1.25 (m, 18H, 9× CH_2), 0.89 (s, 12H, 4× CH_3). The chloride concentration was measured by TXRF and it was found to be below 100 ppm.[32] Water content: 0.02 wt%, viscosity: 1437 cP (22 °C), density: 0.9132 g cm^{-3} at 22 °C Water saturated ionic liquid: Water content: 3.45 wt%, viscosity 260 cP (22 °C), density: 0.9140 g cm^{-3} (22 °C).

4.2.3 Selective leaching and direct magnet dissolution

For the direct magnet powder dissolution and the selective leaching from roasted magnets the procedure reported by Vander Hoogerstraete *et al.,*[33] was followed. A magnet, obtained from the University of Birmingham, UK, and whose composition is shown in Table 4.1 was employed.

Table 4.1. Composition of the employed magnet (wt%).

Element	Content (wt%)	Element	Content (wt%)
Fe	58.16	Pr	0.34
Nd	25.95	C	0.07
Co	4.22	Si	0.06
Dy	4.21	Mn	0.05
B	1.00	Cu	0.04
Nb	0.83	Ni	0.02
O	0.41	N	0.02
Al	0.34	Total	95.72

4.2.3.1 Magnet dissolution

Briefly, 15 g of crushed magnet (particle size < 400 μm) was put into a vial and covered with 15 mL of MilliQ water. Afterwards, 7 mL of concentrated HNO_3 (65 wt%) was carefully and slowly

added; the formation of nitrogen oxides (NO_x) was observed. The vial was closed with a screwcap and heated at 80 °C during 72 h. After this time, the solution was centrifuged during 10 min at 3000 rpm. The aqueous phase was removed and its metal content was measured by TXRF. An orange solution with a pH = 0.41 was obtained. In order to remove the iron that was still present in solution, 1 mL of hydrogen peroxide (35 vol%) was added and the solution was heated at 40 °C for 1 h in order to oxidize the remaining iron(II). A small volume of this solution was poured into a vial that contained 2 mL of MilliQ water and a stirring bar. The pH was monitored with a pH electrode. The initial pH was 0.67. Slowly, under stirring, drop by drop a solution of NaOH 1 M was added to the center of the sample until a pH of 4 was reached. The sample and the solution of NaOH 1 M were gradually added to the vial trying to keep the pH all the time between 3.5 and 4. Afterwards, the sample was stirred for another hour, left to settle during one hour and then it was easily filtered. The resulted solution was pale pink. The metal content was measured by TXRF and no iron could be detected. The precipitate was filtered and analyzed quantitatively by TXRF in order to determine the rare-earth elements that might have been co-precipitated into the precipitate.

4.2.3.2 Selective leaching

The roasting was performed by placing a powder sample (< 400 μm) of the magnet into a porcelain crucible and by heating to 950 °C during 15 h. A sample of the fully roasted powder (15 g) was put into a vial together with 5 mL of HNO_3 (65 wt%) and 10 mL of MilliQ water. A stirring bar was added, the vial was closed with a screwcap and it was stirred for 72 h at 80 °C or during one month at 23 °C. Afterwards, the product was centrifuged for 10 min at 3000 rpm and the aqueous phase was removed and its metal content was measured by TXRF. With this procedure, a very intense pink colored solution of pH = 2.43 was obtained. No iron was detected in this solution. The percentage extraction in the leachate ($\%E_L$) is defined as:

$$\%E_L = \frac{\text{Amount of metal in the leachate}}{\text{Total amount of metal in the leachate and precipitate}} \times 100 \qquad (4.1)$$

4.2.4 Solvent extraction

As the volume of leachate obtained was not enough to carry out all the optimization experiments, a synthetic solution mimicking the concentrations obtained in the selective leaching of rare-earth elements from the roasted NdFeB magnet was prepared. Neodymium(III) nitrate hexahydrate, dysprosium(III) nitrate hexahydrate and cobalt(II) nitrate hexahydrate were dissolved in MilliQ water and acidified with HNO_3 6.5 wt% to pH = 2.0. The final concentrations of these solutions were: 248.54 g L^{-1} of Nd(III), 21.41 g L^{-1} of Dy(III) and 4.37 g L^{-1} of Co(II). To optimize the extraction procedure, the efficiency of the extraction was evaluated in terms of different parameters, such as temperature, concentration of ammonium nitrate, extraction time, effect of the pH, scrubbing agent, selective stripping agent, stirring rate and concentration of EDTA in the case of the separation of neodymium and dysprosium. Only one parameter was varied at the time while keeping the other variables constant.

4.2.4.1 Determination of the efficiency of the extraction

The concentration of Co(II), Nd(III) and Dy(III) distributed between the organic and the aqueous phases was measured using TXRF. The *distribution ratio* (*D*) is defined as follows:

$$D = \frac{[M]_{org}}{[M]_{aq}} = \frac{[M]_i - [M]_{aq}}{[M]_{aq}} \times \frac{V_{aq}}{V_{org}} \qquad (4.2)$$

where $[M]_i$ is the initial metal ion concentration in the aqueous phase. $[M]_{aq}$ is the metal ion concentration in the aqueous phase after the extraction, and V_{org} and V_{aq} are the volumes of the organic and aqueous phases, respectively. In these experiments, equal volumes of organic and aqueous phases have been employed, thus the equation (4.2) can be simplified to:

$$D = \frac{[M]_i - [M]_{aq}}{[M]_{aq}} \qquad (4.3)$$

For poorly extracted metals, the metal concentration in the organic phase was measured and the distribution ratio (*D*) can be expressed as:

$$D = \frac{[M]_{org}}{[M]_i - [M]_{org}} \times \frac{V_{aq}}{V_{org}} \qquad (4.4)$$

The *percentage extraction* (*%E*) is defined as the amount of metal ion extracted to the organic phase over the initial amount of metal ion in case of equal volumes and can be expressed as:

$$\%E = \frac{[M]_i - [M]_{aq}}{[M]_0} \times 100 \qquad (4.5)$$

The efficiency of the separation of two metals can be described with the *separation factor* α, in which D_{M1} and D_{M2} correspond to the distribution ratios *D* of metal M_1 and M_2, respectively:

$$\alpha_{M_1 M_2} = \frac{D_{M_1}}{D_{M_2}} \qquad (4.6)$$

For the scrubbing experiments, the *percentage recovery* (*%S*) can be defined as the amount of metal scrubbed from the organic phase to the total amount of metal in the organic phase before scrubbing.

$$\%S = \frac{V_{aq}[M]_{aq}}{V_{org}[M]_{orgi}} \times 100 \qquad (4.7)$$

where $[M]_{org,i}$ is the metal ion concentration in the organic phase after extraction or before stripping. This formula can be used for both scrubbing and stripping experiments.

4.2.4.2 Separation of Co(II) from Nd(III) and Dy(III)

All extraction experiments were carried out with a pH = 2 water saturated trihexyl(tetradecyl)phosphonium nitrate as organic phase unless stated otherwise. Extractions were performed at 60 °C with intensive shaking (1900 rpm) during 1 h. 10 M NH_4NO_3 was used as source of nitrate ions. After the extraction, the phases were separated by centrifugation at 5000 rpm during 1 min and afterwards they were measured by TXRF. The ratio between the volumes of the organic and the aqueous phase was 1:1.

4.2.4.3 Scrubbing

The scrubbing experiments were carried out at 80 °C, during 90 min with intensive shaking (1900 rpm). A 10 M solution of NH_4NO_3 was used as scrubbing agent. The ratio between the volumes of the organic and the aqueous phase was 1:1. After the extraction, the samples were centrifuged

at 5000 rpm during 1 min and the phases were separated immediately. The metal concentrations in both organic and aqueous phases were measured by TXRF.

4.2.4.4 Purification of the separated cobalt and obtention of cobalt(II) oxide (CoO)

In order to remove the small impurities of neodymium and dysprosium that still could have been present after the separation, the aqueous phase was put in contact with fresh ionic liquid and shaken at 60 °C, during 1 h at 1900 rpm. After the extraction, the phases were immediately separated. Then, a stoichiometric amount of oxalic acid in solution was added to the purified aqueous phase containing the separated cobalt(II). The mixture was shaken during 10 min and then settled during 5 min, afterwards it was centrifuged at 5000 rpm for 1 minute. The white precipitate obtained was filtered and washed twice with water and ethanol. Then, transferred into a previously tared crucible and calcined at 950 °C during 4 h to obtain the corresponding CoO. The purity of the obtained oxide was measured by TXRF. XRD was carried out to confirm that the obtained oxide corresponded to CoO.

4.2.4.5 Loading

For the loading experiments, the metal concentrations in the aqueous phases were 92.0 g L^{-1} of neodymium and 91.2 g L^{-1} of dysprosium. The volume of the aqueous phase was 1 mL and the concentration of NH_4NO_3 was 10 M. The amount of organic phase was varied between 0.4 and 1.6 g for neodymium and between 0.4 and 1.8 g for dysprosium. Extractions were performed for 1 h and 30 min at 70 °C and 1900 rpm. After the extraction, the samples were centrifuged for 1 min at 5000 rpm and the aqueous phase was separated immediately and measured by TXRF.

4.2.5 Separation of Co(II) from Nd(III) and Dy(III)

4.2.5.1 Selective stripping of Dy(III)

A synthetic solution containing only Nd(III) and Dy(III) was prepared (pH = 2). The water-saturated ionic liquid was loaded with this solution in order to obtain the following concentrations in the organic phase, 58.1 g L^{-1} for Nd and 5.5 g L^{-1} for Dy. The ionic liquid was

loaded following the same procedure employed for the separation of Co(II) from Nd(III) and Dy(III). For the selective stripping of Dy(III) from the organic phase containing both Nd(III) and Dy(III), a solution of Na_2EDTA (0.03 M) and NH_4NO_3 (10 M) was employed as striping agent. The experiments were performed at 70 °C during 1 h with vigorous shaking (1900 rpm). After the extraction the phases were separated by centrifugation at 5000 rpm during 1 min and both, organic and aqueous phases were measured by TXRF. The selective stripping with Na_2EDTA (0.03 M) and NH_4NO_3 (10 M) was repeated twice in order to remove the remaining dysprosium and allow the obtention of pure neodymium.

4.2.5.2 Precipitation stripping of neodymium and obtention of Nd_2O_3

The cleaned organic phase (after the two scrubbing steps) was put in contact with 1 mL of a solution 76 g L^{-1} of oxalic acid and shaken for 10 min at 22 °C. As soon as the oxalic acid solution was put in contact with the ionic liquid phase the formation of a white precipitate was observed. After the stripping precipitation, the samples were centrifuged and the organic phase was carefully removed. The aqueous phase, containing the precipitate, was filtered and the solid was washed twice with 1 mL of water and then with 1 mL of ethanol. The solid was put into a previously tared crucible and then calcined at 950 °C during 4 h. A light blue powder was obtained and it was analyzed by TXRF and XRD.

4.2.5.3 Purification of the selectively stripped Dy(III)

The aqueous phase containing dysprosium after the selective stripping with EDTA also contains a considerable amount of neodymium, this is inevitable due to the high percentage of neodymium that is present in the magnet and the low amount of dysprosium. In order to purify this dysprosium, 50 µL of 16 wt% HNO_3 was added to the aqueous phase and it was put in contact with 1 mL of fresh ionic liquid and shaken at 70 °C during 1 h at 1600 rpm. In order to achieve a purity of dysprosium higher than 99% this procedure had to be repeated three times.

4.2.5.4 Obtention of Dy_2O_3

Once the dysprosium has been purified, the aqueous phase can be treated with a stoichiometric amount of oxalic acid in order to precipitate dysprosium(III) oxalate and recover the supernatant

that contains the EDTA which can be reused in the system as stripping agent. The white precipitate corresponding to the dysprosium oxalate was filtered, washed with water and ethanol and then calcined at 950 °C during 1 h. A white powder was obtained and it corresponded to Dy_2O_3 according to XRD.

4.2.5.5 Recycling of the ionic liquid

Once the process is finished and neodymium is removed from the ionic liquid by precipitation stripping, the ionic liquid can be equilibrated with MilliQ water and reused in a new cycle of separations. If an excess of oxalic acid is employed during the precipitation stripping of neodymium, the ionic liquid has to be pre-treated before its reutilization. An easy and green way to purify the ionic liquid is to precipitate the excess of oxalic acid with calcium nitrate. 1 mL of a 1 M solution of calcium nitrate was put in contact with the ionic liquid and shaken during 20 min at 70 °C and 1600 rpm. Afterwards, a white precipitate was obtained and removed after centrifugation. The ionic liquid was then equilibrated with water and reused again without losing its efficiency.

4.3. Results and discussion

4.3.1 Leaching

Two different methods were employed in order to carry out the extraction of rare earths from used NdFeB magnets: leaching of pristine magnets and leaching of roasted magnets The selective leaching from the roasted magnet led to solutions rich in rare earths in which iron was not detected. Table 4.2 shows the %*E* obtained with the two proposed methods, where it can be seen that the magnet dissolution process is not as efficient and convenient as the selective leaching starting from the roasted magnet.

Table 4.2. Percentages extraction in the leachate (%E_L) of the different metals from the dissolution of the non-roasted magnet and the selective leaching of the roasted magnet.

Process	Temperature (°C)	Time	%*E* Fe(III)	%*E* Co(II)	%*E* Nd(III)	%*E* Dy(III)
Selective leaching from the roasted magnet	80.0	15 h	n.d.[a]	14.6	83.3	78.3
	22.5	2 weeks	n.d.[a]	3.72	47.5	42.2
	22.5	1 ½ month	n.d.[a]	12.7	85.5	77.9
Dissolution of the non-roasted magnet	80.0	15 h	23.1	20.7	37.7	21.0
	22.5	2 weeks	6.8	4.9	19.9	14.7

[a] Not detected

The standard reduction potential for iron(III) is more positive than for iron(II),[34] thus during the dissolution of the magnet alloy, iron will go in solution as Fe(II). Indeed, the presence of iron(II) into the solution leads to the formation of NO during the dissolution process. The overall reaction is described as follows

$$3Fe^{2+} + 4H^{+} + NO_3^{-} \rightleftharpoons 3Fe^{3+} + 2H_2O + NO \quad (4.8)$$

Different nitrogen oxides, besides NO can be formed during the process: NO_2, N_2O_4, and N_2O_3.[35] NO_2 is a reddish brown toxic gas and air pollutant. NO and NO_2 are known for being ozone-depleting substances.

The possibility to obtain iron-free leachates from the roasted NdFeB magnets has been already discussed in detail by Vander Hoogerstraete *et al.*[33] Briefly, as a result of the magnet roasting process, iron is present immediately as Fe(III) and will go into solution as Fe(III), then it will be hydrolyzed to $Fe(OH)_3$ when the pH of the leachate rises to pH values above 2. The latter precipitates easily at this pH whereas the rare-earth metal ions stay in solution. In contrast, the dissolution of the non-roasted magnet leads to the formation of hydrated Fe^{2+}, which is more difficult to hydrolyze than hydrated species of Fe^{3+} and thus it remains in solution with the rare-earth metal ions.

The presence of iron in the leachate obtained from the non-roasted magnet represents an interference for the proposed extraction method with ionic liquids because it leads to the formation of undesired precipitates. For instance, after the extraction procedure from the solution obtained by dissolution of the magnet, the presence of a yellowish precipitate was observed at the liquid-liquid interface making it difficult to obtain two clean and separated phases. Formation of iron (hydr)oxide precipitates during extraction processes with ionic liquids have been previously reported and confirmed by TXRF analysis, this is due to acid extraction by the ionic liquid which conduces to an increase of the pH.[29] In order to overcome this issue, it was required to precipitate the iron present in the solution before carrying out the liquid-liquid extraction.

In a first approach, the iron was precipitated by the direct addition of an ammonia solution to the leachate obtained from the non-roasted magnet powder. This led to a brown gelatinous precipitate that was difficult to filtrate and manipulate. Alternatively, many different procedures for the precipitation of iron oxides have been described in detail.[36,37] Different factors such as temperature, pH, the employed base and its concentration, stirring rate, precipitation and ageing times play a key role in the obtention of easily filterable precipitates. The solution was oxidized with hydrogen peroxide and taken to a final pH of 4 with NaOH. The precipitate formed was then removed by filtration and the resulted pink diluted solution was employed for the extraction of rare-earth ions with positive results as no precipitate was observed between the phases. Synthetic iron oxides are of importance because they have a wide range of applications in industry, as pigments, catalysts, sensors and biomedicine, among others.[36] Thus, it is useful to identify the iron oxide phases present in the obtained precipitate. The precipitated iron was analyzed by XRD, founding that it consisted of amorphous goethite (α-FeOOH) and probably iron hydroxide.

It is well known that iron(III) oxyhydroxides have large surface areas and can be effective scavengers of metal ions and oxyanions.[37-39] For this reason, the rare earths that may have been adsorbed onto the precipitate were quantified. The loss of rare earths and cobalt during the precipitation of iron from the dissolution of the non-roasted magnet was equal to 1.5% for Nd, 1.9% for Dy and 1.2% for Co. Even though these are not critical losses, the precipitation of iron by the slow addition of 1 M NaOH requires large volumes of NaOH, and as a consequence dilutes the sample to concentrations that are not of interest for this study.

Taking into account that the oxides of the magnet alloy are less reactive than the magnet powder, it is easier, safer and environmentally friendlier to carry out the selective leaching of roasted magnets rather than the dissolution process with nitric acid. Even though the selective leaching procedure from roasted magnets can be energy consuming (72 h at 80 °C or 1 month and a half week at 22.5 °C), it allows the production of iron-free leachates rich in rare earths that can be directly employed in a solvent extraction process without the need of adding extra steps for the separation of iron by solvent extraction or by precipitation prior the separation of rare earth elements into individual elements. Therefore, iron-free leachates obtained from roasted magnet powder were used for testing the optimized separation system in Co(II), Nd(III) and Dy(III) separation.

4.3.2 Separation of Co(II) from Nd(III) and Dy(III)

The effect of different variables such as, feed solution concentration, ammonium nitrate concentration, extraction time, shaking speed, pH and time, were optimized by the "one variable at a time" method. This optimization was carried out with solutions that mimicked the concentration of rare-earth ions in the obtained iron-free leachates. The first parameter studied was the effect of the concentration of the feed solution. Fig. 4.1 shows the variation of the extraction percentage with respect to the dilution of the initial concentrated feed of Co(II), Nd(III) and Dy(III). At very high concentrations (as the obtained leachate) and where no dilution was carried out, the efficiency of the extraction is relatively low, 80.5% for Nd(III) and 76.4% for Dy(III). When the synthetic solution is diluted with MilliQ water (dilution factor of two), the extraction efficiency increases (*i.e.* 96.9% and 94.6% for Nd(III) and Dy(III), respectively, $\alpha_{Nd/Co}$: 590, $\alpha_{Dy/Co}$: 500). However, as for industrial applications it is more interesting to work with concentrated feed solutions rather than diluted ones, the synthetic solution was diluted only twice for the rest of the optimization experiments even though more diluted solutions presented higher rare-earth extraction percentages.

It is important to notice that when using low feed solution concentrations, the percentage extraction of cobalt into the ionic liquid increases. The latter occurs when the ionic liquid is not saturated with rare-earths ions and part of the cobalt can be solubilized in the water-saturated ionic liquid. Still the small percentage of cobalt that can be solubilized into the ionic liquid can be removed afterwards during the scrubbing step.

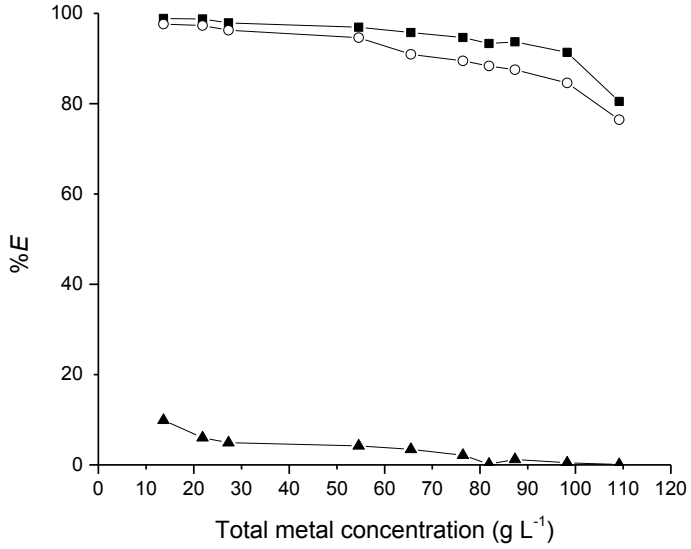

Fig. 4.1. Percentage extraction (%*E*) of cobalt (▲), neodymium (■) and dysprosium (○) as a function of the total concentration of cobalt(II), neodymium(III) and dysprosium(III) together in the aqueous phase. Conditions of extraction: NH_4NO_3 8 M, equilibrium pH = 2, 1900 rpm, 60 min, 60 °C.

The separation of Co(II) from Nd(III) and Dy(III) was also performed at different temperatures, ranging from 40 °C to 80 °C, to determine the influence of the temperature on the extraction process (Fig. 4.2). Higher temperatures provided better extraction percentages for Nd(III) and Dy(III) as they shift the equilibrium of endothermic reactions to the right. On the other hand, high temperatures decrease the viscosity of the ionic liquid and facilitate the transfer of rare earth complexes into the organic phase. A value of 70 °C was chosen as optimal.

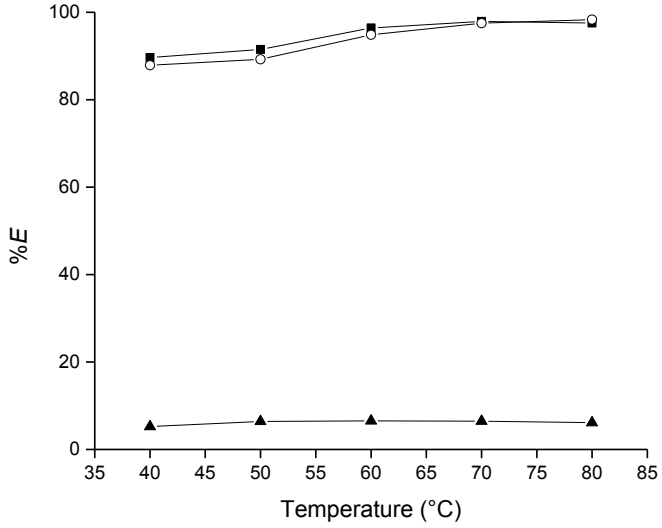

Fig. 4.2. Variation of the percentage extraction (%*E*) of cobalt (▲), neodymium (■) and dysprosium (○) as a function of the temperature. Conditions of extraction: Equilibrium pH = 2, 1900 rpm, 60 min, concentration of NH_4NO_3 8 M.

Furthermore, the ammonium nitrate concentration was evaluated for concentrations up to 10 M (Fig. 4.3). As expected, a higher amount of complexing agent led to a higher extraction percentage for both Nd(III) and Dy(III). The addition of concentrated NH_4NO_3 not only has a positive effect on the extraction percentage of the rare earth metals, but also avoids the formation of emulsions after the vigorous shaking during the extraction. An optimum value of 10 M NH_4NO_3 was chosen to carry out the further optimization experiments. Larger concentrations of NH_4NO_3 could not be obtained because it was not possible to solubilize the salt.

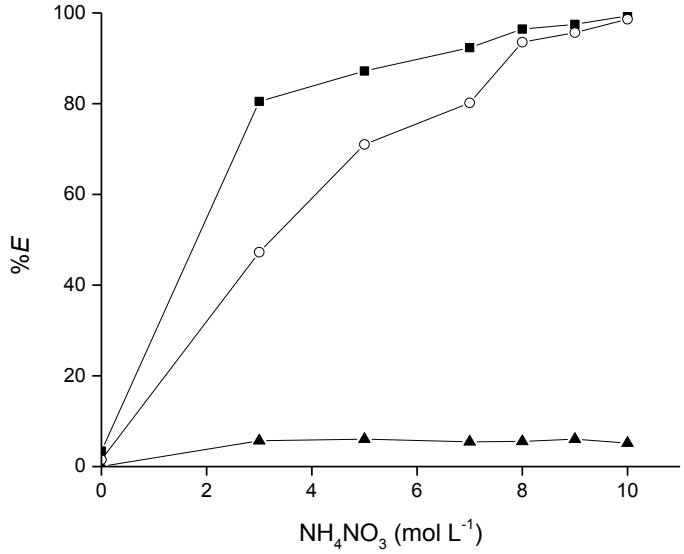

Fig. 4.3. Variation of the percentage extraction (%*E*) of cobalt (▲), neodymium (■) and dysprosium (○) as a function of the concentration of ammonium nitrate. Conditions of extraction: Equilibrium pH = 2, 1900 rpm, 60 min, 70 °C.

For the study of the pH effect on the extraction percentage of Nd(III) and Dy(III), different pH values between 0.25 and 6 were evaluated. The pH did not have a significant effect in the percentage extraction. However, it is important to remark that at pH values higher than 5.8, the rare earths were precipitated and therefore could not be separated and extracted. The influence of the extraction time was evaluated in the range of 10 to 120 min. The results show that by increasing the extraction time from 0 to 40 min, the percentage of extraction is considerably increased (Fig. 4.4). However, since only after an extraction time of 60 min equilibrium was reached, a time of 60 min was kept as optimal value.

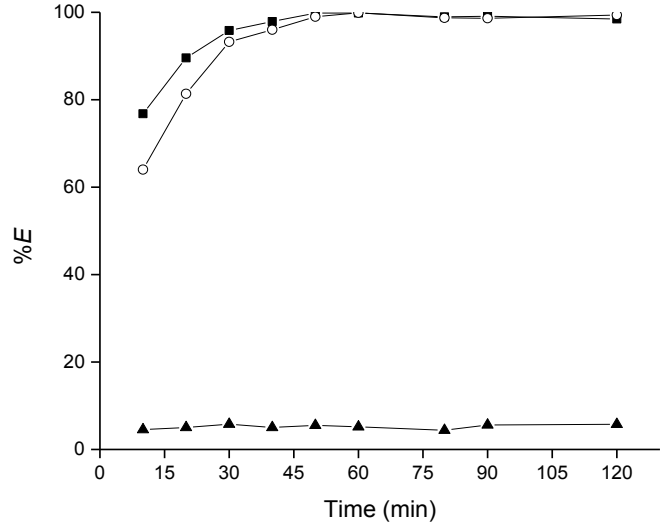

Fig. 4.4. Effect of the extraction time on the percentage extraction (%*E*) of cobalt (▲), neodymium (■) and dysprosium (○). Conditions of extraction: Equilibrium pH = 2, 1900 rpm, 70 °C. NH_4NO_3 10 M.

In general, an increase in the shaking speed generates an improvement in the extraction rate of a process that involves mass transport features. The effect of the shaking speed was evaluated in the range of 0 to 2400 rpm. The extraction percentage becomes higher as the stirring speed increases. Still without mechanical shaking at high temperatures (70 °C), the ionic liquid can get dispersed into the aqueous phase favoring the diffusive processes and mass transport through the phases and thus relatively high percentages of extraction can be obtained. A shaking speed of 1600 rpm was chosen as the optimum value for this extraction process since at higher speeds no improvement of the extraction percentage was observed.

The viscosity of the water-saturated trihexyl(tetradecyl)phosphonium nitrate ionic liquid is 260 cP (at 22 °C), whereas the viscosity of the dried ionic liquid is 1440 cP (at 22 °C). Fig. 4.5 shows the variation of the water-saturated ionic liquid viscosity as a function of the metal loading at two different temperatures. It can be observed how the temperature has a dramatic effect on the viscosity of the ionic liquid. In this system, the viscosity can be decreased in almost a factor of 10 even at high metal loadings (109.2 g L^{-1}), while increasing the temperature to 70 °C. This highlights the importance of working not only with water-saturated ionic liquids, but also at high

temperatures in order to decrease the viscosity of the ionic liquid without the need of adding molecular solvents.

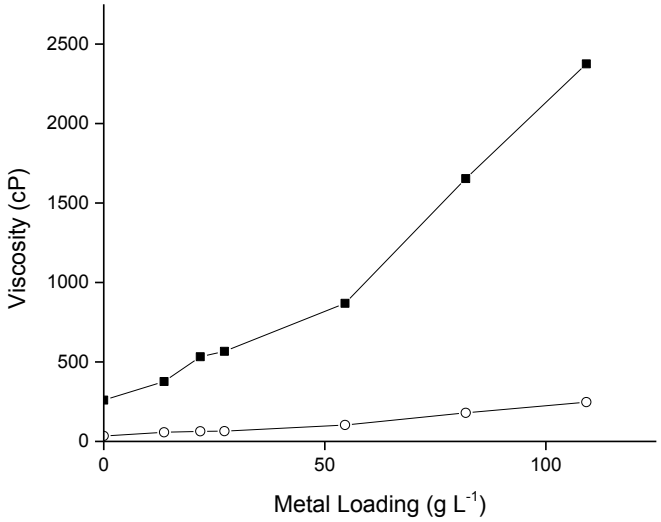

Fig. 4.5. Viscosity of the water-saturated ionic liquid trihexyl(tetradecyl)phosphonium nitrate as a function of the total metal loading (Nd(III) and Dy(III)) at 23 °C (■) and at 70 °C (○).

The principle of separation between Nd(III), Dy(III) and Co(II) is based on the fact that the trivalent rare-earth ions can form anionic complexes with bidentate nitrate ligands. Even though anionic complexes of cobalt with the above mentioned ligands can also be formed in organic solvents,[40] these are more labile to experience water exchange and form the more stable pink hexaaqua complex.[41] For this reason, negative charged complexes formed between the rare earths and the nitrate ions can be extracted into the ionic liquid. The general extraction mechanism for lanthanide extraction can be written as:

$$Ln^{3+} + 3NO_3^- + n\overline{[P_{66614}][NO_3]} \rightarrow \overline{[Ln(NO_3)_{3+n}][P_{66614}]_n} \qquad (4.9)$$

The maximum metal loading experiments (Fig. 4.6) were carried out for the individual elements. The concentration of Nd(III) and Dy(III) was kept constant and the amount of ionic liquid was increased. When the number of ionic liquid equivalents in the separation system is less than two, the molar ratio of the ionic liquid over the number of moles of neodymium or dysprosium extracted in the ionic liquid phase remained almost constant at a value of two. This means that

the anionic nitrate complexes of Nd(III) and Dy(III) are extracted formed by two molecules of ionic liquid at maximum loadings, as indicated in equations 4.10 and 4.11.

$$Nd(NO_3)_3 + \overline{2[P_{66614}][NO_3]} \rightarrow \overline{[P_{66614}]_2[Nd(NO_3)_5]} \quad (4.10)$$

$$Dy(NO_3)_3 + \overline{2[P_{66614}][NO_3]} \rightarrow \overline{[P_{66614}]_2[Dy(NO_3)_5]} \quad (4.11)$$

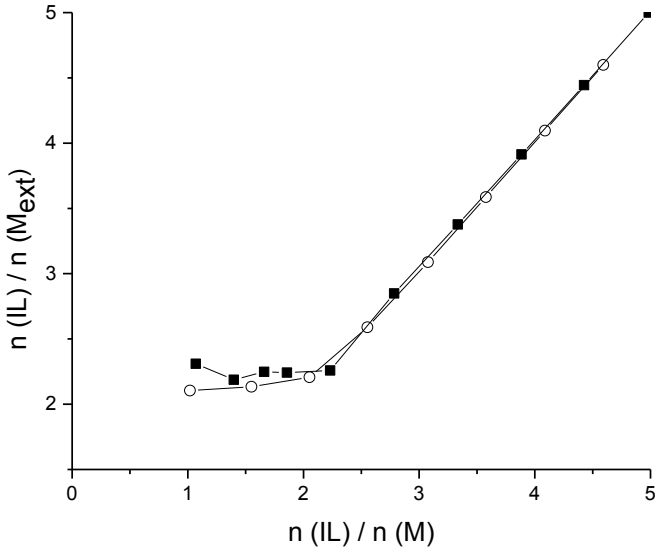

Fig. 4.6. The number of moles of IL over the number of moles of extracted metal ($n(IL)/n(M_{org})$) as a function of the number of ionic liquid equivalents added, at constant initial metal concentrations of neodymium, 1900 rpm, 120 min, 70 °C. Symbols: neodymium (■), dysprosium (○).

As it can be seen in Fig. 4.4, a low percentage of cobalt(II) is still extracted into the ionic liquid together with Nd(III) and Dy(III). Thus, the implementation and optimization of a scrubbing step for the removal of the remaining cobalt is necessary. The following parameters have been optimized for the scrubbing step: shaking speed, concentration of ammonium nitrate, scrubbing time and pH effect. The effect of the NH_4NO_3 concentration in the scrubbing step is shown in Fig. 4.7. An increase in the concentration of the salting-out agent generates higher back-extraction percentages of the remaining Co(II) present in the organic phase. These percentages of

extraction remained almost constant when the NH_4NO_3 concentration was varied between 7 and 10 M. However, when using high concentrations of NH_4NO_3 less Dy(III) and Nd(III) were back-extracted. For this reason, all further scrubbing experiments were carried out using 1 mL of a 10 M NH_4NO_3 solution. Under optimum conditions, Nd(III) and Dy(III) were only back-extracted in extraction percentages of 0.38% and 0.35%, respectively.

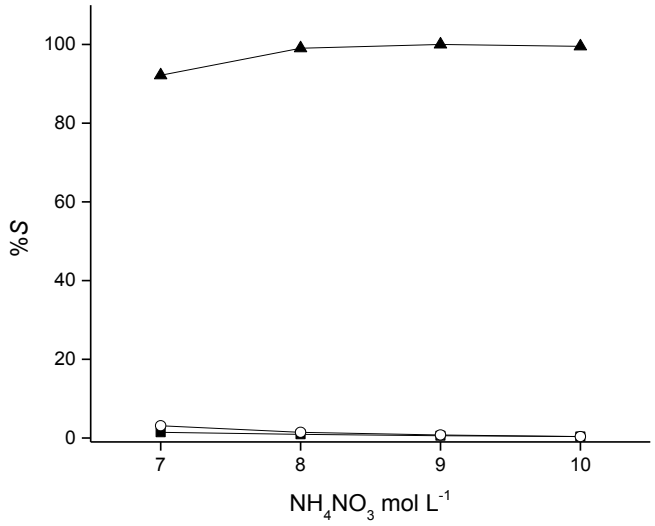

Fig. 4.7. Percentage scrubbing of cobalt(▲), neodymium(■) and dysprosium(○), during the scrubbing step as a function of the concentration of ammonium nitrate. 120 min, 70 °C, 1600 rpm.

Moreover, the purity of the cobalt extract can be further increased by putting the scrubbing aqueous solution containing Co(II) in contact with fresh ionic liquid. Thus a complete removal of Nd(III) and Dy(III) can be achieved. As shown in Fig. 4.8, longer times are required to achieve the total removal of Co(II) from the ionic liquid. This can be explained due to the fact that the viscosity of the ionic liquid loaded with big amounts of Nd(III) and Dy(III) is higher than for the free ionic liquid. Higher temperatures can also be employed, in order to reduce scrubbing times. However, this is not convenient for the scaling up of the process because it would be ideal to have all the extractors working at the same temperature (*e.g.* for simplicity and to avoid losses of heat due to fluctuations in the temperature). A time of 90 min was chosen as the optimum value for the removal of Co(II) from the organic phase.

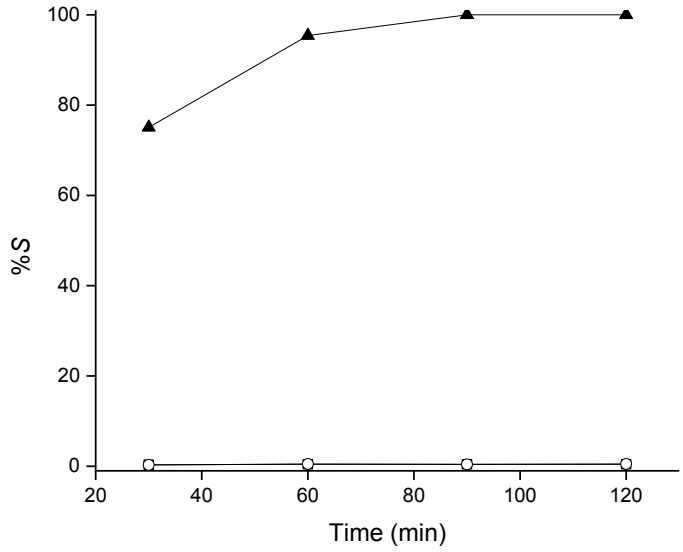

Fig. 4.8. Percentage scrubbing of cobalt(▲), neodymium(■) and dysprosium(○) from the ionic liquid during the scrubbing as a function of the scrubbing time. 70 °C, 1600 rpm. NH_4NO_3 10 M.

As it was previously described in the experimental section, the separated and purified cobalt was recovered by precipitation with oxalic acid and posterior calcination to the corresponding CoO, as it was corroborated by XRD. The purity of the obtained oxide, measured by TXRF was 99.8%, with a yield of 99.4% and Nd as the main impurity.

4.3.3 Separation of Nd(III) and Dy(III)

After having separated and purified cobalt from the magnet leachate, the selective separation between the remaining Dy(III) and Nd(III) has to be performed. With this aim, one can take advantage of the difference in the stability constant that Dy(III) and Nd(III) have for the formation of complexes with EDTA (*i.e.* logarithms of stability constants: 18.0 for Dy(III) and 16.2 for Nd(III)).[42] Indeed, as the affinity of Dy(III) for the EDTA is slightly higher than for Nd(III) this can be used to carry out the stripping of Dy(III) from the organic phase. Chelation with EDTA has been employed for the extraction and separation of rare earths through other different methods.[15,43-45] To explore this possibility, the concentration of EDTA (dissolved as the disodium salt) was varied between 0 and 0.1 M (based on the stoichiometric amount of Dy(III)

present in the ionic liquid), while keeping the concentration of NH_4NO_3 constant at 10 M. The presence of NH_4NO_3 avoided the back-extraction of the Nd(III) into the aqueous phase. As depicted in Fig. 4.9, Dy(III) can be selectively stripped from the organic phase at an EDTA concentration of 0.03 M (and 10 M of NH_4NO_3) with an efficiency of 58.9%. It is important to notice that only a 2.3% of Nd(III) is back-extracted during this procedure.

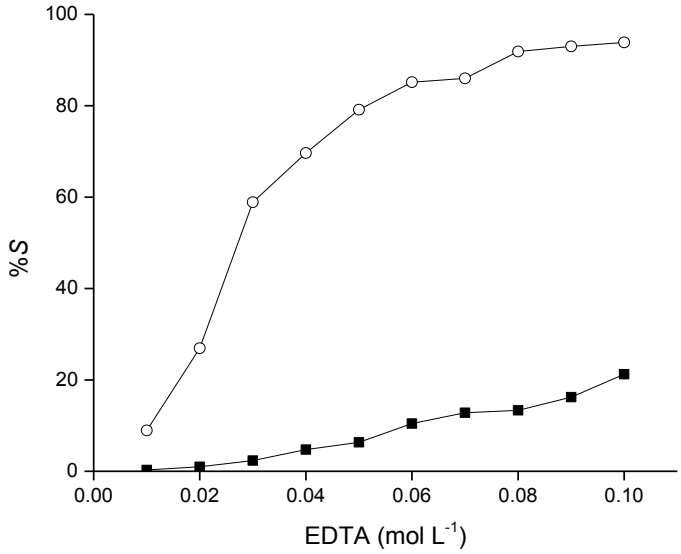

Fig. 4.9. Selective stripping percentage of neodymium (■) and dysprosium (○) as a function of the concentration of EDTA. NH_4NO_3 10 M, shaking speed: 1400 rpm, pH = 5 (initial pH in the aqueous phase) 60 °C.

When only EDTA is employed in absence of NH_4NO_3, no selectivity is achieved for the back-extraction of the rare earths ions. Similar results are observed when only NH_4NO_3 is present at different concentrations and no EDTA is employed.

The temperature effect on the selective stripping of Dy(III) was also studied in the range of 50 to 80 °C. A temperature of 70 °C was chosen since it allowed the obtention of relatively high and low stripping percentages for Dy(III) (79.8%) and Nd(III) (4.0%), respectively. As 70 °C is also the optimized temperature for the other steps, an easier temperature control can be envisaged at a scaled up stage. Another parameter studied for the stripping of Dy(III) was the initial pH in the aqueous phase, which was varied between 0.75 and 7.5. The obtained results show that the pH

does not have any direct effect in the selective stripping of dysprosium(III) when working with a pH from 2.5 to 7. Moreover, it was observed that at pH values higher than 7.5, the extraction could not be carried out because of the formation of a large amount of precipitate. At pH values lower than 2.5, no formation of precipitate was observed, but the stripping efficiency decreased due to the competition of H^+ ions with the rare-earth metal ions for the EDTA.

The stripping time was also evaluated within the range of 5 to 80 min. As the complexation of rare earths with EDTA is fast, it is only required an extraction time of 30 min to carry out this step efficiently (Fig. 4.10).

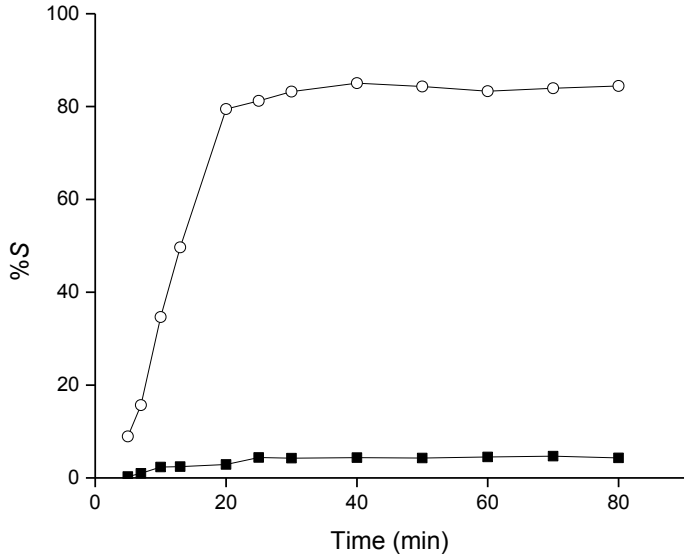

Fig. 4.10. Effect of the scrubbing time in the percentage of selective stripping of Dy(III) (○) and Nd(III) (■). EDTA 0.03 M, NH_4NO_3 10 M. Shaking speed: 1400 rpm, pH = 5 (initial pH in the aqueous phase), 70 °C.

In order to remove the remaining Dy(III) present in the ionic liquid, two more selective stripping steps have to be performed with EDTA and NH_4NO_3. Once the ionic liquid only contains Nd(III), it can be recovered by adding an oxalic acid solution that leads to the formation of a light pink precipitate. Indeed, in only 8 min (at room temperature) the Nd(III) is quantitatively precipitated as the respective oxalate.

$$2\ Nd^{3+} + 3\ H_2C_2O_4 \rightarrow Nd_2(C_2O_4)_3 + 6\ H^+ \qquad (4.12)$$

It was found that a stoichiometric amount of oxalic acid is required (*i.e.* $n(C_2O_4^{2-})/n(Nd^{3+}) = 1.5$) to carry out an effective precipitation of Nd(III) (Fig. 4.11).

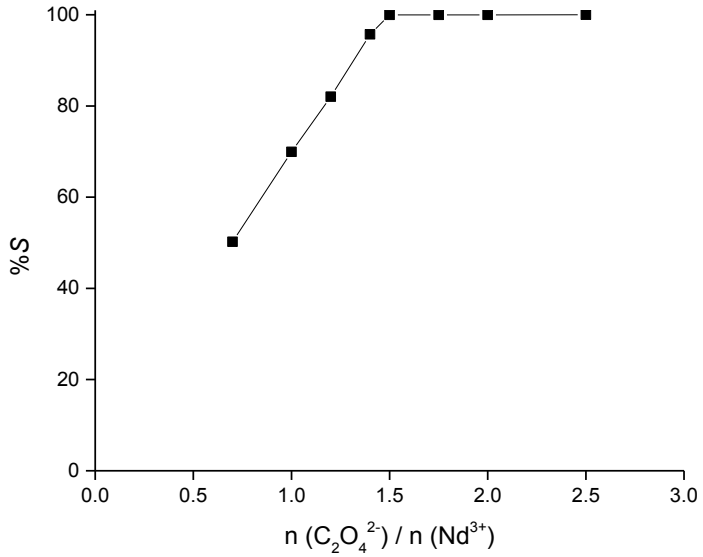

Fig. 4.11. Effect of the ratio $n(C_2O_4^{2-})/nNd^{3+}$ on the percentage of precipitation stripping of Nd(III) from the ionic liquid phase. Shaking speed: 1600 rpm, 23 °C, Time: 10 min.

The obtained precipitate was washed and calcined. The purity of Nd_2O_3 was determined by TXRF and it was found to be 99.6% with the dysprosium as the only impurity. The yield corresponded to 99.3% and it was calculated once the whole process was carried out and all the fractions of neodymium were collected and put together.

Until this point, two of the three major elements in the original leachate have been purified and isolated as oxides. Then Dy(III) remains in the aqueous phase as an EDTA complex. As the magnet is rich in neodymium and has a low amount of dysprosium, it is inevitable that some neodymium also gets back-extracted during the stripping of dysprosium. Even though the stripping percentage of neodymium is low, as it is shown in Fig. 4.10, this is relative because the initial amount of neodymium in the ionic liquid phase is 1000 times larger than the amount of dysprosium. This means that the aqueous phase obtained after the stripping of dysprosium contains a mixture of dysprosium and neodymium that has to be separated through another solvent extraction process.

As $[Nd(EDTA)]^-$ is a less stable complex than $[Dy(EDTA)]^-$, it can be dissociated by the addition of HNO_3 to the aqueous phase, and the Nd(III) that is released can be complexated by the nitrate ions that are present in the ionic liquid. As a result, neodymium(III) can be re-extracted into fresh ionic liquid. This process was optimized in terms of time, concentration of HNO_3 and volume of HNO_3. The optimum conditions found were 20 minutes of extraction time, 16 wt% HNO_3, and 50 μL of HNO_3. Fig. 4.12 shows the effect of the volume of HNO_3 added to the aqueous phase on the extraction percentage of Nd(III) and Dy(III).

This process was carried out three times (in total) in order to remove all the remaining Nd(III), which was further precipitated from the ionic liquid and calcined as described above. The purified Dy(III) in the aqueous phase was precipitated as oxalate and calcined as well. After all the fractions were collected and reunited, Dy_2O_3 was obtained, as confirmed by XRD. The purity of the oxide was analysed by TXRF (99.8%) and the yield of the process was 99.1%.

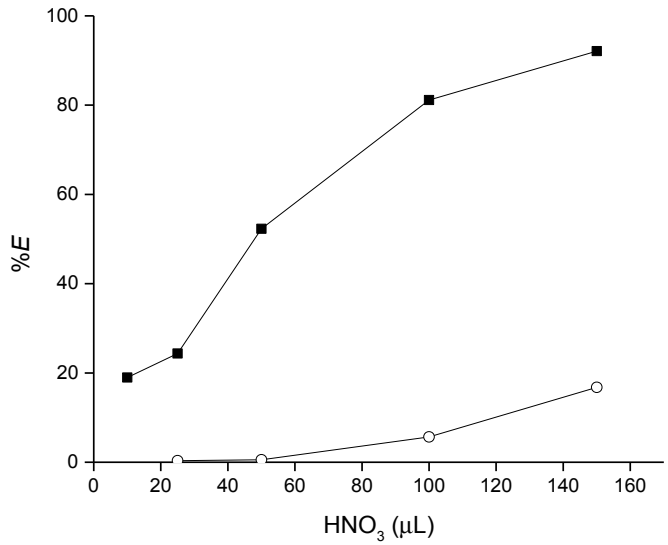

Fig. 4.12. Effect of the volume of nitric acid (16 wt%) added to the aqueous phase on the percentage of extraction of Dy(III) (○) and Nd(III) (■). Shaking speed: 1600 rpm, 70 °C, 40 min.

Finally, free-iron leachates obtained from roasted NdFeB magnets were employed as feed solutions for the separation of rare earths by using the herein implemented liquid-liquid extraction process. The employed experimental conditions corresponded to the optimum ones

determined previously with the synthetic solution. The obtained results are summarized in Table 4.3. High extraction percentages and high rare-earth metal oxide purities were obtained when using the iron-free leachates. For instance, no other impurities were detected on the obtained final oxides, as the concentration of other metals in the starting material was considerably low.

Table 4.3. Percentage of extraction and purity of the oxides obtained when applying the optimized system to leachate samples.

Leachate	Yield Nd_2O_3 % (Purity %)	Yield Dy_2O_3 % (Purity %)	Yield CoO % (Purity %)
Selective leachate at 80 °C	99.2 (99.7)	99.1 (99.8)	99.6 (99.6)
Selective leachate at 22.5 °C	99.3 (99.6)	99.2 (99.6)	99.4 (99.8)

Recycling and recirculation of solvents and reagents is of importance in the industry from both environmental and economic points of view. With this aim, the ionic liquid was recovered and recycled. Once the metals present in the ionic liquid were precipitated with a stoichiometric amount of oxalic acid, then the ionic liquid was washed once with MilliQ water and equilibrated at the desired pH. Table 4.4 summarizes the results obtained for the recycling of the ionic liquid. Three cycles were carried out for the separation of cobalt(II), neodymium(III) and dysprosium(III), the ionic liquid was recovered almost completely after each extraction and it was successfully employed in new cycles of separation without affecting the extraction percentages.

It has to be mentioned that when excesses of oxalic acid are used for the precipitation stripping, the oxalic acid has to be removed first from the ionic liquid in order to avoid precipitation of the rare earths once a new cycle of separations is started. Two methods were tested for the purification of the ionic liquid; the first one comprehends the dilution of the ionic liquid into dichloromethane or toluene and the posterior acid-base extraction with sodium hydroxide. In the second one, the excess of oxalic acid is precipitated with calcium nitrate and then removed after centrifugation. Even though both ways allow the recuperation of the ionic liquid and its reuse

without affecting its efficiency, the second option is easier to carry out and offers an environmentally friendlier approach since it does not involve the use of molecular solvents.

Table 4.4. Recycling of the ionic liquid and efficiency of the separation process using recycled ionic liquid.

Recycle #	Yield Nd_2O_3 % (Purity %)	Yield Dy_2O_3 % (Purity %)	Yield CoO % (Purity %)	Recovery of IL (%)
1	99.2 (99.7)	99.1 (99.8)	99.6 (99.6)	97.8
2	99.3 (99.7)	99.1 (99.6)	99.7 (99.5)	97.2
3	98.9 (99.6)	98.7 (99.6)	99.7 (99.6)	96.8

After the precipitation of dysprosium with oxalic acid, the solution containing EDTA and ammonium nitrate can be recycled. The extraction percentages varied (4.2% for Nd(III), 79.1% for Dy(III) with fresh solution) and (4.5% for Nd(III), 73.8% for Dy(III) with recycled solution). In the same way, the nitric acid employed for the preparation of the leachate can be recovered for its utilization in a new leaching once the cobalt has been precipitated.

Recycling of magnets has a lower environmental impact than mining.[46] Even though the separation of transition metals and rare earths is just a part of the process of the complete recycling chain of NdFeB magnets, it constitutes an important step that can be performed efficiently with more environmental friendly ionic liquids and precipitation stripping methods. Moreover, ionic liquids can be reused without affecting considerably the overall process efficiency. Additionally, phosphonium ionic liquids with nitrate anions, as the one employed in the present work, are not expensive (in comparison to other ionic liquids) and for instance have already been produced in large quantities.[31] With the proposed processes, elements that are required by the industry and usually end up in landfills can be recovered and processed for its use again in NdFeB magnets or any industry requiring of rare-earth elements. Finally, a flow sheet of the process is given in Fig. 4.13.

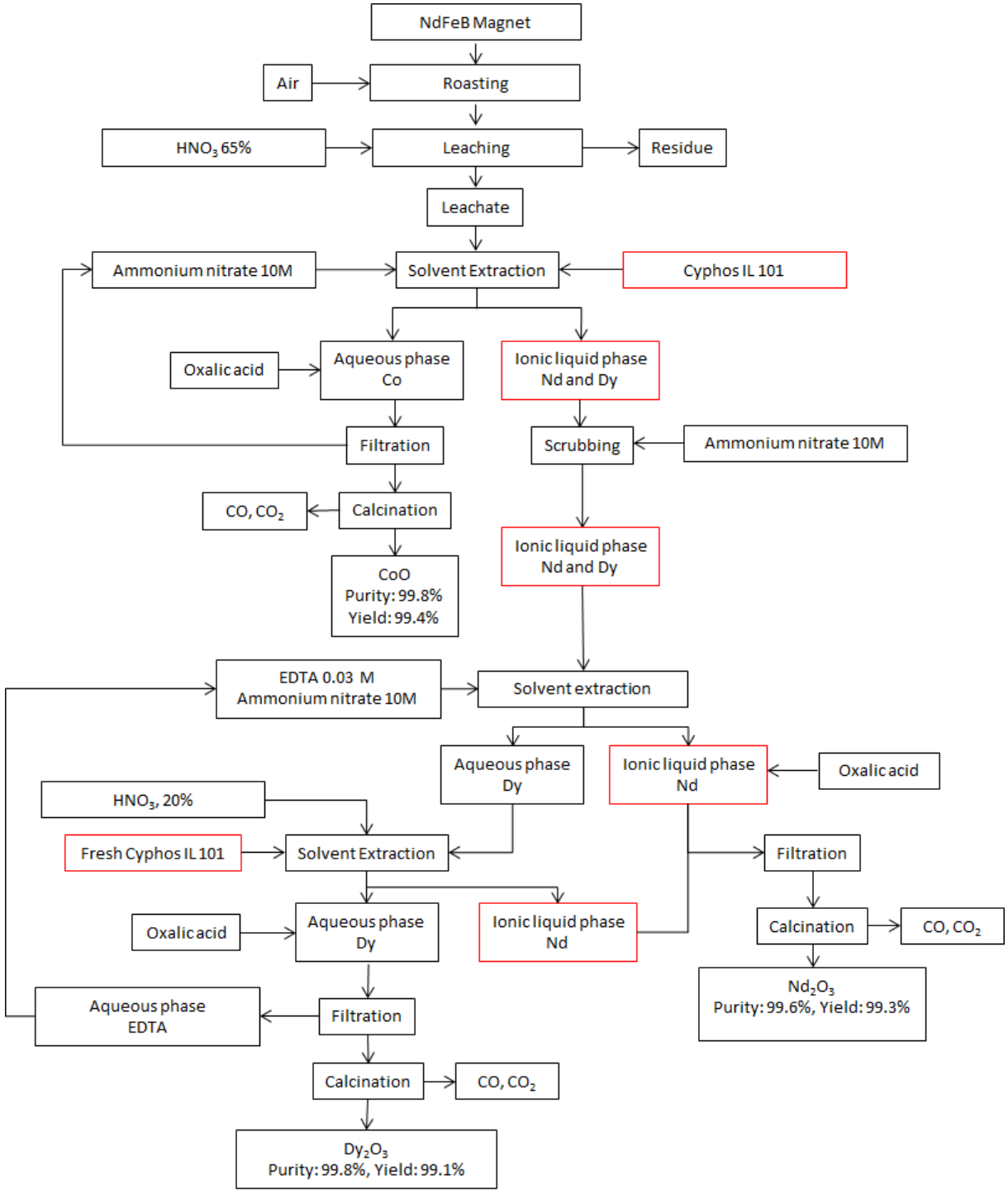

Fig. 4.13. Process flow sheet.

4.4. Conclusions

The ionic liquid trihexyl(tetradecyl)phosphonium nitrate was employed successfully for the liquid-liquid separation of cobalt, neodymium and dysprosium. An efficient and easy to carry out process herein proposed, allowed the recovery of highly valuable metal oxides with high purities, CoO (99.8%), Nd_2O_3 (99.6%), Dy_2O_3 (99.8%). This process was successfully tested in the separation of cobalt(II), neodymium(III) and dysprosium(III) from iron-free leachates in nitric acid. Therefore, it is compatible with the current industrial processes for the separation of rare earths that employ nitric acid leachates and also allows the convenient production of oxalates that can be calcined to produce the respective oxides.

The stripping precipitation consuming only oxalic acid is convenient for the posterior calcination of the products and the obtention of the oxides, as well as, the reuse of the ionic liquid. These oxides are key elements in the recycling chain of permanent magnets because they are the precursors of the alloys needed for the production of the recycled magnets.

The presented process for the separation and recovery of neodymium, dysprosium and cobalt opens the door for the exploration of new and greener systems for the recycling of rare earths in less steps than the currently employed without the use of harmful molecular solvents.

4.5. References

1. K. T. Rim, K. H. Koo and J. S. Park, *Saf. Health Work*, 2013, **4**, 12-26.
2. L. Wang and T. Liang, *Atmos. Environ.*, 2014, **88**, 23-29.
3. U.S., Department of Energy, Critical Materials Strategy, 2011.
4. V. Zepf, Rare earth elements a new approach to the nexus of supply, demand and use: exemplified along the use of neodymium in permanent magnets, Springer, Berlin, 2013.
5. G.-Y. Adachi and N. Imanaka, *Chem. Rev.*, 1998, **98**, 1479-1514.
6. Y. Seo and S. Morimoto, *Resour. Policy*, 2014, **39**, 15-20.
7. J. Li, C. Zhang, Q. Tang, J. Hao, Y. Zhang, Q. Su and S. Wang, *J. Rare Earth*, 2008, **26**, 203-206.
8. D. Brown, B.-M. Ma and Z. Chen, *J. Magn. Magn. Mater.*, 2002, **248**, 432-440.
9. B. Swain, J. Jeong, J.-c. Lee and G.-H. Lee, *Sep. Purif. Technol.*, 2008, **63**, 360-369.

10. S. B. Castor, *Resour. Geol.*, 2008, **58**, 337-347.
11. D. J. Sellmyer, B. Balamurugan, W. Y. Zhang, B. Das, R. Skomski, P. Kharel and Y. Liu, in *PRICM*, John Wiley & Sons, Inc., 2013, pp. 1689-1696.
12. X. Zhang, W. Liu, G. Z. Wei, D. Banerjee, Z. Hu and J. Li, *J. Am. Chem. Soc.*, 2014, **136**, 14230-14236.
13. K. Binnemans, P. T. Jones, K. Acker, B. Blanpain, B. Mishra and D. Apelian, *JOM*, 2013, **65**, 846-848.
14. K. Binnemans, P. T. Jones, B. Blanpain, T. Van Gerven, Y. Yang, A. Walton and M. Buchert, *J. Clean. Prod.*, 2013, **51**, 1-22.
15. F. Xie, T. A. Zhang, D. Dreisinger and F. Doyle, *Miner. Eng.*, 2014, **56**, 10-28.
16. T. P. Thuy Pham, C.-W. Cho and Y.-S. Yun, *Water Res.*, 2010, **44**, 352-372.
17. K. N. Marsh, J. A. Boxall and R. Lichtenthaler, *Fluid Phase Equilib.*, 2004, **219**, 93-98.
18. K. R. Seddon, *J. Chem. Technol. Biot.*, 1997, **68**, 351-356.
19. H. Zhao, S. Xia and P. Ma, *J. Chem. Technol. Biotechnol.*, 2005, **80**, 1089-1096.
20. J. Earle Martyn and R. Seddon Kenneth, in *Clean Solvents*, American Chemical Society, 2002, vol. 819, ch. 2, pp. 10-25.
21. M. Petkovic, K. R. Seddon, L. P. N. Rebelo and C. Silva Pereira, *Chem. Soc. Rev.*, 2011, **40**, 1383-1403.
22. D. Zhao, Y. Liao and Z. Zhang, *CLEAN – Soil, Air, Water*, 2007, **35**, 42-48.
23. M. Freemantle, *Chem. Eng. News*, 1998, **76**, 32-37.
24. G.-c. Tian, J. Li and Y.-x. Hua, *T. Nonferr. Metal. Soc.*, 2010, **20**, 513-520.
25. Z. Kolarik, *Solvent Extr. Ion Exch.*, 2012, **31**, 24-60.
26. P. R. Vasudeva Rao, K. A. Venkatesan, A. Rout, T. G. Srinivasan and K. Nagarajan, *Sep. Sci. Technol.*, 2011, **47**, 204-222.
27. Q. Hu, J. Zhao, F. Wang, F. Huo and H. Liu, *Sep. Purif. Technol.*, 2014, **131**, 94-101.
28. M. G. Freire, C. M. S. S. Neves, I. M. Marrucho, J. o. A. P. Coutinho and A. M. Fernandes, *J. Phys. Chem. A.*, 2009, **114**, 3744-3749.
29. T. Vander Hoogerstraete and K. Binnemans, *Green Chem.*, 2014, **16**, 1594-1606.
30. G. Adamova, R. L. Gardas, L. P. N. Rebelo, A. J. Robertson and K. R. Seddon, *Dalton Trans.*, 2011, **40**, 12750-12764.
31. C. J. Bradaric, A. Downard, C. Kennedy, A. J. Robertson and Y. Zhou, *Green Chem.*, 2003, **5**, 143-152.
32. T. Vander Hoogerstraete, S. Jamar, S. Wellens and K. Binnemans, *Anal. Chem.*, 2014.
33. T. Vander Hoogerstraete, B. Blanpain, T. Van Gerven and K. Binnemans, *RSC Adv.*, 2014, **4**, 64099-64111.

34. W. M. Haynes, D. R. Lide, T. J. Bruno and C. R. C. Press, *CRC handbook of chemistry and physics*, 2013.
35. I. R. Epstein, K. Kustin and L. J. Warshaw, *J. Am. Chem. Soc.*, 1980, **102**, 3751-3758.
36. R. M. Cornell and U. Schwertmann, *The Iron Oxides: Structure, Properties, Reactions, Occurences and Uses*, Wiley-VCH Verlag GmbH & Co. KGaA, 2004.
37. D. Peak and D. L. Sparks, *Environ. Sci. Technol.*, 2002, **36**, 1460-1466.
38. O. Pourret and M. Davranche, *J. Colloid Interface Sci.*, 2013, **395**, 18-23.
39. K. A. Quinn, R. H. Byrne and J. Schijf, *Mar. Chem.*, 2006, **99**, 128-150.
40. L. Zhou, X. H. Liu, H. X. Bai and H. J. Wang, *Chin. Chem. Lett.*, 2011, **22**, 189-192.
41. S. F. Lincoln, D. T. Richens and A. G. Sykes, in *Comprehensive Coordination Chemistry II*, ed. J. A. M. J. Meyer, Pergamon, Oxford, 2003, pp. 515-555.
42. G. Schwarzenbach, *Analyst*, 1955, **80**, 713-729.
43. J. L. Mackey, D. E. Goodney and J. R. Cast, *J. Inorg. Nucl. Chem.*, 1971, **33**, 3699-3706.
44. J. Roosen and K. Binnemans, *J. Mater. Chem. A*, 2014, **2**, 1530-1540.
45. T. Hirokawa, K. Nishimoto, Y. Jie, K. Ito, F. Nishiyama, N. Ikuta and S. Hayakawa, *J. Chromatogr. A*, 2001, **919**, 417-426.
46. B. Sprecher, Y. Xiao, A. Walton, J. Speight, R. Harris, R. Kleijn, G. Visser and G. J. Kramer, *Environ. Sci. Technol.*, 2014, **48**, 3951-3958.

Chapter 5. Separation of neodymium and dysprosium using a phosphonium thiocyanate ionic liquid combined with neutral extractants: a process relevant for the recycling of end-of-life NdFeB magnets

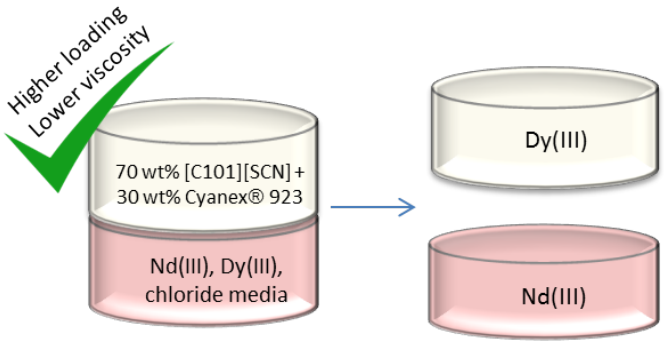

ABSTRACT-A solvent extraction system based on the combination of the ionic liquid trihexyl(tetradecyl)phosphonium thiocyanate ([C101][SCN]) and the neutral extractants Cyanex® 923 and tri-*n*-butyl phosphate (TBP) has been investigated for the separation of Nd(III) and Dy(III) in chloride media. High distribution ratios and separation factors were obtained when using Cyanex® 923 diluted in [C101][SCN] wt% 30:70. The addition of Cyanex® 923 to the ionic liquid brings four main advantages: 1) it enhances the distribution ratios of the rare earths, 2) it decreases the viscosity of the organic phase, therefore it improves the mass transfer, 3) it increases the loading capacity of the ionic liquid and 4) it improves the phase disengagement. Different extraction parameters such as concentration of Cyanex® 923, concentration of chloride in the aqueous phase, equilibration time, pH effect, scrubbing agent and stripping agent were optimized. McCabe-Thiele diagrams were constructed to determine the number of stages needed for the separation of Nd(III) and Dy(III). Stripping of Dy(III) from the organic phase was easily achieved with water. The ionic liquid combined with Cyanex® 923 was recycled up to three times without losing its efficiency. As a result, this process offers a more environmentally friendly alternative for the separation of Nd(III) and Dy(III) than the conventional systems in which molecular solvents are employed as diluents.

Based on the paper
Sofía Riaño, Koen Binnemans. "Separation of neodymium and dysprosium using a phosphonium thiocyanate ionic liquid combined with neutral extractants: a process relevant for the recycling of end-of-life NdFeB magnets". (To be submitted to Hydrometallurgy)

Author contributions:
S.R. performed the experimental work, data analysis and wrote the article.

5.1 Introduction

The rare earth elements (REEs) are a group of 17 metals containing scandium, yttrium and the 15 lanthanides that can be classified into two categories, namely light rare earths elements (LREEs) and heavy rare earths elements (HREEs).[1] The fabrication of permanent magnets based on REEs has gained a considerable attention during the last decades because it has led to the consecution of powerful magnets with improved properties. Around 20% of the consumption of rare earths is employed in neodymium iron boron (NdFeB) permanent magnets that are used in wind turbines, electric motors, hard disc drives, loudspeakers, etc.[2-5] Recycling of rare earths can help mitigate the balance problem and provide supply for scarce elements that are difficult to mine and avoid exhaustion of geological resources.[2,6-11] Magnets can be recycled by manual dismantling or by fragmenting the device that contains the magnet and the magnet itself using shedders. Afterwards, the rare earths can be leached out from these fragments and purified through solvent extraction.[2,3,12,13]

Since the middle fifties, rare earths have been separated into groups or individual elements using different methods such as selective precipitation, solvent extraction and ionic exchange.[14-16] Solvent extraction is one of the most common employed methodologies nowadays, in general, three different kinds of extractants are widely employed in solvent extraction: cation exchangers (acidic extractants), anion exchangers (basic extractants) and solvating extractants (neutral extractants). Carboxylic acids and derivatives of phosphorous acids are acidic extractants usually employed for the separation of rare earths in hydrochloric media, the efficiency of the extraction is pH dependent and usually the stripping process has to be carried out by using concentrated acids.[16-21] Another disadvantage is that at high metal loadings and low acidities, gels can be formed in the organic phase making difficult the separation process.[16] Basic extractants such as primary amines and tertiary amines have been used to extract rare earths as anionic complexes from sulfate and nitrate media. The rare earths can be easily stripped from the loaded organic phase.[20,22-24] Neutral extractants are preferred over acidic and basic extractants to avoid pH influence, as well as high consumption of acid during the stripping steps and gel formation in the organic phase when working at high metal loadings.[2,16,25-27]

Neutral extractants such as tri-*n*-butyl phosphate (TBP) have been widely used for the separation of metal ions.[28] The extractability of the rare earth ions with tributyl phosphate TBP increases

with increasing the atomic number and the extraction is more efficient from nitrate solutions than from chloride solutions. In this kind of extraction, the rare earths in a neutral nitrato complex are coordinated by the phosphoryl group of the TBP.[29] Cyanex® 923 is another neutral extractant that consists of a mixture of different trialkyl phosphine oxides and has been employed in the extraction of mineral acids and metal ions.[30] Cyanex® 923 has been used diluted in heptane to extract lanthanum from nitrate media, the extraction is independent of the pH in the aqueous solution and the mechanism of extraction is similar to the one of TBP.[30] Commercially, Cyanex® 923 and TBP have been also employed for the separation of rare earths from impurities such as calcium in nitric acid.[31] A study on the effect of the diluents in the separation of Pr(III) and Sm(III) with Cyanex® 923 has shown that the extraction percent of the rare-earth ions from nitrate media decreases while increasing the dielectric constant of the diluent.[32]

Ionic liquids (ILs) are organic salts which consist entirely of ions and with melting points below 100 °C. They are characterized for their chemical stability, negligible vapor pressure and low flammability, reasons why they have been used as green solvents in solvent extraction.[33-36] Additionally, they are electrically conductive, which means that there is no risk of accumulating static electricity.[37] Ionic liquids have been mostly used to separate the rare earths from other metals ions, but lately they have also been applied to the separation of rare earths into individual elements.[24,35,38-48] Ionic liquids can be used in split-anion extractions, a new approach in which the ionic liquid phase is used as the source of complex-forming anions. The biggest advantage of this approach is that ionic liquids containing anions such as thiocyanate or nitrate can be used to separate rare-earth mixtures from chloride aqueous media without the need of using acidic extractants.[49] The latter is due to the fact that thiocyanate and nitrate anions have a strong affinity for the organic phase, while chloride anions will remain in the aqueous phase.[50] Indeed, the ionic liquid phase needs to be rich in anions capable to form extractable complexes since the aqueous phase lacks of those anions. In this approach, the rare-earth ions are coordinated by thiocyanate or nitrate ions in the ionic liquid phase, while the chloride ions remain dissolved in the organic phase as counter anions for the ionic liquid cations that are not involved in the extraction of the rare-earth complex. The separation can be easily fine-tuned by the choice of the chloride concentration in the aqueous phase and the stripping can be carried out with water.

Ionic liquids have been used in combination of di(2-ethylhexyl) 2-ethylhexyl phosphonate (DEHEHP), TBP and Cyanex® 925 to enhance the separation of rare-earth ions, increase the extraction capacity and decrease the viscosity of the organic phase.[51-53] In this paper, the effect of molecular extractants on the extraction and separation of rare earths using split-anion was investigated. Since hydrophobic and low viscous ionic liquids with high availability are needed for the development of these processes, phosphonium and quaternary ammonium cations with long alkyl chains combined with nitrate and thiocyanate anions were employed. Special attention was paid to the effect on distribution ratios and separation factors between the rare earths that are most commonly found in NdFeB magnets. Effects on the viscosity and kinetics of the systems were also studied.

5.2 Experimental

5.2.1 Materials and methods

Tricaprylmethylammonium chloride (Aliquat 336, [A336][Cl], 88.2-90.6%), nitric acid (≥ 65%, p.a.) and KSCN (99%) were purchased from Sigma-Aldrich (Diegem, Belgium). KNO_3 (>99%) and tri-*n*-butyl phosphate (TBP) (97%) from Chem-Lab Analytical (Zedelgem, Belgium), trihexyl(tetradecyl)phosphonium chloride (Cyphos IL 101, [C101][Cl], 97.7%) and Cyanex® 923 (93%) were obtained from Cytec Industries (Canada), $Dy(NO_3)_3 \cdot 6H_2O$ (99%) and oxalic acid (99%) were purchased from Acros Oganics (Geel, Belgium), Toluene (99.8%, HPLC grade) and hydrochloric acid (37%, reagent grade) was obtained from Fischer Chemical (UK). $Nd(NO_3)_3 \cdot 6H_2O$ (99%) was obtained from Alfa Aesar (Karlsruhe Germany), $NdCl_3 \cdot 6H_2O$ (99.9%) and $DyCl_3 \cdot 6H_2O$ (99.9%) were obtained from Strem Chemicals (Newburyport, USA). Standard solutions of individual elements (1000 mg L^{-1}) for inductively coupled plasma optical emission spectrometer (ICP-OES) and $CaCl_2 \cdot 2H_2O$ (>99%) were obtained from Merck (Overijse, Belgium). The silicone solution in isopropanol was obtained from SERVA Electrophoresis GmbH (Heidelberg, Germany). Pure water (MilliQ, Millipore, >18 MΩ cm^{-1}) was employed to make all the dilutions. All chemicals were used as received without further purification.

5.2.2 Equipment and characterization

The extraction experiments were performed in 4 mL vials and using a temperature controllable Turbo Thermo Shaker (Model: TMS-200, Hangzhou Allsheng Instrument Co. Ltd., China). The separation of the aqueous and organic phases was speeded up by centrifugation using a Heraeus Megafuge 1.0 centrifuge. Viscosities and densities were measured using an automatic rolling-ball viscosity meter Lovis (Model 2000 M/ME, with a density measuring module MA 4500 ME, Anton Paar GmbH, Graz, Austria). A volumetric Karl Fischer titrator Mettler-Toledo with Stromboli oven operating at 150 °C was used with HYDRANAL®-Composite 5 one-component reagent to determine the water content of the ionic liquids. Analysis of the aqueous phase was performed using a Perkin Elmer Optima 8300 inductively coupled plasma optical emission spectrometer (ICP-OES) in dual view, with a GemTip CrossFlow II nebulizer, a Scott Spray Chamber Assembly, a sapphire injector and a Hybrid XLT ceramic torch. The calibration curve was constructed by fitting through the origin using standard solutions of Nd(III) and Dy(III) prepared in a 1 M HNO3 solution at four different concentrations: 2.5, 5, 10 and 20 mg L–1. Samples of the aqueous phase were prepared by taking an aliquot of 100 µL and diluting it to 10 mL with a 1 M HNO3 solution. A sample of 1 mL of this solution was further diluted to 10 mL with the 1 M HNO3 solution to measure Nd(III), which was in higher concentrations. All measurements were performed in triplicate. The chloride concentration in the organic phase was determined with a bench top total reflection X-ray fluorescence (TXRF) spectrometer (S2 Picofox, Bruker). All the pH measurements were performed using an S220 Seven Compact pH/Ion meter (Mettler-Toledo) and a Slimtrode (Hamilton) electrode.

5.2.3 Solvent extraction

To prepare thiocyanate forms of the ionic liquids, the chloride ionic liquids were preequilibrated three times with a 3 M KSCN solution to exchange the chloride ions for thiocyanate ions. Afterwards, the thiocyanate ionic liquid was washed three times with pure water. This resulted in the water saturated forms of [C101][SCN] and [A336][SCN]. To obtain the nitrate forms of the ionic liquids, the same procedure was followed by using a 3 M KNO_3 solution. The chloride concentration after the equilibrations in these ionic liquid phases was checked by TXRF and was below the detection limits of the TXRF spectrometer.[54] For the solvent extraction experiments, a synthetic solution was prepared by dissolving $NdCl_3 \cdot 6H_2O$ and $DyCl_3 \cdot 6H_2O$ in water, HCl was added to help the dissolution, the final pH of the aqueous solution was 2.5 and the final

concentrations were 64 g L^{-1} Nd(III) and 14 g L^{-1} Dy(III). These concentrations were chosen so that the ratio between the elements mimicked the ratio that is found in some NdFeB magnets. Batch experiments were carried out by contacting 1 mL of the aqueous phase with 1 mL of the organic phase (70% [C101][SCN], 30% Cyanex® 923) unless otherwise is stated in closed 4 mL vials. The vials were shaken at 25 °C and 2000 rpm during 60 min, unless otherwise is stated. Afterwards, the samples were centrifuged and the phases were separated. A sample of the aqueous phase was taken, diluted and measured with ICP-OES. For the scrubbing experiments, the loaded organic phase, 25 g L^{-1} Nd(III) and 9 g L^{-1} Dy(III), was put in contact with 1 mL of scrubbing agent (water, different concentrations of $CaCl_2$) in 4 mL closed vials, and shaken during 60 min at 25 °C. After separation of the phases, a sample of the aqueous phase was taken, diluted and measured with ICP-OES. The maximum loading of Dy(III) and Nd(III) in the undiluted [C101][SCN] or the organic phase containing [C101][SCN] and Cyanex® 923 (70:30 wt%) was determined by equilibrating the organic phase with a solution of Nd(III) and Dy(III), total concentration 14 g L^{-1} in 3.0 M $CaCl_2$ and then removing and measuring the aqueous phase after equilibrium. The organic phase was equilibrated again with fresh solution of the total rare earths and the aqueous phase was removed and measured again. This procedure was repeated six times. The extraction of Nd(III) from the aqueous phase at different concentrations of $CaCl_2$ to [C101][NO_3] was studied from a solution containing 41 g L^{-1} of Nd(III). The recycling was carried out by extracting from a solution containing 64 g L^{-1} Nd(III), 14 g L^{-1} Dy(III) and 3.0 M $CaCl_2$ to the organic phase and stripping completely with water (2 steps), then the organic phase containing [C101][SCN] and Cyanex® 923 (70:30 wt%) was reused in a new cycle of separations.

5.2.4 Theory

The distribution ratio (D) in case of equal volumes is defined as follows:

$$D = \frac{[M]_{org}}{[M]_{aq}} = \frac{[M]_i - [M]_{aq}}{[M]_{aq}} \qquad (5.1)$$

where $[M]_i$ is the initial metal ion concentration in the aqueous phase. $[M]_{aq}$ is the metal ion concentration in the aqueous phase after the extraction. The percentage extraction ($\%E$) is defined as the amount of metal ion extracted to the organic phase over the initial amount of metal ion in case of equal volumes and can be expressed as:

$$\%E = \frac{[M]_i - [M]_{aq}}{[M]_i} \times 100 \qquad (5.2)$$

The efficiency of the separation of two metals can be described with the separation factor α, in which D_{M1} and D_{M2} correspond to the distribution ratios D of metals M_1 and M_2, respectively, $D_{M1}>D_{M2}$:

$$\alpha_{M_1M_2} = \frac{D_{M_1}}{D_{M_2}} \qquad (5.3)$$

5.3. Results and discussion

5.3.1 Extraction parameters

Two different molecular extractants, namely TBP and Cyanex® 923 were tested to study their effect on the separation of Nd(III) and Dy(III) using the split-anion approach. One of the advantages of the split-anion extraction is that it offers the possibility to extract rare earths from chloride solutions using basic extractants. The latter is very useful for the design and development of separation processes, since hydrochloric acid is easier to recycle and thus to be used in a closed-loop process than nitric acid for instance.[49] Therefore, the separation of Nd(III) and Dy(III) was first studied from a chloride media to the undiluted ionic liquid [A336][NO_3] alone or combined with Cyanex® 923 or TBP. The main obtained results are presented in Table 5.1.

Table 5.1. Distribution ratios and separation factors of Nd(III) and Dy(III) to different organic phases.

Organic phase	D_{Nd} [a]	D_{Dy} [a]	$\alpha_{Nd/Dy}$
[A336][NO_3]	0.38	0.20	1.90
[A336][NO_3]:TBP wt% 90:10	0.41	0.22	1.86
[[A336][NO_3]:Cyanex® 923 wt% 90:10	0.44	0.29	1.52

[a] Equilibration time: 60 min, 2000 rpm, 25 °C, Concentration of $CaCl_2$ in the aqueous phase = 2.5 M.

From Table 5.1 it can be seen how the addition of TBP or Cyanex® 923 to the ionic liquid slightly increases the distribution ratios of both metals. The distribution ratio of Nd(III) changes

from 0.38 in the undiluted ionic liquid to 0.41 when 10 wt% TBP is added, and to 0.44 when 10 wt% Cyanex® 923 is added. However, since the distribution ratios of Dy(III) are also increasing the separation factors decrease. In this case the undiluted ionic liquid offers the best separation factor. This could be due to the fact that the extraction of rare earths from nitrate media follows a negative sequence (*i.e.* the LREES are extracted more than the HREES), in contrast to the fact that Cyanex® 923 and TBP extract from nitrate media following a positive sequence (*i.e.* the HREES are extracted more than the LREES).[16,49,55]

Taking into account that the separation of rare earths from chloride media when employing [C101][SCN] or [A336][SCN] follows a positive sequence, which means that Dy(III) is preferentially extracted, the addition of TBP and Cyanex® 923 was studied in thiocyanate-based ionic liquids and the results are presented in Table 5.2.

Table 5.2. Distribution ratios and separation factors of Nd(III) and Dy(III) to different organic phases.

Organic phase	D_{Nd} [a]	D_{Dy} [a]	$\alpha_{Dy/Nd}$
[A336][SCN]	0.27	0.54	2.11
[A336][SCN]:TBP wt% 90:10	0.28	0.59	2.10
[A336][SCN]:Cyanex® 923 wt% 90:10	0.32	0.72	2.25
[C101][SCN]	0.16	0.37	2.31
[C101][SCN]:TBP wt% 90:10	0.19	0.49	2.57
[C101][SCN]:Cyanex® 923 wt% 90:10	0.23	0.79	3.43

[a] Equilibration time: 60 min, 2000 rpm, 25 °C, Concentration of $CaCl_2$ in the aqueous phase = 2.5 M.

Comparing the results from Table 5.1 and Table 5.2, it can be seen that the separation is more efficient when using ionic liquids with thiocyanate anions than when using ionic liquids with nitrate anions. Thiocyanate-based ILs had larger separation factors than the nitrate-based ILs. The fact that the distribution ratios are higher for Dy(III) than for Nd(III) in the thiocyanate-based systems is also beneficial in the case of the recycling of NdFeB magnets since it will facilitate the removal of the low amount of dysprosium present in the magnet. When extracting to [A336][SCN], higher distribution factors for Dy(III) and Nd(III) are obtained than in the case of

[C101][SCN], but the separation factors are smaller. This is because ammonium ILs trend to extract the light rare earths more strongly than the phosphonium ILs, which is in part due to the fact that the ammonium ionic liquid has a higher loading capacity due to its lower molecular mass. Besides this, the aqueous media has a high content of Nd(III) (*i.e.* 64 g L^{-1}) which is 4.5 times the amount of Dy(III) present (*i.e.* 14 g L^{-1}). The addition of TBP to the thiocyanate-based ionic liquids slightly increased the distribution ratios. Instead, the addition of Cyanex® 923 increased the distribution ratios and separation factors for both thiocyanate-based ionic liquids due to the stronger capacity of extraction of Cyanex® 923. Since larger separation factors were obtained when using Cyanex® 923 combined with the ionic liquid [C101][SCN], it was decided to further optimize this system for the separation of Nd(III) and Dy(III).

The effect of the concentration of Cyanex® 923 in [C101][SCN] on the extraction was studied only from 0 to 50 wt%, since percentages higher than 50 wt.% resulted in the formation of a third phase.

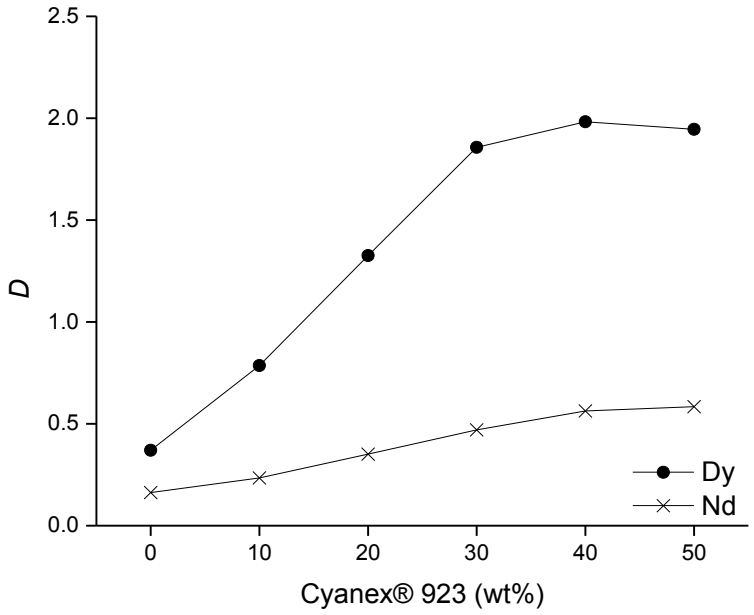

Fig. 5.1. Effect of the concentration of Cyanex® 923 diluted in [C101][SCN] on the separation of Nd(III) and Dy(III) in 2.5 M $CaCl_2$. Equilibration time: 60 min. Shaking speed: 2000 rpm at 25 °C.

From Fig. 5.1, it can be seen how the distribution ratios of both metals increase while increasing the concentration of Cyanex® 923 in [C101][SCN] and especially for Dy(III). The separation factors also increase up to a concentration of 30 wt% Cyanex® 923 (α=3.95), after this concentration the separation factors decrease as well as the distribution ratios due to the decrease of the thiocyanate concentration in the organic phase. A concentration of 30 wt% was chosen as optimal.

The chloride concentration has a major impact on the distribution ratios and can be used to fine-tune the extraction. Therefore the effect of the concentration of $CaCl_2$ in the aqueous phase was studied (Fig. 5.2).

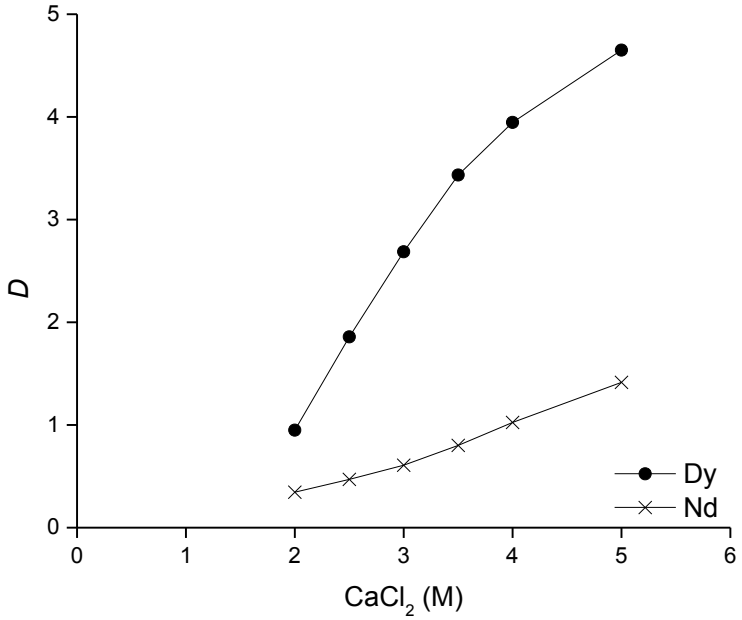

Fig. 5.2. Effect of the concentration of $CaCl_2$ on the separation of Nd(III) and Dy(III). Equilibration time: 60 min. Shaking speed: 2000 rpm at 25 °C, 30 wt% Cyanex® 923 in [C101][SCN].

In a split anion extraction process, the thiocyanate ions in the ionic liquid phase coordinate the rare earths because under the conditions of the present extraction, the rare-earth ions form more easily extracted complexes with thiocyanate ions than with chloride ions. Therefore, the addition of $CaCl_2$ to the aqueous phase has a major impact on the distribution ratios of dysprosium. The

best separation factors were obtained when working with a concentration of 3 M $CaCl_2$ (α = 4.42). When working at higher concentrations than 3 M, the selectivity is lost due to the co-extraction of neodymium. The marked effect that the concentration of $CaCl_2$ has over the distribution factors is also an indication that it could be used for the stripping and the scrubbing steps.

The next parameter evaluated was the kinetics of the extraction and the results are presented in Fig. 5.3.

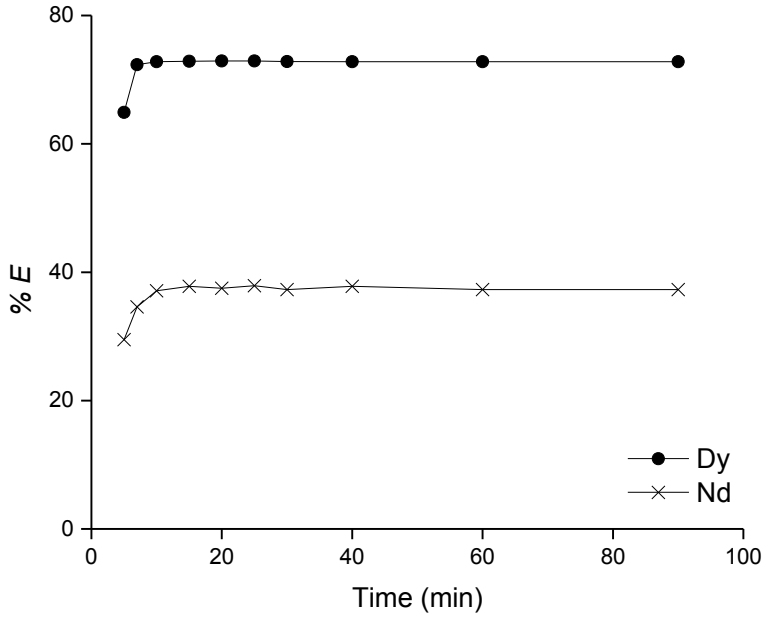

Fig. 5.3. Kinetics of extraction of Nd(III) and Dy(III) from a 3 M $CaCl_2$ matrix to an organic phase composed of 30 wt% Cyanex® 923, 70 wt% [C101][SCN] Shaking speed: 2000 rpm at 25 °C.

The separation equilibrium is reached somewhere in between 7 and 10 min (Fig. 5.3), which is a short time confirming the feasibility and potential of proposed system. For the study of the pH effect on the distribution ratios of Nd(III) and Dy(III), different pH values between 0.25 and 4 were evaluated.

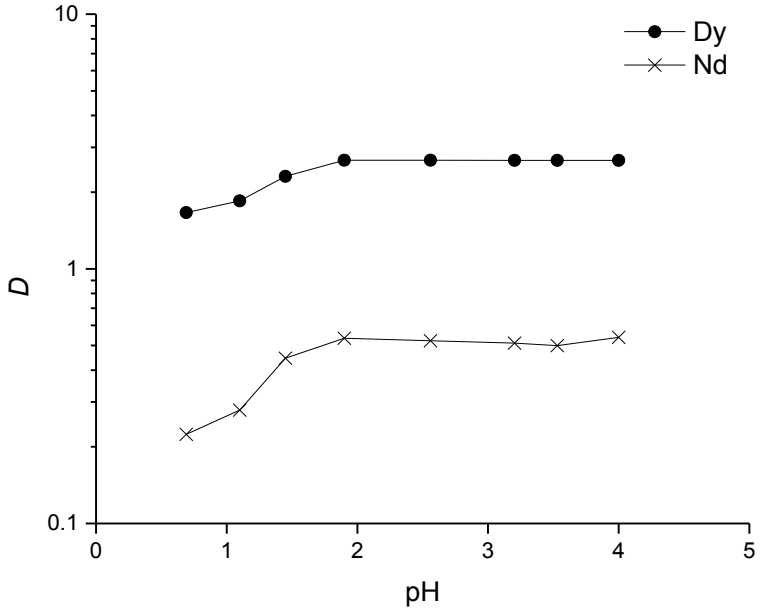

Fig. 5.4. Distribution ratio of Dy(III) and Nd(III) as a function of the equilibrium pH. $CaCl_2$ in the aqueous phase 3.0 M, 22 °C, 15 min equilibration time.

As it can be seen in Fig. 5.4, the pH did not have a significant effect in the percentage extraction. Below a pH of 1.5 the distribution ratios decreased for both metals probably due to the competition between the extraction of protons and the extraction of the metal complex by the neutral extractant.[56] Above pH values equal to 2, the distribution ratios remained constant and therefore a pH of 2 was chosen as optimal. pHs higher than 5 are not recommended since at these values the rare earths can undergo hydrolysis.

When studying the influence of the concentration of Cyanex® 923 it was observed how the addition of it decreased the viscosity of the organic phase and also accelerated the phase disengagement (except at concentrations higher than 50 wt% in which a third phase was formed). For this reason it was decided to compare the viscosity of the loaded undiluted ionic liquid [C101][SCN] against the viscosity of the loaded organic phase composed of Cyanex® 923 30 wt% and [C101][SCN] 70 wt%. The loading capacity of the organic phases was calculated by contacting them with a solution containing 14 g L^{-1} total concentration of rare earths, after equilibrium, the aqueous phase was removed and the previously loaded organic phase was contacted again with fresh solution. This process was repeated 6 times to reach a maximum

loading capacity. The results obtained regarding the loading capacity are presented in Table 5.3 and the viscosity values of the organic phases before and after loading are reported in Table 5.4.

Table 5.3. Loading capacity of the organic phase (Cyanex® 923 30 wt% and [C101][SCN] 70 wt%).

Organic phase	Total loading (g L^{-1})[a]
[C101][SCN]	26.3
70 wt% [C101][SCN] + 30 wt% Cyanex® 923	39.8

[a] $CaCl_2$ in the aqueous phase = 3 M, 25 °C, shaking speed: 2000 rpm.

Table 5.4. Viscosities of the organic phases before and after loading at 25 °C.

Organic phase	Viscosity (cP)
[C101][SCN]	391
70 wt% [C101][SCN] + 30 wt% Cyanex® 923	220
[C101][SCN] loaded with 26.3 g L^{-1} REE	958
70 wt% [C101][SCN] + 30 wt% Cyanex® 923 loaded with 39.8 g L^{-1} REE	468

The loading capacity of the organic phase is an important parameter in split-anion extraction. This is because the HREES have a crowing effect on the extraction of LREES (i.e. the rare earths with higher D values displaces the ones with lower D values at high loading values). The total loading increased from 26.3 g L–1 to 39.8 g L–1 when adding 30 wt% Cyanex® 923 (Table 5.3). This effect is most likely due to the greater solubility of the extracted rare earth complexes in the ionic liquid phase due to the presence of Cyanex® 923. At the same time, the addition of Cyanex® 923 decreased the viscosity of the loaded organic phase and improved the phase disengagement. The high loading, the low viscosity and the easy phase disengagement are parameters that are crucial in solvent extraction. In industrial processes in which concentrated

feeds are treated, higher loading capacities are beneficial because allow to increase the process capacity.

A McCabe Thiele diagram was constructed to determine the number of stages required to separate Dy(III) from Nd(III) with the optimized system. As a result, it was estimated that two stages would be needed for the removal of Dy(III) using an O:A ratio of 1:1 (Fig. 5.5).

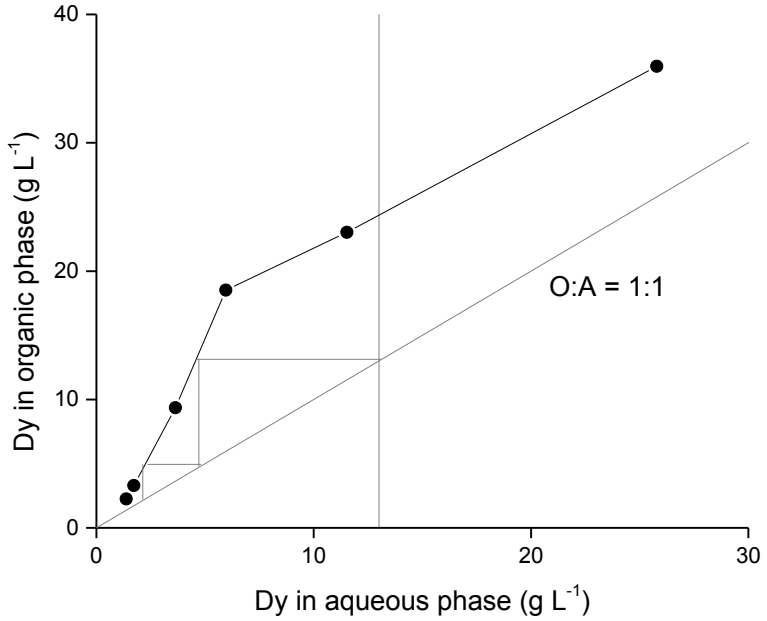

Fig. 5.5. McCabe-Thiele diagram for the extraction of dysprosium from a mixture of Dy(III) and Nd(III) to the organic phase (30 wt% Cyanex® 923 and 70 wt% [C101][SCN]). $CaCl_2$ in the aqueous phase = 3.0 M. Phase contact time: 30 min, O:A ratios varied between ratios between 0.5:5 and 5:1.5).

5.3.2 Scrubbing and Stripping

The next parameters investigated were the stripping and the scrubbing of Nd(III). Scrubbing is important since due to the large content of Nd(III) in the aqueous phase, it can get coextracted along Dy(III). Taking into account that large concentrations of chloride ions increase the

distribution of Dy(III) in the organic phase, the effect of the concentration of $CaCl_2$ on the percentage scrubbing was studied.

Table 5.5. Percentage of scrubbing (%*S*) of Nd(III) and Dy(III) from the loaded organic phase (70 wt% [C101][SCN] and 30 wt% Cyanex® 923) using $CaCl_2$.

$CaCl_2$ (M)	%*S* Nd(III)[a]	%*S* Dy(III)[a]
5.0	9.6	0.99
4.0	25.5	9.06
3.0	53.3	38.6
2.0	75.9	66.7
1.0	93.6	90.5
Water	99.8	97.7

[a] Equilibration time 60 min, 25 °C, 2000 rpm.

From Table 5.5, it can be seen how different concentrations of $CaCl_2$ can offer selectivity in the scrubbing step. For instance, high concentrations of $CaCl_2$ allow the scrubbing of Nd(III) while keeping most of the Dy(III) in the loaded organic phase. Concerning the stripping, it can be seen in Table 5.5 that it can be achieved with water or with a diluted solution of $CaCl_2$ since the presence of the salt helps additionally the phase disengagement.

Up to this point it has been shown how Dy(III) can be extracted, refined and stripped from the initial rare earth mixture. However, a part of Nd(III) will still remain in the aqueous phase together with calcium(II). Another advantage of the split anion approach is that it allows the possibility to change the organic phases depending on the needs of the extraction, for example the distribution ratios of Nd(III) are larger when extracting to nitrate-based ionic liquids than when extracting to thiocyanate-based ionic liquids (Tables 5.1 and 5.2). Therefore, the aqueous phase containing Nd(III) can be contacted with [C101][NO_3] or [A336][NO_3] to separate it from Ca(II) (see Table 5.6).

From Table 5.6, it can be seen how the addition of $CaCl_2$ to the aqueous feed can be beneficial for the extraction of Nd(III). The percentage extraction of Ca(II) was very low and without significant deviations between the percentage extraction using the phosphonium or the ammonium forms of the ionic liquid. After extraction with [C101][NO3], Nd(III) can be stripped from the loaded ionic liquid using water as well (i.e. with a stripping efficiency up to 99.6%).

Table 5.6. Percentage extraction Nd(III) from aqueous phases containing different concentrations of $CaCl_2$ to [A336][NO_3] and [C101][NO_3].

Organic phase	Aqueous phase $CaCl_2$ (M)	*%E* Nd [a]	*%E* Ca [a]
[A336][NO_3]	3.0	25.6	0.09
	4.0	56.7	0.12
	5.0	92.9	1.41
[C101][NO_3]	3.0	27.5	0.05
	4.0	57.9	0.27
	5.0	93.2	0.90

[a] 60 min equilibration time, pH aqueous phase = 2, Nd(III) 41 g L^{-1}

5.3.3 Mechanism of extraction

In general, the mechanism of extraction of a split-anion extraction of a rare-earth ion Ln^{3+} can be written as follows,[49]

$$Ln^{3+} + 3SCN^- + (x-3)\overline{PR_4SCN} \rightarrow \overline{\left(\left(\left(PR_4{}^+\right)_{(x-3)}\right)\left((Ln(SCN)_x)^{3-x}\right)\right)} \qquad (5.4)$$

The bars in the equation mean that the species is in the organic phase, and $x \geq 3$. Due to an anion exchange between the aqueous and the ionic liquid phase there is small amount of SCN^- anions in the aqueous phase. The extracted complex is probably formed in the aqueous phase rather than in the ionic liquid, therefore coordinated water molecules could be present in the extracted species.

On the other hand, Cyanex® 923 can form complexes of the form Ln(SCN)3·n(Cya) with n=4 and 3 for the light and heavy rare earths, respectively when extracting to Cyanex® 923 diluted in xylene.57 If the solvating mechanism is assumed for all the complexation reactions with Cyanex® 923, slope analysis can be used to determine the number of molecules of Cyanex® 923 that are involved in the extraction.

$$Ln^{3+} + 3SCN^{-} + \overline{n(Cya)} \rightarrow \overline{Ln(SCN)_3 \cdot n(Cya)} \qquad (5.5)$$

$$K = \frac{\overline{Ln(SCN)_3 \cdot n(Cya)}}{[Ln^{3+}][SCN^{-}]^3\overline{[n(Cya)]}} \qquad (5.6)$$

Replacing by *D* and taking the logarithm,

$$\log D = n\log[Cya] + 3\log[SCN] + \log K \qquad (5.7)$$

By plotting log*D* vs. log[Cyanex® 923] it is possible to determine the number of molecules of Cyanex® 923 involved in the solvation of the extracted complex. The slope analysis was carried out for dysprosium (Fig. 5.6.).

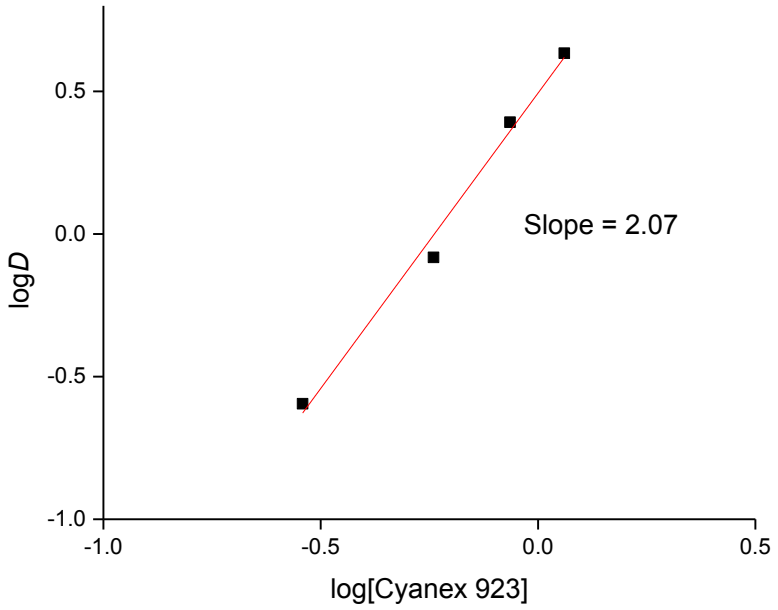

Fig. 5.6. Distribution ratios for 14 g L^{-1} Dy(III) in a 3 M chloride solution as a function of the concentration of Cyanex® 923 varied between 0.28 - 1.15 M.

The slope obtained is 2.07, meaning that 2 molecules of Cyanex® 923 would be solvating the extracted species. However, different species can be formed when extracting to ionic liquids[58] and the slope analysis method has limitations. A correct way to determine the structure of the complexes that are being extracted would be using extended X-ray absorption fine structure (EXAFS).

5.3.3 Recycling of the organic phase

The organic phase composed of 70 wt% [C101][SCN] and 30 wt% Cyanex® 923 was recovered after the stripping of dysprosium and recycled. With this aim, the ionic liquid was re-equilibrated with acidulated water to a pH = 2 and then contacted again with fresh feed. This procedure was repeated three times. The distribution ratios remained almost the same (0.61 ± 0.06 for Nd(III) and 2.69 ± 0.15 for Dy(III), which indicates the feasibility of recycling the organic phase. It has to be highlighted that the prolonged exposition of thiocyanate ionic liquids to sunlight and high temperatures leads to some degradation of the thiocyanate ions.[49] No degradation was observed

(constant distribution ratios) in the experiments carried out at 25°C. As a precaution, the thiocyanate ionic liquids were stored in the dark. Finally, a flow sheet of the complete process is given in Fig. 5.7.

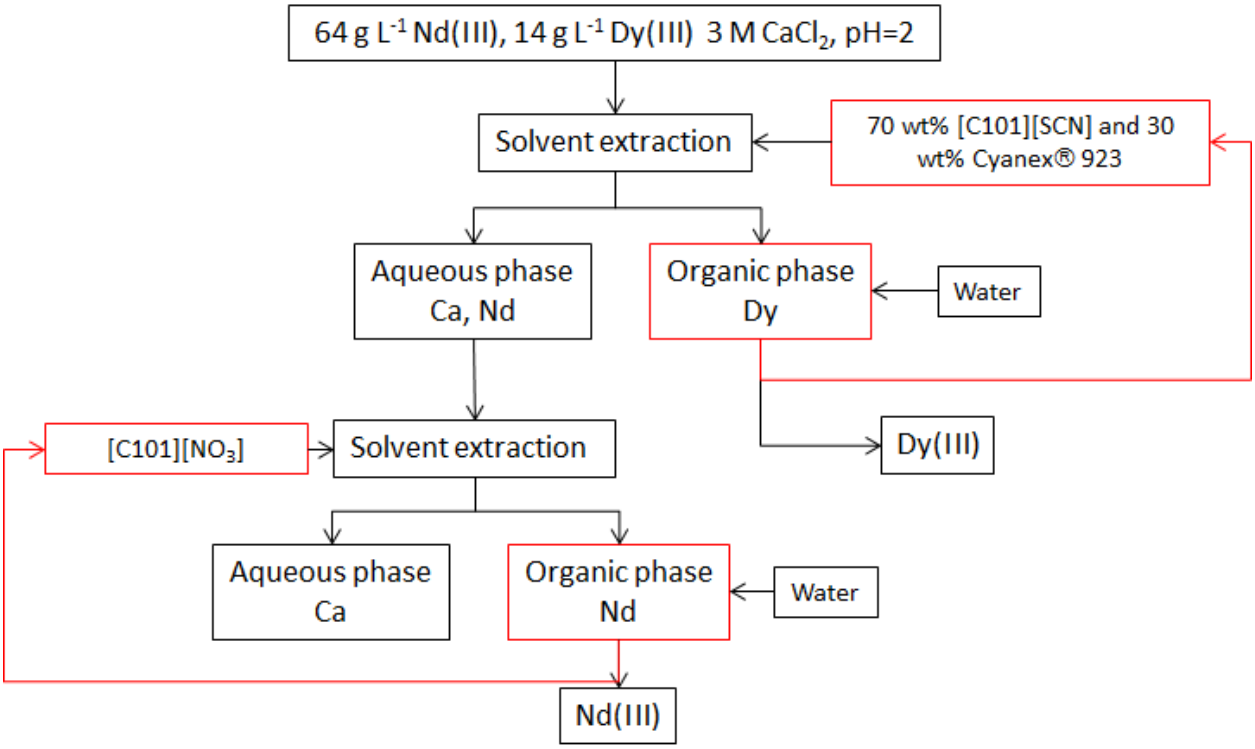

Fig. 5.7. Flow sheet of the developed and optimized process for the extraction and purification of Nd(III) and Dy(III) mixtures in highly concentrated chloride media.

5.4. Conclusions

This paper proposes an environmentally friendly process based on the ionic liquid trihexyl(tetradecyl)phosphonium thiocyanate combined with Cyanex® 923 for the separation of Nd(III) and Dy(III) from highly concentrated chloride aqueous solutions. By introducing Cyanex® 923 into the system, the distribution ratios of Dy(III) increased, a higher metal loading was allowed while decreasing the viscosity and enhancing the phase disengagement process. As a result, the presented process is of relevance for the separation of Nd(III) and Dy(III) from used NdFeB magnets. Dy(III) was separated from Nd(III) by using [C101][SCN] combined with

Cyanex 923 and easily stripped with water. Nd(III) was recovered from the aqueous phase using the ionic liquid [C101][NO_3]. The latter demonstrated one of the biggest advantages of split-anion extractions: since the organic phase is the source of the complexing anion and not the aqueous phase, different extractions can be carried out from the same type of feed by changing the source of complexing anions in the organic phase. The proposed strategy is compatible with current industrial processes for the separation of rare earths elements from chloride media allowing the separation of two critical metals in few steps.

5.5. References

1. A. Golev, M. Scott, P. D. Erskine, S. H. Ali and G. R. Ballantyne, *Resour. Policy*, 2014, **41**, 52-59.

2. K. Binnemans, P. T. Jones, B. Blanpain, T. Van Gerven, Y. Yang, A. Walton and M. Buchert, *J. Clean. Prod.*, 2013, **51**, 1-22.

3. Y. Yang, A. Walton, R. Sheridan, K. Güth, R. Gauß, O. Gutfleisch, M. Buchert, B.-M. Steenari, T. Van Gerven, P. T. Jones and K. Binnemans, *J. Sustain. Metall.*, 2017, **3**, 122-149.

4. D. Brown, B.-M. Ma and Z. Chen, *J. Magn. Magn. Mater.*, 2002, **248**, 432-440.

5. V. Zepf, Rare earth elements a new approach to the nexus of supply, demand and use: exemplified along the use of neodymium in permanent magnets, Springer, Berlin, 2013.

6. E. Machacek, J. L. Richter, K. Habib and P. Klossek, *Resour. Conserv. Recy.*, 2015, **104**, 76-93.

7. K. Binnemans, P. T. Jones, K. Acker, B. Blanpain, B. Mishra and D. Apelian, *JOM*, 2013, **65**, 846-848.

8. A. Golev, M. Scott, P. D. Erskine, S. H. Ali and G. R. Ballantyne, *Resour. Policy*, 2014, **41**, 52-59.

9. A. Rollat, D. Guyonnet, M. Planchon and J. Tuduri, *Waste Manage.*, 2016, **49**, 427-436.

10. G. G. Zaimes, B. J. Hubler, S. Wang and V. Khanna, *ACS Sustain. Chem. Eng*, 2015, **3**, 237-244.

11. J. H. Rademaker, R. Kleijn and Y. Yang, *Environ. Sci. Technol.*, 2013, **47**, 10129-10136.

12. B. Sprecher, Y. Xiao, A. Walton, J. Speight, R. Harris, R. Kleijn, G. Visser and G. J. Kramer, *Environ. Sci. Technol.*, 2014, **48**, 3951-3958.

13. J. Kooroshy, G. Tiess, A. Tukker and A. Walton, *Strenghthening of the European Rare Earths Supply-chain,*, The european rare earths competency network (ERECON), 2015.
14. K. A. Gschneidner, J. C. G. Bünzli and V. K. Pecharsky, *Handbook on the Physics and Chemistry of Rare Earths*, Elsevier, Amsterdam, 2006.
15. C. K. Gupta and N. Krishnamurthy, *Int. Mater. Rev.*, 1992, **37**, 197-248.
16. F. Xie, T. A. Zhang, D. Dreisinger and F. Doyle, *Miner. Eng.*, 2014, **56**, 10-28.
17. Y. Wang, F. Li, Z. Zhao, Y. Dong and X. Sun, *Sep. Purif. Technol.*, 2015, **151**, 303-308.
18. X. Wang, W. Li and D. Li, *J. Rare Earth.*, 2011, **29**, 413-415.
19. S. Radhika, B. N. Kumar, M. L. Kantam and B. R. Reddy, *Sep. Purif. Technol.*, 2010, **75**, 295-302.
20. R. Safarbali, M. R. Yaftian and A. Zamani, *J. Rare Earth.*, 2016, **34**, 91-98.
21. M. Anitha, M. K. Kotekar, D. K. Singh, R. Vijayalakshmi and H. Singh, *Hydrometallurgy*, 2014, **146**, 128-132.
22. M. Černá, E. Volaufová and V. Rod, *Hydrometallurgy*, 1992, **28**, 339-352.
23. J. Liu, W. Wang and D. Li, *Colloids Surf., A*, 2007, **311**, 124-130.
24. Y. Zuo, J. Chen and D. Li, *Sep. Purif. Technol.*, 2008, **63**, 684-690.
25. K. Larsson, C. Ekberg and A. Ødegaard-Jensen, *Hydrometallurgy*, 2013, **133**, 168-175.
26. D. F. Haghshenas, D. Darvishi, H. Rafieipour, E. K. Alamdari and A. A. Salardini, *Hydrometallurgy*, 2009, **97**, 173-179.
27. W. Liao, Q. Shang, G. Yu and D. Li, *Talanta*, 2002, **57**, 1085-1092.
28. K. R. Barnard, N. J. Kelly and D. W. Shiers, *Hydrometallurgy*, 2014, **146**, 1-7.
29. D. F. Peppard, J. P. Faris, P. R. Gray and G. W. Mason, *J. Phys. Chem.*, 1953, **57**, 294-301.
30. T. Hui, L. De-qian, W. Yi-ge and L. Jia-heng, *Wuhan Univ. J. Nat. Sci.*, 2003, **8**, 871-874.
31. S. E. E. A.W. Al-Shawi, O.B. Jenssen, T.R. Jorgensen, M., *Proc. ISEC 2002*, 2002, **2**, 1064–1069.
32. Y. A. El-Nadi, *J. Rare Earth.*, 2010, **28**, 215-220.
33. J. Earle Martyn and R. Seddon Kenneth, *Pure Appl. Chem.*, 2000, **72**, 1391.
34. G.-T. Wei, Z. Yang and C.-J. Chen, *Anal. Chim. Acta*, 2003, **488**, 183-192.

35. T. Vander Hoogerstraete, S. Wellens, K. Verachtert and K. Binnemans, *Green Chem.*, 2013, **15**, 919-927.
36. L. Zaijun, C. Jie, S. Haixia and P. Jiaomai, *Rev. Anal. Chem.*, 2007, **26**, 109.
37. J. N. Chubb, P. Lagos and J. Lienlaf, *J Electrostat.*, 2005, **63**, 119-127.
38. Y. Baba, F. Kubota, N. Kamiya and M. Goto, *J. Chem. Eng. Jpn.*, 2011, **44**, 679-685.
39. D. Dupont and K. Binnemans, *Green Chem.*, 2015, **17**, 856-868.
40. T. Vander Hoogerstraete and K. Binnemans, *Green Chem.*, 2014, **16**, 1594-1606.
41. T. Vander Hoogerstraete, B. Blanpain, T. Van Gerven and K. Binnemans, *RSC Adv.*, 2014, **4**, 64099-64111.
42. S. Riano and K. Binnemans, *Green Chem.*, 2015, **17**, 2931-2942.
43. X. Q. Sun, B. Peng, J. Chen, D. Q. Li and F. Luo, *Talanta*, 2008, **74**, 1071-1074.
44. X. Sun, C.-L. Do-Thanh, H. Luo and S. Dai, *Chem. Eng. J.*, 2014, **239**, 392-398.
45. Y. Wang, C. Huang, F. Li, Y. Dong, Z. Zhao and X. Sun, *Sep. Purif. Technol.*, 2016, **162**, 106-113.
46. Y. Liu, J. Chen and D. Li, *Sep. Sci. Technol.*, 2012, **47**, 223-232.
47. Y. Dong, X. Sun, Y. Wang, C. Huang and Z. Zhao, *ACS Sustain. Chem. Eng*, 2016, **4**, 1573-1580.
48. L. Guo, J. Chen, L. Shen, J. Zhang, D. Zhang and Y. Deng, *ACS Sustain. Chem. Eng*, 2014, **2**, 1968-1975.
49. K. Larsson and K. Binnemans, *Hydrometallurgy*, 2015, **156**, 206-214.
50. D. Dupont, D. Depuydt and K. Binnemans, *J. Phys. Chem. B*, 2015, **119**, 6747-6757.
51. J. Chen, C. Huang, Y. Wang, B. Huang and X. Sun, *J. Rare Earth.*, 2016, **34**, 1252-1259.
52. X. Sun, D. Wu, J. Chen and D. Li, *J. Chem. Technol. Biotechnol.*, 2007, **82**, 267-272.
53. Y. Xiong, W. Kuang, J. Zhao and H. Liu, *Sep. Purif. Technol.*, 2017, **179**, 349-356.
54. T. Vander Hoogerstraete, S. Jamar, S. Wellens and K. Binnemans, *Anal. Chem.*, 2014, **86**, 1391-1394.
55. M. Reddy, R. Luxmi Varma, T. Ramamohan, S. K. Sahu and V. Chakravortty, *Solvent Extr. Ion Exc.*, 1998, **16**, 795-812.
56. A. M. Wilson, P. J. Bailey, P. A. Tasker, J. R. Turkington, R. A. Grant and J. B. Love, *Chem. Soc. Rev.*, 2014, **43**, 123-134.

57. M. L. P. Reddy, R. Luxmi Varma, T. R. Ramamohan, S. K. Sahu and V. Chakravortty, *Solvent Extr. Ion Exc.*, 1998, **16**, 795-812.
58. C. H. C. Janssen, N. A. Macías-Ruvalcaba, M. Aguilar-Martínez and M. N. Kobrak, *Int. Rev. Phys. Chem.*, 2015, **34**, 591-622.

Chapter 6. Separation of rare earths and other valuable metals from deep-eutectic solvents: a new alternative for the recycling of used NdFeB magnets

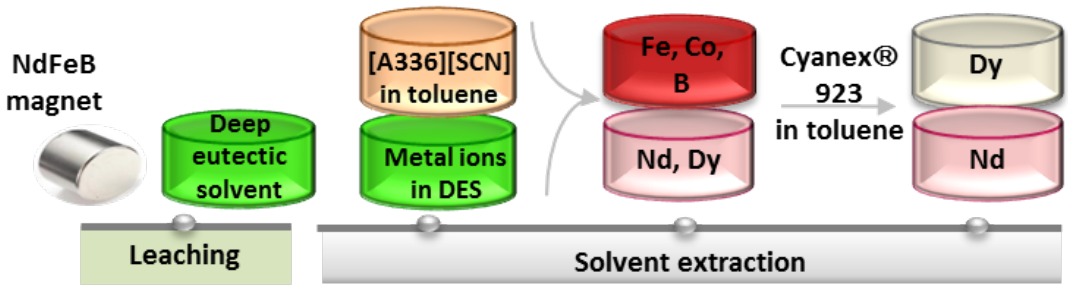

ABSTRACT-Deep-eutectic solvents (DESs) are used as a promising alternative to aqueous solutions for the recovery of valuable metals from NdFeB magnets. A deep-eutectic solvent based on choline chloride and lactic acid (molar ratio 1:2) was used for the leaching of rare earths and other metals from NdFeB magnets. A process for the separation of Fe, B and Co from Nd and Dy in the deep-eutectic solvent was developed by using the ionic liquid tricaprylmethylammonium thiocyanate (Aliquat 336 SCN, [A336][SCN]) diluted in toluene (0.9 M). The extraction parameters were optimized and stripping of B was efficiently carried out by HCl, while EDTA was employed for the recovery of Fe and Co. The separation of Nd and Dy was assessed by using two different types of extractants, a mixture of trialkylphosphine oxides (Cyanex® 923) and bis(2-ethylhexyl)phosphoric acid (D2EHPA). Based on the distribution ratios, separation factors and the easiness of the subsequent stripping, Cyanex® 923 was chosen as the most adequate extractant. The purified Dy present in the less polar phase was easily recovered by stripping with water, while the Nd present in the deep-eutectic solvent was recovered by precipitation stripping with a stoichiometric amount of oxalic acid. Nd_2O_3 and Dy_2O_3 were recovered with a purity of 99.87% and 99.94%, respectively. The feasibility to scale up this separation process was corroborated by a setup of mixer-settlers. The new proposed system based on a deep-eutectic solvent combined with traditional organic extraction phases presented higher selectivities and efficiencies than the analogous aqueous system. Extended X-

ray absorption fine structure (EXAFS) was employed to elucidate the different mechanisms for extraction of Co and Fe from the deep-eutectic solvent and from an aqueous solution.

Based on the submitted paper
Sofía Riaño, Martina Petranikova, Bieke Onghena, Tom Vander Hoogerstraete, Dipanjan Banerjee, Mark R.StJ. Foreman, Christian Ekberg, and Koen Binnemans.
"Separation of rare earths and other valuable metals from deep-eutectic solvents: a new alternative for the recycling of used NdFeB magnets". (Submitted to Dalton Transactions)

Author contributions:
S.R. performed the experimental work, data analysis and wrote the article. B.O. and T.V.D.H. solved the EXAFS data of Co and Fe, respectively.

6.1 Introduction

The recycling of rare-earth permanent magnets continues to be of high importance since it represents a promising strategy against the global supply crisis of rare-earth elements.[1] During the last years, the environmental and economic benefits of NdFeB magnet recycling have been discussed, analyzed and investigated.[1-4] Diverse methodologies have been proposed, including the use of mechano-chemical treatment without external heating,[5] the recovery of neodymium from NdFeB magnets at high temperatures using molten magnesium metal as extractant[6] and hydrogen gas to separate the NdFeB magnets from waste.[7-10] As an alternative to these processes, rare earths and other valuable metals present in magnet scrap can be recovered and purified through leaching and solvent extraction.[3,11-13] The separation and purification of metals by solvent extraction is a well-known strategy that has been used at laboratory and industrial scale for decades.[14-21] To start the separation process, a leachate or a concentrate containing the metals of interest must be obtained. With this aim, strong mineral acids and bases, leaching agents such as cyanide or chelating agents are normally used to leach the metals into an aqueous solution that is later processed by solvent extraction.[11,22-25] The metal ions are extracted into an organic phase that usually consists of an extractant, a molecular solvent, and if needed, a phase modifier (to avoid the formation of a third phase and/or to improve phase disengagement).[17] In case non-target metals are co-extracted together with the desired metals, a scrubbing step can be performed to improve the purity of the previously obtained organic phase. The metal ions can be removed from the organic phase using an appropriate striping agent. Afterwards, they can be precipitated and calcined in order to obtain metal oxides.

In solvent extraction, attention has been paid to the replacement of commonly used organic solvents. New organic phases that provide new and tunable functionalities to improve the selectivity and efficiency of the extraction process are preferred, especially when they benefit workplace safety and are less harmful to the environment. With this aim, ionic liquids have been successfully employed as an organic phase in solvent extraction for the purification of metal ions, including transition metals and rare-earth elements.[11-13,26-33] In contrast, less effort has been made in order to replace the aqueous phase by other liquid media able to facilitate the separation process. Deep-eutectic solvents (DESs) could act as a new functionalized, more polar phase for the leaching, solvent extraction, separation and purification of metal ions.[34-37]

DESs are systems formed from a eutectic mixture of Lewis or Brønsted acids and bases which can contain a variety of anionic and/or cationic species.[36] DESs have been defined by Abbott *et al.*[38] with the general formula $R_1R_2R_3R_4N^+X^-\cdot Y$ and can be classified into four different groups: (1) type I, in which Y corresponds to $ZnCl_2$, $SnCl_2$, $AlCl_3$, $GaCl_3$, $FeCl_3$; (2) type II, in which hydrated metal halides are used as for instance Y = $MCl_x\cdot yH_2O$, M = Cr, Co, Cu, Ni, Fe; (3) type III, in which Y is an hydrogen bond donor (HBD) that can be an amide, alcohol or carboxylic acid; (4) type IV, in which DESs are composed of metal chlorides mixed with HBDs such us urea, ethylene glycol, acetamide or hexanediol. DESs are structurally different from ionic liquids (ILs) which are composed entirely by ions and usually contain only one type of anion and cation.[36,39] Ionic liquids and DESs share some common physical properties such as low vapor pressure and non-flammability. Besides these properties, DESs are easier and cheaper to prepare than ionic liquids since their synthesis relies on the mixture of two components which is 100% atom economic (beneficial for their scaling up and industrial use). Moreover, DESs have excellent dissolution properties due to their ability to donate or accept electrons or protons to form hydrogen bonds.[36,39] DESs are able to selectively dissolve various metal oxides depending on the deep eutectic solvent that is employed.[34,40] This makes DESs good candidates for the dissolution of end-of-life NdFeB magnets.

In this paper the preparation of a NdFeB magnet leachate with a deep-eutectic solvent (choline chloride and lactic acid, molar ratio 1:2, see Fig 6.1) and a subsequent solvent extraction procedure for the separation of neodymium, dysprosium, iron, cobalt and boron from the leachate in two steps are reported for the first time. In the first step, the ionic liquid [A336][SCN] diluted in toluene (0.9 M) is employed for the extraction of iron, cobalt and boron. Afterwards, Cyanex® 923 diluted in toluene (0.9 M) is employed for the separation of neodymium and dysprosium. One of the main advantages of this process is that the leaching can be carried out using a cheap and easily available solvent that can be re-used or easily discarded since its components are biodegradable. Moreover, higher distribution ratios are obtained when extracting from deep-eutectic solvent media than from conventional aqueous feeds. The system is versatile. First, only the transition metals and B are separated and afterwards, dysprosium can be separated. Neodymium remaining in the deep-eutectic solvent can be easily stripped. The feasibility of the proposed extraction was tested in larger scale by using a mixer-settler setup.

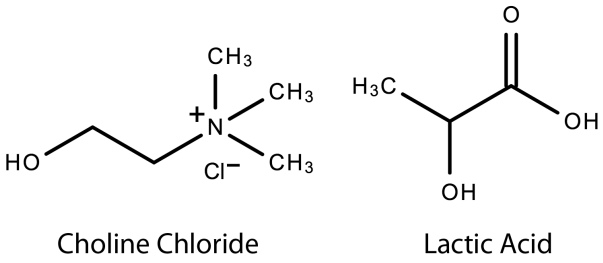

Fig 6.1. Chemical structure of choline chloride and lactic acid.

6.2 Experimental

6.2.1 Materials and methods

Tricaprylmethylammonium chloride (Aliquat® 336, 88.2-90.6%), nitric acid (≥ 65%, p.a.), bis(2-ethylhexyl) phosphate (D2EPHA, 97%) and KSCN (99%) were obtained from Sigma-Aldrich (Diegem, Belgium). Cyanex® 923 (93%) was obtained from Cytec Industries (Canada), tri-n-butyl phosphate (97%) from Chem-Lab Analytical (Zedelgem, Belgium), choline chloride (99%), L(+)-lactic acid (90%), iron(III) chloride (98%), citric acid (99.6%), disodium ethylenediaminetetraacetate dihydrate (99%), sulfuric acid (96%), $CoCl_2 \cdot 6H_2O$ (99.9%) and oxalic acid (99%) was purchased from Acros Oganics (Geel, Belgium). Toluene (99.8%, HPLC grade) and hydrochloric acid (37%, reagent grade) was obtained from Fischer Chemical (UK). Boric acid (99%) was obtained from VWR Chemicals (Leuven, Belgium). Solvent 70 was obtained from Statoil (Norway). $NdCl_3 \cdot 6H_2O$ (99.9%) and $DyCl_3 \cdot 6H_2O$ (99.9%) were obtained from Strem Chemicals (Newburyport, USA). Standard solutions of individual elements (1000 mg L^{-1}) for ICP analysis and $CaCl_2 \cdot 2H_2O$ were obtained from Merck (Overijse, Belgium). Pure water (MilliQ, Millipore, >18 MΩ cm^{-1}) was employed to make all the dilutions. All chemicals were used as received without further purification.

6.2.2 Equipment and characterization

A disc mill (Benelux Scientific) was used to ground the magnet pieces, which were later sieved to obtain <400 μm powders. A planetary ball mill (Retsch PM4000, 5 mm stainless steel balls) was used to further grind the samples to obtain a particle size below 100 μm. The ball-milling conditions were: 30:1 ball-to-powder ratio (g/g), 2 h duration at 200 rpm. A muffle furnace was used for roasting (950 °C, 15 h). Leaching experiments were conducted in 4 mL vials, with magnetic stirring. After leaching, the samples were centrifuged in a Heraeus Megafuge 1.0

centrifuge at 5000 rpm during 3 min to separate the residue from the leachate. Solvent extraction experiments were carried out in temperature controllable Turbo Thermo Shakers (Model: TMS-200, Hangzhou Allsheng Instrument Co. Ltd, China). ^{1}H NMR spectra were recorded on a Bruker Avance 300 spectrometer, operating at a frequency of 300 MHz. Samples for ^{1}H NMR measurements were prepared in deuterated dimethyl sulfoxide (DMSO-d_6). UV-VIS absorption spectra were recorded with a Varian Cary 5000 spectrophotometer. The viscosity and density of the DES was measured using an automatic rolling-ball viscosity meter Lovis (Model 2000 M/ME, with a density measuring module MA 4500 ME, Anton Paar GmbH, Graz, Austria). A volumetric Karl Fischer titrator Mettler Toledo with Stromboli oven operating at 150 °C was used with HYDRANAL®-Composite 5 one-component reagent to determine the water content of the DES. Analysis of the deep-eutectic solvent phase was performed using a Perkin Elmer Optima 8300 inductively coupled plasma optical emission spectrometer (ICP-OES) in dual view, with a GemTip CrossFlow II nebulizer, a Scott Spray Chamber Assembly, a sapphire injector and a Hybrid XLT ceramic torch. The calibration curve was constructed by fitting through the origin using standard solutions of Fe, Co, Nd and Dy prepared in a 1 M HNO_3 solution at four different concentrations: 2.5, 5, 10 and 20 mg L^{-1}. Samples of the deep-eutectic solvent phase were prepared by taking an aliquot of 300 µL and diluting it to 10 mL with a 1 M HNO_3 solution. A sample of 1 mL of this solution was further diluted to 10 mL with the 1 M HNO_3 solution in case of more concentrated solutions. All measurements were performed in triplicate.

Extended X-ray Absorption Fine Structure (EXAFS) spectra of the Fe K-edge (7112 eV) and Co K-edge (7709 eV) were collected at the Dutch-Belgian Beamline (DUBBLE, BM26A) at the European Synchrotron Radiation Facility (ESRF) in Grenoble (France). The energy of the X-ray beam was tuned by a double-crystal monochromator operating in fixed-exit mode using a Si(111) crystal pair. The measurements were done in transmission mode using ionization chambers filled with Ar/He gas at ambient pressure. A brass sample holder with Kapton® windows and a flexible polymeric spacer (VITON®) with a thickness of 2 mm was used as a sample holder. Samples of the less polar phase (0.9 M [Aliquat336][SCN]) were taken after equilibrating it with solutions of approximately 5000 ppm of Fe and 5000 ppm Co in DES. For the aqueous solutions the same concentrations of Fe and Co were employed and the total concentration of $CaCl_2$ was 5 M. Standard procedures were used for pre-edge subtraction and data normalization in order to isolate the EXAFS function (χ). The isolated EXAFS oscillations were accomplished by a smoothing

spline as realized in the program VIPER.[41] The data were fitted using the ab initio code FEFF 7.0[42] which was used to calculate the theoretical phase and amplitude functions that subsequently were used in the non-linear least-squares refinement of the experimental data. The chloride concentration in both phases was determined with a bench top total reflection X-ray fluorescence (TXRF) spectrometer (S2 Picofox, Bruker). X-ray diffraction powder patterns were recorded at room temperature with a Seifert 3003 T/T X-ray diffractometer equipped with a scintillation detector. X-ray type: Cu K_α operating at 40 kV and 40 mA, scanning range: 10–80° (2θ), step width: 0.02°, step scan: 2.00 s. The X-ray diffractograms were processed by "X'pert HighScore Plus" PANalytical software with ICDD database.

6.2.3 Synthesis of DES

Batches of approximately 1 liter of DES based on chloline chloride and lactic acid as hydrogen bond donor were prepared by mixing choline chloride (1 molar eq.) and lactic acid (2 molar eq.) and shaking manually in a bottle until the mixture was completely homogeneous.

6.2.4 Leaching

Two different samples of small NdFeB magnets (one round-shaped of approximately 25D × 10H mm and one rectangular-shaped of approximately 25W × 10H × 33L mm) were kindly provided by BEC Gesellschaft für Produktmanagement GmbH (Moers, Germany) and Magneti Ljubljana (Ljubljana, Slovenia), respectively. The magnets were demagnetized by heating them during 5 h at 300 °C in a furnace. Afterwards, they were crushed, milled and sieved to collect the fraction <400 μm from which a part was further ball-milled and sieved to obtain the <100 μm fraction. The chemical composition of the magnet samples was determined by carefully dissolving a sample of the magnet powder in concentrated hydrochloric acid and quantifying the solution with ICP-OES. For the roasting process, a magnet powder sample of 5 g was placed in a porcelain crucible without lid and heated at 950 °C in a muffle furnace during 15 h.

Magnet samples of 100 mg were dissolved in 5 mL of deep-eutectic solvent and heated at 70 °C during 12 h, unless stated otherwise. Afterwards, the leachate was centrifuged and filtered. A sample of the leachate was diluted with 1 M HNO_3 and the metal concentration was measured with ICP-OES. The solid residue was dissolved in 6 M HNO_3 and quantified by ICP-OES.

6.2.5 Solvent extraction

The chloride ion in the ionic liquid Aliquat® 336 was exchanged by a thiocyanate anion by equilibrating it three times with a 2.5 M KSCN solution. Afterwards, the thiocyanate ionic liquid was washed. For the solvent extraction experiments, a synthetic solution was prepared by dissolving $NdCl_3 \cdot 6H_2O$, $DyCl_3 \cdot 6H_2O$, $CoCl_2 \cdot 6H_2O$, $FeCl_3$ and H_3BO_3 in the DES and stirring the mixture while heating at 40 °C. The final concentrations ± the standard deviation were: (2375±10) mg L^{-1} for Nd, (6813±9) mg L^{-1} for Fe, (54±3) mg L^{-1} for B, (102±5) mg L^{-1} for Dy and (153±6) mg L^{-1} for Co. For the removal of iron, cobalt and boron, batch experiments were carried out by contacting 1 mL of DES with 1 mL of the less polar phase ([A336][SCN] diluted in toluene (0.9 M) in closed 4 mL vials. The vials were shaken at 25 °C and 2000 rpm during 20 min, unless otherwise is stated. Batch experiments for the separation of Nd and Dy were carried out using a synthetic solution which was prepared by dissolving $NdCl_3 \cdot 6H_2O$ and $DyCl_3 \cdot 6H_2O$ in the deep-eutectic solvent (choline chloride and lactic acid, molar ratio 1:2). The final concentrations ± the standard deviation were (2370±8) mg L^{-1} for Nd and (102±4) mg L^{-1} for Dy. A sample of 1 mL of this solution was put in contact with 1 mL of less polar phase (Cyanex® 923 or D2EPHA diluted in toluene 0.9 M unless otherwise is stated) and shaken during 20 min at 25 °C and 2000 rpm. For the stripping experiments, the loaded less polar phase was put in contact with 1 mL of stripping agent (different concentrations of HCl, oxalic acid, citric acid or EDTA) in 4 mL closed vials, and shaken during 60 min at 25 °C. A sample of the aqueous phase was taken, diluted and measured with ICP-OES.

For comparison reasons, solvent extraction experiments from aqueous solutions containing (2155±9) mg L^{-1} Nd, (6380±12) mg L^{-1} Fe, (68±3) mg L^{-1} B, (112±4) mg L^{-1} Dy and (148±4) mg L^{-1} Co were carried out. $CaCl_2$ was used as source of chlorides and its concentration in the aqueous phase was 1.5 M, unless otherwise stated. For the separation of Nd and Dy the concentrations in the aqueous phase were (2218±7) mg L^{-1} for Nd and (121±3) mg L^{-1} for Dy. The extraction was carried out in 4 mL vials at 25 °C and 2000 rpm during 60 min to assure that equilibrium was achieved.

A counter-current mixer-settler system comprised of five extraction units in polyvinylidene fluoride (PVDF) was used to evaluate the scaling up feasibility of the developed process for the separation of iron, cobalt and boron from neodymium and dysprosium and subsequently

dysprosium from neodymium. The mixer-settler unit consists of: a) the mixing chamber, where the less polar phase and the more polar phase are mixed using a motor stirrer, b) the settling chamber, where the phases are separated by density difference and c) a more polar phase outlet compartment, from which the more polar phase exits the unit.[43] The more and less polar phases were pumped into the mixer-settlers using electromagnetic pumps (Iwaki). Each mixer-settler unit has a volume of 120mL/unit (MYMEKO, Sweden). The light phase:heavy phase ratio (LP:HP) was 1:1. The light phase corresponds to 0.9 M [A336][SCN] or Cyanex® 923 in toluene, while the heavy phase corresponds to the DES chlorine chloride:lactic acid (molar ratio 1:2). The flow rates for the deep-eutectic solvent and organic feeds were 1.5 mL/min, the mixing speed in the mixer chambers was 900 rpm. The retention time corresponded to 13.3 min. For the separation of dysprosium from neodymium, the LP:HP phase ratio was 2:1. The flow rates for the deep eutectic solvent and organic feeds were 3 and 1.5 mL/min, respectively, the mixing speed in the mixer chambers was 900 rpm. The retention time corresponded to 8.8 min.

6.3 Results and discussion

6.3.1 Dissolution

The composition of two different NdFeB magnets that were employed for the dissolution experiments was determined with ICP-OES (Table 6.1). The composition of a NdFeB magnet varies depending on the type of application it is used for. Generally, cobalt is added to the magnets to increase their Curie temperature, while dysprosium and gadolinium are added when it is required to operate at high temperatures as they increase the coercivity of the magnet.[44,45] Praseodymium is often present together with neodymium to reduce production costs since its complete separation from neodymium requires multiple steps and they share similar properties.[46] Both magnets contained 4 different rare earths, Nd, Dy, Pr and Gd. Magnet 2 contains higher amounts of Gd and Pr but a lower amount of Dy compared to Magnet 1.

Table 6.1. Main composition (wt%) of two NdFeB magnets determined with ICP-OES.

	Main composition (wt%)	
Element	Magnet 1	Magnet 2
Fe	58.52 ± 6.22	56.62 ± 5.67
Nd	22.96 ± 3.45	21.38 ± 4.96
Co	2.66 ± 0.10	2.76 ± 0.17
Dy	5.06 ± 0.56	0.26 ± 0.05
B	1.26 ± 0.09	1.30 ± 0.08
Nb	n.d.[a]	0.09 ± 0.04
Gd	1.86 ± 0.19	5.5 ± 0.9
Al	1.39 ± 0.05	4.00 ± 0.23
Pr	3.87 ± 0.07	5.47 ± 0.28
Si	0.05 ± 0.01	0.10 ± 0.05
Cu	n.d.[a]	0.10 ± 0.06
Ni	n.d.[a]	0.44 ± 0.09
Ga	0.22 ± 0.03	0.09 ± 0.01
Total	97.85	98.11

[a] n.d. = not detected (below detection limit)

The *percentage metal leached* (%*L*) was calculated as follows,

$$\%L = \frac{\text{Amount of metal in the leachate}}{\text{Total amount of metal in the leachate and precipitate}} \times 100 \quad (6.1)$$

To the best of our knowledge, the solubility of rare-earth oxides has not been reported in any DESs yet. Magnet samples (<100 μm particle size) were roasted and leached using three different deep-eutectic solvents based on choline chloride (ChCl), ChCl:urea, ChCl:ethylene glycol and

ChCl:lactic acid, all of them with a molar ratio 1:2. High %*L* were obtained when using the deep-eutectic solvent composed of ChCl:lactic acid (1:2) and no significant deviations were obtained between both roasted magnets. The mixtures ChCl:urea (1:2) and ChCl: ethylene glycol (1:2) allowed the poor dissolution of Nd and Fe and did not dissolve any of the other metal oxides from the roasted magnets. Since physicochemical properties of deep-eutectic solvents depend on the kind of moieties and substituents present in the mixture, the high solubility of the oxides in the choline chloride:lactic acid (1:2) DES can be explained by the fact that the protons present in the lactic acid react with the oxides to form water (Eq. 6.2) and probably the coordinating abilities of lactic acid and the choline help dissolution.

$$Nd_2O_{3(s)} + 6CH_3CHOHCOOH_{(DES)} \rightarrow 2Nd(CH_3CHOHCOO)_{3(DES)} + 3H_2O_{(DES)} \qquad (6.2)$$

Since the best results were obtained with the DES based on choline chloride and lactic acid (1:2), it was decided to carry out the dissolution of metals from the NdFeB magnets with this solvent. The effect of the liquid:solid (L/S) ratio on the two different roasted magnet powders was investigated (Fig. 6.2). As expected, the percentage of metal leached increased when using L/S ratios larger than 20 mL g^{-1}. When trying to dissolve the magnet using lower quantities of DES, low %*L* values were obtained. This can be explained because of the poor agitation due to the low amount of liquid and the large amount of solid, which probably makes it difficult for the DES to reach all the metals in the magnet powder. At high L/S ratios, all metals were dissolved almost completely. No selectivity was observed at any ratio and there were not significant differences when using magnets with different compositions. The effect of the water content in the DES choline chloride:lactic acid (1:2) on the percentage of metal leached was evaluated (Fig. 6.3).

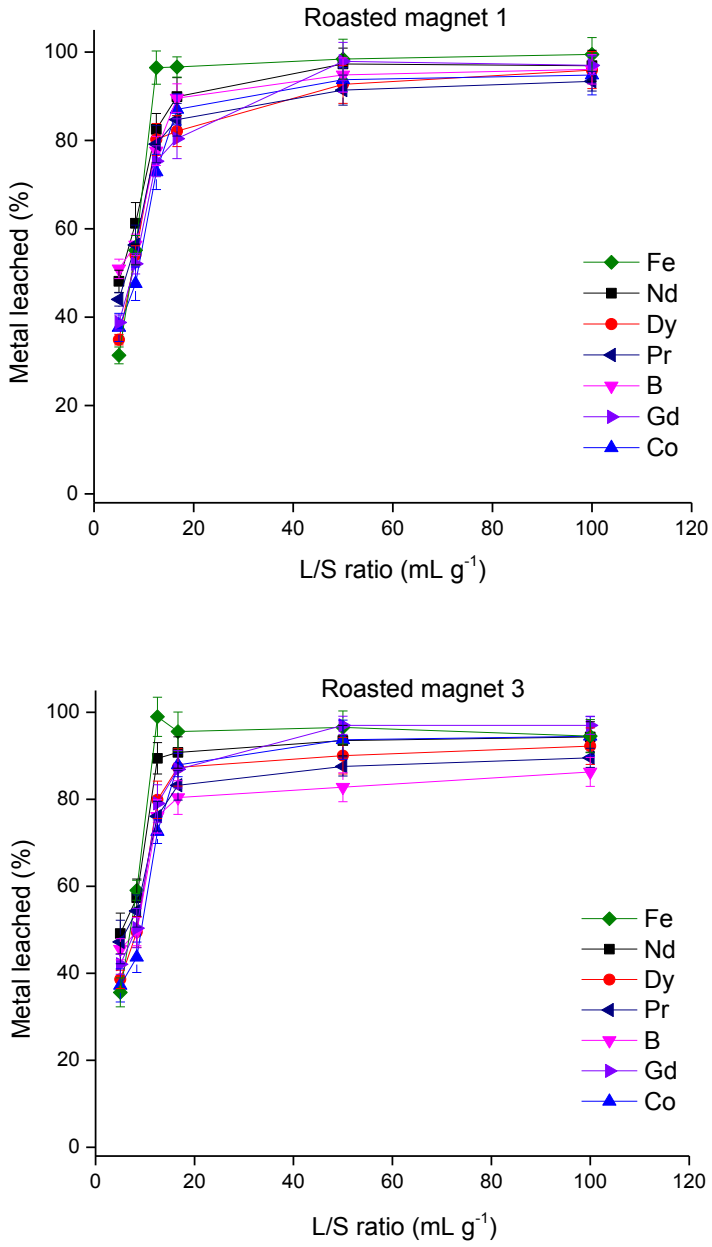

Fig. 6.2. Effect of the liquid:solid ratio (L/S) on the percentage metal leached from two different roasted magnet powders (<100 μm particle size), 70 °C leaching temperature, 24 h leaching duration.

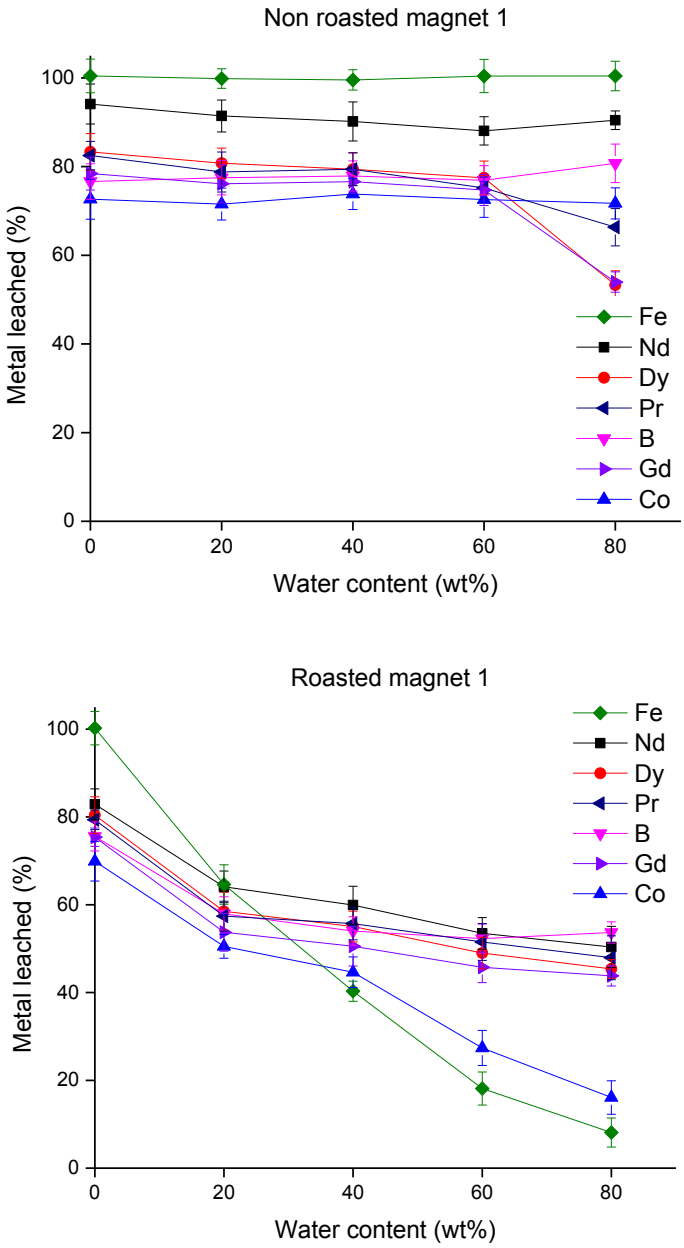

Fig. 6.3. Effect of the water content (wt%) in the deep-eutectic solvent choline chloride:lactic acid (1:2) on the percentage metal leached from non-roasted (<100 µm particle size) and roasted NdFeB magnet 1 (<100 µm particle size), leaching temperature: 70 °C, 24 h leaching duration, L/S = 12.5 mL g^{-1}.

The effect of roasting the magnets was investigated by comparing the leaching of non-roasted and roasted magnets. The magnet powders (<100 µm particle size) were roasted at 950 °C before dissolving them in the DES at 70 °C during 24 h. In the case of non-roasted magnets (<100 µm

particle size), the dissolution was started by contacting the non-roasted magnets with DES without heating or stirring to avoid potential spillage because of the production of hydrogen gas during the dissolution (Eq. 6.3).

$$2Nd_{(s)} + 6CH_3CHOHCOOH_{(DES)} \rightarrow 2Nd(CH_3CHOHCOO)_{3(DES)} + 3H_{2(g)} \quad (6.3)$$

or the dissolution of the non-roasted magnet with the DES choline chloride:lactic acid (1:2), an increase in water content (up to 60 wt%) had no significant effect on the percentage metal leached. After 60 wt% water content, a decrease on the dissolution of the metals was observed. As expected, no dissolution of metals occurred when pure water was used.

For the leaching of the roasted magnets, selectivity can be achieved when adding water to the DES (Fig. 6.3). During the roasting process, different kinds of metal oxides such as Fe_2O_3, $NdBO_3$ and $NdBO_3$ are formed.[47] In the same way as explained in equation 6.2, lactic acid reacts with the corresponding oxides to form water (Eq. 6.4):

$$Fe_2O_3 + 6CH_3CHOHCOOH_{(DES)} \rightarrow 2Fe(CH_3CHOHCOO)_{3(DES)} + 3H_2O \quad (6.4)$$

In the case of non-roasted magnets, iron is released into the DES as iron (II), as follows,

$$Fe_{(s)} + 2CH_3CHOHCOOH_{(DES)} \rightarrow Fe(CH_3CHOHCOO)_{2(DES)} + H_{2(g)} \quad (6.5)$$

Iron (II) is more stable against hydrolysis than iron (III), thus, in the case of non-roasted magnets, no selectivity can be achieved since iron (II) can go in solution as long as there is not an oxidizing environment. In the case of roasted magnets (Eq. 6.4), as the lactic acid is consumed and water is produced, the pH increases allowing the hydrolysis of iron (III) and precipitation of $Fe(OH)_3$. The advantage of such situation is not only the selectivity but also that the eutectic mixture is not decomposed since no redox reactions occur upon dissolution of the roasted magnets. The dissolution of magnets in mixtures of water and DESs is promising and might result after optimizing some leaching parameters (*e.g.* kinetics, temperature, nature of the carboxylic acid in the DES) in leachates containing mostly rare earths. Still, since the highest *%L* was achieved with the DES choline chloride:lactic acid (1:2) without the addition of water, this DES was employed as the more polar phase for the further solvent extractions.

6.3.2 Solvent extraction

The leachate from the roasted magnet produced with the DES choline chloride:lactic acid (1:2) without water was employed as the more polar phase for solvent extraction. Foreman has studied the solvent extraction of transition metals and lanthanides from DES using Aliquat® 336 and D2EHPA diluted in an aromatic solvent and a saturated aliphatic hydrocarbon respectively.[37] Since the recovery of metals from NdFeB magnets using DES has not been widely explored yet, it was decided to carry out the separation of only the most typical elements present in NdFeB magnets (*i.e.* Nd, Dy, Fe, B, Co) through solvent extraction.

To evaluate and quantify the efficiency of the solvent extraction, parameters such as, percentage extraction (*%E*), distribution ratio (*D*) and separation factor *($\alpha_{A,B}$)* were evaluated. The *percentage extraction (%E)* is defined as the initial amount of metal ion in the more polar phase ($[M]_i$) minus the amount of metal ion in the more polar phase after extraction ($[M]_f$) over the initial amount of metal ion ($[M]_i$). In case of equal volumes it can be expressed as:

$$\%E = \frac{[M]_i - [M]_f}{[M]_i} \times 100 \qquad (6.6)$$

The *distribution ratio (D)* of a metal is defined in equation 6.7 as the ratio of its concentration in the less polar phase by its concentration in the more polar phase ($[M]_f$) after extraction and phase separation.

$$D = \frac{[M]_i - [M]_f}{[M]_f} \qquad (6.7)$$

The *separation factor ($\alpha_{A,B}$)* between two metals is the ratio of the distribution ratios of the metals *A* and *B*, where *A* and *B* are chosen so that $\alpha > 1$ (Eq. 6.8).

$$\alpha = \frac{D_A}{D_B} \qquad (6.8)$$

Ionic liquids were chosen as the less polar phase for the solvent extraction because they are effective extractants for metal ions.[11-13,27,29,32,33] Since the available mixer settlers operated exclusively at room temperature, ionic liquids were diluted with organic solvents to avoid longer equilibration times due to the relatively high viscosities. Toluene and Solvent 70 (one of the fractions of kerosene) were tested because they are very common diluents for solvent extraction

systems.[48-55] Despite the fact that toluene is not a green solvent,[56] it was chosen as diluent since it allowed higher separation factors as well as faster and better phase disengagements in comparison to Solvent 70. Besides this, no problems with third phase formation were encountered when using toluene.

Table 6.2 shows the results obtained for the extraction of Nd, Fe, B, Dy and Co from a synthetic solution, mimicking the concentrations of a leachate of NdFeB magnet, where two ionic liquids (Aliquat® 336 with two different anions, chloride and thiocyanate, diluted in toluene) were employed.

Table 6.2. Distribution ratios of neodymium, dysprosium, iron, boron and cobalt.[a]

	D for [A336][Cl] in toluene (0.7 M)	*D* for [A336][SCN] in toluene (0.7 M)
Nd	0.041 ± 0.009	0.029 ± 0.006
Fe	187 ± 6	47.8 ± 0.7
B	2.73 ± 0.30	0.78 ± 0.08
Dy	0.023 ± 0.005	0.026 ± 0.007
Co	0.74 ± 0.07	192 ± 10

[a] Shaking time: 60 min, 2000 rpm, 25 °C. Each value represents the average of three measurements.

Both [A336][SCN] and [A336][Cl] extracted Fe and higher distribution ratios were obtained for B when [A336][Cl] was employed, while [A336][SCN] allowed a more efficient extraction of Co. In both cases, there was almost no extraction of the rare earths. Since in general, high *D* were obtained for Co with less co-extraction of the rare earths when using [A336][SCN], this extractant was chosen to carry out the first separation stage. In terms of equilibration time, it was found that a period between 15 to 20 min was adequate to reach equilibrium. An equilibration time of 20 min was chosen as the optimal time to make sure that equilibrium was reached. This relatively long equilibration time is needed because of the slow mass transfer process occurring under the operating conditions (*i.e.* viscosity of the DES phase at 25 °C = 155.8 cP).

Dilutions of [A336][SCN] in toluene were prepared in order to optimize the concentration of the extractant. Poor phase mixing and slow phase disengagement were observed when working with concentrations of [A336][SCN] higher than 0.9 M. A concentration of 0.9 M of [A336][SCN] in

toluene was chosen as optimal since it allowed the highest D for B, Fe and Co without facing problems with viscosity. It is important to notice that there was hardly any extraction of the rare earths during this step (Fig. 6.4).

As chloride is a good inner-sphere ligand it is possible to generate extractable chlorometallate complexes as expressed as follows,

$$\mathrm{M}^{n+} + n\mathrm{Cl}^- + \overline{m[\mathrm{A336}]} \rightleftharpoons \overline{[\mathrm{MCl}_n[\mathrm{A336}]_m]} \qquad (6.9)$$

The equilibrium constant can be expressed as

$$K_{\mathrm{eq}} = \frac{\overline{[\mathrm{MCl_n[A336]_m}]}}{[\mathrm{M^{n+}}][\mathrm{Cl^-}]^{\mathrm{n}}\overline{[\mathrm{A336}]^{\mathrm{m}}}} = \frac{D_{\mathrm{M}}}{[\mathrm{Cl^-}]^{\mathrm{n}}\overline{[\mathrm{A336}]^{\mathrm{m}}}} \qquad (6.10)$$

By plotting log *D* vs. log[A336] when the chloride concentration is constant, it is possible to determine the number of molecules of ionic liquid that are involved in the extraction of the metal ion (Eq. 6.11).

$$\log D = \mathrm{m}\log[\mathrm{A336}] + \mathrm{n}\log[\mathrm{Cl^-}] + \log K\mathrm{eq} \qquad (6.11)$$

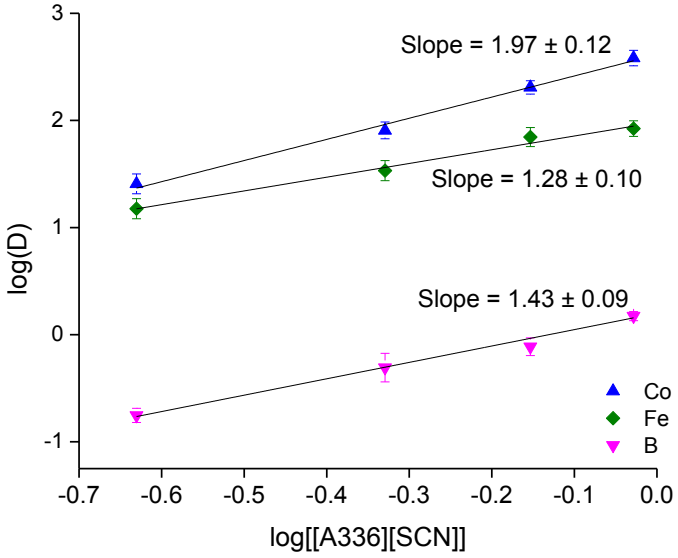

Fig. 6.4. Effect of the concentration of [A336][SCN] in toluene on the extraction of Fe, B and Co from a mixture of Nd, Dy, Fe, B and Co in the DES choline chloride:lactic acid (molar ratio 1:2). Shaking speed: 2000 rpm at 25 °C, equilibration time: 20 min. Concentration of [A336][SCN] = 0.2 - 0.9 M.

It can be seen that the distribution ratios for B, Fe and Co increase with the [A336][SCN] concentration. The distribution ratios of Co and Fe are in concordance with what has been reported previously for the extraction of these metals from the same DES.[37] The stoichiometric ratios between Fe, B and Co and the extractant were determined by plotting the log*D* vs. log[[A336][SCN]] and then doing the linear regression to determine the stoichiometric ratio between the metal ion and the extractant (Fig 6.4). The results show that the slope values are close to 2 for Co and 1 for Fe, this would suggest that the complexes formed could correspond to $[FeCl_4][A336]$ and $[Co(Cl)_4][A336]_2$. In the case of boron, a value of 1.43 was obtained for the slope, indicating that most likely more than one kind of complex is formed. It is known that boric acid can form 1:1 or 1:2 anionic complexes with lactic acid, $[B(OH)_2(C_4H_5O_3)]^-$ or $[B(C_4H_5O_3)_2]^-$.[57] In the presence of an excess of lactic acid, the complex $[B(C_4H_5O_3)_2]^-$ would be predominant. This complex could be extracted by the ionic liquid present in the less polar phase as $[B(C_4H_5O_3)_2][A336]$. However, estimations by slope analysis do not give complete information about the structure of the extracted metal complex. EXAFS was used to determine

the environment of the extracted complexes of Fe and Co and the results will be discussed in the section EXAFS.

Since industrial processes using ambient temperature are usually less expensive and preferred over those that use high temperatures, the effect of the temperature was not studied. However, it must be stressed that working at higher temperatures could help to reduce the viscosity of the system and thus, to increase the mass transfer of the extraction process. Additionally, it could also allow the use of the ionic liquid in its undiluted form, which will possibly increase the extraction of boron.

After the removal of Fe, Co and B (*i.e.* by countercurrent solvent extraction in mixer settlers), a process for the separation of Nd and Dy present in the DES was developed. Two conventional extractants were tested: Cyanex® 923 and D2EHPA. D2EHPA is a well-known acidic extractant that is widely employed for the separation of rare earths due to its high selectivity and extractant capacity.[17,58] Cyanex® 923 is a solvating extractant that has been widely used for the separation of rare earths in nitrate media.[17,58] Table 5.3 shows the distribution ratios of Nd and Dy when extracted from the DES using Cyanex® 923 and D2EHPA.

Table 6.3. Distribution ratios of neodymium(III) and dysprosium(III) from the eutectic mixture of choline chloride and lactic acid (molar ratio 1:2).[a]

	D_{Nd}	D_{Dy}
Cyanex® 923 (0.9 M in toluene)	0.14 ± 0.07	1.79 ± 0.10
D2EHPA (0.9 M in toluene)	2.23 ± 0.09	28.85 ± 2.53

[a] Shaking speed: 2000 rpm, equilibration time: 60 min, 25 °C.

D2EHPA allowed the obtention of higher distribution ratios than Cyanex® 923 but the separation factors were similar, $\alpha_{Dy/Nd}$ = 12.93 and 12.79 for D2EHPA and Cyanex® 923 respectively. Since solvent extraction processes must not be analyzed only in terms of their distribution ratios, but also considering the stripping procedure and their feasibility to be scaled up, it was decided to study both systems to compare them and choose the most adequate one. The kinetics of

extraction of both systems was studied at 25 °C and in both cases, the equilibrium is reached somewhere in between 5 and 10 min. Taking this into account, 15 min was chosen as the optimal time to carry out further experiments.

The next parameter investigated was the effect of the concentration of extractant in the less polar phase. In both cases the distribution ratios for both rare-earth metals increase as the concentration of extractant increases (Fig. 6.5 and 6.6). Concentrations of extractant higher than 0.9 M resulted in higher distribution ratios but also in a loss of the selectivity.

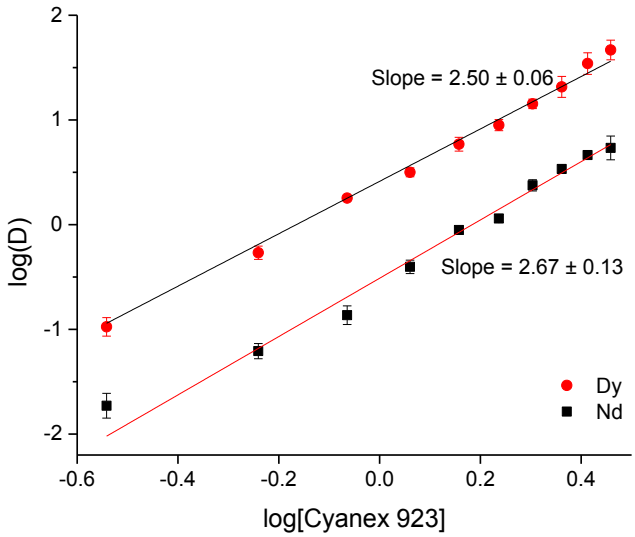

Fig. 6.5. Effect of the concentration of Cyanex® 923 diluted in toluene on the separation of neodymium and dysprosium in the DES choline chloride:lactic acid (molar ratio 1:2). Equilibration time: 15 min. Shaking speed: 2000 rpm at 25 °C.

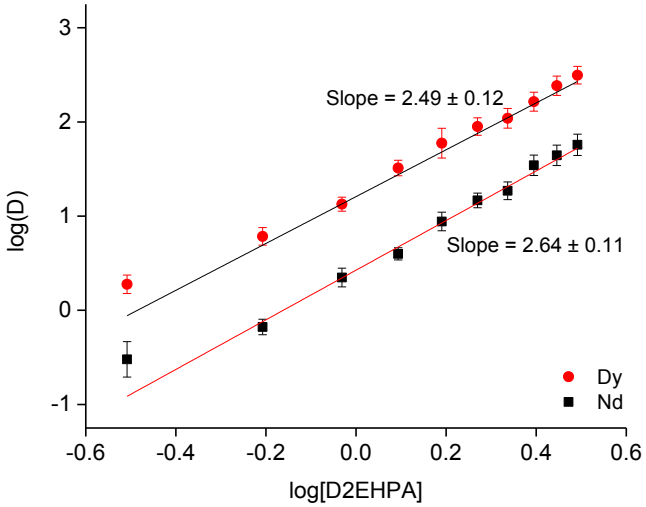

Fig. 6.6. Effect of the concentration of D2EHPA diluted in toluene on the separation of neodymium and dysprosium in the DES choline chloride:lactic acid (molar ratio 1:2). Equilibration time: 15 min. Shaking speed: 2000 rpm at 25 °C.

In general, the extraction of rare earths by organophosphorous acids, such as D2EHPA, can be expressed as follows,[17]

$$RE^{3+} + \overline{3(HA)_2} \rightleftharpoons \overline{REA_3(HA)_3} + 3H^+ \qquad (6.12)$$

Where $(HA)_2$ represents the dimer of D2EHPA, and RE denotes a rare earth element. The equilibrium constant *K* of the reaction can be written as follows,

$$K = \frac{\overline{[REA_3(HA)_3]}[H^+]^3}{[RE^{3+}]\overline{[(HA)_2]}^3} = \frac{D[H^+]^3}{\overline{[(HA)_2]}^3} \qquad (6.13)$$

Taking logarithm on both sides, the following equation is obtained,

$$\log D = -3\log[H^+] + 3\log[(HA)_2] + \log K(HA)_2 \qquad (6.14)$$

When the concentration of $[H^+]$ is constant, the plot of log$D$ against log$[(HA)_2]$ should give a straight line with a slope of three.

On the other hand, the extraction reaction using Cyanex® 923 can be expressed by Eq. 6.15,[59]

$$RE^{3+} + 3Cl^- + 3B \rightleftharpoons RECl_3 \cdot 3B \qquad (6.15)$$

The equilibrium constant can be written as,

$$K_B = \frac{[RECl_3 \cdot 3B]}{[RE^{3+}][Cl^-]^3[B]^3} = \frac{D}{[Cl^-]^3[B]^3} \qquad (6.16)$$

Where B represents Cyanex® 923. The logarithm of the distribution ratio depends only on the concentrations of Cyanex® 923 and Cl^-, as shown in Eq. 6.17,

$$\log D = 3\log[Cl^-] + 3\log[B] + \log K_B \qquad (6.17)$$

When the chloride concentration is constant, the plot of log$D$ against log[B] should give a slope of 3.

From Fig. 6.5 and 6.6 it can be observed that the slopes had values close to 2.5 for both Nd and Dy extracted from DES with Cyanex® 923 or D2EHPA. The slopes are non-integral indicating that more than one type of complex is involved in the extraction. These slopes are in concordance with what has been published previously by other authors.[17,60-64] Cyanex® 923 has been widely used in the extraction of rare earths from nitrate media.[64-66] In general, solvating extractants have been mostly used when extracting from nitrate media because they offer higher distribution ratios and separation factors than from chloride media.[67] Therefore, the use of solvating extractants to extract rare earths from chloride media has been barely reported.[59,67] Lee and co-workers reported the extraction of La, Ce, Pr, Nd and Sm from chloride media using Cyanex® 923 and D2EHPA

as the extractant for a solvent-impregnated resin.[59] The distribution ratios for heavy rare earths were higher than those for light rare earths, which is in agreement with what has been found in this work for the extraction of Nd and Dy from DES and also with other works on the extraction of REEs with Cyanex® 923 from different aqueous feeds.[62,63 64]

6.3.2.1 Stripping

The percentage of stripping is defined in equation 6.18.

$$\%S = \frac{[\mathrm{M}]_{aq}}{[\mathrm{M}]_{bs}} \times 100 \qquad (6.18)$$

where $[M]_{aq}$ corresponds to the concentration of metal ion in the more polar phase after stripping and phase separation and $[M]_{bs}$ is the concentration in the less polar phase before stripping.

The stripping of Fe, Co and B from the less polar phase consisting of the ionic liquid [A336][SCN] diluted in toluene (0.9 M) was studied. Diluted and concentrated acids were employed as well as NaOH, EDTA and citric acid (Table 6.4).

The use of NaOH as stripping agent allowed precipitation stripping of Fe and Co. B was only back-extracted to the aqueous phase when using high concentrations of NaOH (8 M). It has been reported that at very high concentrations of NaOH or KOH, B can be stripped by the formation of $Na_2B_4O_7$ and $K_2B_4O_7$ at high pH.[68] One disadvantage of this method is the formation of the non-coarse precipitate of hydroxides of iron and cobalt that is difficult to filter, besides the fact that high concentrations of NaOH are required to precipitate all the metals. HCl was also tested but it was not a good stripping agent for Fe(III) and Co(II) due to the strong complexes formed between the thiocyanate ions and these metal ions. When HCl was used as stripping agent, Fe and Co were not back-extracted, however, B could easily be stripped since it is less strongly extracted. As expected, EDTA was a good complexing agent for stripping Fe and Co, but a poor one for B. Citric acid was not a better alternative than EDTA because the stability constants for the formation of the complexes are smaller with citric acid (log K_{Co}= 4.4 and log K_{Fe}= 11.8) than with EDTA (log K_{Co}= 16.21 and log K_{Fe}= 14.3).[69,70] To achieve complete stripping, the solution can be treated with 6 M HCl to remove B, followed by a treatment with 1.2 M EDTA to remove Fe and Co.

Table 6.4. Distribution ratio of the stripping of Fe, B and Co from [A336][SCN] in toluene (0.9 M).[a]

Stripping agent	Concentration (M)	D_{Fe} ± SD	D_B ± SD	D_{Co} ± SD
NaOH	8.0	0.66 ± 0.02	2.20 ± 0.13	0.47 ± 0.01
	2.0	1.18 ± 0.04	n.d.[b]	3.95 ± 0.33
	1.0	1.31 ± 0.02	n.d.[b]	13.5 ± 1.6
	0.5	3.78 ± 0.11	n.d.[b]	> 200
HCl	6.0	> 200	0.32 ± 0.01	122 ± 8
	3.0		0.53 ± 0.02	107 ± 10
	2.0	42.5 ± 7	0.90 ± 0.05	82.3 ± 6.2
	1.0	26.8 ± 2.9	1.20 ± 0.06	17.9 ± 6.1
EDTA	1.2	0.03 ± 0.01	n.d.[b]	0.03 ± 0.01
	0.4	1.44 ± 0.03	n.d.[b]	1.35 ± 0.03
	0.1	2.52 ± 0.12	n.d.[b]	61.5 ± 1.5
	0.05	5.13 ± 0.28	n.d.[b]	> 200
Citric acid	0.4	8.43 ± 0.23	n.d.[b]	29.3 ± 3.7

[a] Equilibration time 60 min, 25 °C, 2000 rpm. [b] n.d.: not detected (below detection limit).

After the removal of Fe, Co and B, Dy can be separated from Nd by using either Cyanex® 923 or D2EHPA diluted in toluene (0.9 M) as previously discussed. Since Nd is one of the main components of the magnet, it is present in the leachate in higher concentrations (*i.e.* 2370 ppm) than Dy (*i.e.* 102 ppm). Therefore, Nd is also co-extracted during the removal of Dy using the above mentioned extractants. To remove the Nd that is co-extracted with Dy to the less polar phase, a scrubbing procedure is necessary. $CaCl_2$ at different concentrations was tested as scrubbing agent (Table 6.5).

Table 6.5. Effect of the $CaCl_2$ concentration on the scrubbing of Nd and Dy from the less polar phase (Cyanex® 923 in toluene 0.9 M).[a]

$CaCl_2$ (M)	D_{Nd}	D_{Dy}
5.6	0.64 ± 0.06	> 200
4.2	0.73 ± 0.08	57.8 ± 3.8
2.8	0.63 ± 0.10	3.69 ± 0.09
1.4	0.65 ± 0.06	0.38 ± 0.05
0.7	0.45 ± 0.05	0.16 ± 0.03

[a] 25 °C, 2000 rpm, 40 min. Concentrations in the less polar phase: (431±6) mg L^{-1} for Nd and (270±4) mg L^{-1} for Dy (concentrations of the raffinate obtained from the mixer settler).

From Table 6.5 it can be seen that no selectivity can be achieved at very low concentrations of $CaCl_2$ since both Nd and Dy are stripped. However, selectivity can be achieved when working at higher concentrations of $CaCl_2$ because the presence of chloride anions increases the distribution of heavy rare earths towards the less polar phase. When D2EHPA was used as extractant, this scrubbing step with $CaCl_2$ could not be carried out since the metals are not easily stripped by water and the presence of high chloride concentrations favours their distribution in the less polar phase. Thus, 6.6 M $CaCl_2$ was selected as scrubbing agent and was employed to purify the Dy-rich less polar phase obtained after running the mixer-settlers using 0.9 M Cyanex® 923 in toluene. No co-extraction of Ca was observed when using Cyanex® 923 as extractant. The stripping of Dy was evaluated using different stripping agents and the results are summarized in Table 6.6.

Table 6.6. Distribution ratios of Dy stripping from Cyanex® 923 in toluene (0.9 M) and D2EHPA in toluene (0.9 M).[a]

Stripping agent	D_{Dy} from Cyanex® 923 in toluene 0.9 M	D_{Nd} from D2EHPA in toluene 0.9 M
Water	0.016 ± 0.007	> 200
0.5 M HCl	0.012 ± 0.006	0.31 ± 0.09
0.1 M citric acid	0.019 ± 0.009	> 200
0.1 M EDTA	0.24 ± 0.09	> 200

[a] Equilibration time: 40 min, 25 °C, 2000 rpm. Concentration of Dy in the less polar phase after the scrubbing: 245 mg L^{-1}.

From Table 6.6, a clear difference in the stripping behaviour of the two systems is observed since the *D* were lower for all the stripping agents that were used when stripping from the Cyanex® 923 in comparison to stripping from the D2EHPA phase. This can be explained because of the high affinity of the acidic extractant D2EHPA for the rare earths. With this extractant very high distribution ratios can be achieved for heavy rare earths, but the stripping is difficult. Because of the easiness of scrubbing and stripping when Cyanex® 923 is used, Cyanex® 923 was chosen as optimal extractant for the separation of Dy from Nd and water was selected as stripping agent. Once Dy was removed from the DES phase (*i.e.* by counter-current extraction), it was necessary to find a way to strip Nd from the DES. With this aim, precipitation stripping with oxalic acid was explored. Different amounts of oxalic acid were contacted with the DES and then stirred at 25 °C and 2000 rpm during 25 min. After this time, the precipitate was removed and the aqueous phase quantified by ICP-OES. As it can be seen in Fig. 5.7, a stoichiometric amount of oxalic acid was needed to precipitate all Nd present in the DES, as stated in equation 5.19. Using an excess of oxalic acid is not recommended since the deep eutectic solvent choline chloride:oxalic acid can be formed.

$$2Nd^{3+} + 3H_2C_2O_4 \rightarrow Nd_2(C_2O_4)_3 + 6H^+ \qquad (6.19)$$

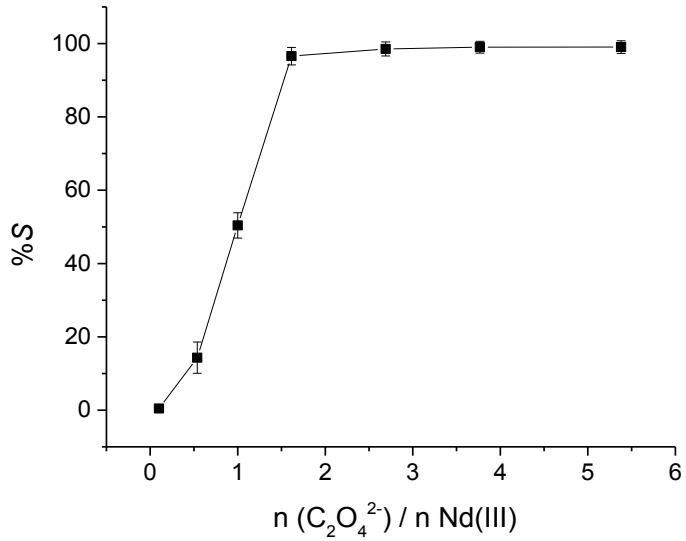

Fig. 6.7. Precipitation stripping of Nd from the eutectic mixture of choline chloride and lactic acid (molar ratio 1:2). Equilibration time 40 min, 25 °C and 2000 rpm.

6.3.3 Separation by mixer-settlers

The feasibility of scaling up the extraction processes was tested using small mixer-settlers (Fig. 6.8). Besides determining the extractant, the composition of the less polar phases, the contact time, the stripping agent and evaluating other parameters such as phase disengagement, the number of stages needed for the separation of Fe, B and Co from Nd and Dy was also determined.

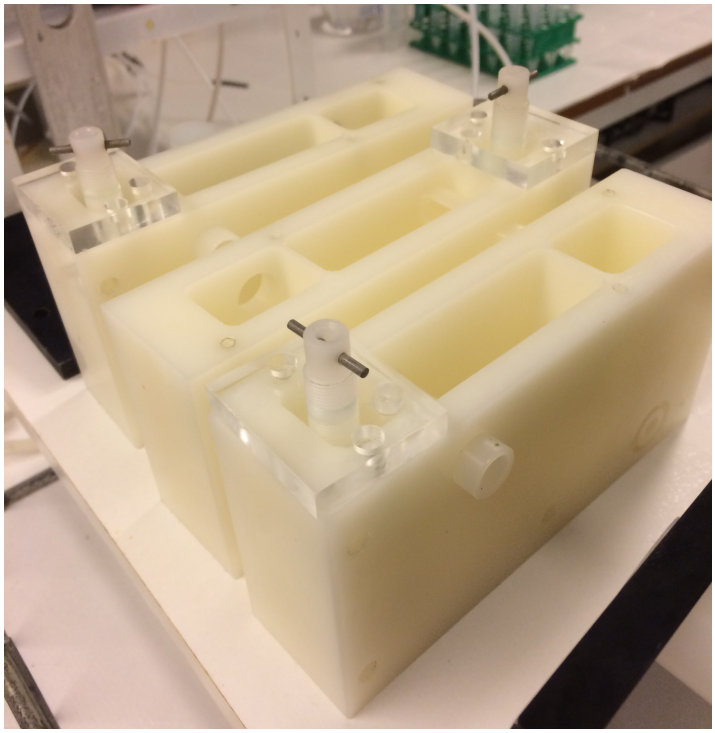

Fig 6.8. Photograph of employed mixed-settlers.

McCabe Thiele diagrams showing the loading of Fe, Co and B at different light phase:heavy phase ratios (LP:HP) from a solution containing all the metals (Fe, B, Co, Nd and Dy) were constructed. It was estimated that one stage was needed for Fe and Co extraction, approximately three for B extraction when using an LP:HP ratio of 1:1. At a LP:HP ratio of 2:1 one stage is needed for Fe and Co and two for B (Fig. 6.9, 6.10, 6.11). In total, three stages would be necessary for the complete extraction of Fe, Co and B from Nd and Dy. However two more stages were put as precaution in case more stages were needed due to the relative high viscosity of the more polar phase.

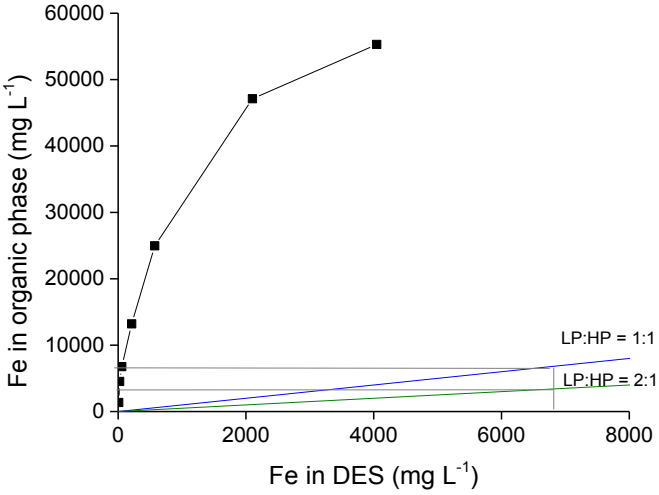

Fig. 6.9. McCabe-Thiele diagram for Fe from a mixture of Fe, Co, B, Nd and Dy in the DES choline chloride:lactic acid (molar ratio 1:2) with 0.9 M [A336][SCN] in toluene (phase contact time 20 min, LP:HP ratios between 0.05:1 and 10:1).

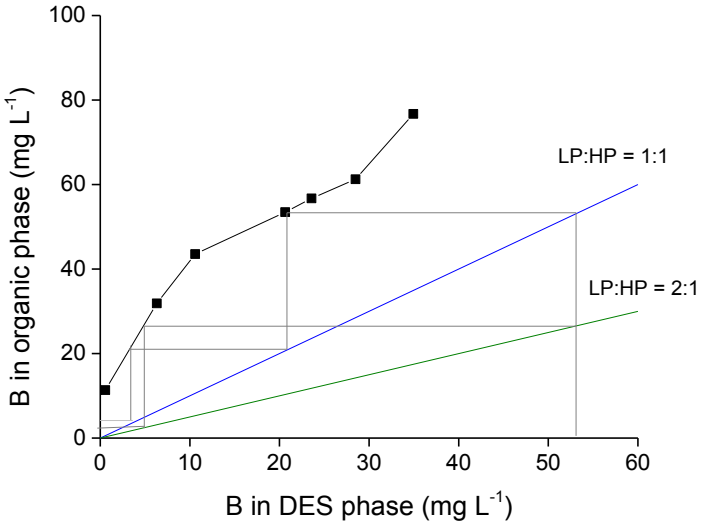

Fig. 6.10. McCabe-Thiele diagram for B from a mixture of Fe, Co, B, Nd and Dy in the DES choline chloride: lactic acid (molar ratio 1:2) with 0.9 M [A336][SCN] in toluene (phase contact time 20 min, LP:HP phase ratios between 0.25:1 and 10:1).

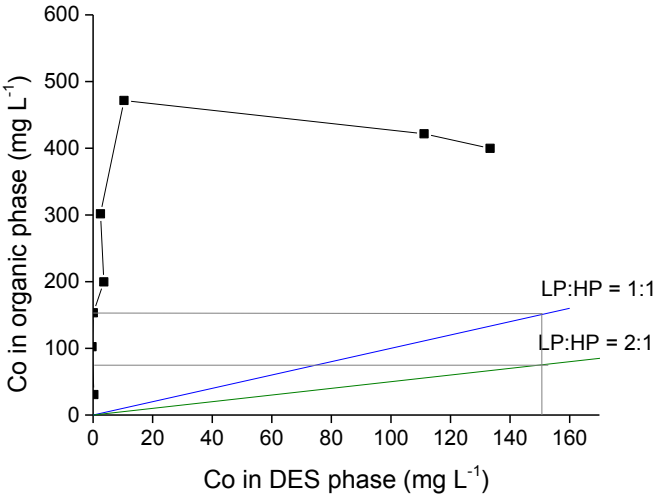

Fig. 6.11. McCabe-Thiele diagram for Co from a mixture of Fe, Co, B, Nd and Dy in the DES choline chloride:lactic acid (molar ratio 1:2) with 0.9 M [A336][SCN] in toluene (phase contact time 20 min, LP:HP ratios between 0.05:1 and 10:1).

The extraction behaviour of Fe, Co and B in the mixer-settler is presented in Fig. 6.12. Every hour a sample was taken from each extraction chamber throughout the day and analysed by ICP-OES. The extraction system showed a good stability over time, with minor variations in metal concentrations between the samples. In the first stage, the concentration of Fe and Co in the DES decreased considerably. On the other hand, B required three stages to be completely recovered from the DES. During the whole time of operation, no precipitate or third phase formation was observed. The experimental data obtained with the mixer-settlers showed that the fourth and fifth stages were not needed since at those stages Fe, Co and B were not detected in the more polar phase.

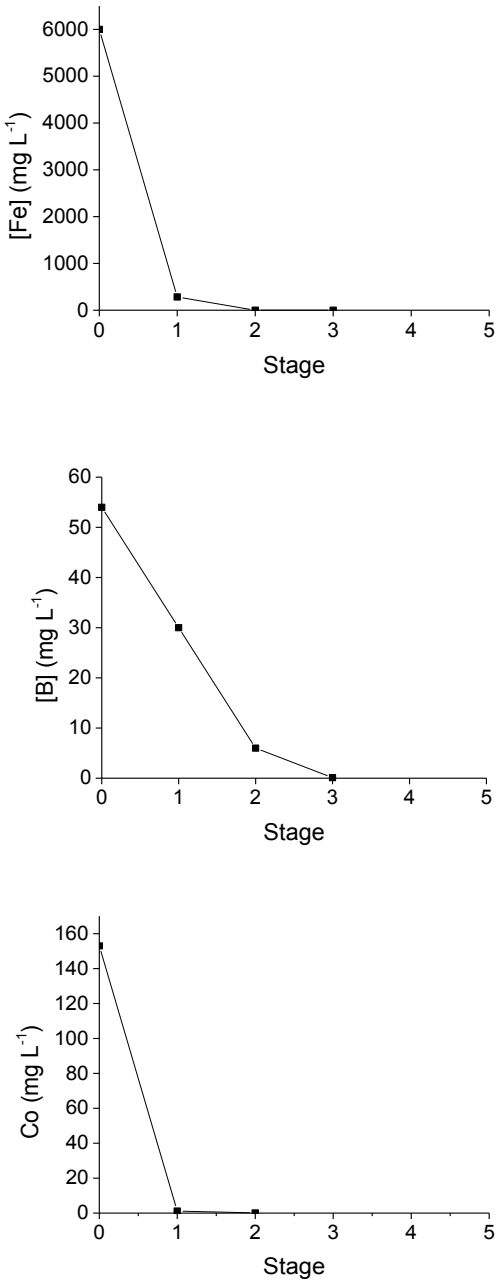

Fig. 6.12. Extraction behaviour of iron (top), boron (center) and cobalt (bottom) from the DES choline chloride:lactic acid (molar ratio 1:2). The extraction was carried out with [A336][SCN], (0.9 M in toluene). The LP:HP ratio was 1:1.

After the removal of Fe, Co and B, Nd and Dy remained in the DES solution. As it was previously discussed, the extractant, its concentration, the kinetics and the stripping agent were

evaluated. Cyanex® 923 (0.9 M in toluene) was selected as the less polar phase to carry out the separation of Dy from Nd in the mixer settlers since good separation factors were achieved, the stripping could be carried out efficiently using water and the system presented fast and good phase disengagement (important when running mixer settlers). Fig. 6.13 shows the extraction isotherm of Dy at different LP:HP ratios from an eutectic mixture of choline chloride and lactic acid (molar ratio 1:2) containing only Nd and Dy. It was estimated that approximately three stages were needed when working at an LP:HP ratio of 1:1 and two stages when using an LP:HP ratio of 2:1. An LP:HP ratio of 2:1 was chosen since it allows the less number of stages and a better and faster phase disengagement when removing the Nd from Dy than when removing Fe, Co, and B from Nd and Dy, partly because of the lower viscosity of the system. No formation of a third phase, precipitate or gel was observed at any point of the separation study. One extra stage was added to the system in order to assure complete extraction of the Dy in the case that two stages were not enough when testing the separation system in the mixer settlers.

The extraction behaviour of Dy is presented in Figure 6.14. Every hour a sample was taken from each extraction chamber throughout the day and analysed with ICP-OES. The extraction showed good stability over time, with minor variations in metal concentrations between the samples. In the first stage, the concentration of Dy in the more polar phase was decreased by almost the half and on the second stage it was close to 0 mg L^{-1}. No Dy was detected on the third stage. The experimental data with the mixer settlers showed that two stages, when working at an LP:HP phase ratio of 2:1 were needed to successfully separate Dy from the Nd.

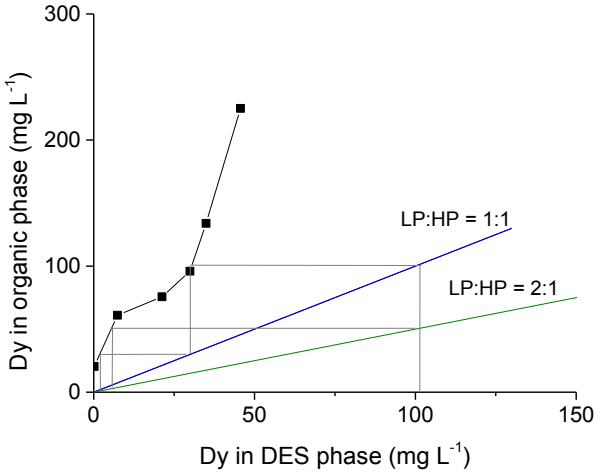

Fig. 6.13. McCabe-Thiele diagram for Dy from a mixture of Nd and Dy in the DES of choline chloride and lactic acid (molar ratio 1:2) with 0.9 M Cyanex® 923 in toluene (phase contact time 20 min, LP:HP phase ratios between 0.25:1 and 10:1).

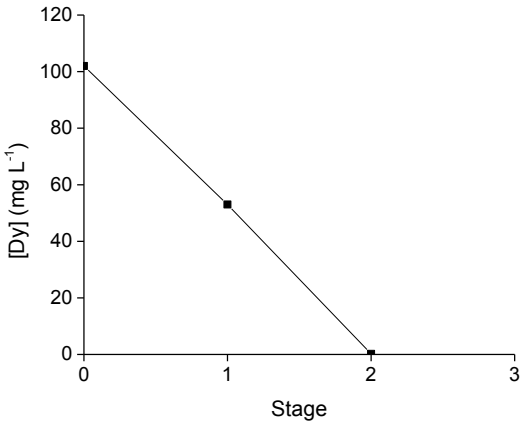

Fig. 6.14. Extraction behaviour of Dy from the deep-eutectic solvent choline chloride: lactic acid (1:2). The extraction was carried out with Cyanex® 923 (0.9 M in toluene). The LP:HP phase ratio was 2:1.

After extraction, part of the raffinate containing mainly Nd was contacted with a stoichiometric amount of oxalic acid and stirred at 25 °C during 30 min. The light pink precipitate that was obtained was filtered, washed with water and ethanol and then calcined at 950 °C during 3 hours. The blue powder that was obtained was analyzed by XRD and corresponded to Nd_2O_3.[71] The

dissolution of this powder in concentrated HCl and its quantification with ICP-OES indicated a purity of 99.87% and 0.13% of Dy. The less polar phase obtained from the mixer settler, rich in Dy and containing Nd was scrubbed manually in a separatory funnel, 5 times, with 6 M $CaCl_2$ and then the Dy was stripped with water, precipitated with oxalic acid and calcined at 950 °C. The obtained white powder was analyzed by XRD which indicated that it corresponded to Dy_2O_3,[72] the purity was determined by ICP and it corresponded to 99.94% Dy and 0.06% Nd as impurity.

6.3.4 Recycling of the less polar phase

After the removal of Fe, B and Co from the feed solution with the ionic liquid [A336][SCN] (0.9 M in toluene) and the stripping of these elements using 6 M HCl and 1.5 M EDTA pH 5.6, the less polar phase, without any further treatment, was put in contact with a fresh DES mixture containing Fe, B, Co, Nd and Dy. In a similar experiment, the less polar phase was equilibrated with KSCN before its reuse in a new extraction. Results are presented in Table 6.7.

Table 6.7. Re-use of the less polar phase (0.9 M [A336][SCN] in toluene) for the extraction of Fe, B and Co.[a]

Less polar phase	D_{Fe} ± SD	D_B ± SD	D_{Co} ± SD
Without treatment	30.3 ± 1.4	2.6 ± 0.2	65.7 ± 2.4
Equilibrated with $[SCN]^-$	52.9 ± 4.9	0.84 ± 0.07	199 ± 8

[a] 25 min equilibration time, 2000 rpm, 25 °C.

Table 6.7 shows how after the stripping of Fe, B and Co with HCl and EDTA, the less polar phase can be re-used for the extraction of these metals. The percentages of extraction for Fe and Co are comparable to the ones obtained when carrying out the extraction for the first time (Table 6.2). However, in the case of B, higher percentages extraction were obtained and they are comparable to the ones obtained when [A336][Cl] was used as extractant. When the less polar phase is equilibrated with 2.5 M KSCN before its re-use, the percentages extraction that are obtained are similar to those observed when working with [A336][SCN]. This could indicate that there is an anionic exchange mechanism when using [A336][SCN], therefore, after extraction, the less polar phase is richer in chloride ions, which explains why the higher percentages of extraction for boron when the less polar phase is reused without equilibration with KSCN. In fact,

the analysis of the less polar phase with TXRF after extraction indicated the presence of chloride peaks.

After stripping with water, the less polar phase (Cyanex® 923 diluted in toluene 0.9 M), was re-used to extract Dy from the mixture of Nd and Dy in the DES of choline chloride:lactic acid (molar ratio 1:2) and no significant deviations from the results obtained when using the extractant for the first time were encountered.

6.3.5 Comparison with conventional systems

The developed system was compared to the traditional liquid-liquid extraction systems composed by an aqueous phase and an organic phase. Since the concentration of chloride anions in the DES is close to 3 M, it was decided to carry out the experiments with an aqueous phase containing 1.5 M $CaCl_2$ to have a concentration of chloride anions close to the one present in the DES, a concentration of 5 M $CaCl_2$ in the aqueous phase was also tested for comparison (Table 6.8).

Table 6.8. Comparison between the proposed system and a traditional liquid-liquid extraction system from an aqueous solution for the removal of Fe, B and Co using 0.9 M [A336][SCN] in toluene.[a]

More polar phase	D_{Fe} ± SD	D_{B} ± SD	D_{Co} ± SD	D_{Nd} ± SD	D_{Dy} ± SD
ChCl:lactic acid (molar ratio 1:2)	44.5 ± 2.6	0.78 ± 0.10	193 ± 2	0.029 ± 0.007	0.025± 0.008
Aqueous phase (without $CaCl_2$)	5.7 ± 0.3	n.d.[b]	10.0 ± 1.4	n.d.[b]	0.080 ± 0.009
Aqueous phase ($CaCl_2$ 1.5 [M])	20.0 ± 1.6	n.d.[b]	29.8 ± 1.2	0.10 ± 0.02	0.23 ± 0.04
Aqueous phase ($CaCl_2$ 5 [M])	49.6 ± 1.5	0.09 ± 0.03	72 ± 3	0.31 ± 0.08	0.45 ± 0.07

[a] Equilibration time: 60 min, 2000 rpm, 25 °C. [b] n.d. = not detected (below limit of detection).

From Table 6.8 it can be seen how higher *D* for Fe and Co are obtained when extracting from DESs. Moreover, the extraction of B is not possible from the aqueous system. The extraction of metal ions from the aqueous system can be improved by addition of $CaCl_2$ but by doing this, the

selectivity is lost since Dy and Nd are co-extracted. The use of a DES as the more polar phase was also beneficial for the separation of Nd and Dy in comparison to conventional aqueous systems (Table 6.9).

Table 6.9. Comparison between the proposed system and a traditional liquid-liquid extraction system with an aqueous solution for the removal of Dy using 0.9 M Cyanex® 923 in toluene.[a]

More polar phase	D_{Nd} ± SD	D_{Dy} ± SD
ChCl:lactic acid (molar ratio 1:2)	0.17 ± 0.09	1.89 ± 1.2
Aqueous phase (without $CaCl_2$)	0.19 ± 0.02	0.43 ± 0.06
Aqueous phase ($CaCl_2$ 1.5 [M])	0.29 ± 0.06	0.55 ± 0.12
Aqueous phase ($CaCl_2$ 5 [M])	0.45 ± 0.05	0.77 ± 0.13

[a] Equilibration time: 60 min, 2000 rpm, 25 °C.

When extracting Nd and Dy at these concentrations from aqueous systems, low *D* and SF are obtained. When extracting from DESs, better separation factors are obtained. This can be due to the presence of lactic acid in the more polar phase. It has been reported how a complexing agent that can form complexes with rare-earth cations (with different equilibrium constants) can significantly increase the possibility of selectively separate the different rare earth cations. The complexation of rare-earth cations with enhances the sorption performance and improves the selectivity.[73-75] This highlights the importance of these new systems and the importance of studying and improving them. Fig. 6.15 shows the flow sheet for a process to separate Fe, B and Co from Nd and Dy in a DES and afterwards to separate Dy from Nd using [A336][SCN] (0.9 M in toluene) and Cyanex® 923 (0.9 M in toluene), respectively.

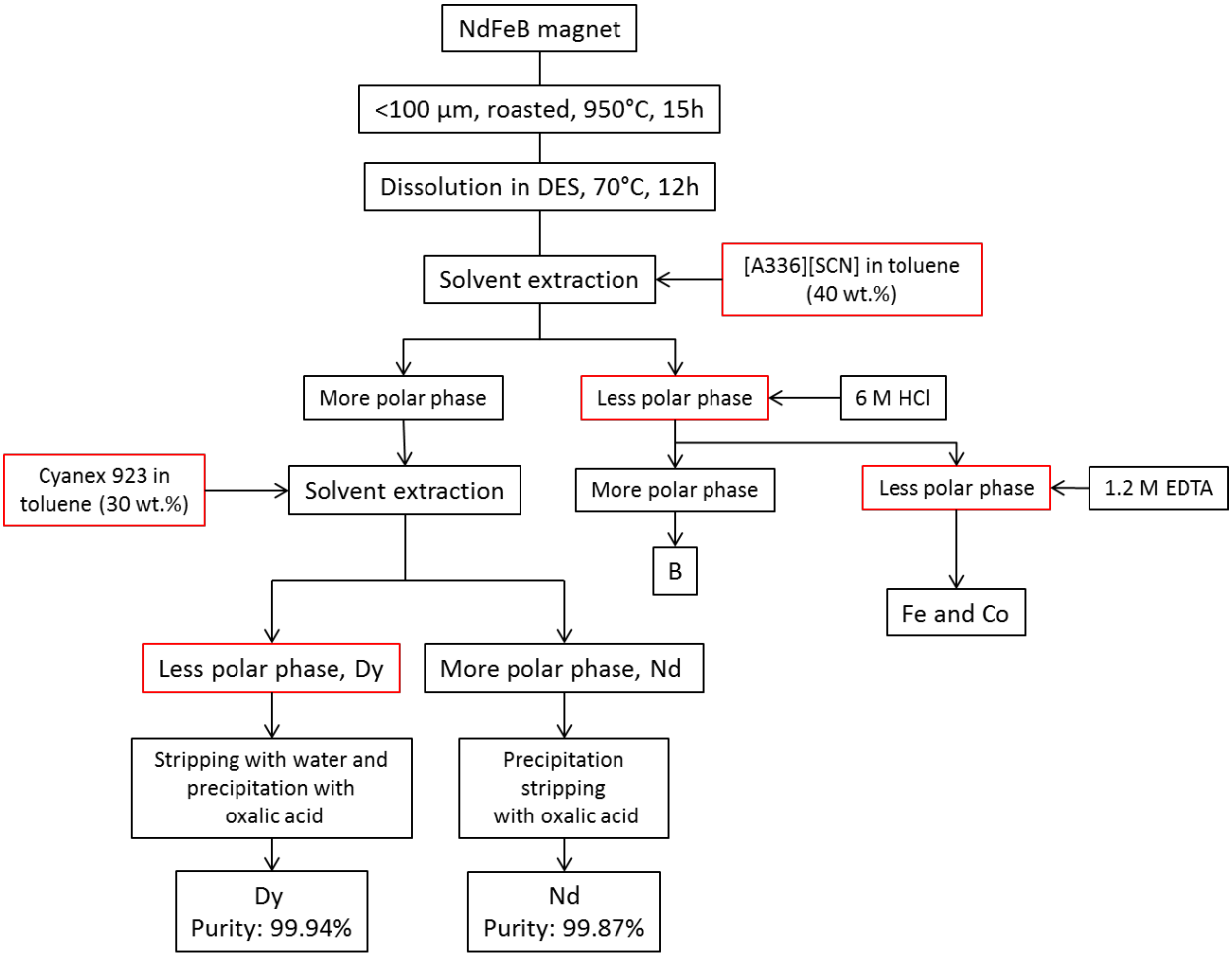

Fig. 6.15. Flow sheet for a process consisting of dissolution of a NdFeB magnet in the DES choline chloride: lactic acid (molar ratio 1:2), followed by the removal of Fe, B and Co with [A336][SCN] 0.9 M in toluene and afterwards, the separation of Nd and Dy with Cyanex® 923 0.9 M in toluene.

6.3.6 EXAFS

Understanding of the mechanism of extraction is crucial in every single extraction process. When it is understood how the extraction occurs, the process can be optimized and redesigned in order to create better systems in terms of efficiency and consumption of chemicals. The extraction of transition metals and rare earths using conventional extractants from aqueous systems is described extensively in the literature.[15,17,58] However, the mechanism of extraction from DESs has not been studied yet. The mechanism of extraction of Fe and Co with [A336][SCN] 0.9 M in

toluene was studied from the DES phase and compared against the extraction of the same metals from aqueous solutions.

A fit of the first coordination shell of iron extracted from the aqueous to the [A336][SCN] phase showed 6 nitrogen atoms. Therefore, a model containing 6 coordinating thiocyanate anions was used to fit the experimental data. A model including a linear Fe-N-C bond showed bad fits. In case of a non-linear Fe-N-C bond, four-leg scattering paths can be excluded if the bond angle is not close to 180°. A model including three two-leg scattering paths (Fe-N, Fe-C and Fe-S) and three three-leg scattering paths resulted in a good fit of the data. The degeneracy of the different paths was constrained but S_0 was allowed to vary resulting in a value of 0.95. The distances to N, C and S also proof the non-linearity of the Fe-N-C bond as the total sum of the bond lengths (*r*) in Fe-N-C-S is around 5 Å and the fact that the three leg scattering paths to carbon and sulphur are significantly larger in distance than the two leg scattering paths to carbon and sulphur, respectively (Table 6.10, Fig. 6.16., Fig. 6.17). *N* is the coordination number, *r* is the bond distance, and σ^2 is the mean-square-displacement in the bond distance.

Table 6.10. Fitting results of the EXAFS data for the $[Fe(SCN)_6]^{3-}$ complex in [A336][SCN], extracted from an aqueous phase.[a]

Scattering path	N	*r* (Å)	σ^2 (Å^2)
Fe-N	6	2.076(3)	0.010(1)
Fe-C	6	3.085(46)	0.015(2)
Fe-S	6	4.503(29)	0.009(2)
Fe-N-C	12	3.254(13)	0.009(1)
Fe-S-C	12	4.614(19)	0.008(1)
Fe-S-N	12	4.937(11)	0.008(2)

[a] The data were Fourier-transformed between k = 3.0 and 12.9 Å with a Gaussian rounded ends function and fitted to the model between r = 0 and 4.92 Å^{-1}.

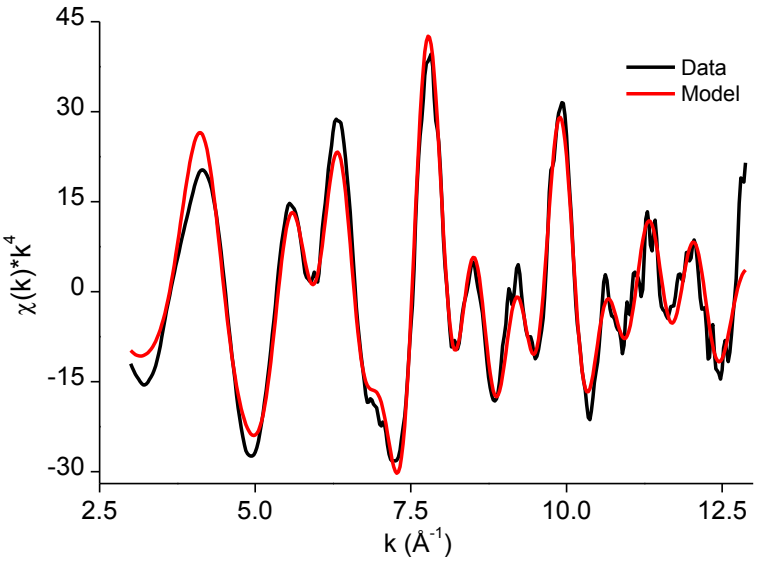

Fig. 6.16. EXAFS function $\chi(k)*k^4$ and model of the $[Fe(SCN)_6]^{3-}$ complex.

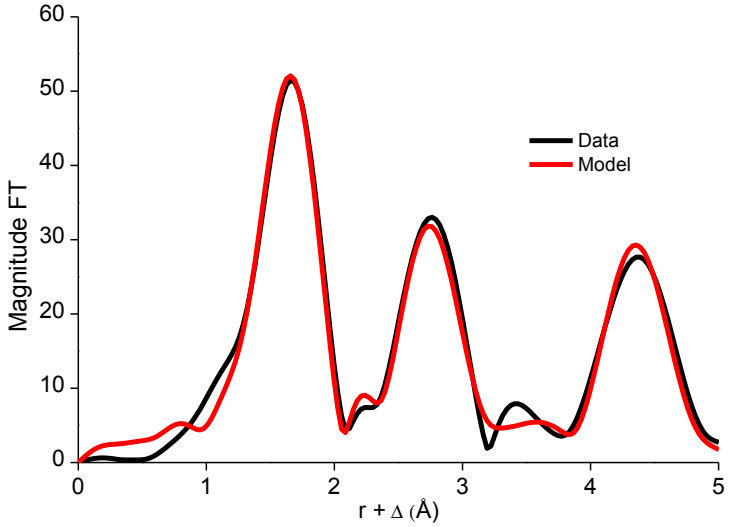

Fig. 6.17. Fourier transform and model of the $[Fe(SCN)_6]^{3-}$ complex. The data were Fourier-transformed between k = 3.0 and 12.9 Å with a Gaussian rounded ends function and fitted to the model between r = 0 and 4.92 $Å^{-1}$.

The edge structure of the iron(III) complex extracted from the DES looked very similar to the edge structure previously observed for $[FeCl_4]^-$ complexes.[76,77] A fit of the EXAFS region, including only Fe-Cl single scattering paths resulted in a fit degeneracy of 3.4, a bond distance of 2.208 Å and a Debye Waller factor of 0.004 $Å^2$. A slightly better fit was obtained when including also one Fe-O path. However, this is contradictory to the rest of the Fourier transform (FT) as coordinating oxygen atoms can only come from lactic acid or choline. This suggests that there

should be contributions to the FT at slightly higher r values as well, which is not the case. Therefore, it can be concluded that iron extracts as a $FeCl_4$ complex to the less polar phase (Fig. 6.18, 6.19, 6.20).

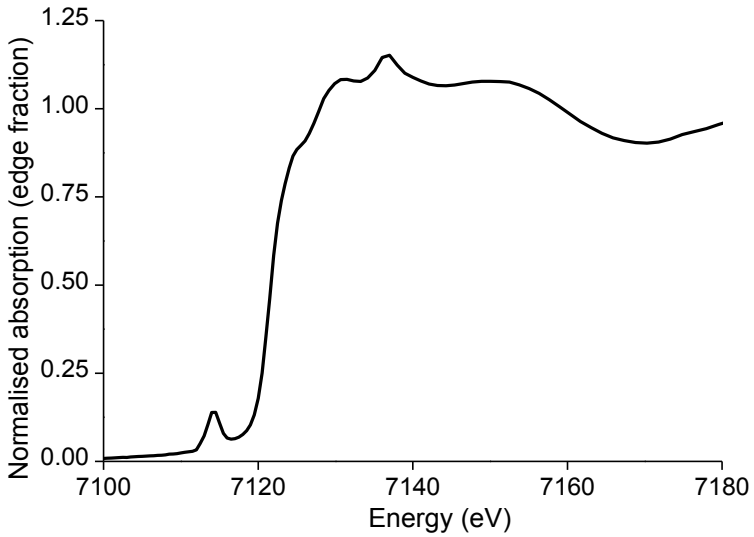

Fig. 6.18. X-ray absorption spectrum around the Fe K-edge of the less polar phase (0.9 M [A336][SCN]) of the extraction from the DES.

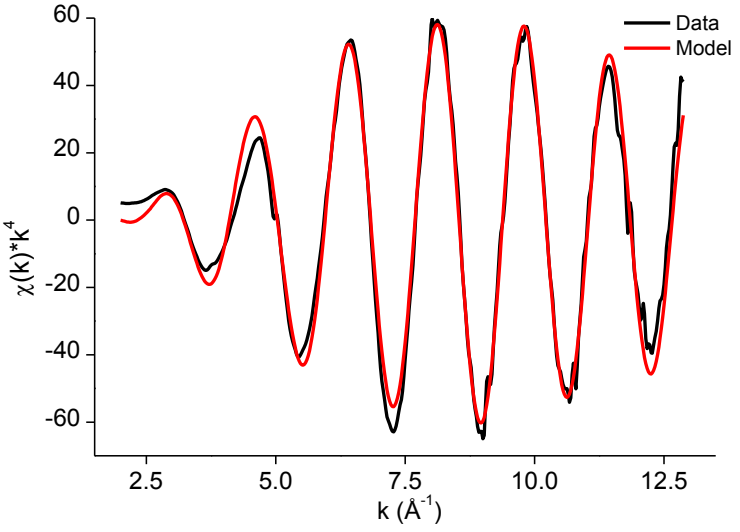

Fig. 6.19. EXAFS function $\chi(k)*k^4$ and model of the $[FeCl_4]^-$ complex in 0.9 M [A336][SCN] diluted in toluene, as extracted from the DES.

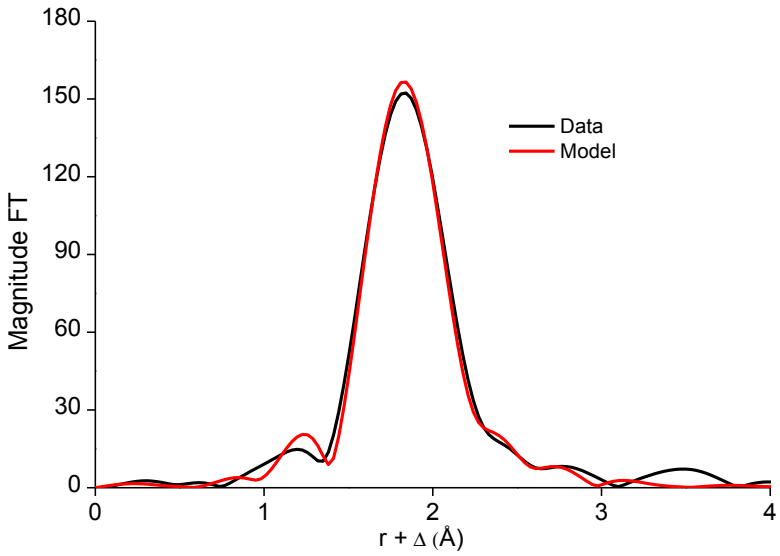

Fig. 6.20. Fourier transform and model of the $[FeCl_4]^-$ complex in [A336][SCN] diluted in toluene (0.9 M), as extracted from DES. The data were Fourier-transformed between k = 2.0 and 12.9 Å with a Gaussian rounded ends function and fitted to the model between r = 0 and 3 $Å^{-1}$.

Fitting of the first shell of the Co complex in the [A336][SCN] phase, as extracted from an aqueous solution, showed the presence of four nitrogen atoms. Therefore, a model consisting of four thiocyanate ligands was used to fit the experimental data. Three single scattering paths and three three-leg scattering paths were included, and of which the degeneracy was constrained. The amplitude reduction factor S_0 was set to 0.95. Similarly to the $[Fe(SCN)_6]^{3-}$ complex in [A336][SCN], the three-leg scattering paths Co-C-N, Co-S-C and Co-S-N are larger than the distances between Co and N, C and Co, which indicates the non-linearity between the Co-N-C angle and the N-C-S angle (Table 6.11). The EXAFS function of the Co complex extraction from the DES and from 5 M $CaCl_2$ was very similar to the EXAFS function of Co extracted from an aqueous solution, which indicates that the $[Co(SCN)_4]^{2-}$ complex is formed in both cases (Fig. 6.21, 6.22, 6.23). This result is in contrast to the extraction of iron, where $[Fe(SCN)_6]^{3-}$ complex is formed when extraction occurred from an aqueous solution, while a $[FeCl_4]^-$ complex is formed when extracted from DES.

Table 6.11. Fitting results of the EXAFS function of cobalt extracted from aqueous solution to [A336][SCN].[a]

Scattering path	N	*r* (Å)	σ^2 (Å^2)
Co-N	4	1.962(4)	0.005(1)
Co-C	4	3.992(12)	0.004(1)
Co-S	4	4.606(9)	0.005(1)
Co-C-N	8	3.128(4)	0.004(1)
Co-S-C	8	4.776(15)	0.005(1)
Co-S-N	8	4.909(60)	0.005(1)

[a] The data were Fourier transformed between k = 4.0 and 13.0 Å without any window function and fitted to the model between r = 0 and 5 Å^{-1}.

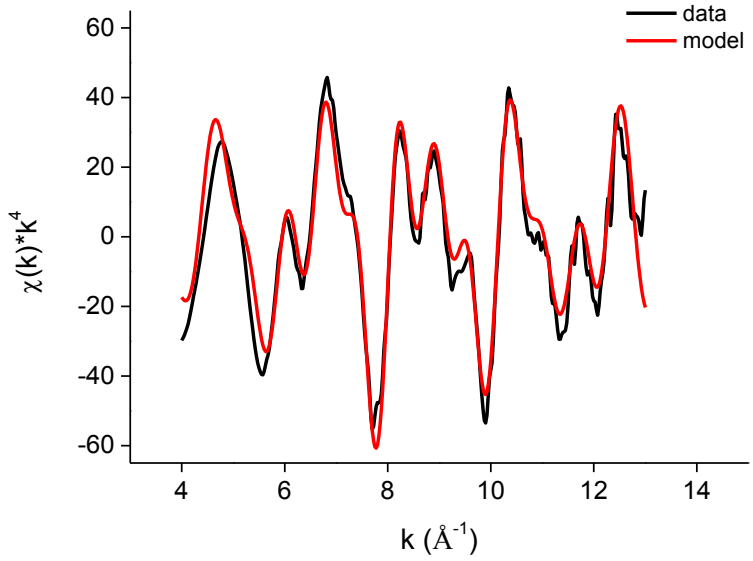

Fig. 6.21. EXAFS function $\chi(k)*k^4$ and model of the $[Co(SCN)_4]^{2-}$ complex.

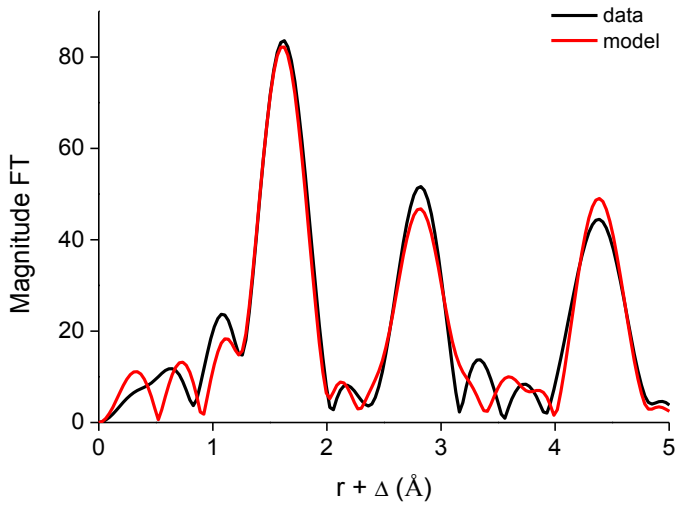

Fig. 6.22. Fourier transform and model of the $[Co(SCN)_4]^{2-}$ complex in the ionic liquid [A336][SCN], as extracted from aqueous solution.

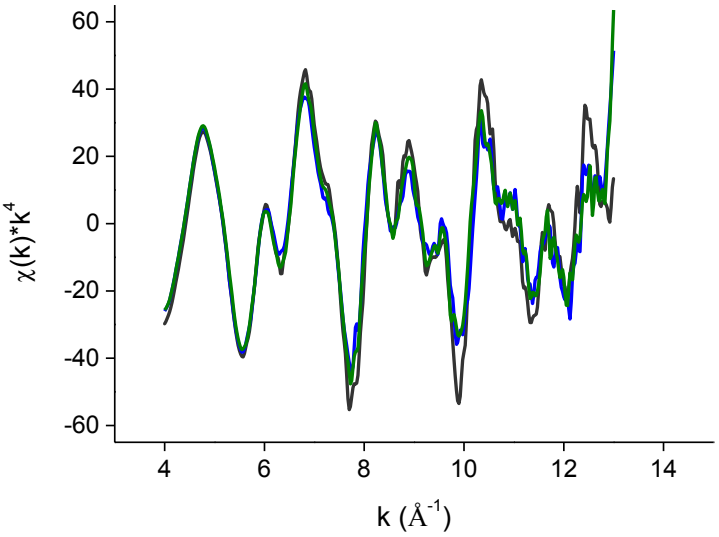

Fig. 6.23. EXAFS function $\chi(k)*k^4$ of the $[Co(SCN)_4]^{2-}$ complex in the ionic liquid [A336][SCN] as extracted from water (black), 5 M $CaCl_2$ (green) and DES (blue).

Furthermore, samples of the organic and the DES phase after extraction of Fe were taken and analyzed by ^{1}H NMR. Components of the DES were not detected in the less polar phase nor the Aliquat® 336 cation was detected in the DES. The latter results in addition with the ones

obtained by EXAFS, suggest that the mechanism of extraction of Fe from the DES choline chloride:lactic acid (1:2) corresponds to an anionic exchange (Eq. 6.20).

$$Fe^{3+} + 4Cl^- + \overline{[A336][SCN]} \rightarrow \overline{[FeCl_4][A336]} + SCN^- \qquad (6.20)$$

This means that part of the thiocyanate anions are being exchanged by chloride anions from the DES phase and thus, the ionic liquid in the less polar phase is being degraded. This issue can be solved by contacting the less polar phase with $[SCN]^-$ and regenerating the ionic liquid after extraction (Table 6.7).

6.4 Conclusions

For the first time, a DES composed of choline chloride and lactic acid (molar ratio 1:2) was successfully employed for the complete dissolution of NdFeB magnets. Fe, Co and B were removed from this leachate using the ionic liquid [A336][SCN] as extractant diluted in toluene (0.9 M). Cyanex® 923 diluted in toluene (0.9 M) was a better extractant for the separation of Dy from Nd than D2EHPA diluted in toluene, since it allowed easier scrubbing and stripping. As demonstrated by EXAFS measurements, the extraction mechanism from DESs is different from those from aqueous solutions, thus different distribution ratios and separation ratios were achieved. As a result, the use of DESs allowed higher selectivity for the removal of Fe, Co and B from Nd and Dy and also for the separation of Dy from Nd in comparison with conventional liquid-liquid extraction systems. The feasibility of scaling up the proposed process was further confirmed by its implementation in a mixer-settler setup. It was found that the studied DES can be used at room temperature without any issue related to high viscosity, poor phase disengagement or third-phase formation. The metals were stripped by HCl and EDTA (for Fe, B and Co) and water (for Dy) from the less polar phase and a stoichiometric amount of oxalic acid for the removal of Nd from the DES. Nd_2O_3 and Dy_2O_3 were recovered with purities of 99.87% and 99.94%, respectively.

6.5 References

1. J. H. Rademaker, R. Kleijn and Y. Yang, *Environ. Sci. Technol.*, 2013, **47**, 10129-10136.
2. M. Zakotnik, C. O. Tudor, L. T. Peiró, P. Afiuny, R. Skomski and G. P. Hatch, *Environmental Technology & Innovation*, 2016, **5**, 117-126.
3. K. Binnemans, P. T. Jones, B. Blanpain, T. Van Gerven, Y. Yang, A. Walton and M. Buchert, *J. Clean. Prod.*, 2013, **51**, 1-22.
4. Y. Yang, A. Walton, R. Sheridan, K. Güth, R. Gauß, O. Gutfleisch, M. Buchert, B.-M. Steenari, T. Van Gerven, P. T. Jones and K. Binnemans, *J. Sustain. Metall.*, 2017, **3**, 122-149.
5. R. Sasai and N. Shimamura, *J. Asian. Cer. Soc.*, 2016, **4**, 155-158.
6. O. Takeda, T. H. Okabe and Y. Umetsu, *J. Alloys Compd.*, 2006, **408–412**, 387-390.
7. A. Walton, H. Yi, N. A. Rowson, J. D. Speight, V. S. J. Mann, R. S. Sheridan, A. Bradshaw, I. R. Harris and A. J. Williams, *J. Clean. Prod.*, 2015, **104**, 236-241.
8. M. Zakotnik, I. R. Harris and A. J. Williams, *J. Alloys Compd.*, 2008, **450**, 525-531.
9. M. Zakotnik, I. R. Harris and A. J. Williams, *J. Alloys Compd.*, 2009, **469**, 314-321.
10. X. Li, M. Yue, M. Zakotnik, W. Liu, D. Zhang and T. Zuo, *J. Rare Earth.*, 2015, **33**, 736-739.
11. D. Dupont and K. Binnemans, *Green Chem.*, 2015, **17**, 856-868.
12. S. Riano and K. Binnemans, *Green Chem.*, 2015, **17**, 2931-2942.
13. T. Vander Hoogerstraete, S. Wellens, K. Verachtert and K. Binnemans, *Green Chem.*, 2013, **15**, 919-927.
14. D. Beltrami, G. Cote, H. Mokhtari, B. Courtaud, B. A. Moyer and A. Chagnes, *Chem. Rev.*, 2014, **114**, 12002-12023.
15. S. Nishihama, T. Hirai and I. Komasawa, *Ind. Eng. Chem. Res.*, 2001, **40**, 3085-3091.
16. P. J. Panak and A. Geist, *Chem. Rev.*, 2013, **113**, 1199-1236.
17. F. Xie, T. A. Zhang, D. Dreisinger and F. Doyle, *Miner. Eng.*, 2014, **56**, 10-28.
18. Z. Zhu, W. Zhang and C. Y. Cheng, *Hydrometallurgy*, 2011, **105**, 304-313.
19. M. K. Jha, D. Gupta, J.-c. Lee, V. Kumar and J. Jeong, *Hydrometallurgy*, 2014, **142**, 60-69.
20. V. S. Kislik, in *Solvent Extraction*, Elsevier, Amsterdam, 2012, ch. 1, pp. 3-67.
21. V. S. Kislik, in *Solvent Extraction*, Elsevier, Amsterdam, 2012, ch. 3, pp. 113-156.
22. M. A. R. Önal, C. R. Borra, M. Guo, B. Blanpain and T. Gerven, *J. Sustain. Metall.*, 2015, **1**, 199-215.
23. M. Al-Harahsheh and S. W. Kingman, *Hydrometallurgy*, 2004, **73**, 189-203.

24. S. S. Konyratbekova, A. Baikonurova and A. Akcil, *Miner. Process. Extr. Metall. Rev.*, 2015, **36**, 198-212.
25. M. Sahin, A. Akcil, C. Erust, S. Altynbek, C. S. Gahan and A. Tuncuk, *Sep. Sci. Technol.*, 2015, **50**, 2587-2595.
26. Y. Dong, X. Sun, Y. Wang and Y. Chai, *Hydrometallurgy*, 2015, **157**, 256-260.
27. T. Vander Hoogerstraete, B. Onghena and K. Binnemans, *J. Phys. Chem. Lett*, 2013, **4**, 1659-1663.
28. X. Sun, C.-L. Do-Thanh, H. Luo and S. Dai, *Chem. Eng. J.*, 2014, **239**, 392-398.
29. X. Sun, H. Luo and S. Dai, *Talanta*, 2012, **90**, 132-137.
30. J. Wang, J. Zhao, D. Feng, X. Kang, Y. Sun, L. Zhao and H. Liang, *J. Rare Earth.*, 2016, **34**, 83-90.
31. H.-L. Yang, W. Wang, H.-M. Cui and J. Chen, *Chinese, J. Anal. Chem.*, 2011, **39**, 1561-1566.
32. K. Larsson and K. Binnemans, *Hydrometallurgy*, 2015, **156**, 206-214.
33. A. Rout and K. Binnemans, *Dalton Trans.*, 2014, **43**, 1862-1872.
34. A. P. Abbott, G. Capper, D. L. Davies, K. J. McKenzie and S. U. Obi, *J. Chem. Eng. Data*, 2006, **51**, 1280-1282.
35. G. R. T. Jenkin, A. Z. M. Al-Bassam, R. C. Harris, A. P. Abbott, D. J. Smith, D. A. Holwell, R. J. Chapman and C. J. Stanley, *Miner. Eng.*, 2016, **87**, 18-24.
36. E. L. Smith, A. P. Abbott and K. S. Ryder, *Chem. Rev.*, 2014, **114**, 11060-11082.
37. M. R. S. Foreman, *Cogent Chemistry*, 2016, **2**, 1139289.
38. A. P. Abbott, J. C. Barron, K. S. Ryder and D. Wilson, *Chemistry*, 2007, **13**, 6495-6501.
39. Q. Zhang, K. De Oliveira Vigier, S. Royer and F. Jerome, *Chem. Soc. Rev.*, 2012, **41**, 7108-7146.
40. A. P. Abbott, G. Capper, D. L. Davies, R. K. Rasheed and P. Shikotra, *Inorg. Chem.*, 2005, **44**, 6497-6499.
41. K. V. Klementev, *Nucl. Instrum. Methods Phys. Res., Sect. A*, 2000, **448**, 299-301.
42. M. Newville, *J. Synchrotron Radiat*, 2001, **8**, 96-100.
43. J. O. Liljenzin, G. Persson, I. Svantesson and S. Wingefors, in *Transplutonium Elements—Production and Recovery*, American Chemical Society, 1981, vol. 161, ch. 13, pp. 203-221.
44. B. Sprecher, Y. Xiao, A. Walton, J. Speight, R. Harris, R. Kleijn, G. Visser and G. J. Kramer, *Environ. Sci. Technol.*, 2014, **48**, 3951-3958.
45. W. Yan, S. Yan, D. Yu, K. Li, H. Li, Y. Luo and H. Yang, *J. Rare Earth.*, 2012, **30**, 133-136.
46. P. C. Dent, *J. Appl. Phys.*, 2012, **111**, 07A721.

47. L. K. Jakobsson, G. Tranell and I.-H. Jung, *Metall. Trans. B*, 2016, 1-13.
48. M. I. Saleh, M. F. Bari and B. Saad, *Hydrometallurgy*, 2002, **63**, 75-84.
49. A. A. Mhaske and P. M. Dhadke, *Hydrometallurgy*, 2001, **61**, 143-150.
50. G. A. Clark, R. M. Izatt and J. J. Christensen, *Sep. Sci. Technol.*, 1983, **18**, 1473-1482.
51. A. Cieszynska and M. Wisniewski, *Sep. Purif. Technol.*, 2010, **73**, 202-207.
52. J. Yang, T. Retegan and C. Ekberg, *Hydrometallurgy*, 2013, **137**, 68-77.
53. Y. Jin, Y. Ma, Y. Weng, X. Jia and J. Li, *J. Ind. Eng. Chem.*, 2014, **20**, 3446-3452.
54. N. Panda, N. Devi and S. Mishra, *J. Rare Earth.*, 2012, **30**, 794-797.
55. S.-m. Liu, H.-h. Liu, Y.-j. Huang and W.-j. Yang, *Trans. Nonferrous Met. Soc. China*, 2015, **25**, 329-334.
56. D. Prat, A. Wells, J. Hayler, H. Sneddon, C. R. McElroy, S. Abou-Shehada and P. J. Dunn, *Green Chem.*, 2016, **18**, 288-296.
57. R. Pizer and R. Selzer, *Inorg. Chem.*, 1984, **23**, 3023-3026.
58. M. K. Jha, A. Kumari, R. Panda, J. Rajesh Kumar, K. Yoo and J. Y. Lee, *Hydrometallurgy*, 2016, **165, Part 1**, 2-26.
59. G. S. Lee, M. Uchikoshi, K. Mimura and M. Isshiki, *Sep. Purif. Technol.*, 2009, **67**, 79-85.
60. K. Ohto, M. Yano, K. Inoue, T. Yamamoto, M. Goto, F. Nakashio, S. Shinkai and T. Nagasaki, *Anal. Sci.*, 1995, **11**, 893-902.
61. D. Zheng, N. B. Gray and G. W. Stevens, *Solvent Extr. Ion Exc.*, 1991, **9**, 85-102.
62. C. Tunsu, C. Ekberg, M. Foreman and T. Retegan, *Solvent Extr. Ion Exc.*, 2014, **32**, 650-668.
63. N. K. Batchu, T. Vander Hoogerstraete, D. Banerjee and K. Binnemans, *Sep. Purif. Technol.*, 2017, **174**, 544-553.
64. B. Gupta, P. Malik and A. Deep, *Solvent Extr. Ion Exc.*, 2003, **21**, 239-258.
65. Y. A. El-Nadi, *J. Rare Earth.*, 2010, **28**, 215-220.
66. M. L. P. Reddy, R. Luxmi Varma, T. R. Ramamohan, S. K. Sahu and V. Chakravortty, *Solvent Extr. Ion Exc.*, 1998, **16**, 795-812.
67. D. F. Peppard, J. P. Faris, P. R. Gray and G. W. Mason, *J. Phys. Chem.*, 1953, **57**, 294-301.
68. A. Fortuny, M. T. Coll, C. S. Kedari and A. M. Sastre, *J. Chem. Technol. Biotechnol.*, 2014, **89**, 858-865.
69. T. E. Furia, in *CRC Handbook of Food Additives*, ed. C. Press, CRC Press, Boca Raton (Florida), 1972.
70. G. Schwarzenbach, *Analyst*, 1955, **80**, 713-729.
71. T. Liu, Zhang, Shao and Li, *Langmuir*, 2003, **19**, 7569-7572.

72. A. Bassano, V. Buscaglia, M. Sennour, M. T. Buscaglia, M. Viviani and P. Nanni, *J. Nanopart. Res.*, 2010, **12**, 623-633.
73. F. V. P. Blondet, T.Guibal, in *Ion Exchange and Solvent Extraction*, CRC Press, Boca Raton (Florida), 2007, pp. 151-292.
74. S. Yin, W. Wu, X. Bian, Y. Luo and F. Zhang, *Ind. Eng. Chem. Res.*, 2013, **52**, 8558-8564.
75. S. Yin, W. Wu, X. Bian and F. Zhang, *Hydrometallurgy*, 2013, **131–132**, 133-137.
76. A. Kiyotaka, N. Masaharu and K. Haruo, *Bull. Chem. Soc. Jpn.*, 1985, **58**, 1543-1550.
77. M. Bauer and C. Gastl, *Phys. Chem. Chem. Phys.*, 2010, **12**, 5575-5584.

Chapter 7. Conclusions and outlook

Solvent extraction processes based on ionic liquids are a safer and more environmentally friendly alternative for the recycling of NdFeB magnets. Their low flammability, negligible volatility and recyclability make them good candidates for the replacement of conventional less environmentally friendly organic phases in solvent extraction.

This PhD dissertation mainly focused on the use of ionic liquids for the separation of rare earths, especially neodymium and dysprosium, the principal rare earths present in NdFeB magnets. [C101][NO_3] and [C101][SCN] were successfully employed in the separation of two rare earths and both represented a safer alternative than the conventional molecular extractants. The ionic liquid [C101][SCN] combined with the molecular extractant Cyanex® 923 allowed the extraction of rare earths from chloride media without the need of employing an acidic extractant. In both cases, soft stripping conditions were necessary to recover the rare earths from the ionic liquid phase.

Concretely, an iron-free leachate from end-of-life NdFeB magnets was prepared and the ionic liquid [C101][NO_3] was used to separate neodymium(III) and dysprosium(III) from cobalt(II). The partition of both rare-earth metal ions towards the organic phase was assessed by increasing the nitrate concentration of the aqueous feed. The separation of dysprosium(III) from neodymium(III) was achieved using EDTA as selective stripping agent. Different parameters of extraction were optimized and cobalt(II), dysprosium(III) and neodymium(III) were recovered as their respective oxides. The ionic liquid was recovered and reused, as well as part of the EDTA with the aim of reducing waste streams and the impact to the environment. While working on this approach, that also included the handling of very concentrated feeds, the problem of the relatively high viscosity of the ionic liquids was solved by working at high temperatures and using water-saturated ionic liquids. The issues with a high viscosity related to a highly-loaded ionic liquid phase were also approached by an alternative strategy in another process. The split-anion extraction approach was applied to the separation of neodymium(III) and dysprosium(III) from a chloride feed. The system was improved by the addition of a molecular extractant (*i.e.* Cyanex® 923) to the organic phase, which resulted not only in a lower viscosity and improved phase

disengagements, but also in an increase in the distribution ratios of dysprosium(III) and in the loading capacity of the ionic liquid. After optimization and removal of dysprosium(III) with [C101][SCN], the recovery of neodymium(III) was achieved by contacting the chloride aqueous feed with [C101][NO_3], which highlighted the versatility of the split-anion extraction.

A novel approach consisting in the dissolution of the magnets in a deep-eutectic solvent was proposed. Compared to the two processes based on ionic liquids, in which the leaching step was carried out with mineral acids, this one demonstrated that there are alternative ways of dissolving the magnets using environmentally friendly and less expensive reagents. It was demonstrated that it is possible to carry out solvent extraction from deep eutectic solutions to diluted ionic liquids or using conventional extractants. The pregnant deep-eutectic solution was further processed by solvent extraction and the separations were much more efficient and selective than the analogous aqueous traditional system. The leachate was contacted with the ionic liquid [A336][SCN] diluted in toluene to remove iron, boron and cobalt. Then, the raffinate containing neodymium and dysprosium was contacted with the neutral extractant Cyanex® 923 diluted in toluene to separate the dysprosium from the neodymium. The system based on the deep-eutectic solvent was tested in a small mixer-settler setup and it was successfully scaled up without facing problems, which demonstrated the feasibility of the proposed separation process.

Finally, in the third part of this PhD dissertation, attention was paid to the development of a procedure for the correct preparation of aqueous samples for TXRF analysis. The proposed procedure allows making more reliable analysis of metal ions in aqueous solutions with low matrix content. The key observation was that it is important that both analyte and internal standard have closer X-ray line energies, as well as that the concentration ratio of the standard should be close to the one of the analyte in order to assure good recovery rates.

Outlook

There are still a lot of opportunities related to the development of environmentally friendly processes for the recycling of NdFeB magnets. New studies should include more rare earths such as gadolinium, terbium and praseodymium and not be limited to only neodymium and dysprosium. In the same way, more studies on the recovery of transition metals such as cobalt are needed since it is a valuable metal that can be present in considerable quantities in the NdFeB magnets. In this PhD dissertation only two neutral extractants were studied to enhance the properties of the ionic liquid phase, but more extractants can be included in the future in order to assess the possibility to enhance further the separation factors between rare earths. More research is needed at larger scales to prove the feasibility and robustness of the developed processes including the use of feeds with different concentrations of metals and real leachates. On the other hand, the recycling of sintered magnets has gotten more attention than the recycling of resin-bonded magnets, therefore, new environmentally friendly hydrometallurgical processes for the recycling of resin-bonded-NdFeB magnets should be studied.

There is still plenty of room for improvement of the extraction from deep-eutectic solvents. One approach that can be explored is the development of solvent extraction processes based on undiluted ionic liquids. Since both phases will suffer of relatively high viscosity issues, higher temperatures would have to be employed. However, the presence of complexing anions in the deep-eutectic solvent can enhance the distribution ratios on the less polar phase if the ionic liquid is chosen properly. Studies on the mechanism of extraction of the rare earths from these types of solvents to ionic liquids should be studied with EXAFS.

Safety aspects

The experimental work performed during this PhD thesis was executed in compliance with the code of practice for safety in the lab (http://chem.kuleuven.be/en/hse/procedures/liab1.htm) and the Introduction Safety Guidelines of the Department of Chemistry (http://chem.kuleuven.be/veiligheid/documenten/safety-brochure.pdf).

The following safety precautions were taken:

- Risk assessments were approved before each experiment and are available: https://www.groupware.kuleuven.be/sites/depchemrisico/Risk%20Assessments/Forms/Per%20division.aspx
- For unsupervised experiments, additional risk assessments were prepared and approved by the necessary people according to the procedure: https://admin.kuleuven.be/sab/vgm/kuleuven/EN/riskactivities/ue/continuous-activities
- Safety googles, labcoat and gloves were worn while performing the experiments.

Safety training:

- Introductory safety course 23/01/2014
- Safety in the lab 07/03/2014
- Radiation protection 22/09/2014

List of publications

S. Riaño, K. Binnemans; Extraction and separation of neodymium and dysprosium from used NdFeB magnets: an application of ionic liquids in solvent extraction towards the recycling of magnets. *Green Chemistry* **2015**, 17, 2931-2942

S. Riaño, M. Regadío, K. Binnemans, T. Vander Hoogerstraete; Practical guidelines for best practice on Total Reflection X-ray Fluorescence spectroscopy: Analysis of aqueous solutions. *Spectrochimica Acta part B* **2016**, 24, 109-115

M. Regadío, S. Riaño, K. Binnemans, T. Vander Hoogerstraete; Direct analysis of metal ions in solutions with high salt concentrations by Total Reflection X-ray Fluorescence (TXRF). *Analytical Chemistry*, **2017**, 89, 4595-4603.

S. Riaño, M. Petranikova, B. Onghena, T. Vander Hoogerstraete, D. Banerjee, M. R.StJ. Foreman, C. Ekberg, K. Binnemans; Separation of rare earths and other valuable metals from deep-eutectic solvents: a new alternative for the recycling of used NdFeB magnets. *RSC Advances*. **(**Accepted).

S. Riaño, K. Binnemans. "Separation of neodymium and dysprosium using a phosphonium thiocyanate ionic liquid combined with neutral extractants: a process relevant for the recycling of end-of-life NdFeB magnets". (To be submitted to *Hydrometallurgy*)

D. Kontoulis, B. Sprecher, T. Vander Hoogerstraete, S. Riaño, K. Van Acker; "Environmental assessment of newly developed rare earth recycling routes out of end-of-life NdFeB permanent magnets". (To be submitted to *Journal of cleaner production*).

Attended conferences and trainings

Attended conferences

- **9th international conference on f-elements (ICfE 9)**

  6th-9th September 2015, Oxford, United Kingdom.

  Flash presentation + poster presentation.

  S. Riano, K. Binnemans, "Ionic-liquid based process for the recovery of neodymium and dysprosium from used NdFeB magnets"

Secondments (EREAN)

- **Chalmers University of Technology, Gothenburg, Sweden**
  20th August – 21st November, 2015
  Separation of rare earths and other metals from deep eutectic solvents.
  Training on the use of mixer-settlers.

- **Treibacher Industrie AG, Althofen, Austria**

  1st – 30th June, 2016

  Project management training.

  R&D: Optimization of already existing processes in the production floor.

Attended courses, workshops and summer schools

- 12th February 2014, Lab safety and IP training, EREAN Kick off meeting, KU Leuven, Belgium.
- 24-26th April 2014, EXIL Workshop 2014 "Liquid-liquid extraction with Ionic Liquids". Strasbourg, France.
- 19-20th June 2014, ESOF "MSCA event at ESOF 2014". Copenhagen, Denmark.

- 18-21st August 2014, EREAN summer school on rare earth technology. KU Leuven, Belgium.
- 18th September 2014, Team working, critical path analysis and introduction to project management, marketing and total quality management. University of Birmingham, UK.
- 15th Dec 2014, Managing my PhD. KU Leuven, Belgium.
- 16-17th March 2015, Leadership in a complex and uncertain world. Chalmers University of Technology, Sweden.
- 22-24th April 2015, SACSESS 1st international workshop "Towards safe and optimized separation processes, a challenge for nuclear scientists". Warsaw, Poland.
- 29th September 2015 The art of scientific writing. Darmstadt, Germany.
- 1st October 2015 Scientific presentations, Darmstadt, Germany.
- 7th April 2016 Curriculum for career –course. University of Helsinki, Helsinki, Finland.
- 24th-26th August 2016 DEMETER Summer school on rare earths and full hybrid electric vehicles
- 4th October 2016 Application of electrochemistry in metals extraction and refining. / Metals science and sustainable processing. TU Delft, The Netherlands.